

Title	Discovery and pharmacological characterisation of angiotensin-(1-7) receptors and identification of their importance in diabetes mellitus
Authors	Tetzner, Anja
Publication date	2018
Original Citation	Tetzner, A. 2018. Discovery and pharmacological characterisation of angiotensin-(1-7) receptors and identification of their importance in diabetes mellitus. PhD Thesis, University College Cork.
Type of publication	Doctoral thesis
Rights	© 2018, Anja Tetzner. - http://creativecommons.org/licenses/by-nc-nd/3.0/
Download date	2023-05-05 07:57:55
Item downloaded from	http://hdl.handle.net/10468/7333

Ollscoil na hÉireann

The National University of Ireland

Coláiste na hOllscoile, Corcaigh

University College Cork



UCC

Coláiste na hOllscoile Corcaigh, Éire
University College Cork, Ireland

**Discovery and pharmacological characterisation
of angiotensin-(1-7) receptors and identification of their importance in
diabetes mellitus**

Thesis presented by

Anja Tetzner, MSc.

Under the supervision of

Professor Thomas Walther

For the degree of

Doctor of Philosophy

DEPARTMENT OF PHARMACOLOGY AND THERAPEUTICS

Head of Department Professor Thomas Walther

April, 2018

1 Contents

1	Contents.....	2
2	Declaration	7
3	Abstract	8
4	Introduction	11
4.1	The renin-angiotensin system	11
4.1.1	General structure of the renin-angiotensin system	11
4.1.2	The circulating and local renin-angiotensin system	14
4.1.3	The “new” renin-angiotensin system.....	15
4.1.4	Physiological effects mediated by angiotensin-(1-7)	20
4.2	The G-protein coupled receptors AT2, Mas and MrgD	29
4.2.1	Signalling pathways of G-protein coupled receptors	29
4.2.2	The AT2 receptor	34
4.2.3	The family of the Mas related G-protein coupled receptors	38
4.2.4	The Mas receptor	39
4.2.5	The MrgD receptor	43
4.2.6	The constitutive activity of Mas and MrgD	47
4.3	Diabetes mellitus: a pandemic disease	48
4.3.1	What is diabetes mellitus?	48
4.3.2	Diabetes type 1.....	49

4.3.3	Diabetes type 2.....	50
4.3.4	Insulin resistance and hyperinsulinemia	52
4.3.5	Complications associated with hyperglycaemia.....	53
4.3.6	Treatment of diabetes type 1 and 2	55
4.3.7	The connection between diabetes mellitus and the renin-angiotensin system	57
5	Aim of the study.....	61
6	Results	63
6.1	The G protein-coupled receptor MrgD is a receptor for angiotensin-(1-7) involving adenylyl cyclase, cAMP, and phosphokinase A	63
6.2	Decarboxylation of Ang-(1-7) to Ala ¹ -Ang-(1-7) leads to significant changes in pharmacodynamics	94
6.3	The AT ₂ receptor agonist, C21, also stimulates the Mas and MrgD receptor	116
6.4	The Angiotensin-(1-7)/Mas axis improves pancreatic β -cell function in vitro and in vivo..	142
7	General discussion	174
7.1	cAMP is the primary second messenger activated by Ang-(1-7).....	174
7.2	Mas is a functional receptor for Ang-(1-7)	176
7.3	MrgD is a receptor for Ang-(1-7)	177
7.4	Ala ¹ -Ang-(1-7) can also act through the Mas receptor.....	178
7.5	Ang-(1-7) and Ala ¹ -Ang-(1-7) possess different pharmacodynamics	180
7.6	The AT ₂ specific blocker, PD123319, also blocks Mas and MrgD	182
7.7	The AT ₂ specific compound C21 also stimulates Mas and MrgD.....	183
7.8	Ang-(1-7) improves beta cell function.....	186

7.9	Ang-(1-7) does not improve the blood glucose levels in STZ induced diabetic animals	188
8	Conclusion.....	191
9	Perspectives	194
10	Appendix part 1: Supplemental data	197
10.1	Proof of successful overexpression of Mas and MrgD in HEK293 cells.....	197
10.2	Preliminary data for mesangial cells derived from single knockout mice.....	198
10.2.1	Ala ¹ -Ang-(1-7) stimulates cAMP in single receptor knockout cells mesangial cells	198
10.2.2	C21 still stimulates PKA activity in mesangial cells derived from AT2 knockout mice	200
10.3	Effects of angiotensin-(1-7) administration on blood glucose levels in STZ induced diabetic mice	201
10.3.1	STZ-study performed by Invitek	201
10.3.2	No significant difference in blood glucose concentrations between the Ang-(1-7) receptor knockouts and wild-type animals	202
10.3.3	No significant effect of Ang-(1-7) administration on the hyperglycaemic status	204
10.3.4	Negative effects of high concentrations of Ang-(1-7) on blood glucose concentration in wild-type mice	206
10.3.5	Effects of high concentrations of Ang-(1-7) on organ weights.....	207
10.3.6	Gender depending effects of Ang-(1-7) on blood glucose concentration in wild-type mice	209
11	Appendix part 2: Materials and methods	212
11.1	Materials.....	212
11.1.1	Special equipment	212
11.1.2	Complete systems (kits)	213

11.1.3	Oligonucleotides.....	213
11.1.4	Antibodies.....	214
11.1.5	Chemicals.....	215
11.1.6	Buffer	216
11.2	Cell biological methods	219
11.2.1	Cultivation of eukaryotic cells	219
11.2.2	Isolation of mesangial cells from mouse kidney	219
11.2.3	Cell count.....	221
11.2.4	Cryopreservation and reactivation of eukaryotic cells.....	222
11.2.5	Transfection of eukaryotic cells.....	222
11.2.6	Stimulation and treatment of eukaryotic cells.....	224
11.2.7	Isolation and stimulation of mouse islets of Langerhans.....	224
11.3	Microbiological methods.....	225
11.3.1	Transformation of prokaryotic cells	225
11.3.2	Multiplication of prokaryotic cells.....	226
11.3.3	Isolation of plasmid DNA.....	227
11.4	Molecular biological methods.....	228
11.4.1	Genotyping mice.....	228
11.4.2	Isolation of RNA.....	231
11.4.3	Quantification of nucleic acids	232
11.4.4	Synthesis of complementary DNA (cDNA)	232
11.4.5	Quantitative real time PCR (qRT-PCR)	233

11.4.6	Dual luciferase assay (DLR).....	235
11.5	Protein biochemical methods	237
11.5.1	Protein extraction.....	237
11.5.2	Protein concentration determination according to Biuret (BCA).....	238
11.5.3	Sodium dodecyl sulphate polyacrylamide gel electrophoresis (SDS-PAGE).....	238
11.5.4	Immunoblot analysis	239
11.5.5	Cyclic Adenosine monophosphate enzyme-linked immunosorbent assay (cAMP ELISA)...	242
11.5.6	Protein kinase A (PKA) activity analysis.....	243
11.6	<i>In vivo</i> studies	245
11.6.1	STZ induced diabetes.....	245
12	Acknowledgements.....	247
13	Publications, posters and oral presentations	248
13.1	Publications	248
13.2	Posters	249
13.3	Oral presentations	251
14	Abbreviations.....	252
15	Figures	258
16	Tables.....	261
17	Literature	262

2 Declaration

This is to certify that the work I am submitting is my own and has not been submitted for another degree, either at University College Cork or elsewhere. All external references and sources are clearly acknowledged and identified within the contents. I have read and understood the regulations of University College Cork concerning plagiarism.

Anja Tetzner, M.Sc (Dipl. Biochemistry)

3 Abstract

The renin-angiotensin system (RAS) is known to be the main regulator of blood pressure and fluid balance. Within the RAS, angiotensin (Ang)-(1-7) is known to have cardiovascular protective effects. It represents the opponent of the often detrimental Ang II, which is known to stimulate the angiotensin receptor type 1 (AT1), causing negative effects such as a pathological rise in blood pressure. Beside the well accepted fact that the G-protein coupled receptor Mas is a receptor for the heptapeptide, it was not possible to characterise the ligand/receptor pharmacology or to identify further receptors, since there was a lack in the understanding of the initial intracellular signalling pathways stimulated by Ang-(1-7).

In this study, cyclic adenosine monophosphate (cAMP) was identified as a second messenger stimulated by Ang-(1-7). The heptapeptide elevates cAMP concentration in various cell lines, as well as in Mas transfected HEK293 cells, confirming that Mas is a functional receptor for Ang-(1-7). Even more important, MrgD was identified as a second receptor for the peptide, while AT2 could be excluded to be targeted by the heptapeptide.

It was also examined, if there are any changes in the intracellular signalling if the first amino acid of the peptide is decarboxylated. The receptor fingerprint for Ala¹-Ang-(1-7) was discovered, and the consequences for pharmacodynamics characterised. The dose-response curves were clearly different from the curves generated with Ang-(1-7). They showed a much lower EC₅₀ and a bell-shaped curve for Ala¹-Ang-(1-7). Furthermore, pharmacological proof was provided that both, Mas and MrgD, are functional receptors for Ala¹-Ang-(1-7).

Interestingly, it was also discovered that the AT₂ receptor blocker PD123319 is not AT₂ specific, but can also block the effects of Ang-(1-7) and Ala¹-Ang(-1-7) in Mas and MrgD-transfected and in primary cells. This raised the question whether the selective non-peptidic AT₂ receptor agonist, Compound 21 (C21), is also unspecific and stimulates Mas and MrgD too. This hypothesis was supported by the fact that the chemical structure of C21 is similar to the Mas receptor specific, non-peptidic agonist AVE0991. Using cAMP and downstream molecules as readouts, pharmacological proof that Mas and MrgD are functional receptors for C21 was generated.

The last part of the study examined the role of Ang-(1-7) and its receptors in diabetes mellitus (DM). Previous studies demonstrated that the ACE2/ Ang-(1-7)/ Mas axis has beneficial effects on glucose homeostasis, but the underlying mechanisms remained unknown. The effects of Ang-(1-7) and its receptor Mas on the function of β -cells were investigated. Islets isolated from Mas-deficient and wild-type mice were stimulated with Ang-(1-7) or its antagonists and effects on insulin secretion were determined. It was found that Ang-(1-7) was able to increase the insulin secretion from wild-type islets, but not from islets derived from Mas deficient animals. Interestingly, Ang-(1-7) antagonist D-Pro, but not A779 could block the Ang-(1-7) mediated effects indicating the involvement of another Ang-(1-7) receptor. However, the heptapeptide did not affect the insulin gene expression or the excitation-secretion coupling, but increased intracellular cAMP involving exchange protein activated directly by cAMP (EPAC), leading to a higher insulin secretion by the β -cells.

Ang-(1-7) was also applied to normo-glycaemic mice for 14 days using osmotic pumps. The effects of the heptapeptide *in vivo* had only marginal effects on glucose tolerance in wild-type mice. However, Ang-(1-7) had improved the insulin secretion in islets isolated

from these mice. Interestingly, although less pronounced than in wild-types, Ang-(1-7) still affected insulin secretion in islets derived from Mas deficient mice. The effect of Ang-(1-7) in mice with STZ-induced diabetes was marginal, as in normo-glycaemic mice.

Taken together, these results lead to an expansion and partial revision of the renin-angiotensin system, by identifying a second receptor for Ang-(1-7), and by excluding AT₂ as a receptor for the heptapeptide. Furthermore, the identification of Ala¹-Ang-(1-7) as a peptide with specific pharmacodynamic properties can be used as a basis for the design of more potent and efficient Ang-(1-7) analogues, which can be useful in therapeutic interventions in a rapidly growing number of diseases. The proof that C21 and PD123319 are not AT₂ receptor specific as generally assumed, but also interact with the two Ang-(1-7) receptors, Mas and MrgD, might be an explanation for the partial overlap in beneficial effects of both compounds. Thus, the better understanding of the interaction of small molecules like C21 with their receptors, lays the foundation for the development of small molecules which stimulate all or just one of the Ang-(1-7) receptors, which may be beneficial in diseases like diabetes mellitus. Since it could be shown that Ang-(1-7) plays a significant role in the regulation of insulin secretion from mouse islets *in vitro* and *in vivo*, mainly, but not exclusively, by Mas-dependent signalling, modulating the accessory pathway of insulin secretion via increase in cAMP, makes clear that Ang-(1-7) and its receptors are very promising therapeutic targets.

4 Introduction

4.1 The renin-angiotensin system

4.1.1 General structure of the renin-angiotensin system

Historically, the renin-angiotensin system (RAS) was believed to be a system with endocrine properties, whose active metabolite angiotensin (Ang) II was also the final product of the system [1, 2]. After activation, the first step is the secretion of renin by specialised cells in the kidney tissue, known as the juxtaglomerular apparatus [3]. The juxtaglomerular apparatus responds to blood pressure changes in *vas afferens*, the salt content of the urine, signals from the autonomic nervous system and various hormones. Renin is stored in myoepithelial cells of the *vasa afferentia*. Decreased blood flow, reduced blood pressure, reduced glomerular filtration rate, lower concentration of chloride ions in the urine (measured by the salt sensors of the *macula densa*) and the activation of the sympathetic nervous system lead to an increased release of renin [4, 5].

Whereas renin is secreted by the kidneys, the precursor of angiotensin, the 452 amino acid long angiotensinogen, is secreted by the liver and circulates free in the blood. The pro-hormone is cleaved by renin into the 10 amino acid long Ang I (Ang-(1-10)), which then is cleaved by the angiotensin converting enzyme (ACE) to the octapeptide Ang II (Ang-(1-8)) [6].

Two receptors have been identified as targets for Ang II, the angiotensin receptor type I (AT1), and the angiotensin receptor type II (AT2) [7, 8] (Figure 4.1.1). The induced intracellular signalling then results in different physiological effects such as increase in blood pressure, cardiac contractility, vascular and cardiac hypertrophy, and proliferation

[7, 8]. While the mentioned effects are AT1 mediated, AT2 opposes most of these effects [7, 8].

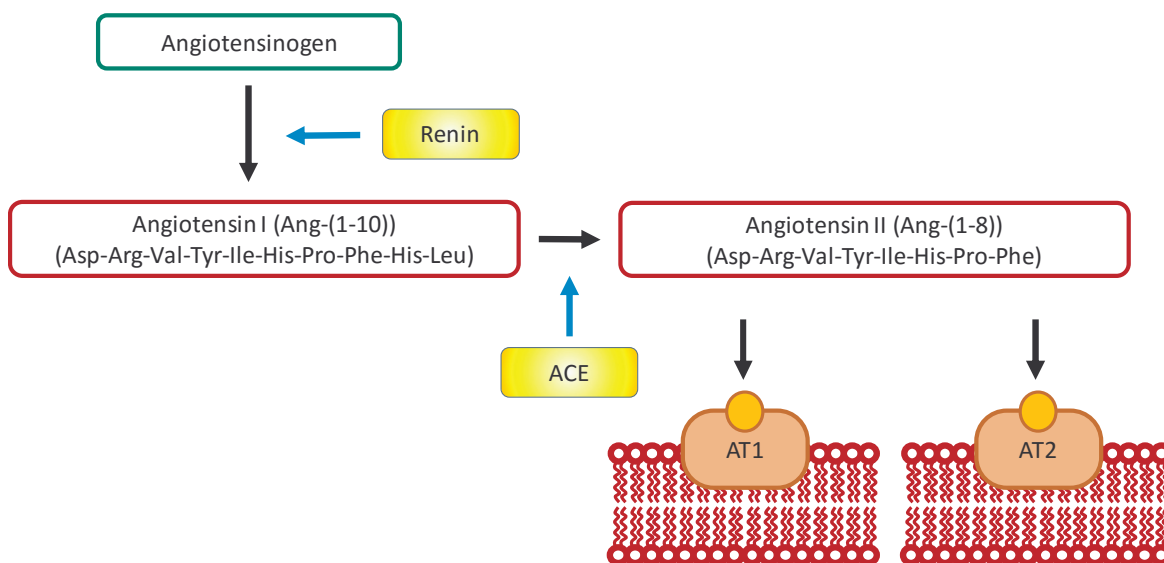


Figure 4.1.1 The general structure of the renin-angiotensin system

The kidney secretes renin when blood pressure drops or the glomerular filtration rate decreases. In the blood circulating angiotensinogen is cleaved by renin to Angiotensin I (Ang I). The angiotensin converting enzyme (ACE) cleaves two amino acids from the c-terminal end of Ang I to generate Ang II [6], which then interacts with the AT1 and AT2 receptor.

4.1.1.1 The carboxypeptidase ACE

The glycoprotein ACE is the key enzyme for the production of Ang II. It is a zinc metalloprotease and converts the inactive decapeptide Ang I into the biologically active Ang II by cleaving the n-terminal dipeptide histidine-leucine [9]. ACE has been found in several tissues, such as heart, blood vessels, kidneys, and intestine [10]. A soluble form also exists, which has been found in blood plasma, amniotic fluid, seminal plasma, and other body fluids [11].

ACE inhibitors were initially used to treat hypertension, but are also very effective in cardiovascular events such as acute myocardial infarction (heart attack), cardiac failure (left ventricular systolic dysfunction), but also in kidney complications (diabetic nephropathy). ACE inhibitors lower arteriolar resistance and increase venous capacity. Furthermore, they decrease the cardiac function (cardiac output, cardiac index, stroke work, and volume) and increase excretion of sodium in the kidney tubules, by decreasing the Ang II production which results in reduced aldosterone release [12].

4.1.1.2 Angiotensin II and its receptors AT1 and AT2

The functions of Ang II include the regulation of blood pressure and electrolyte balance, release of aldosterone and vasopressin, sympathetic activity, as well as the control of thirst and water intake [13].

The effects of Ang II are mediated by AT1 and AT2. Both receptors are G-protein coupled receptors (GPCRs) of the rhodopsin subclass with comparable properties in ligand binding (see Chapter 4.2.1). The difference between them lies in their tissue distribution, as well as their transcriptional regulation and signal transduction [14]. The AT2 receptor will be further discussed in Chapter 4.2.2.

The AT1 receptor is the major receptor for Ang II [7, 15]. It interacts with various heterotrimeric G-proteins and activates second messengers, such as inositol trisphosphate (IP3), diacylglycerol (DAG) and reactive oxygen species (ROS). The binding of Ang II to AT1 activates receptor and non-receptor tyrosine kinases, serine/threonine kinases, mitogen-activated protein kinases (MAPKs), p70S6K, protein kinase B (PKB/ AKT),

and protein kinase C (PKC) and has a negative effect on adenylyl cyclase (AC) [16]. In general, the activation of the AT1 receptor induces strong vasoconstriction. It stimulates the release of aldosterone from the adrenal glands, which in turn promotes sodium reabsorption. In the kidney, the activation of the receptor is associated with renal vasoconstriction and anti-natriuresis [3, 17]. In addition, AT1 activates the sympathetic nervous system and is involved in the development of hypertension, arteriosclerosis and heart failure [18, 19]. In the heart, AT1 stimulates hypertrophy and the proliferation of cardiac fibroblasts [20]. The ACE/ Ang II/ AT1 axis is seen as the harmful arm of the RAS.

4.1.2 The circulating and local renin-angiotensin system

Since the first description of renin by Tigerstedt and Bergmann in 1898 [21], the RAS has been the focus of intense research. Researchers came to the understanding that the RAS has not just endocrine, but also paracrine functions [22]. They concluded that the primary function of the circulating RAS was not the delivery of Ang II to tissues, but rather the delivery of renin and angiotensinogen [23]. The generation of Ang I and Ang II then occurs in the target tissue through ACE, respectively.

Two systems can be distinguished, the circulating RAS and the local (tissue specific) RAS [24]. In the 1970s, components of the RAS could be identified in different tissues such as heart [25], lung [26], kidney [27, 28], blood vessels [29, 30], adrenal glands [31-33], brain [34, 35] and even reproductive organs [36]. Although, those findings initially faced big criticism, with the development of new techniques it was no longer deniable that local RAS exists.

Whereas the plasma RAS is responsible for short-term changes and the regulation of the cardiovascular system, the local RAS can cause long-term effects. Those effects include changes in cell proliferation, protein synthesis and organ function. The local RAS seems to work independent from the circulating system [3, 37].

4.1.3 The “new” renin-angiotensin system

For a long time, Ang II was believed to be the final product and functional component of the RAS. The discovery of other components such as new receptors, angiotensin peptides and alternative ways of generating them, fundamentally changed the understanding of the RAS in the past 100 years (Figure 4.1.2).

These new components contain the peptides Ang III (Ang-(2-8)), Ang IV (Ang-(3-8)), Ang-(1-9) and Ang-(1-7) (see also Figure 4.1.2) [38, 39]. Enzymes responsible for the generation of these angiotensin peptides are primarily, but not exclusively, the carboxy peptidases ACE and ACE2, the neutral endopeptidase (neprilysin, NEP), and the aminopeptidases (AP) APA, APN and APD [39].

Jankowski *et al.* have been the first who described Ala¹-Ang II in human plasma [40]. Also known as Ang A, this peptide is generated by the decarboxylation of the first amino acid. The detailed mechanism and the enzyme responsible remain unknown. Ang A acts through the same receptor as Ang II, AT1 [41].

In 2013, Lautner *et al.* identified Ala¹-Ang-(1-7). This peptide can be generated through the decarboxylation of the first amino acid of Ang-(1-7), as the authors have demonstrated by analysing Ang-(1-7) perfused rat heart [42]. Additionally, they also

demonstrated that the peptide can be converted from Ang A through ACE2, by cleaving the last amino acid from Ang A. The effects of Ala¹-Ang-(1-7) seem to be the same as those from Ang-(1-7), such as vasorelaxation and anti-hypertensive effects, as demonstrated in spontaneous hypertensive rats [42].

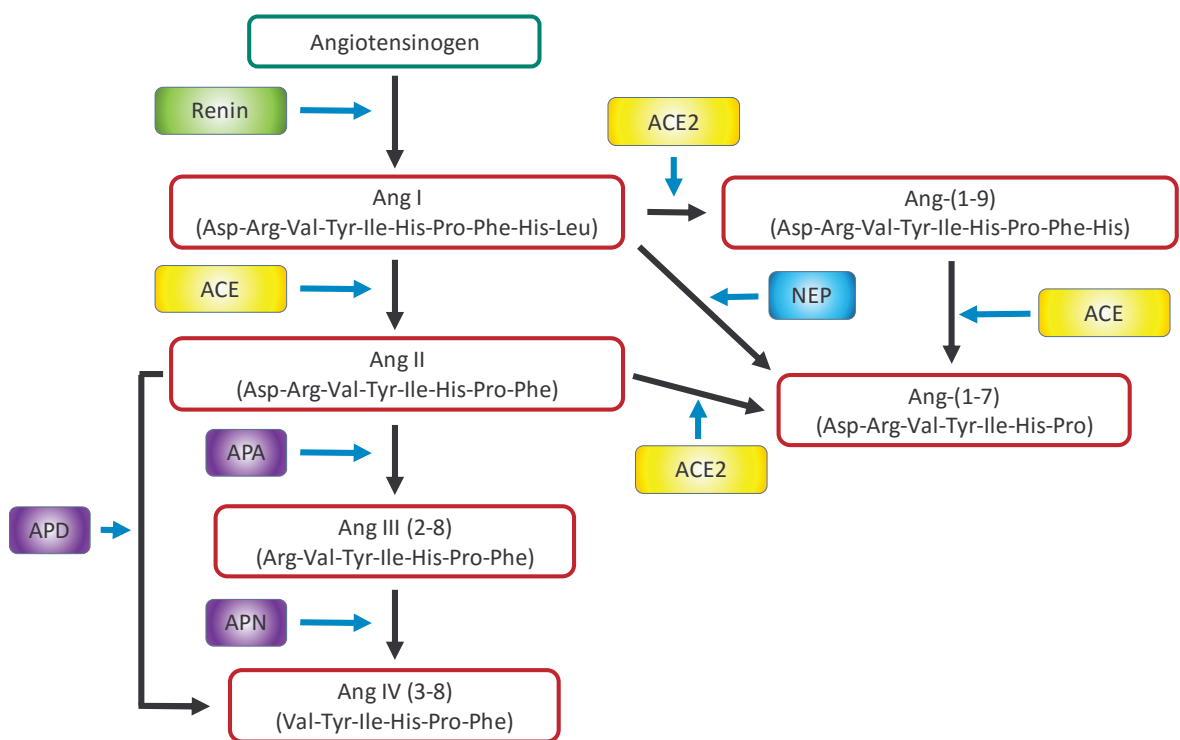


Figure 4.1.2 Biologically active angiotensin peptides and their generation

Schematic overview of the biologically active angiotensin peptides and their generation through the main targeting peptidases [43, 44]. (AP: amino peptidase, ACE: angiotensin converting enzyme, NEP: neutral endopeptidase)

Additionally, the number of receptors within the RAS has expanded over the past 70 years (Figure 4.1.3). Researchers have found that Ang III, like Ang II, can stimulate AT1 and AT2 and has the same, if not better potency compared to Ang II [44]. The hexapeptide Ang IV can bind to AT1 and AT4 (later identified as the insulin regulating amino peptidase (IRAP)) [45, 46]. Ang-(1-9) was found to bind to AT2 [47], whereas Ang-(1-7) has been linked to

the Mas receptor. However, in certain circumstances and tissues, AT2 seemed to be involved in the Ang-(1-7) mediated effects [48, 49]. The receptor identified for the newly described Ala¹-Ang-(1-7) was MrgD, a Mas like receptor [42].

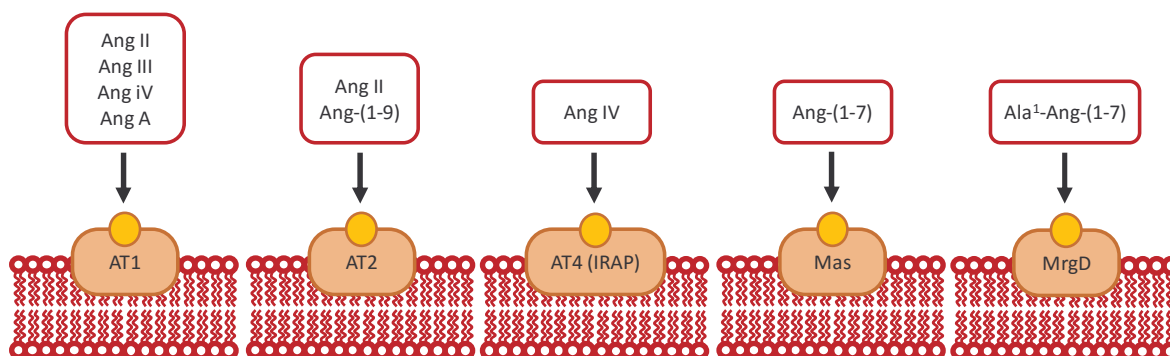


Figure 4.1.3 The receptors of the RAS

Schematic overview of the receptors of the RAS and the estimated ligands.

In contrast to Ang II, Ang III and Ang IV, have vasoconstrictive properties, while Ang-(1-9) and Ang-(1-7) are vasorelaxant [43, 50].

Nowadays, the RAS is divided into two antagonistic axes, as the discovery of ACE2 and the Mas receptor extended the concept of RAS. Now the RAS no longer just consists of the “bad” ACE/ Ang II/ AT1 axis, but also the “good” ACE2/ Ang (1-7)/ Mas axis. While the classical axis is characterised by proliferative, fibrotic, vasoconstrictive, and hypertrophic effects, the “new” axis opposes those effects [51].

4.1.3.1 The carboxy peptidase ACE2

ACE2 was first described in 2000 by two independent research teams [52, 53]. Like ACE, it is a zinc dependent metallopeptidase. Both show 42 % identity in their catalytic domain [52, 53]. In addition, the catalytic mechanism of both peptidases is quite similar. The

difference from ACE is the number of amino acids cleaved from the substrate. ACE splits two amino acids from the C-terminal end, while ACE2 is a mono-carboxy peptidase and cleaves only one amino acid from the C-terminal end.

At first, it was assumed that ACE2 expression was restricted to heart, kidney, and testis [53, 54], as Donoghue *et al.* could show. They cloned the human ACE2 from a cDNA library and performed northern blot analysis with several human tissue [53]. However, recent findings demonstrated that it is expressed in a wide variety of cardiovascular tissues (myocytes, lung epithelial cells, vascular smooth muscle cells) and noncardiovascular tissues (ileum, duodenum, jejunum, caecum, and colon) [54]. ACE2 is an integral type I membrane protein [55], but can also be shed from the membrane to a still active soluble form [56].

Initially, the decapeptide Ang I was considered to be the primary substrate for ACE2, generating the biologically active peptide Ang-(1-9) [53]. However, investigations of ACE2 activity demonstrated that the catalytic activity of the carboxypeptidase for Ang II is 400 times higher than for Ang I, concluding Ang II as the main substrate of ACE2, which is metabolised to the heptapeptide Ang-(1-7) [57, 58] .

4.1.3.2 The protective angiotensin-(1-7) and its receptor Mas

For a long time, it was assumed that Ang-(1-7) was a peptide without biological activity. The first proof of its biological activity was in 1988. Schiavone *et al.* [59] demonstrated in *in vitro* experiments that the heptapeptide induces the release of vasopressin from the

hypothalamic neurohypophyseal explant. At the same time, the formation of Ang-(1-7) from Ang I via an ACE-dependent pathway was described [60].

Since 1988, Mas was presumed to be a functional angiotensin receptor [61]. As the binding of Ang II to Mas could never be shown, this hypothesis was questioned for a long time [61]. In 2003, the Walther group described Ang-(1-7) as a ligand for the Mas receptor [62]. Santos *et al.* showed that the knockout of Mas in mice completely abolished the vasodilatory effects of Ang-(1-7) in aortic rings isolated from those animals. Furthermore, they showed that the transfection of COS cells with the Mas receptor resulted in Ang-(1-7) mediated release of arachidonic acid (AA) [62].

However, the results of several studies suggest that the peptide interacts with several receptors of the RAS. Beside Mas [62], researchers found that Ang-(1-7) also binds to the AT1 receptor, using replacement assays with I125-AngII [63]. However, the affinity of the heptapeptide for the AT1 receptor is much lower than for the Mas receptor, since high concentrations ($\geq 10^{-6}$ M) of Ang-(1-7) has been required in those studies. In addition, Ang-(1-7) has a low affinity for the AT2 receptor [64]. However, since pharmacological studies implicated that many Ang-(1-7) mediated effects are AT2 receptor independent, the receptor might be only involved in certain conditions and in certain tissues [64]. Furthermore, the peptide might also interact with the Mas-like receptors MrgD and Mrg, as the peptide was able to increase the AA release in COS cells overexpressing these receptors. [65].

Interestingly, most effects mediated by Ang-(1-7) are counteracting the effects caused by Ang II activating the AT1 receptor [66]. The signalling of the AT2 receptor will be described in detail in Chapter 4.2.4.4.

4.1.4 Physiological effects mediated by angiotensin-(1-7)

The main function of the RAS is the regulation of blood pressure, fluid balance and salt homeostasis including thirst. Beside those classical functions, the RAS is also involved in other processes.

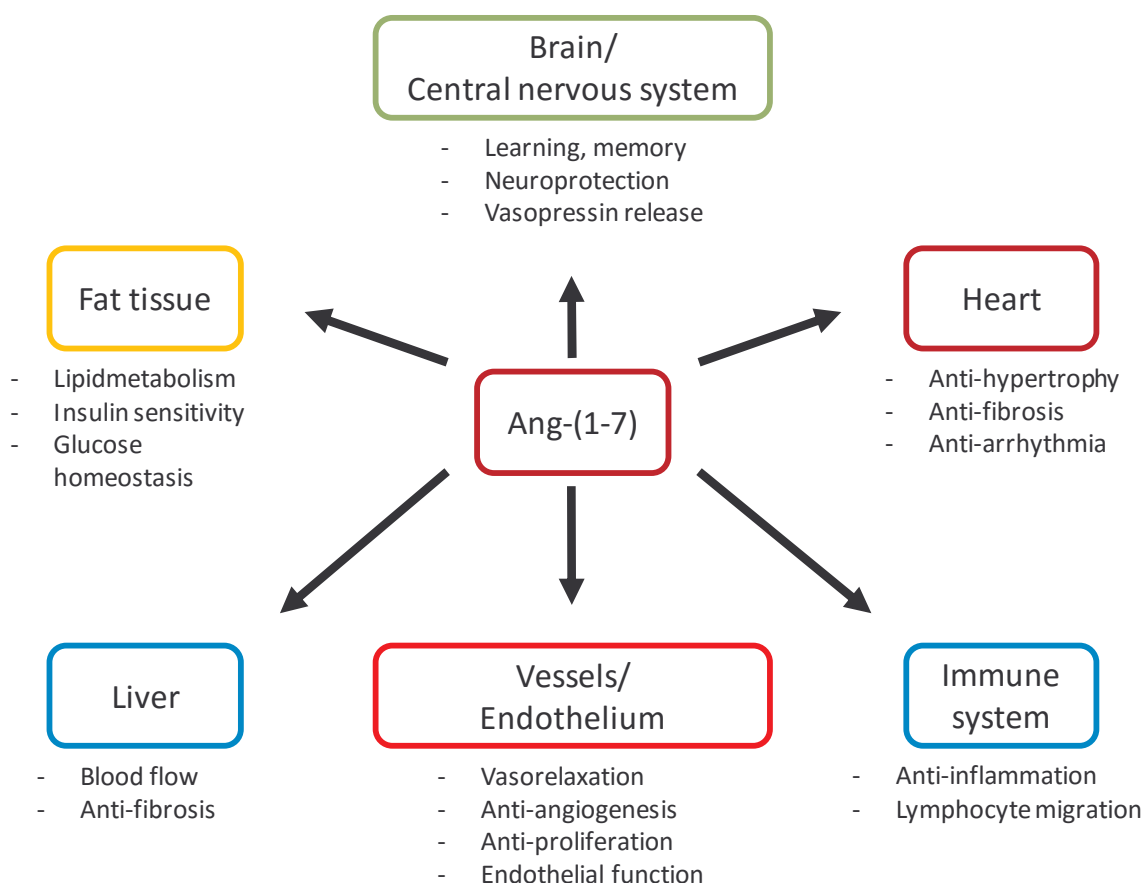


Figure 4.1.4 Ang-(1-7) tissue specific effects

Overview of the beneficial effects mediated by Ang-(1-7) in different tissues such as brain, central nervous system, heart, blood vessels, fat tissue and liver. Furthermore, Ang-(1-7) plays a role in the modulation of the immune response.

The system plays a role in certain diseases, such as Alzheimer's disease [67, 68], Parkinson's disease [69], epilepsy [70], alcoholism [71, 72], depression and diabetes [73] (see also Chapter 4.3). It also influences the blood flow in the brain and kidney [74, 75].

Ang-(1-7) often counteracts the cardiovascular effects of Ang II/ AT1, but it is also involved in other tissue specific processes (Figure 4.1.4).

4.1.4.1 Angiotensin-(1-7) mediated effects in the kidney

The function of the heptapeptide in the renal system is contradictory. Many studies could show positive effects of Ang-(1-7) in renal diseases. The heptapeptide improved glomerulosclerosis [76] and had positive effects on general renal parameters (microalbuminuria and serum albumin levels) in a murine model of adriamycin-induced nephropathy [77]. In a genetic mouse model for diabetes type 2, Ang-(1-7) has been renoprotective against diabetic nephropathy. This was associated with lower levels of inflammatory markers (reduced macrophage levels in perirenal adipose tissue), less oxidative stress (less superoxide production) and less fibrosis in renal tissue [78]. In kidney epithelial cells, the heptapeptide modulates the activity of transporters, limiting the transcellular sodium flux. The modulation of transporter activity occurs by activation of phospholipase A2 (PLA2) [79].

On the other hand, it seems that Ang-(1-7) has detrimental effects under certain conditions. In streptozotocin (STZ) induced diabetic rats, for example, the infusion of the heptapeptide worsened the renal function and did not improve the renal injury [80]. In murine models of renal insufficiency (unilateral ureteral obstruction and ischemia/ reperfusion injury), the administration of Ang-(1-7) had pro-inflammatory effects, increased fibrosis and apoptosis and worsened the conditions. Furthermore, the knockout of the Mas receptor reduced the renal damage, indicating that the Ang-(1-7)/

Mas axis plays an important role in the pathogenesis and progression of subsets of renal failure [81].

In cells isolated from the proximal tubules of rats, Ang-(1-7) displayed growth inhibitory properties by counteracting the Ang II mediated phosphorylation of the mitogen-activated protein kinase (MAPK) [82]. The pre-incubation of rat mesangial cells with Ang-(1-7) in addition to Ang II, opposed several Ang II mediated responses, like the production of ROS, the activation of the nuclear factor kappa-light-chain-enhancer of activated B cells (NF- κ B), and MAPK phosphorylation [83]. In contrast, in human mesangial cells the heptapeptide stimulated cell growth pathways by increasing AA release and MAPK phosphorylation [84]. While Liu *et al.* showed that the heptapeptide promotes Erk1/2 (MAPK1/2) phosphorylation [85], Oudit *et al.* demonstrated that Ang-(1-7) inhibited high glucose-stimulated nicotinamide adenine dinucleotide phosphate (NADPH) oxidase (NOX) via Mas receptor activation [86].

Animals lacking the Mas receptor showed a reduced volume of urine and sodium excretion, and an increase in glomerular filtration. Furthermore, the knockout mice showed an increased proteinuria [87].

4.1.4.2 Angiotensin-(1-7) mediated effects in the heart

The heptapeptide has been detected in heart areas such as, aortic root, coronary sinus, sinus node, right atrium, and in the hermus cells [88, 89].

Ang-(1-7) activated the sodium pumps, reduced the frequency and duration of ischemia-reperfusion arrhythmias [90, 91], and improved heart function after ischemia-

reperfusion-induced cardiac injury in rats [92]. Furthermore, Ang-(1-7) seems to play an important role in the regulation of cardiac remodelling and expression of extracellular matrix proteins in rat heart [93]. In a rat model of myocardial infarction, the chronic infusion of the heptapeptide resulted in many beneficial effects. It increased the coronary perfusion, preserved the cardiac function, and reversed the vascular endothelial dysfunction in aortic rings [94]. In addition, chronic Ang-(1-7) treatment ameliorated cardiac hypertrophy and fibrosis and attenuated the growth-promoting pathways in the heart of insulin-resistant rats [95]. In hypertensive rats, the administration of Ang-(1-7) was also cardio protective. The heptapeptide significantly reduced the Ang II induced cardiac remodelling by the upregulation of a MAPK specific phosphatase (dual-specificity phosphatase 1, DUSP-1) [96]. The administration of Ang-(1-7) in models of cardiac fibrosis in Sprague-Dawley rats prevented the Ang II induced fibrosis in the rat heart [97]. Also in hypertensive rats, the treatment with Ang-(1-7) upregulated Mas and AT₂ and resulted in decreased fibrosis [98].

The deletion of Mas resulted in a marked increase in fibronectin and collagen type I and III in the heart compared to wild-type mice, indicating the importance of the Ang-(1-7)/Mas axis in the modulation of the extracellular matrix [99, 100]. In addition, the Mas-deficient mice showed a gender-specific difference in heart rate variability and blood pressure variability compared to wild-type animals, suggesting that Mas has a significant influence on both [101].

4.1.4.3 Angiotensin-(1-7) mediated effects in endothelium and blood vessels

Ang-(1-7) has a significant impact on endothelial function. Ang-(1-7) failed to cause vasodilation in coronary arteries of dogs where the endothelium was removed [102], indicating that the vasodilatory effect of Ang-(1-7) is endothelium dependent. Not only are endothelial cells crucial for Ang-(1-7)-mediated vascular effects, they are also important for the generation and catabolism of the heptapeptide. Santos *et al.* could demonstrate that the incubation of ¹²⁵I-Ang I with bovine and human endothelial cells resulted in a time-dependent generation of 125I-Ang-(1-7), 125I-Ang II and 125I-Ang-(1-4) [103]. In endothelial cells, the heptapeptide induces the release of hyperpolarizing factors and vasodilators such as prostanoids and nitric oxide (NO) [104-106] by activating the endothelial nitric oxide synthase (eNOS) [107].

Most of the Ang-(1-7) mediated vasodilatory effects seem to be Mas receptor-dependent. The Ang-(1-7) induced decrease in the perfusion pressure in isolated rat hearts was abolished by A779 [108]. Mesenteric microvessels isolated from Mas-deficient mice showed no response to Ang-(1-7). Furthermore, in wild-type mesenteric microvessels the pre-incubation with the Mas antagonists A779 or D-Pro totally abolished the vasodilatory effect of Ang-(1-7), indicating that this effect is Mas dependent [109].

In addition, the vasodilatory effects are gender specific. Experiments with hypertensive rats showed that oestrogen promotes the generation of Ang-(1-7) and potentiates its effects [110]. In rats fed on a high salt diet (model for diet-induced hypertension), the anti-oxidative effects of the ACE2/Ang-(1-7)/Mas axis helped to maintain and restore normal endothelial function in cerebral vessels. The chronic infusion of Ang-(1-7) reduced

vascular superoxide levels and restored the NO-dependent dilatation. The administration of A779 blocked those effects [111].

The knockout of Mas on a mixed FVBN and C57BL/6 background, showed an endothelial dysfunction [112, 113]. The Walther group could show that microvessels isolated from mice deficient in Mas lose the ability to respond to bradykinin with a vasorelaxation [113]. Furthermore, Mas deletion resulted in an imbalance between NO and ROS [114]. Interestingly, there is a significant difference in the pronounced phenotype depending on the genetic background [115]. Mas-deficiency on a pure C57BL/6 background showed a less prominent endothelial dysfunction compared to a pure FVB/N background. Additionally, C57BL/6Mas-deficient mice remained normotensive, whereas the FVB/N developed an elevated blood pressure [115].

4.1.4.4 Angiotensin-(1-7) mediated effects on the central nervous system

In the brain, Ang-(1-7) influences processes such as, learning, memory, and neuroprotection. Most of these effects are Mas dependent [116].

The activation of the Mas receptor resulted in the activation of neuronal NOS (nNOS) and NO synthesis. The activation of nNOS is important for object recognition memory and long-term potentiation in the hippocampus and amygdala [116, 117]. Rats lacking the Mas receptor developed a deficiency in object recognition and memory, showing that the Ang-(1-7)/ Mas axis plays an important role in learning and memory [118].

The ACE2/ Ang-(1-7)/ Mas axis has also neuroprotective effects in ischemic stroke. In rats with induced ischemic stroke, the central infusion of the Mas receptor agonist, A779,

resulted in larger infarct volumes compared to the control animals. Furthermore, the central infusion of an angiotensin-converting enzyme 2 inhibitor (MLN-4760) worsened neurological function [119].

Animals lacking the Mas receptor showed an increased maintenance of long-term potentiation in the brain. The hippocampal morphology, basal synaptic transmission, and presynaptic function was not changed. Male mice displayed an increased anxiety behaviour compared to wild-type animals, which was not observed in female mice, indicating a gender-specific effect of Mas expression effects [120].

4.1.4.5 Angiotensin-(1-7) mediated effects in fat tissue

Components of the RAS can also be found in adipose tissue [121]. The activation and expression is depending on the state of ingestion. For example, in sucrose-fed rats the concentration of ACE2 and Ang-(1-7) are elevated in adipose tissue [122].

In rats, which were fed with high-fructose or high-fat diets, the long-term administration of Ang-(1-7) reduced the total fat mass, adipocyte size, adipose inflammation, and superoxide production by NADPH [123, 124]. A study in 2010 used the over expression of an Ang-(1-7)-releasing fusion protein in rats to increase plasma Ang-(1-7) levels. This resulted in a significantly reduced adipose tissue mass and decreased plasma triacylglycerides [125]. Besides the beneficial effects on lipid metabolism, Ang-(1-7) also influences the glucose homeostasis and insulin resistance in adipose tissue, which will be discussed in Chapter 4.3.7.

The deletion of Mas in mice resulted in a metabolic syndrome-like state. Mas-knockout mice had a normal body weight, but showed dyslipidemia, increased insulin levels and leptin, and increased abdominal fat mass. Furthermore, a glucose intolerance and reduced insulin sensitivity was observed [126]. In addition, the KO mice showed a reduced response of adipocytes to the anti-lipolytic effect of insulin [127].

4.1.4.6 Regulation of inflammation through angiotensin-(1-7)

Several studies could show that the Ang-(1-7)/ Mas axis plays a role in inflammatory responses. Ang-(1-7) reduced leukocyte migration, cytokine expression and release, and activation of fibrogenic pathways.

Using a rat model of autoimmune myocarditis, Sukumaran *et al.* [128, 129] could demonstrate that the ACE2/ Ang-(1-7)/ Mas axis plays an important role in the anti-inflammatory effects of Telmisartan and Olmesartan (AT1 blockers). The increase of myocardial protein levels of ACE2, Ang-(1-7) and Mas was correlated with an increase of the anti-inflammatory cytokine, interleukin (IL)-10, and a reduction of pro-inflammatory cytokines such as tumour necrosis factor (TNF)- α , interferon (IFN)- γ , IL-1 β , IL-6. This was associated with less myocardial fibrosis and the down-regulation of phosphatidylinositol 3-kinases (PI3K), phospho-Akt (pAkt), phospho-p38, phospho-c-Jun N-terminal kinases (pJNK), phospho-MAPK1 and phospho-MAPK2 (pErk1/2) [128, 129]. Ang-(1-7) counteracted the Ang II induced inflammation in human aortic smooth muscle cells by inhibiting the activation of NADPH oxidase and nuclear factor kappa-light-chain-enhancer of activated B cells (NF- κ B), which results in the prevention of inducible NOS (iNOS)

generation. Those effects were blocked by A779 and D-Pro, indicating that this is Mas-dependent [130].

Mas-deficient mice showed a reduced concentration of intra-renal NFκB compared to the wild-type animals after unilateral ureteral obstruction, indicating that the absence of the Mas gene suppresses inflammation in the kidneys. These mice also had a decreased matrix deposition, apoptosis and inflammatory cell infiltration [131]. Macrophages from C57BL/6 Mas deficient mice showed an increased migratory and pro-inflammatory phenotype, which led to an increased immune cell infiltration in the spinal cord or in atherosclerotic plaques [132].

4.1.4.7 Regulation of cell proliferation through angiotensin-(1-7)

Many studies demonstrated that the Ang-(1-7)/ Mas axis has anti-proliferative effects in vascular smooth muscle cells [133, 134], liver tissue [135, 136], cardiomyocytes [134] and tumors [137-139]. In VSMC, Ang-(1-7) inhibited the growth via increasing the prostacyclin (PGI₂) [133]. Using a rat model of hepatic fibrosis (induced by bile duct ligation), it was possible to show that Ang-(1-7) and the Mas agonist AVE 0991 improved fibrosis significantly [136]. In a mouse model for hepatocellular carcinoma (tumour growth in mice was induced by injecting H22 cells), Ang-(1-7) administration reduced the tumour growth and inhibited the angiogenesis [137]. In *in vitro* experiments, Ang-(1-7) abolished the AngII-induced migration, invasion, VEGF expression, and MMP-9 activity in breast cancer cells (MDA-MB-231 and LM3) [139].

The molecular mechanisms that promote the anti-proliferatory effects of Ang-(1-7) include the inhibition of MAPK and the stimulation of prostaglandin synthase and cyclic adenosine monophosphate (cAMP) production [133, 140, 141].

Mas KO mice showed an increased renal expression of transforming growth factor (TGF) β 1 and extracellular matrix proteins [87]

4.2 The G-protein coupled receptors AT2, Mas and MrgD

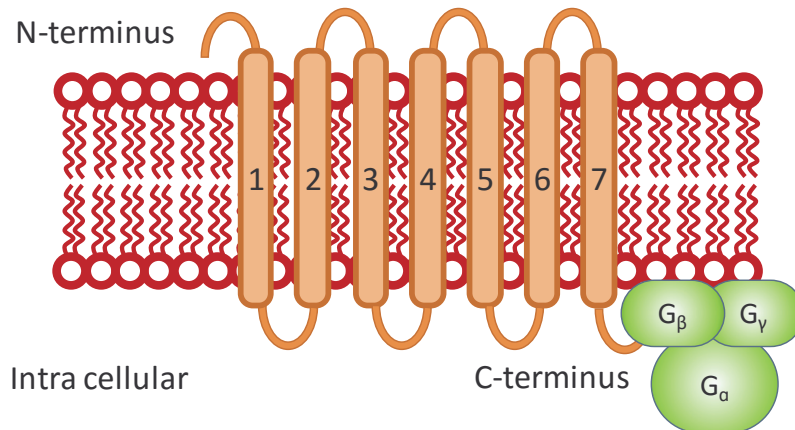
GPCRs, also known as seven transmembrane receptors (7TMR), are the largest group of membrane bound receptors, and are only found in eukaryotes and animals [142]. This receptor family is a widely used target for the pharmaceutical industry for the treatment of diseases such as diabetes, obesity and Alzheimer's disease [143]. Approximately 34 % of all modern drugs target GPCRs [143]. The GPCRs in vertebrates are divided into six categories: Class A (or 1) (Rhodopsin-like), Class B (or 2) (Secretin receptor family), Class C (or 3) (Metabotropic glutamate/ pheromone), Class D (or 4) (Fungal mating pheromone receptors), Class E (or 5) (cAMP receptors) and Class F (or 6) (Frizzled/ Smoothed) [144].

4.2.1 Signalling pathways of G-protein coupled receptors

The name, GPCR or 7TMR, comes from their structure (Figure 4.2.1), as they possess seven membrane-spanning domains (transmembrane helices) [145].

Extra cellular

N-terminus



Intra cellular

C-terminus

Figure 4.2.1 G-Protein coupled receptor

Schematic structure of a G-protein coupled receptor.

The binding of an agonist to the GPCR leads to a conformational change and activates intracellular responses. The majority of the signalling is G-protein dependent, but G-protein independent signalling, such as phosphatase activation, also exists [146-148].

G-proteins are trimers of α , β , and γ subunits (G_α , G_β , and G_γ) (Figure 4.2.1) [149]. In their inactive state, they are bound to guanosine diphosphate (GDP). If the GPCR is activated, the guanine exchange factor (GEF) domain activates the G-protein by exchanging GDP for guanosine triphosphate (GTP) at the G_α -subunit. This leads to a dissociation of the subunits from the receptor. The G_α -GTP-monomer and a $G_{\beta\gamma}$ -dimer, are now able to modulate the activity of other intracellular proteins and ion channels [150, 151].

There are four sub-classes of G_α -proteins distinguished from each other by sequence differences and function/ downstream signalling ($G_{\alpha s}$, $G_{\alpha i/o}$, $G_{\alpha q/11}$, and $G_{\alpha 12/13}$) [149]. $G_{\alpha s}$ and $G_{\alpha i/o}$ are modulating the cAMP-generating enzyme adenylate cyclase (AC) [152]. AC catalyses the conversion of cytosolic adenosine triphosphate (ATP) to cAMP (Figure 4.2.2). The interaction with $G_{\alpha i/o}$ inhibits AC from generating cAMP, while $G_{\alpha s}$ activates AC (Figure 4.2.2).

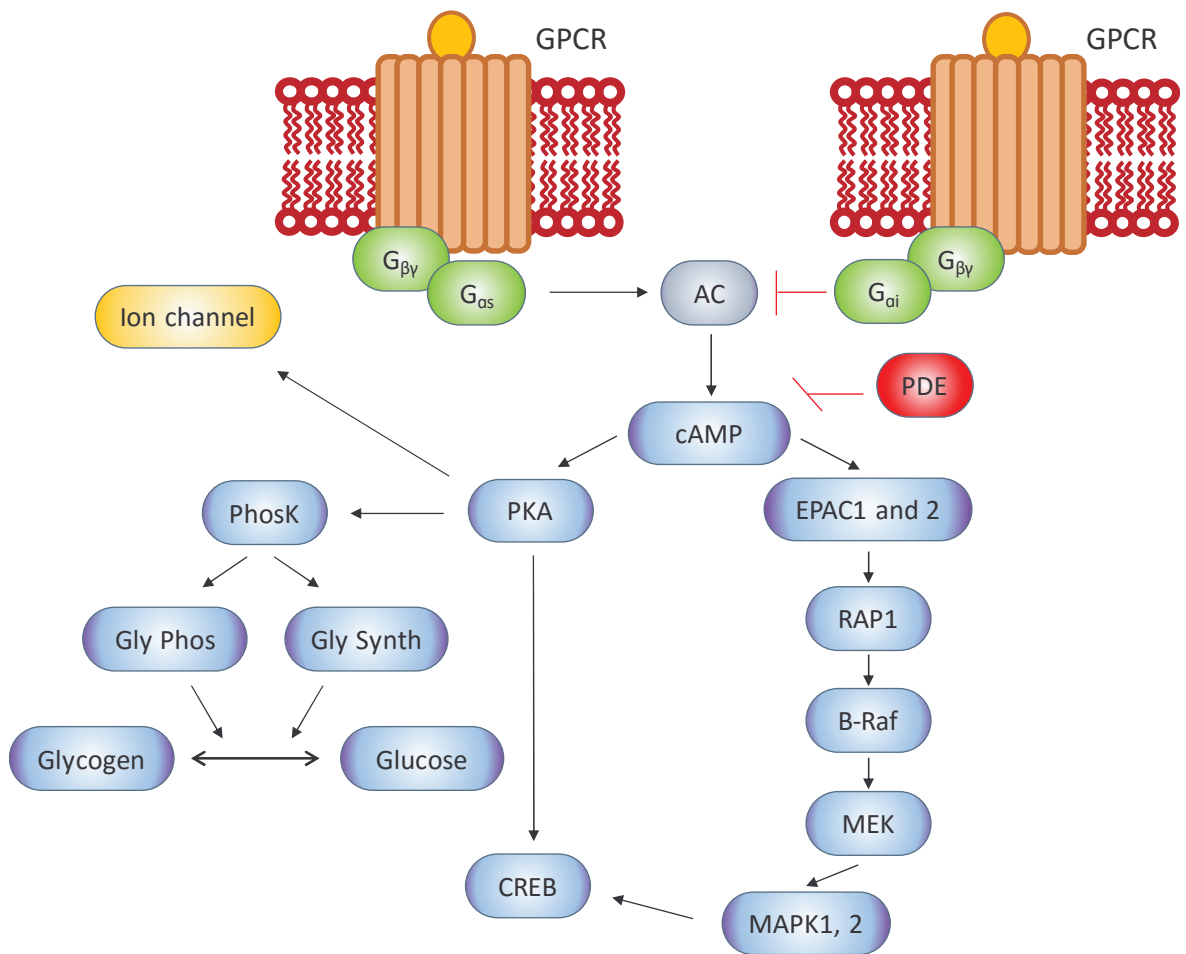


Figure 4.2.2 The $G_{\alpha s}$ and $G_{\alpha i}$ pathway

Schematic overview of the $G_{\alpha s}$ and $G_{\alpha i}$ mediated intracellular pathways. The generation of cAMP activates multiple intra cellular responses, including ion channels, transcription factors, and metabolic enzymes (AC: Adenylyl cyclase, B-Raf: Mitogen activated protein kinase kinase kinases, cAMP: Cyclic adenosine monophosphate, CREB: cAMP response element-binding protein, EPAC: Exchange factor directly activated by cAMP, Gly Phos: Glycogen phosphorylase, Gly Synth: Glycogen synthase, MAPK: Mitogen-activated protein kinase, MEK: MAPK/ERK kinase, PDE: Phosphodiesterase, PhosK: Phosphorylase kinase, PKA: Protein kinase A, RAP1: Ras-related protein 1).

Cytosolic cAMP activates the guanine-nucleotide-exchange factor directly activated by cAMP (EPAC), but also the serine/ threonine-specific protein kinase A (PKA) [153], and both can activate the cAMP response element-binding protein (CREB) (Figure 4.2.2) [144].

Phosphorylated CREB (pCREB) translocates to the nucleus, binds to the CREB response element (CRE) and acts as a transcription factor. CREB plays an important role in neuronal plasticity and long-term memory and is important for the survival of neurons. Mouse studies showed that the lack of CREB during the embryogenesis leads to the death of the mice immediately after birth, indicating a crucial role in developmental processes during embryogenesis [154]. Furthermore, EPAC 2 proteins are known to regulate exocytosis in different cell types, such as insulin secretion from pancreatic β -cells [155]. Additionally, the activation of PKA initiates a cascade, which is responsible either for the breakdown or the synthesis of glycogen, as phosphorylase kinase activates both glycogen synthase (Gly Synth) and glycogen phosphatase (Gly Phos), indicating the importance of the cAMP pathway in the regulation of glucose homeostasis [156].

Phospholipase C (PLC) β is the main effector of the $G_{\alpha q/11}$ subunit [157]. Briefly, PLC β catalyses the cleavage of membrane-bound phosphatidylinositol 4,5-bisphosphate (PIP₂) into IP₃ and DAG. IP₃, as a second messenger, binds to IP₃-receptors found in the membrane of the endoplasmic reticulum (ER) to induce Ca^{2+} -release from the ER. The increase in Ca^{2+} activates calmodulins, which in turn activate enzymes such as Ca^{2+} /calmodulin-dependent kinases (CAMKs). At the end of this pathway (Figure 4.2.3) is the activation of nuclear factor of activated T-cells (NFAT). NFAT plays an important role in the immune response and is involved in the expression of a number of immunologically important genes [151, 158]. DAG diffuses along the plasma membrane where it activates PKC. This results in an activation of the MAPK pathway, which promotes cell growth and plays an important role in the regulation of the cell cycle [159].

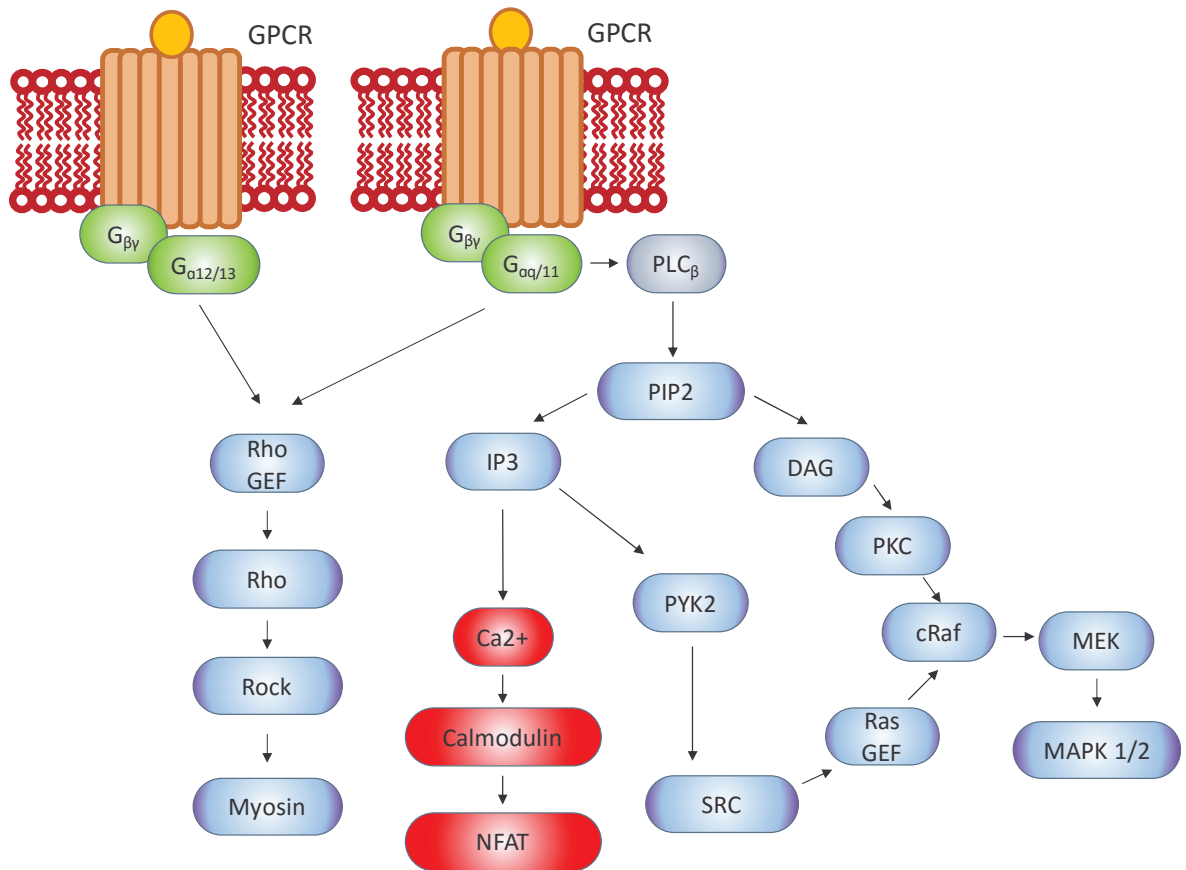


Figure 4.2.3 The $G_{\alpha q/11}$ and $G_{\alpha 12/13}$ pathway

Overview of the $G_{\alpha q/11}$ and $G_{\alpha 12/13}$ mediated intracellular pathways (DAG: Diacylglycerol, GEF: Guanine exchange factor, IP3: Inositol trisphosphate, MAPK (Erk): Extracellular signal-regulated kinase or mitogen activated protein kinase, MEK: mitogen-activated protein kinase kinase, NFAT: Nuclear factor of activated T-cells, PIP2: Phosphatidylinositol 4,5-bisphosphate, PKC: Protein kinase c, PLC: Phospholipase C, PYK2: Protein tyrosine kinase 2, Rho: Small GTPase, Rock: Rho-associated protein kinase, Raf: Serine/threonine-specific protein kinase, Ras: Small GTPase, SRC: Proto-oncogene tyrosine-protein kinase)

RhoGEFs (p115-RhoGEF, PDZ-RhoGEF, and LARG) are the effectors of the $G_{\alpha 12/13}$ pathway. They activate the cytosolic small GTPase, Rho, which activates the Rho-associated protein kinase (ROCK) (Figure 4.2.3) [160]. The activation of ROCK induces the formation of actin stress fibres, which promotes cellular contraction, and increases the formation of stable

actin filaments, leading to the loss of actin monomers and resulting in reduced cell migration [161]. Many GPCRs that couple to $G_{\alpha_{12/13}}$ also couple to $G_{\alpha_q/11}$ [151].

4.2.2 The AT2 receptor

4.2.2.1 Expression pattern of the AT2 receptor

AT2 is strongly expressed in foetal tissue. After birth, the expression of the receptor decreases significantly, indicating that AT2 plays an important role in development and differentiation processes [162, 163]. In addition, the AT2 receptor is involved in the regulation of growth, differentiation and regeneration of nervous tissue [164, 165]. In adults, AT2 has been found in just a few tissues such as brain, adrenal gland, heart, vascular endothelium, kidney, myometrium and ovary [14, 166-169]. However, under pathological conditions, such as vascular injury [170, 171], myocardial infarction [172, 173], congestive heart failure [174], renal failure [175, 176], brain ischemia [177, 178], sciatic or optic nerve transection, an increase of AT2 expression has been observed [179-181].

4.2.2.2 AT2 receptor agonists

Apart from Ang II, Ang III [44] and Ang-(1-9) have also been reported as ligands for the AT2 receptor [47]. In rats, renal cortical interstitial infusion of Ang III has been shown to induce natriuresis. The Ang III-induced natriuresis was abolished by co-infusion with PD123319 (AT2 antagonist, see also Chapter 4.2.2.3) which indicated that this effect was AT2 mediated [182]. In *in vivo* studies, the Ang-(1-9) mediated effects (anti-hypertensive,

anti-fibrotic, anti-hypertrophic) in the hearts of hypertensive rats could also be blocked by PD123319 [183].

The semipeptide CGP42112 is another specific agonist for the AT₂ receptor. Studies with radio labelled CGP42112 could show that the agonist only bound to human myometrium (expressing AT₂), but not to vascular smooth muscle cells (no AT₂ expression). Furthermore, in rat adrenal glomerulosa membranes, expressing AT₁ and AT₂, only binding to AT₂ was observed [14, 184].

In 2004, Wan *et al.* developed an orally accessible, nonpeptidic AT₂ receptor agonist, named Compound 21 (C21) [185]. In *in vivo* studies, C21 improved post-myocardial infarction [186] and provided vasodilatory effects in spontaneously hypertensive rats [187]. The ligand also reduced myocardial fibrosis and vascular injury in hypertensive stroke-prone rats [188]. From this, the interest in AT₂ as a therapeutic target increased. Because of its specificity, C21 is widely used to define *in vivo* function of AT₂ in many physiologic and pathophysiological states [189].

4.2.2.3 AT₂ receptor antagonists

The two non-peptidic antagonists, PD123319 and PD123177, are widely used tools for defining the pharmacology and functions of the AT₂ receptor in several cell types, tissues and *in vivo*. PD123319 is approximately 10,000-fold more selective for AT₂ than AT₁ and more selective than PD123177 [190-192].

More recently, another antagonist has been developed. EMA401 ((S)-2-(diphenylacetyl)-1,2,3,4-tetrahydro-6-methoxy-5-(phenylmethoxy)-3-isoquinolinecarboxylic acid) is a

highly selective, non-peptidic AT₂ receptor antagonist [193]. In a phase-two clinical trial, the compound has been found to be efficient against post-herpetic neuralgia [194, 195]. The compound might be useful to treat chronic neuropathic pain, as EMA401 inhibited capsaicin-evoked calcium influx in human and rodent sensory neuron cultures [196].

Another antagonist of the AT₂ receptor is the small molecule EMA300 (5-[2,2-di(phenyl)acetyl]-4-[(4-methoxy-3-methylphenyl)methyl]-1,4,6,7-tetrahydroimidazo[4,5-c]pyridine-6-carboxylic acid). The small molecule eased neuropathic pain in mice with a chronic constriction injury of the sciatic nerve, by inhibiting p38 MAPK and p44/p42 MAPK activation [193]. Recently, EMA200 and EMA300 were tested in a rat model of dideoxycytidine-induced anti-retroviral toxic neuropathy. Administration of EMA200 and EMA300 induced dose-dependent analgesia in dideoxycytidine rats [197].

4.2.2.4 AT₂ mediated intracellular signalling

The signalling mediated by the AT₂ receptor is unique among the G-protein coupled receptors, as the receptor displays an atypical signal transduction mechanism and G-protein coupling [198]. The signalling mechanisms are diverse, and not fully understood. AT₂ has been reported to couple to G_{αi}, as the pre-treatment of cultured rat neurons with pertussis toxin (PTX), an G_{αi} inhibitor, abolished the Ang II mediated increase in outward K⁺ current [199]. However, focusing on the signalling related to growth inhibition, Na⁺ transport and neuronal activation, the main three pathways activated by AT₂ include 1) protein phosphatases, 2) NO/ cGMP and 3) phospholipase A/ AA-release (Figure 4.2.4).

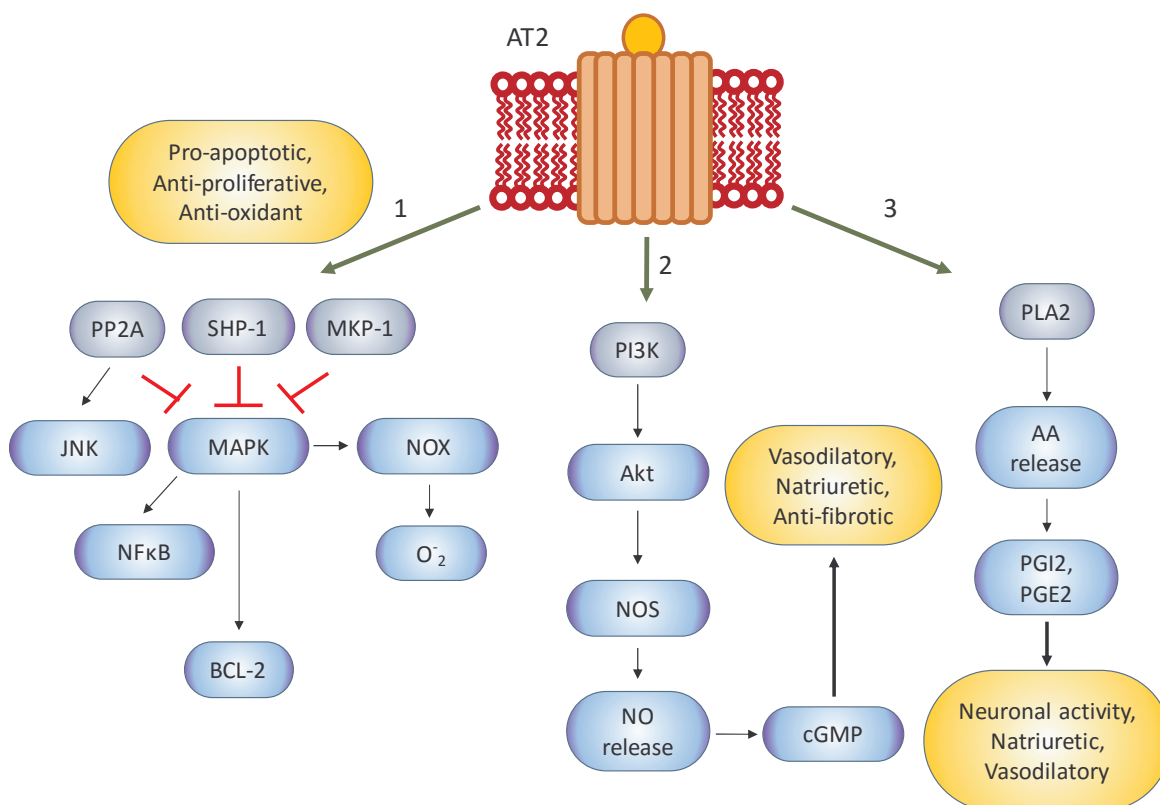


Figure 4.2.4 AT2 mediated intracellular signalling

Major AT2 mediated signalling pathways. (AA: arachidonic acid, Akt: Protein kinase B, BCL-2: B-cell lymphoma 2, cGMP: Cyclic guanosine mono phosphate, JNK: C-Jun n-terminal kinase, MAPK: Mitogen activates protein kinase, MKP-1: MAP kinase phosphatase-1, NFκB: Nuclear factor kappa-light-chain-enhancer of activated B cells, NOS: Nitric oxide synthase, NOX: NADPH oxidase, PGE2: Prostaglandin E2, PGI2: Prostaglandin I2, PI3K: Phosphatidylinositol-4,5-bisphosphate 3-kinase, PLA2: Phospholipase A2, PP2A: Protein phosphatase 2A, SHP-1: Src homology region 2 domain-containing phosphatase-1) [200].

The activation of three main protein phosphatases (PP) has been described: Protein phosphatase 2A (PP2A) [201], the Src homology region 2 domain-containing phosphatase-1 (SHP-1) [202] and the MAP kinase phosphatase-1 (MKP-1) [203]. All three play a role in the dephosphorylation, and consequently the activation, of the MAPK [204]. This has a negative impact on downstream pathways such as NFκB, BCL-2 phosphorylation and activation, and ROS generation, resulting in growth inhibitory, pro-apoptotic and anti-

oxidative effects of AT₂ [165]. For example, in the neuronal cell line PC12W, AT₂-induced apoptosis by ERK inactivation and B-cell lymphoma 2 (BCL-2) dephosphorylation through MKP-1 [203] and SHP-1 activation [202]. In cultured neurons, the AT₂ receptor induces apoptosis through PP2A dependent activation of JNK [205].

An AT₂ mediated increase in NO with a subsequent increase in intracellular cGMP has been observed in cultured rat heart endothelial cells [206], dog coronary microvessels or large coronary arteries [207] and isolated perfused rat renal arteries [208], where it mediates vasorelaxation. Additionally, in the kidney, NO production resulted in natriuresis [209]. In PC12W [210] and NG-108-15 [211], neuronal cell lines, NO production via AT₂ stimulation, mediated differentiation and neuronal outgrowth.

In vivo studies have shown that Ang II activates phospholipase A₂ in an AT₂ dependent manner [212], which leads to AA release and activation of a Na⁺/HCO₃⁻ symporter system, an intracellular pH regulator [213].

4.2.3 The family of the Mas related G-protein coupled receptors

Mas was the first identified member of the Mas-related G-protein coupled receptors (Mrgpr) [214]. Receptors of this family all belong to the class A family. They share a high homology of 30 to 41 % with Mas [215]. The Mrgprs have been found in humans and in rodents [216-220] and they are divided in 9 subfamilies. Mrgpr (Mrg) A, B, C, and H are just found in rodents. The MrgX are specific for primates. Mrg D, E, F and G are expressed in different mammalian species, including rodents and primates. Ten subtypes in the human and about 50 in rodents have been described for the Mrgpr family. However, the

Mrgpr's found in humans are MAS, MRG, MrgD, MrgE, MrgF, MrgG, and MrgX1-MrgX4 [216, 218, 220-222].

4.2.4 The Mas receptor

4.2.4.1 Expression pattern of the Mas receptor

Discovered in 1986 by Young *et al.* [214], the Mas receptor was originally isolated from DNA of a human epidermoid carcinoma cell line [214]. However, there is one main misleading fact about Mas. The term proto-oncogene, which is widely used for the receptor, is wrong. Mas was never found to be amplified in primary tumours, but it can transform cells when excessively overexpressed. The Mas 5'-region is a hotspot for recombination. The rearrangement of the 5'-noncoding sequence, which can occur during transfection has been the reason for the oncogenic activity of the receptor and was the reason for transformation of NIH-3T3 cells [214, 215].

Mas has been found in several tissues. It is highly expressed in the testis [223] and in different regions of the brain, such as hippocampus and cerebral cortex, the olfactory tubercle, the piriform cortex, and the olfactory bulb, neocortex and frontal lobe [224, 225]. Low expression levels has been detected in kidney, heart, lung, spleen, liver, tongue and skeletal muscle [226-228]. Furthermore, Mas can be found in the endothelial layers from several organs [229, 230].

4.2.4.2 Mas receptor agonists

Initially it was believed that Mas is a receptor for Ang II [61]. Jackson *et al.* [61] used transiently transfected *Xenopus* frog oocytes and a stably transfected mammalian cell line to study whether Ang II acts via Mas. Whereas the untransfected oocytes showed a dose-dependent induction of an inward current in response to the Ang I, II, and III, the Mas-transfected cells, responded to Ang II and III with mobilization of intracellular Ca^{2+} . This led to the conclusion that Mas is a functional Ang II receptor.

In 2003, studies with Mas-deficient mice were able to demonstrate that Mas is not the receptor for Ang II, and Ang-(1-7) was then identified as a agonist for Mas [62]. The binding of the heptapeptide was completely abolished in kidneys of mice lacking the Mas receptor. Furthermore, no anti-diuretic effect of Ang-(1-7) could be detected in those animals after acute dehydration. In addition, the vasorelaxing effect in aortic rings isolated from Mas deficient animals was not longer detectable. Contrary, transfection of COS cells with the Mas receptor induced AA release after Ang-(1-7) administration [62].

However, Ang-(1-7) is not the only agonist for Mas. Ang II and Ang IV have been shown to activate the Mas receptor. Both peptides induced AA release in Mas transfected COS cells [65], implicating that there might be more unknown agonists for this receptor. In 2011, angiotensin was identified in the blood of healthy humans and patients with end-stage renal failure [231].

Angiotensin is an Ang II-like octapeptide with the sequence Pro-Glu-Val-Tyr-Ile-His-Pro-Phe. The similarity to the sequence of Ang II raised the hypothesis that angiotensin may be derived from Ang II, but no evidence was found [231]. Angiotensin alone had no vasorelaxant effect on rat aortic rings, but was able to antagonise the vasoconstriction

mediated by Ang II. Furthermore, Ang II had no significant effect on the binding of CY3 labelled angiotensin to mouse microvascular endothelial cells, indicating AT1 and AT2 are not the receptors. This study could show that those effects are Mas mediated, as angiotensin had a significant vasodilatory effect in wild-type mice, but not in Mas receptor-deficient mice, [231].

Initially AVE0991, a non-peptidic agonist for Mas, was developed to mimic Ang-(1-7) for therapeutic applications [232]. AVE0991 has been 10-fold more potent in binding to bovine aortic endothelial cell membranes than the heptapeptide, and 5-fold more potent in inducing NO release from bovine aortic endothelial cells [232]. A number of *in vivo* studies could show that AVE0991 prevents diabetes-induced cardiovascular dysfunction [233], attenuated cardiac hypertrophy [234], protects against post-ischemic heart failure in rats [235], improved inflammation in experimental arthritis [236] and inhibited atherogenesis in apoE-knockout mice [237, 238]. Although these results from animal studies have been very promising, no clinical trial for AVE0991 is currently registered since its development.

4.2.4.3 Mas receptor antagonists

In 1994, Santos *et al.* first characterised a Mas specific antagonist, A779 (Asp-Arg-Val-Tyr-Ile-His-D-Ala), also known as D-Ala⁷-Ang-(1-7). The blocker differs from Ang-(1-7) in amino acid seven. A779 blocked the anti-diuretic effect of Ang-(1-7) in water-loaded rats and abolished the Ang-(1-7) mediated changes in blood pressure. In contrast, A779 did not block Ang II, vasopressin, Ang III, bradykinin, or substance P [239]. Since its characterisation, A779 is a well-accepted and widely used antagonist for Mas.

4.2.4.4 Mas mediated intracellular signalling

The effects mediated by Mas (Chapter 4.1.4) involve a various number of signalling pathways as shown in Figure 4.2.5. The main pathways activated by Ang-(1-7) involve AA release and Ca^{2+} -independent activation of NOS via PI3K. [62, 65, 232].

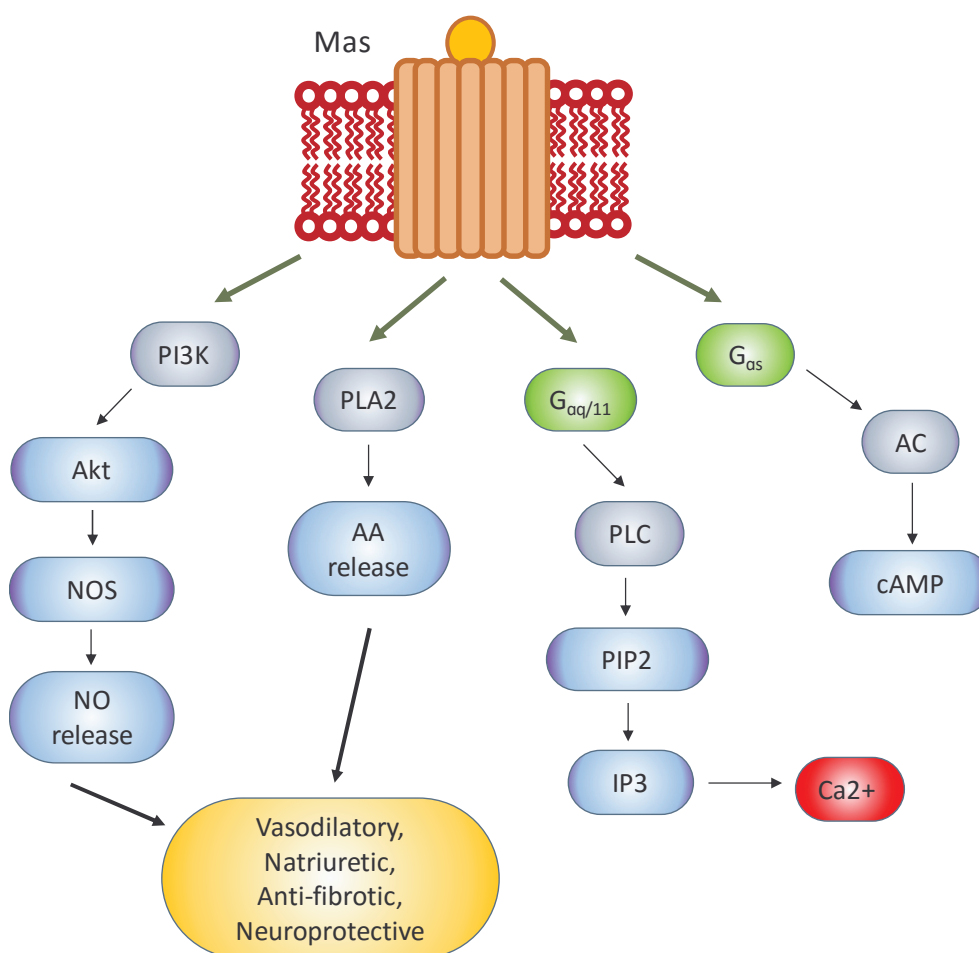


Figure 4.2.5 Intracellular signalling pathways of Mas

Mas mediated signalling pathways. (AA: Arachidonic acid, Akt: Protein Kinase B, IP3: Inositol trisphosphate, NOS: Nitric oxide synthase, NOX: NADPH oxidase, PI3K: Phosphatidylinositol-4,5-bisphosphate 3-kinase, PIP2: Phosphatidylinositol 4,5-bisphosphate, PLA2: Phospholipase A2, PLC: Phospholipase C,).

In Mas-transfected COS and CHO cells, Ang-(1-7) was able to induce AA release [62, 65].

In bovine endothelial cells, the stimulation with the heptapeptide resulted in NOS

activation and NO release [232]. Another study has shown that Mas overexpression in HEK293 cells activated PLC, indicating that Mas couples to $G_{\alpha q/11}$ [240] (Figure 4.2.5). While Ang-(1-7), A779 and AVE0991 failed to initiate the G-protein interaction [232, 241, 242], other researchers reported that mesangial cells and VSMC showed an increase in cAMP and activation of protein kinase A after Ang-(1-7) stimulation [133, 141]. A779 blocked the increase in cAMP in MC, suggesting $G_{\alpha s}$ is involved in the signalling mediated by Mas [141].

4.2.5 The MrgD receptor

4.2.5.1 Expression pattern of the MrgD receptor

MrgD (MrgprD), also known as GPCR45 [219] or TGR7 [243], is mainly expressed in dorsal root ganglia [222]. The Mas-like receptor seems not to be essential for the development and wiring of these neurons, as mice deficient in MrgD showed a normal development and functionality [216, 218, 222].

MrgD has also been found in other tissues, such as arteries, heart, lung, cerebellum, testis, uterus, urinary bladder, skin, trachea, thymus, diaphragm, skeletal muscle, prostate, seminal vesicle, and white and brown adipose tissue [220, 222, 243-245].

MrgD is upregulated in *in vivo* models of neuropathic pain [243]. Furthermore, increased MrgD expression was reported to be associated with inflammatory bowel disease [245], atherosclerotic aorta [246], or lung cancer [247]. In NIH-3T3 cells, stably expressing MrgD, the receptor promoted cell proliferation and anchorage independent growth, indicating a tumour promoting effect [247].

4.2.5.2 MrgD receptor agonists

The first agonist identified for MrgD was β -alanine [243]. MrgD knockout mice showed significantly reduced scratching after drinking β -alanine-infused water, compared to wild-type mice [248]. In addition, growth promoting effects of β -alanine in MrgD transfected NIH-3T3 cells has been reported [247].

Recently, Ala¹-Ang-(1–7), also known as alamandine, was described as a potent agonist of MrgD [42]. The interaction with the receptor seems to be different to the one with β -alanine, as β -alanine does not inhibit the vasodilatory actions of Ala¹-Ang-(1–7) [42]. Ala¹-Ang-(1–7) is a heptapeptide with amino acid sequence Ala–Arg–Val–Tyr–Ile–His–Pro, differing from Ang (1–7) only in the N-terminal alanine instead of aspartate. It was postulated that Ala¹-Ang-(1–7) is generated directly from Ang-(1–7) by the decarboxylation of its aspartate residue or by catalytic hydrolysis of Ang A through ACE2 [42]. Ala¹-Ang-(1–7) plasma levels were increased in patients with renal disease [249]. The beneficial effects of this heptapeptide are similar to those of Ang-(1-7). In aortic rings isolated from mice, Ala¹-Ang-(1–7) induced endothelial-dependent vasorelaxation. This effect was still detectable when using aortic rings isolated from Mas knockout animals, indicating that this effect was Mas independent [42, 250]. Furthermore, Ala¹-Ang-(1–7) can counteract the vasoconstriction induced by its potential precursor Ang A [246]. However, the Ala¹ Ang (1–7) mediated effects could not be blocked with the Mas receptor antagonist A779, but with D-Pro, which can also block the MrgD receptor [246]. Furthermore, Ala¹-Ang-(1–7) induced NO-release in MrgD-transfected cells but not in Mas-transfected cells, confirming that Ala¹-Ang-(1–7) is a natural ligand for MrgD receptor [42, 251].

Additional agonists with lower potency than β -alanine or Ala¹-Ang-(1-7) for MrgD have been described. One compound is the inhibitory neurotransmitter gamma-aminobutyric acid (GABA). GABA weakly stimulates the calcium flux in HEK293 cells expressing human and rat MrgD [243, 252, 253]. β -aminoisobutyric acid, and diethylstilbestrol, a synthetic estrogen hormone, were also reported as novel agonists for MrgD, as they increased calcium flux in MrgD transfected HEK293 cells [253].

4.2.5.3 MrgD receptor antagonists

In 2003, Santos *et al.* initially described the heptapeptide Asp-Arg-Val-Tyr-Ile-His-D-Pro (D-Pro) as a potent Ang-(1-7) antagonist. They demonstrated that the specific binding of ¹²⁵I-labeled Ang-(1-7) to mouse kidney slices was completely abolished by D-Pro. This heptapeptide analog did not block the binding of ¹²⁵I-labeled Ang II to AT1 in receptor-transfected CHO cells or to adrenal medulla, further indicating its specificity as an Ang-(1-7) antagonist [254]. Additionally, they found that D-Pro blocked the vasorelaxation and the anti-diuresis produced by Ang-(1-7) [254]. However, Lautner *et al.* demonstrated that the binding of Ala¹-Ang-(1-7) to MrgD-transfected COS cells was competed by D-Pro, but not by A779. This indicated that D-Pro is not Mas specific but also blocks the MrgD receptor [42].

A more specific antagonist of MrgD is MU-6840. This molecule was obtained as an MrgD antagonist through a high-throughput-screening of a large small chemical library and is a possible anti-cancer compound. It inhibits the spheroid formation in cells expressing MrgD [253]. However, the compound can also be described as inverse agonist. It inhibits

the constitutive and β -alanine-induced activity of MrgD-transfected cells, as it was demonstrated using IP assays [253].

4.2.5.4 MrgD mediated intracellular signalling

As shown in Figure 4.2.6, the signalling of MrgD involves different pathways.

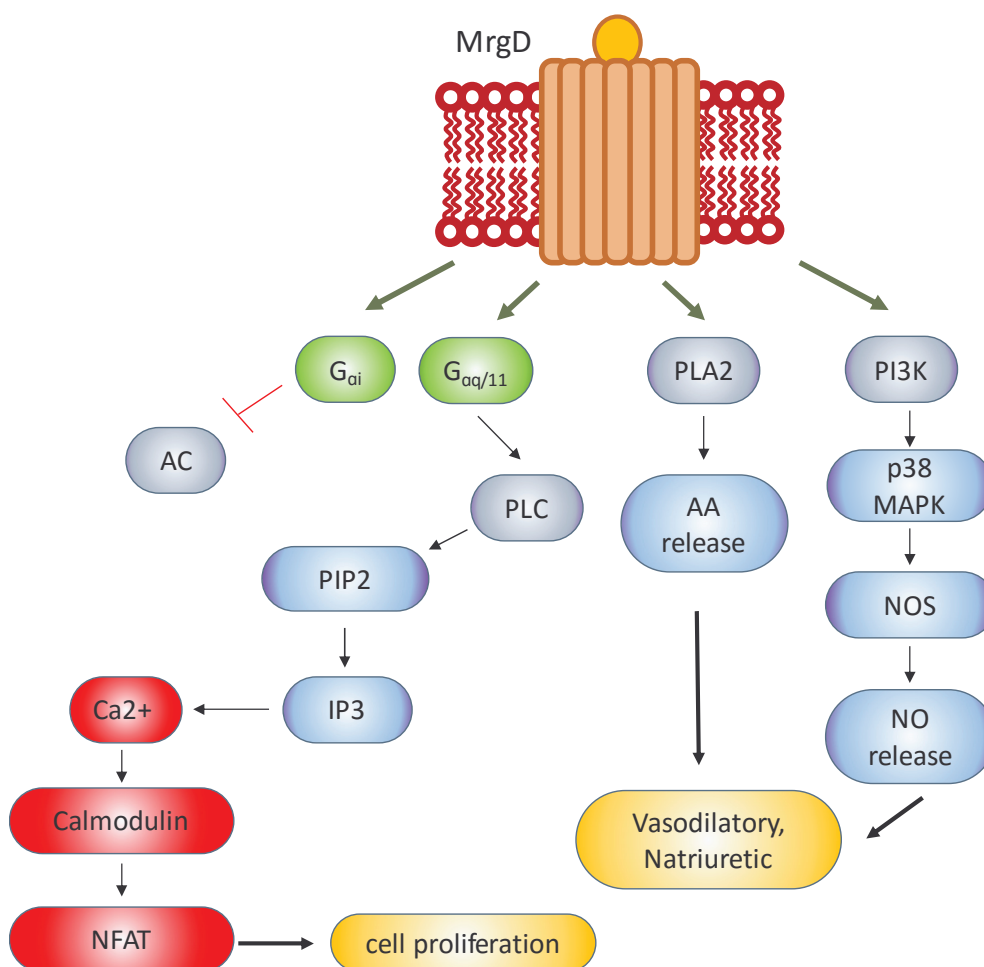


Figure 4.2.6 Intracellular MrgD signaling pathways

MrgD mediated signalling pathways. (AA: arachidonic acid, AC: Adenylate cyclase, IP3: Inositol trisphosphate, p38 MAPK: Mitogen activated protein kinase p38, NOS: Nitric oxide synthase, NOX: NADPH oxidase, PI3K: Phosphatidylinositol-4,5-bisphosphate 3-kinase, PIP2: Phosphatidylinositol 4,5-biphosphate, PLA2: phospholipase A2, PLC: Phospholipase C).

In HEK293 cells transfected with MrgD, a constitutive coupling to $G_{\alpha q}$ and $G_{\alpha i}$ proteins has been reported, as an increased luciferase signal for NFAT and Elk1 was detected [253]. Consequently, the activation of $G_{\alpha q}$ and $G_{\alpha i}$ led to changes of intracellular Ca^{2+} and cAMP levels [243, 249]. In MrgD-transfected COS cells, Ang-(1-7) was able to induce AA release [65]. In isolated adipocytes from rats, Ala¹-Ang-(1-7) activated iNOS expression and NO production via activation of MrgD and p38 MAPK, and decreased the leptin expression and secretion [255].

4.2.6 The constitutive activity of Mas and MrgD

Certain GPCRs, including members of the Mrgpr family, exhibit agonist-independent signal transduction, known as constitutive activity. Constitutive activity of a receptor is the ability to spontaneously produce elevated basal cellular activity, in the absence of a ligand [256]. Previously, Canals *et al.* demonstrated that in HEK293 transfected cells, the Mas receptor exhibits constitutive activity, activating $G_{\alpha q/11}$ followed by PKC signalling without ligand stimulation [240]. Uno *et al.* could demonstrate a constitutive coupling to $G_{\alpha q}$ and $G_{\alpha i}$ proteins using a reporter assay for MrgD receptor transfected HEK293 cells [252, 253]. This inherent activity of the receptor can be manipulated by certain ligands, known as inverse agonists. As already mentioned, the synthetic chemical compound MU-6840 was the first proposed inverse agonist of MrgD, as the compound inhibited spheroid proliferation of MrgD-transfected NIH3T3, which was dependent on basal activity of the receptor [253]. AR244555 and AR305352 were described as inverse agonists of Mas. Using HTRF IP1 assays as readout for $G_{\alpha q/11}$ coupling of Mas, Zhang *et al.* demonstrated that both compounds were able to decrease the IP1 concentrations in HEK cells stably expressing Mas, indicating their function as inverse agonists [257].

4.3 Diabetes mellitus: a pandemic disease

4.3.1 What is diabetes mellitus?

Diabetes mellitus (DM) is a chronic metabolic disease, which is caused by the insufficiency of secretion or action (insulin resistance, see also chapter 4.3.4) of endogenous insulin. Diabetes is a severe public health problem as both the number of cases and the prevalence of diabetes have been increasing over the past few decades [258].

According to the World Health Organization in 2016, about 422 million people suffer from DM worldwide, which equals 8.5 % of the world's population. The number of cases have dramatically increased since 1980, when about 108 million cases were reported (4.7 % of the world's population) [259]. About 90 % of all diagnosed diabetic cases are type 2 (T2DM) [258, 259]. In 2015, about 1.6 million deaths were directly caused by diabetes, which makes DM to the eighth leading cause of death [246]. It is predicted that the number of DM cases will raise to over 600 million cases by 2045, showing that DM is a huge problem in the modern world [260, 261].

Over time, diabetes causes damage to the heart, blood vessels, eyes, kidneys, and nerves. Diabetes is the leading cause of kidney failure [262]. Diabetes increases the risk of stroke and heart attack [263, 264]. The reduced blood flow and nerve damage in the feet increases the chance of foot ulcers, infections, and might lead to limb amputation [265, 266]. Long-term accumulated damage to the small blood vessels in the retina causes diabetic retinopathy, which can result in blindness [267].

Symptoms of hyperglycaemia are frequent urination (polyuria), increased thirst (polydipsia), increased hunger (polyphagia), fatigue, and weight loss. DM can be

associated with other symptoms such as blurred vision, itchiness, peripheral neuropathy, recurrent vaginal infections, and fatigue [268]

4.3.2 Diabetes type 1

In diabetes mellitus type 1 (T1DM), not enough insulin is produced due to the loss of β -cell function. This results in high blood glucose (BG) levels in the body. This form of diabetes normally develops in children and young adults.

About 5–10 % of all diabetes cases are T1DM. The exact number of people affected globally is unknown, but it is estimated that about 80,000 children develop the disease each year [269].

It has to be noted, that T1DM can be associated with depression (12% of the patients) [270]. Coeliac disease affects about 6 % of T1DM [271, 272].

4.3.2.1 What causes type 1 diabetes and how can it be prevented?

The causes of T1DM are not fully understood. Genetic predisposition, environmental triggers or certain chemicals or drugs might be reasons for this type of diabetes [273].

There are more than 50 genes which are associated with T1DM [274]. They can be dominant or recessive, depending on the locus position and combination. For instance, certain variants of the gene IDDM1 (Insulin-dependent (type I) diabetes mellitus) increase the risk for DMT1 [275]. In families with no history of T1DM, the risk of developing this type of diabetes is approximately 0.4%. In the case, that one parent is affected, the risk increases depending if the mother or the father is affected. If the

mother is affected, the risk is about 1% - 4%, and if the father is affected the risk is about 3% to 8%. If both parents are affected the likelihood of the offspring to develop T1DM is about 30% [276].

Thus, studies showed that 50–70 % of identical twins, where one has the disease, the other will not develop it, indicating that genetic factors alone are not a risk factor [277]. In addition to genetic factors, environmental factors can influence the frequency for this type of diabetes. This is also supported by the observation of the different appearance of T1DM among Caucasians, which are living in different areas of Europe [278, 279]. However, further research is required to fully understand possible environmental triggers and also protective factors, such as dietary agents [280], gut microbiota [281] and viral infections [282].

Pancreatitis or tumours (either malignant or benign) can also cause a loss of insulin production [269]. Furthermore, drugs, which selectively destroy β -cells, can also cause T1DM. One of those drugs is the anti-neoplastic agent Streptozotocin (STZ, Zanosar). STZ is used to treat metastatic pancreatic cancer if the cancer cannot be removed by surgery [283]. STZ is widely used in research for inducing a preclinical model of DMT1 in rodents [284]. Currently DMT1 cannot be prevented, as the factors relevant for the development of the disease have not been finally determined [269].

4.3.3 Diabetes type 2

T2DM is characterised by insufficient insulin production as a result of insulin resistance. The inability or reduced response to insulin, mainly in muscles, liver, and fat tissue is called insulin resistance [268]. The glucose uptake is disrupted and blood glucose levels

elevate. Insulin normally suppresses glucose release and increases the glucose uptake. However, in the case of insulin resistance, the liver releases glucose into the blood. An increased breakdown of lipids within fat cells is also associated with T2DM [285]. Furthermore, high blood glucagon levels, increased salt and water retention by the kidneys, and dysregulation of the metabolism by the central nervous system are characteristics of T2DM [268]. As a long term consequence of insulin resistance, patient develop a disturbance of insulin secretion by pancreatic β -cells [268].

4.3.3.1 What causes type 2 diabetes and how can it be prevented?

T2DM is caused by a combination of different factors. An unhealthy lifestyle can significantly increase the risk of developing T2DM. Factors include an unhealthy diet resulting in obesity [286, 287], lack of physical activity, smoking [288, 289], stress, and lack of sleep [290].

The main cause of T2DM is obesity. Excess body fat is associated with 60–80 % of T2DM cases in European countries [287]. Sugar-sweetened drinks [291, 292], saturated fats and trans fatty acids are also increasing the risk of T2DM [293]. Only 7 % of T2DM cases seem to be caused by a lacking exercise [294].

More than 36 genes were identified which may contribute to the risk of T2DM. Most of the genes are linked to β -cell function. However, only 10 % of the T2DM cases can be linked to genetic predisposition [295].

In addition, some medications like glucocorticoids, thiazides, beta-blockers, atypical antipsychotics, and statins, can lead to a predisposition to T2DM [296, 297]. Other factors

like gestational diabetes [23], Cushing's syndrome, hyperthyroidism, pheochromocytoma, certain cancers (such as glucagonomas) [298] and testosterone deficiency are also associated with the development of T2DM [299].

The best way to prevent T2DM is a healthy lifestyle, a healthy diet, regular exercise and weight reduction lowers the risk of developing a T2DM [300, 301].

4.3.4 Insulin resistance and hyperinsulinemia

Insulin resistance is a pathological condition in which cells (e.g muscle cells) fail to respond normally to the insulin. The most common type of insulin resistance is associated with being overweight or obese, a condition known as the metabolic syndrome [302]. As the cells do not respond to insulin anymore, blood sugar levels keep increasing [303]. Under normal conditions, insulin triggers the transport of glucose into body cells, where it is used for energy production, causing the decrease of blood sugar levels. Furthermore, it inhibits the lipolysis (using fat as energy source). However, during the state of insulin resistance, even in the presence of insulin, excess glucose is not sufficiently transported into the cells, causing an increase in the level of blood sugar [303]. Insulin resistance is often associated with T2DM [302].

As a compensation, β -cells in the pancreas subsequently increase their production of insulin, which contributes to an increase of plasma insulin levels resulting in hyperinsulinemia [304]. The constant exposure to high insulin levels further triggers insulin resistance, resulting in an endless circle of both conditions. High levels of insulin lead to an increase in inflammation and are associated with hypertension and a higher risk for cancer [304, 305].

Therefore, it is important to reduce insulin resistance in T2DM patients rather than further increase hyperinsulinemia by just using insulin therapy.

4.3.5 Complications associated with hyperglycaemia

In general, the harmful effects of hyperglycaemia can be distinguished into macrovascular complications (such as coronary artery disease, peripheral arterial disease, and stroke) and microvascular complications (such as diabetic nephropathy, neuropathy, and retinopathy) [306].

4.3.5.1 Macrovascular complications

The main reason for macrovascular complications is atherosclerosis [306]. In the peripheral or coronary vascular system, atherosclerosis is caused by chronic inflammation and injury of the arterial walls. Briefly, oxidized lipids from low-density lipoprotein (LDL) particles accumulate in the endothelial wall of arteries, causing chronic inflammation, resulting in smooth muscle cell proliferation and collagen accumulation in the arterial walls. The end result is a lipid-rich atherosclerotic lesion with a fibrotic cap, which causes a narrowing of the arterial walls. It should be mentioned that Ang II may promote the oxidation of LDL [307].

Other macrovascular events include increased coagulability (due to impaired NO generation, increased free radical formation in platelets, and altered calcium regulation) and impaired fibrinolysis (increase of plasminogen activator inhibitor type 1), which further increases the risk of vascular occlusion and cardiovascular events and diseases in patients with diabetes [308].

4.3.5.2 Microvascular complications

Microvascular complications include diabetic retinopathy, nephropathy and neuropathy [306].

Diabetic retinopathy occurs due to the damage of small blood vessels and neurons in the retina, which results in impaired visual function and dysfunction of the blood-retinal barrier (endothelial dysfunction) [309]. Briefly, the narrowing of the retinal arteries (reduced retinal blood flow), leads to a dysfunction of the neurons of the inner retina, this is later followed by changes in the function of the outer retina [310]. In late stages, the capillaries degenerate, which causes a loss of blood flow, progressive ischemia, and microscopic aneurysms, leading to further dysfunction and degeneration of the neurons and glial cells of the retina [309, 310].

The mechanisms causing diabetic nephropathy are the same as in diabetic retinopathy. The damage to the small blood vessels due to high blood sugar levels, results in impaired blood flow and endothelial dysfunction. As a result, the glomeruli, which are responsible for selective filtration of blood entering the kidney, are damaged and allows proteins in the blood leaking through, leading to proteinuria and chronic loss of kidney function [306, 311].

Diabetic neuropathy also occurs as a result of the damage of small blood vessels resulting in neuronal ischemia. This nerve damage cause several symptoms, as it can affect all organs and systems in the body [306].

4.3.6 Treatment of diabetes type 1 and 2

In general, the treatment of diabetes focuses on lowering BG levels, near to the normal range (80–140 mg/dl (4.4–7.8 mmol/l), and keeping HbA1c (amount of glycated haemoglobin) at around 7 % [312, 313].

4.3.6.1 Management of type 1 diabetes

The administration of insulin, either via subcutaneous injection or via insulin pump, is necessary for all patients. Thus, a healthy diet and exercise do not help to normalise the blood glucose levels, but they are still an important part of the therapy [314]. In some cases, a pancreas transplant can restore proper glucose regulation. However, the surgery and accompanying immunosuppression required may be more dangerous than continued insulin replacement therapy [315]. Furthermore, an islet (β -cell) transplantation may be an option for some people with T1DM that is not well controlled with insulin [316]. Difficulties include finding compatible donors, survival of the islets, and the side effects from the medications used to prevent rejection [317]. The limited options for the management of T1DM clarifies the need for alternative treatment options, which are less invasive and have more beneficial long-term effects. One possibility would be to restore or to improve the function of the remaining β -cells.

4.3.6.2 Managing type 2 diabetes

A long-term change in life style and diet is the main way to manage T2DM in the early stage. A proper diet and exercise decrease HbA1c and improve insulin sensitivity and can completely reverse the hyperglycaemic status [286, 318].

Before the administration of insulin becomes necessary, there are various oral drugs available. Metformin is the first line treatment for T2DM which mainly is used in overweight patients. It should not be used in patients with severe kidney or liver problems [319]. Other classes of medications are sulfonylureas, thiazolidinediones, dipeptidyl peptidase-4 inhibitors, sodium–glucose cotransporter 2 (SGLT2) inhibitors, and glucagon-like peptide-1 analogues [320].

Also, the treatment of cardiovascular risk factors such as hypertension, high cholesterol, and microalbuminuria, improves the long term perspective of a patients with T2DM [321]. Interestingly, in a large-scale clinical trial (EMPA-REG OUTCOME trial), SGLT2 inhibitors significantly reduced the mortality of T2DM patients with high risk of cardiovascular events, indicating a significant connection between DM and the cardiovascular system [322]. Furthermore, blood pressure lowering medications such as ACE inhibitors and angiotensin receptor blockers (ARBs) appear to be renoprotective, probably by decreasing intraglomerular pressure. These drugs are highly recommended as a pharmacological first-line treatment of microalbuminuria, even in patients without hypertension [323]. Additionally, the blockade of the RAS using either an ACE inhibitor or ARBs reduced cardiovascular events in patients with diabetes more effective, compared to other antihypertensive agents [306].

4.3.7 The connection between diabetes mellitus and the renin-angiotensin system

The association of DM with retinopathy, nephropathy, hypertension and cardiovascular diseases, strongly implicates that the RAS plays an important role in the progression and development of DM, as it is also a well-known driver of such diseases [324].

The increased blood glucose levels in DM can activate the RAS through several mechanisms. Hyperglycaemia induces the formation of Nepsilon-(carboxymethyl)-lysine (CML) [325, 326]. Studies have found that CML leads to the activation of iNOS, which then induces NO production in rat glomerular mesangial cells [327]. The released NO leads to a release of renin through the upregulation of cGMP/cAMP-mediated renin exocytosis, which results in an over activation of the RAS [328]. In addition, the accumulation of succinate as a result of high blood glucose levels seems to activate the RAS. Succinate initiates an intracellular signalling pathway in cells from the macula or endothelial cells of the afferent arteriole, resulting in the elevation of intracellular calcium levels, production of NO and activation of prostaglandin E₂ (PGE₂). This induces renin secretion via the pathway shown in Figure 4.3.1 [329-331].

Studies in diabetic rats found that high blood glucose levels increase the expression of pro-renin receptors on cellular surfaces. This also results in activating RAS [332]. The activation of the RAS then results in an upregulation of Ang II, which leads to various physiological pathways. Ang II induces oxidative stress [333, 334], endothelial dysfunction, inflammation and proliferation [335], which may lead to cardiac problems [336], diabetic retinopathy [337] and nephropathy [338].

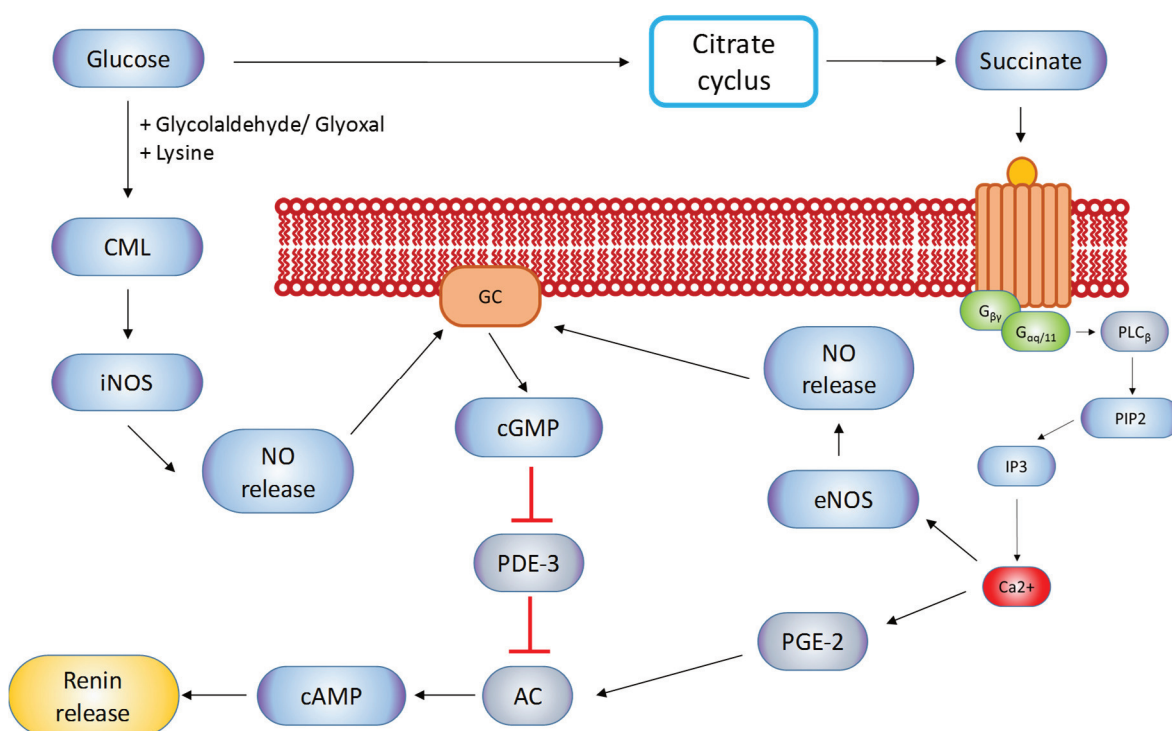


Figure 4.3.1 Mechanism of renin release by high levels of blood glucose

This diagram shows the pathways involved in the release of renin caused by hyperglycaemic conditions. (AC: Adenylate cyclase, cAMP: Cyclic adenosine monophosphate, cGMP: Cyclic guanosine monophosphate, CML: Nε-(carboxymethyl)-lysine, eNOS: Endothelial nitric oxide synthase, GC: Guanylate cyclase, iNOS: Inducible nitric oxide synthase, IP3: Inositol trisphosphate, NO: Nitric oxide, PDE-3: Phosphodiesterase 3, PGE-2: Prostaglandin E2, PIP2: Phosphatidylinositol 4,5-bisphosphate, PLCβ: Phospholipase C beta,)

Furthermore, by interfering with the insulin receptor signalling, Ang II causes insulin resistance [339]. In *in vivo* studies, using rat heart, Ang II was able to stimulate the tyrosine phosphorylation of the insulin receptor substrates (IRS) 1 and 2, which resulted in an inhibition of PI3K, instead of activation, preventing normal insulin signalling [339].

Consequently, the blockage of the ACE/Ang II/ AT1 axis in DM patients showed beneficial and protective effects [340]. ACE inhibitors or AT1 blockers are used to treat hypertension, in DM patients. The use of those inhibitors and blockers significantly reduce the number of patients with vascular complications [341, 342]. They seem to increase the insulin sensitivity [343], and improve the glucose transport [344]. Furthermore, protective effects on pancreatic islets were observed. It could be shown that ACE inhibitors protected islets against glucotoxicity and decreased oxidative stress [345]. Additionally, they seem to be very useful in the prevention and treatment of diabetic retinopathy and nephropathy [346, 347].

The ACE2/Ang-(1-7)/Mas axis counteracts Ang II mediated effects, this part of the RAS also is a useful tool and target for the treatment of DM and associated symptoms. Recent studies in rat and mice models reported beneficial effects of Ang-(1–7) on glucose homoeostasis. These effects were associated with the improvement of insulin sensitivity and glucose uptake in peripheral tissues (muscle, fat) [73, 125, 348, 349]. In a study using a rat model of inducible T2DM, the oral administration of Ang-(1–7) reduced the hyperglycemia [348]. Another study showed that the chronic administration of Ang-(1–7) in rats with metabolic syndrome resulted in the normalisation of insulin sensitivity and insulin mediated signal transduction of skeletal muscle, liver, and adipose tissue. Furthermore, a normalisation of blood glucose levels and serum triglyceride levels was reported [73]. A third study demonstrated that Ang-(1–7) administration to primary epididymal adipocytes of mice and to 3T3-L1 adipocytes resulted in an improved glucose uptake. This was associated with reduced production of ROS due to a reduction in the expression of a NOX subunit, mediated by Ang-(1-7) [349]. In transgenic rats with Ang-(1-7) overexpression, an increased glucose uptake in adipocytes, an improved insulin

sensitivity and a reduction of cholesterol and triglycerides in plasma has been observed [125]. Furthermore, Ang-(1–7) was able protect the β -cell function of rats with STZ-induced diabetes mellitus. The heptapeptide prevented the shrinkage of the cytoplasm and condensation of nuclear chromatin and significantly improved the insulin production of pancreatic β -cells [350].

In vivo studies in diabetic mice and rats demonstrated that the intraocular administration of ACE2 or Ang-(1-7) significantly reduced the diabetes-induced retinal vascular leakage, acellular capillaries, infiltrating inflammatory cells and oxidative damage in both [351]. Furthermore, Ang-(1-7) ameliorated diabetic renal injury in STZ-induced DM in rats by reducing oxidative stress and inhibiting TGF β 1 and vascular endothelial growth factor (VEGF)-mediated pathways [352].

Taken together, in addition to the blockage of the ACE/ Ang II/ AT1 axis, the stimulation of the ACE2/ Ang-(1-7)/ Mas axis might play an important role in the treatment of DM related symptoms, such as diabetic nephropathy, hypertension and retinopathy.

5 Aim of the study

Over the past years, the number of publications on Ang-(1-7) and its beneficial effects significantly increased. Despite this, the underlying intracellular mechanisms remain unclear. Studies have shown that Mas is associated with Ang-(1-7)-stimulated signalling [62]. Whereas Ala¹-Ang-(1-7), a peptide very similar to Ang-(1-7), has been associated with MrgD [42]. Furthermore, the Mas and MrgD receptors showed a significant increase in AA release in response to the Ang-(1-7) [65], indicating that other receptors might be involved in the Ang-(1-7) mediated signalling. Therefore, the first aims of the first study were:

- 1) Identification of intracellular pathways activated by Ang-(1-7)
- 2) Confirmation of Mas as a functional receptor for the heptapeptide
- 3) Identification of other receptors involved in Ang-(1-7)-mediated signalling
- 4) Investigation of the receptor fingerprint of Ala¹-Ang-(1-7)

Over the past decades, there has been an increasing interest in the association between the RAS and certain diseases like diabetes mellitus, neurodegenerative diseases and. With that, the interest in Ang-(1-7) as therapeutic target is now huge. Diabetes Mellitus is just one example. Initial work could show that Ang-(1-7) had beneficial effects on glucose metabolism and islet function [125, 348, 350].

In order to evaluate whether Ang-(1-7) is a promising tool for the treatment of Diabetes Mellitus, *ex vivo* and *in vivo* experiments will be used for:

- 1) Identification of intracellular pathways activated by Ang-(1-7) in β -cells
- 2) Identification of receptors involved in Ang-(1-7)-mediated signalling

- 3) *In vivo* investigation of the Ang-(1-7) mediated effect on blood glucose in STZ induced diabetic animals

6 Results

6.1 The G protein-coupled receptor MrgD is a receptor for angiotensin-(1-7) involving adenylyl cyclase, cAMP, and phosphokinase A

Anja Tetzner, MSc^{1, 2*}; Kinga Gebolys, PhD^{1*}; Christian Meinert, PhD^{1,3}; Sabine Klein, PhD⁴; Anja Uhlich, MSc¹; Jonel Trebicka, MD, PhD⁴; Óscar Villacañas Pérez, PhD⁵; Thomas Walther, PhD^{1,2}

¹Dept. Pharmacology and Therapeutics, School of Medicine and School of Pharmacy, University College Cork (UCC), Cork, Ireland;

²Departments Obstetrics and Pediatric Surgery, University of Leipzig, Leipzig, Germany;

³Inst. Experimental and Clinical Pharmacology and Toxicology, Medical Faculty Mannheim - University Heidelberg, Mannheim, Germany;

⁴Internal Medicine I, University of Bonn, Bonn, Germany;

⁵Intelligent Pharma, Barcelona, Spain.

*Both authors contributed equally to this work

Address for correspondence: Prof. Thomas Walther, Department Pharmacology & Therapeutics, Western Gateway Building, Western Road, University College Cork, Cork, Ireland; Phone: +353-21-420-5973, fax: +353-21-4205471, E-mail: t.walther@ucc.ie

Published in *Hypertension*, 2016 July, 68(1):185-94.

Hypothesis

Ang-(1-7) does not stimulate AT₂, but acts through the Mas receptor. Furthermore, other receptors from the Mas-like family might be a target for the heptapeptide.

Aim of the study

The aim of the study was to identify a second messenger stimulated by Ang-(1-7) and to use this as a readout to proof that Mas is a functional receptor for the heptapeptide. Additionally, the new method was used to identify other receptors for Ang-(1-7) by working with primary and receptor-transfected cells.

Author contributions

Anja Tetzner performed experiments for Figure 1-5, developed the images for the figures and worked on the manuscript.

Kinga Gebolys performed experiments for Figure 1-5 and worked on the manuscript.

Christian Meinert performed the experiments for Figure 1C and 1D.

Sabine Klein performed the experiment for Figure 5E

Anja Uhlich performed part of the experiments for Figure 1D

Óscar Villacañas analysed the ligand-protein interactions and supervised the modelling part.

Thomas Walther initiated the work, coordinated the experiments, advised, drafted the main text body, and finalized the manuscript.

Abstract

Angiotensin (Ang)-(1-7) has cardiovascular protective effects and is the opponent of the often detrimental Ang II within the renin-angiotensin system. Although it is well-accepted that the G-protein coupled receptor Mas is a receptor for the heptapeptide, the lack in knowing initial signalling molecules stimulated by Ang-(1-7) prevented definitive characterisation of ligand/receptor pharmacology as well as identification of further hypothesized receptors for the heptapeptide. The study aimed to identify a second messenger stimulated by Ang-(1-7) allowing confirmation as well as discovery of the heptapeptide's receptors.

Ang-(1-7) elevates cAMP concentration in primary cells such as endothelial or mesangial cells. Using cAMP as readout in receptor-transfected HEK293 cells, we provided pharmacological proof that Mas is a functional receptor for Ang-(1-7). Moreover, we identified the G-protein coupled receptor MrgD as a second receptor for Ang-(1-7). Consequently, the heptapeptide failed to increase cAMP concentration in primary mesangial cells with genetic deficiency in both Mas and MrgD. Mice deficient in MrgD showed an impaired hemodynamic response following Ang-(1-7) administration. Furthermore, we excluded the Ang II type 2 receptor AT2 as a receptor for the heptapeptide but discovered that the AT2 blocker PD123319 can also block Mas and MrgD receptors.

Our results lead to an expansion and partial revision of the renin-angiotensin system, by identifying a second receptor for Ang-(1-7), by excluding AT2 as a receptor for the heptapeptide, and by enforcing the revisit of such publications which concluded AT2 function by only using PD123319.

Keywords: Angiotensin-(1-7), AT₂ receptor, Mas receptor, MrgD receptor, renin-angiotensin system

Introduction

The renin-angiotensin system (RAS) is an important regulator of arterial blood pressure, electrolyte homeostasis, and water and sodium intake [353], but is also involved in other processes like tissue regeneration [354]. The RAS is a complex cascade in which precursor peptides are processed by specific enzymes to their active forms. Angiotensinogen is metabolised by renin to the biologically inactive decapeptide angiotensin (Ang) I that is then cleaved by the Ang converting enzyme (ACE) to Ang II, the primary active peptide of the RAS.

A homologue of ACE, termed ACE2, cleaves a single amino acid from the octapeptide Ang II, which produces Ang-(1-7) [58]. Since Ang-(1-7) can counter-regulate adverse effects of AngII, [58] the interest in this peptide significantly increased over the last decade [355].

In previous work, we identified the G protein-coupled receptor Mas to be associated with Ang-(1-7)-induced signalling, since e.g. genetic deletion of Mas abolishes the binding of Ang-(1-7) to mouse kidney [62]. This binding could be also blocked by co-treatment with D-Ala⁷-Ang-(1-7), also named A779, a specific Ang-(1-7) antagonist [62].

There is still intense discussion about the interaction of Ang-(1-7) with the Ang II type 2 (AT₂) receptor. For example, Walters and colleagues described the vaso-depressing effect of Ang-(1-7) in AT₁ blocker-treated rats can be markedly blocked by PD123319, an AT₂ blocker, suggesting that Ang-(1-7) acts via the AT₂ receptor [356].

Furthermore, we and others described that D-Pro⁷-Ang-(1-7) (D-Pro) blocks Ang-(1-7) effects [254, 357]. Interestingly, the two distinct Ang-(1-7) receptor blockers, A779 and D-Pro, reversed the normalising effects of Ang-(1-7) on systemic and pulmonary hemodynamics in a model of acute lung injury, but only D-Pro blocked the protection from lung oedema and protein leak, whereas A779 restored the infiltration of neutrophils indicating that Ang-(1-7) may act via distinct receptors [357].

Therefore, we aimed to identify and quantify a second messenger stimulated by Ang-(1-7) allowing pharmacological confirmation of Mas as a functional heptapeptide receptor, to understand the postulated interaction between AT₂ and Ang-(1-7), and to discover the hypothetical second receptor, by working with primary and receptor-transfected cells and *in vivo* approaches.

Methods

Most of the techniques have been previously described in detail by our group including culture of primary cells [358] and culture and transfection of HEK-293 cells [65]. A detailed description of techniques, where there is no reference by our group, is provided including cAMP measurement, quantification of PKA activity and CREB phosphorylation, and measurement of acute hemodynamic effects.

Mice deficient in Mas and MrgD (double knockout) have been generated through breeding of single Mas [120] and MrgD [359] (strain #36050, [B6.129S1-Mrgprd^{tm5Mjz}/Mmnc](#), The Mutant Mouse Regional Resource Center 8U42OD010924-13, Chapel Hill, NC, USA) knockouts in the animal facilities at UCC, Ireland.

Chemicals and reagents

Angiotensin (Ang)-(1-7), D-Ala⁷-Ang-(1-7), D-Pro⁷-Ang-(1-7) were from Biosynthan (Berlin, Germany). Adrenaline, Forskolin, HOE 140 (Icatibant), IBMX, isoproterenol, RPMI1640, trypsin/EDTA, PMSF, protease inhibitor cocktail, phosphatase inhibitor cocktail were purchased from Sigma Aldrich (St. Louise, Missouri, USA). DMEM was purchased from BioScience (Dun Laoghaire, Dublin, Ireland). Fetal Bovine Serum (FBS) was purchased from GIBCO (Life Technologies, Carlsbad, California, USA). L-NAME was from Cayman Chemical Company (Ann Arbor, Michigan, USA). PD123319 was from Parke-Davis Pharmaceutical Research (Detroit, Michigan, USA). Transfection reagent was purchased from Qiagen (Venlo, Limburg, Netherlands).

Cell culture conditions, transfection and stimulation

Human embryonic kidney (HEK-293) cells were cultured in DMEM medium supplemented with FBS (10%), HEPES buffer (1%), sodium pyruvate (1%), and L-glutamine (1%) and maintained under standard conditions (5% CO₂, 95% humidity and 37°C). Cells were cultured in 75 cm²-tissue culture flasks and seeded in 48-well plates at density of 75,000 cells per well. The next day, HEK-293 cells were transfected using transient transfection procedure following manufacturer's instructions. Briefly, 150ng of pcDNA3.1 or a combination of 50ng of pcDNA3.1 and 100ng of Mas, MrgD, AT2, or Mrg [65] were mixed with serum-free medium and PolyFect transfection reagent. After 10min incubation at room temperature which allowed the complex formation, the medium containing serum and other supplements was added and the total volume was transferred into appropriate wells of 48-well plate. The cells were incubated for 16-20h. The next day, the medium

was replaced by serum-free medium 1h before stimulation. After stimulated with A779, D-Pro, IBMX, HOE 140, L-NAME, PD123319, forskolin or IBMX (all 10^{-6} M) for 10min, the solvent, Ang-(1-7) or isoproterenol (all 10^{-7} M) were added for 15min. Then, the cells were lysed by adding 180 μ l/well 0.1N hydrochloric acid with 0.1% Triton X-100, and the lysates were stored at -80°C until further use. The protein concentration was determined using Pierce BCA Protein Assay Kit according to the manufacturer's protocol (Thermo Fisher Scientific, Waltham, Massachusetts, USA).

Isolation and culture of primary cells and their stimulation

Primary aortic smooth muscle cells (VSMC) were isolated from the thoracic aortas of 6 to 8-week old male C57/BL6 mice and cultured as described previously [358]. Kidney mesangial cells (MC) were isolated from 10 to 12-week old female mice deficient in Mas [120], MrgD [359] (strain #36050, B6.129S1-*Mrgprd*^{tm5Mjz}/Mmnc, The Mutant Mouse Regional Resource Center 8U42OD010924-13, MMRRC, Chapel Hill, North Caroline, USA) or in both (generated through cross-breeding of both single knocks in the animal facilities at UCC, Cork, Ireland) and from their age- and gender-matched C57/BL6 control according to the protocol previously described.[358] VSMC were used between passage 2 and 3 whereas MC were used at passage 2. Cardiac fibroblasts (CFB) were isolated from ventricles of adult male C57/BL6 mice as described previously [360]. Primary human dermal microvascular endothelial cells (HDMEC) were purchased from European Collection of Cell Cultures (Salisbury, UK). Primary human umbilical vein endothelial cells (HUVEC) were purchased from LONZA BioResearch (Basel, Switzerland). Mouse endothelial cells from cerebral cortex, bEnd.3, were a gift from Dr. Siems from FMP

(Forschungsinstitut fuer Molekulare Pharmakologie, Berlin, Germany). All primary cells were cultured in 75cm² tissue culture flasks and seeded for cAMP assay in 24-well plates at density of 75,000 cells per well. For protein isolation, cells were cultured in 50mm dishes until 80% confluence. The stimulation with Ang-(1-7) or blockers was carried out as described above. For the test of the adenylyl cyclase inhibitor (SQ22536), cells were pre-stimulated with 2x10⁻⁶M for 15min, followed by stimulation with Ang-(1-7) at 10⁻⁷M for 15min.

Measurement of cAMP in cell lysates

cAMP concentration in cell lysates was determined using Direct cAMP ELISA kit (Enzo Life Sciences Ltd., Exeter, United Kingdom). Briefly, wells of 96-well plate (Goat Anti-Rabbit IgG pre-coated) were neutralized with 50µl of Neutralizing Reagent. Next, 100µl of acetylated cAMP standard or cell lysate was added, followed by 50µl of blue cAMP-Alkaline Phosphatase Conjugate and 50µl of yellow EIA Rabbit Anti-cAMP antibody. The plate was then incubated on a shaker (~ 400rpm) at room temperature for 2h. Next, the wells were aspirated and rinsed three times with Wash Buffer (1:10, Tris buffered saline containing detergents and sodium azide in deionized water). After the final wash, the plate was tapped against clean paper towel to remove any remaining Wash Buffer. To each well 200µl p-Nitrophenyl Phosphate Substrate Solution was added, and the plate was incubated for 1h at room temperature. The enzymatic reaction was stopped by adding 50µl of Stop Solution, and the absorbance at 405nm was measured immediately. The cAMP concentration was determined from non-linear standard curve using GraphPad Prism 5.0 software.

Western blot analyses

Cells were lysed in RIPA buffer containing protease and phosphatase inhibitor cocktails (Sigma, St. Louis, MO, USA). Protein quantification was measured with Pierce BCA Protein Assay Kit according to the manufacturer's protocol. Twenty five μ g protein were separated on 10% SDS-polyacrylamide gels and transferred to Immobilon®-P PVDF membrane (Merck KGaA Darmstadt, Germany) using a Semi Dry Blotter PEGASUS (PHASE Gesell. für Phorese, Analytik und Separation mbH, Luebeck, Germany). After blocking with 5% dry milk powder in TBS-T buffer for 1h, the PVDF membrane was incubated with the primary antibodies: CREB, pCREB, (1:1000 dilution in 5% BSA/TBS-T) purchased from Cell Signaling Technology (Danvers, MA, USA) or the anti-GAPDH (1:5000 in 5% milk/TBS-T) from Sigma Aldrich (St. Louise, Missouri, USA), at 4°C overnight. After three washing steps with TBS-T buffer, blots were incubated with the appropriate horseradish peroxidase (HRP)-conjugated secondary antibodies: anti-rabbit IgG in the dilution of 1:2000 in 5% milk/TBS-T (Cell Signaling Technology) or 1:1000 in 5% milk/TBS-T (Sigma Aldrich) at room temperature for 2h. The membranes were developed employing the enhanced chemiluminescence (ECL)-based system (Roche Holding AG, Basel, Switzerland). Densitometric evaluation was performed with ImageJ software (National Institute of Health, USA).

Protein Kinase A activity assay

The measurement of Protein Kinase A (PKA) activity was performed using the PKA Colorimetric Activity Kit (Arbor Assays Headquarters, Ann Arbor, Michigan, USA) following manufacturer's instruction. Briefly, HEK293 cells (75,000 per well) were seeded into 48-

well plates. On the next day, cells were transiently transfected using PolyFect reagent as described above. For HUVEC cells, 24-well plates (75,000 per well) were used and plated overnight. Sixteen to 20h later, the medium containing serum and other supplements was replaced by serum-free medium 1h before stimulation. Then, cells were stimulated with Ang-(1-7) (10^{-7}M , 10^{-8}M or 10^{-9}M) for 15min. For experiments with the adenylyl cyclase inhibitor (SQ22536), the cells were pre-stimulated for 15min with $2 \times 10^{-6}\text{M}$, followed by stimulation with Ang-(1-7) at 10^{-7}M for 15min. Cells were lysed in 50 μL (HEK293) or 100 μL (HUVEC) activated cell Lysis Buffer provided by the kit, containing 1mM PMSF, 1 $\mu\text{L}/\text{mL}$ protease and phosphatase inhibitor cocktail (Sigma) and incubated for 30min on ice. The lysates were transferred to 1.5ml reaction tubes and centrifuged at 10,000rpm at 4°C for 10min. The supernatant was directly used for analysis or stored at -80°C till measurement.

For measurement, all samples were diluted 1:10 in Kinase Assay Buffer provided by the Kit. For the measurement 40 μL of the sample (in triplicates) or standard (in duplicates) were pipetted in to each well. Afterwards, 10 μL of ATP was added to each well and incubated for 1.5h at 30°C on a shaker. Next, the wells were aspirated and rinsed four times with Wash Buffer (1:20 in deionized water). After the final wash, the plate was tapped against clean paper towel to remove any remaining Wash Buffer. Twenty-five μL of the Goat anti-rabbit IgG HRP and 25 μL of the Rabbit Phospho PKA Substrate antibody were added to each well and incubated at room temperature for 60min with shaking. The wells were aspirated again and rinsed four times with Wash Buffer (1:20 in deionized water). After the final wash, the plate was tapped against clean paper towel to remove any remaining Wash Buffer. Next, 100 μL of the TMB Substrate Solution were added to

each well and incubated for 30min at room temperature. Afterwards, 50µL of stop solution was added to each well and the optical density was measured in a plate reader at 450nm. The PKA activity (U/ml) was determined from linear standard curve using linear regression from Excel.

Dual-luciferase reporter assay

For Dual-Luciferase reporter assays, HEK293 cells were seeded into 48-well plates (75,000 cells/well). About 24h later, cells were transiently transfected with 100ng eukaryotic expression vectors of AT1 [65], AT2 or Mrg together with 25ng pNFAT-TA-Luc-, (BD Biosciences; Heidelberg; Germany) or pELK-Luc Reporter Vector (Signosis, Santa Clara, California, USA) luciferase reporter plasmids and 25ng pRL-TK (Promega GmbH, Mannheim, Germany) using the protocol described above. Next day, the medium was replaced by serum-free medium 1h before stimulation. After 6 hours of stimulation with Ang-(1-7) or Ang II (10^{-7} M and 10^{-6} M), cells were lysed with 65µL/well passive lysis buffer provided with the Dual Luciferase Reporter Assay kit (Promega GmbH, Mannheim, Germany) and incubated on a shaker for 15min at room temperature. The activity for Firefly and Renilla Luciferase was measured with Orion L Microplate Luminometer (Berthold Detection Systems GmbH, Pforzheim, Germany) according to the manufactures protocol. Briefly, 30µL of lysed cells where transferred into a white 96-MicroWell plate (Thermo Fisher Scientific, Waltham, Massachusetts, USA), and 100µL of Luciferase Assay Reagent II was added. After quantifying the firefly luminescence, the reaction was quenched by adding 100µL of Stop&Glo reagent and renilla activity was measured. For calculations, the ratio of firefly and renilla luciferase was used.

mRNA isolation and Real-time PCR

Total cellular RNA was isolated using the NucleoSpin RNA isolation kit (MACHEREY-NAGEL, Düren, Germany) according to the manufacturer's protocol. After isolation, 2,000ng total RNA was transcribed into cDNA using the RevertAid H Minus First Strand cDNA Synthesis kit (MBI Fermentas, Hanover, MD, USA) and oligo(dT)18 primer. After synthesis, RNase free water was added to the single cDNA to a final volume of 100µl. Quantification of gene expression was performed by real-time quantitative PCR (RT-PCR) on the StepOne™ Real-Time PCR System (Thermo Fisher Scientific, Waltham, Massachusetts, USA) employing the Platinum SYBR Green qPCR SuperMix-UDG (Invitrogen) and specific primers: Mas forward: CCTCCCATTCTTCGAAGCTGTA, Mas reverse: GCCTGGGTTGC-ATTTTCATCTTT, MrgD forward: TCTACTGGGTGGATGTGAAACG, MrgD reverse: TCATTAGTACACGTGGATGGCG, AT2 forward: GAATTACCCGTGACCAAGTCCT, AT2 reverse: GGAACTCTAAACACACTGCGGA. Real time quantitative PCR amplifications were performed in a final volume of 20µl at 95°C for 15min followed by 40 cycles with denaturation at 95°C for 30sec, annealing at 58°C for 30sec and elongation at 72°C for 30sec. PCR products were finally subjected to a melting curve analysis. The mRNA levels were quantified with the StepOne™ analysis software in comparative quantitation mode and normalized to beta-Actin expression levels. All quantitative RT-PCRs were done at least three times using RNA from independent experiments.

Measurement of arterial pressure and heart rate

The acute mean arterial pressure response to Ang-(1-7) injection was measured by direct cannulation in anesthetized 10 to 14-week old male mice of wild-type and MrgD-deficient genotype [361]. The mice were anesthetized with a combination of ketamine (78mg/kg body weight) and Xylacine (17.1mg/kg body weight) given intraperitoneal. Body temperature was maintained at 37°C. The right caroid artery was cannulated with PE-10 tubing and connected to a physiological pressure transducer (MEMSCAP, Skoppum, Norway), and the mean arterial pressure was continuously recorded with a digital data recorder (Lab Chart, ADInstruments Ltd, Oxford, United Kingdom). The heart rate was recorded using mouse needle electrodes (ADInstruments Ltd). After stabilization, Ang-(1-7) (30µg/kg body weight) was injected in the tail vein. The mean arterial pressure and heart rate were monitored continuously for 30min.

In silico modelling

The 3D structure of Ang-(1-7) was prepared by minimising their NMR experimental structures (PDB:2JP8) with AMBER* force field and in water solvent using Schrödinger's MacroModel (MacroModel, version 9.7, Schrödinger, LLC, New York, NY, 2009). It was further docked (keeping the backbone rigid) with Autodock 4.2.3 [362] into a modelled structure of Mas receptor [363], in which the F112 side chain conformation was modified to create a larger binding site and to expose specific binding residue [364, 365]. The complex was minimized as before. The resulting conformation of Ang-(1-7) was considered the bioactive conformation. Hercules software (Intelligent Pharma S.L., Barcelona, Spain) was applied to superpose PD123319 over Ang-(1-7). PD123319 non-ring

bonds were treated as flexible (amide bonds set to either 0° or 180°) while flexible ring conformations were computed with Corina (Corina_Linux2 3.46, Molecular Networks GmbH, Erlangen, Germany) using an energy window value of 20kJ/mol. Ionization states were estimated with Schrödinger's Epik (Epik version 2.8017, Schrödinger, LLC, 2009, New York, NY, USA), and Gasteiger's charges were assigned to atoms in both molecules as implemented in Openbabel [366].

Statistical Analyses

Data presented are mean \pm SEM. Data were analysed by Student's t-test or 1-way and 2-way ANOVA tests accompanied by Bonferroni post hoc test using GraphPad Prism 6.0 (GraphPad Software Inc., San Diego, CA, USA). A *P*-value of <0.05 was considered statistically significant.

Results

Angiotensin-(1-7) increases intracellular cAMP in different cell-types

Tallant and Clark described an increase in cAMP in VSMC stimulated by Ang-(1-7) [133]. Furthermore, Liu *et al.* described the stimulation of intracellular signalling by Ang-(1-7) in glomerular mesangial cells. Their data indicated that the heptapeptide can increase intracellular cAMP [141]. As we aimed to identify the receptors associated with Ang-(1-7) signalling, we initially examined whether cAMP would be an efficient readout to quantify changes in intracellular signalling following Ang-(1-7) stimulation. Ang-(1-7) increased cAMP in a dose-dependent manner in primary mesangial cells with highest efficacy at 10^{-7} M and an EC₅₀ value of 6.2nM (Figure 6.1.1 A). This increase was blocked by the two Ang-(1-7) antagonists, A779 and D-Pro, but also by the AT2 receptor blocker PD123319 (Figure 6.1.1 B). As a variety of papers described the blocking effect of the bradykinin B₂ receptor blocker, Icatibant, as well as the inhibitory effect of the NO synthase inhibitor L-NAME, on Ang-(1-7) mediated signalling [367], we tested both substances in our primary-cell assay. While Icatibant failed to block an Ang-(1-7)-mediated increase in cAMP, L-NAME inhibited the effects of Ang-(1-7). The heptapeptide could not add to the increased concentration of cAMP reached by L-NAME treatment alone (Figure 6.1.1 B). To test the ability of Ang-(1-7) to increase cAMP in other cell types, we stimulated primary cardiac fibroblasts (CFB) and vascular smooth muscle cells (VSMC) with the heptapeptide. While CFBs did not respond to Ang-(1-7) (Figure 6.1.1 C), it increased cAMP in VSMC, and the same compounds blocked the effect as described for primary mesangial cells (Figure 6.1.1 D).

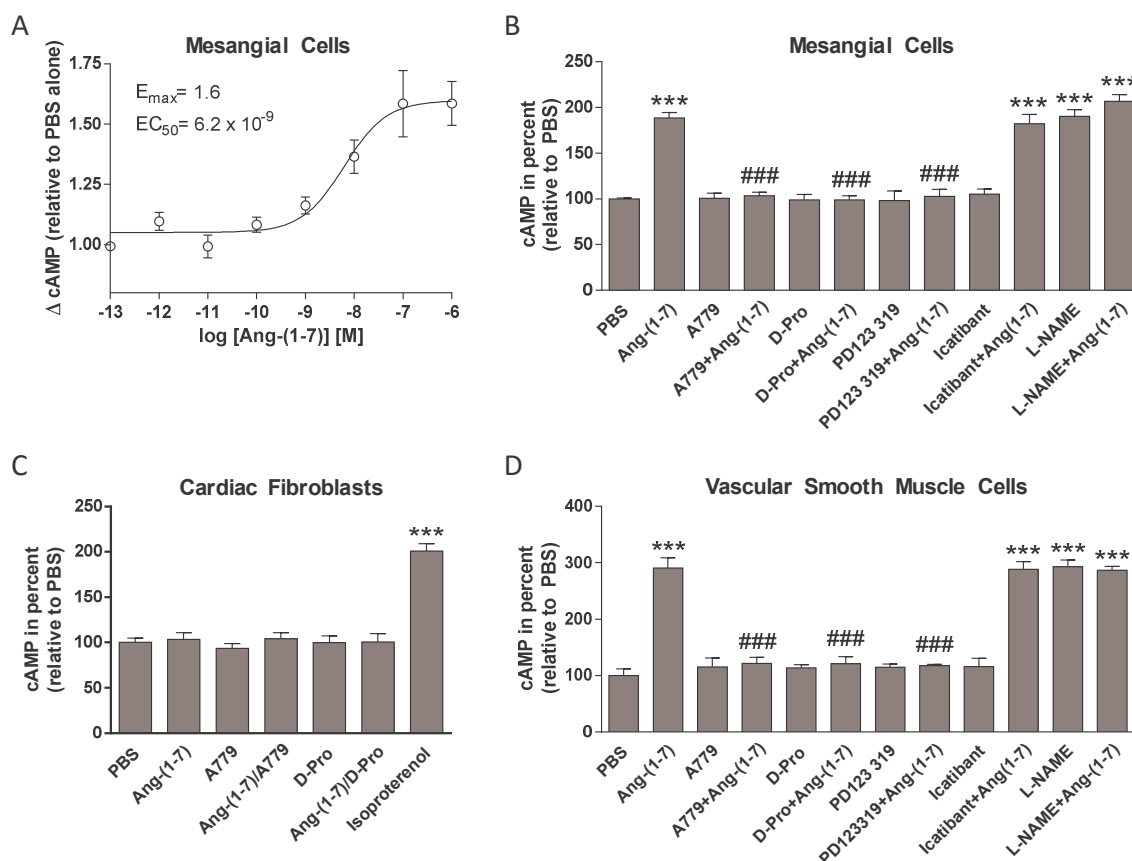


Figure 6.1.1 Intracellular cAMP is increased in angiotensin-(1-7) in various cell types

(A) concentration-dependent increase in cAMP level in primary mesangial cells, (B) effect of A779, D-Pro⁷-Ang-(1-7) (D-Pro), PD123319, Icatibant, and L-NAME (all 10^{-6} M) on Ang-(1-7) (10^{-7} M)-mediated increase in cAMP in mesangial cells, (C) lack of increase in intracellular cAMP in cardiac fibroblasts, (D) effect of the receptor blockers and L-NAME on Ang-(1-7)-mediated increase in cAMP in primary vascular smooth muscle cells. Data are presented as mean \pm SEM. *** $P < 0.001$ vs. PBS, ### $P < 0.001$ vs. Ang-(1-7), $n = 3 \times 3$.

Angiotensin-(1-7) stimulates the generation of intracellular cAMP in endothelial cells

Since Ang-(1-7) relaxes vessels in an endothelium-dependent manner [368], we tested the most commonly used endothelial cell-line, human umbilical vein endothelial cells (HUVEC), for its response to Ang-(1-7). As described before for other cell-lines, the peptide-mediated increase in intracellular cAMP could be blocked by A779, D-Pro,

PD123319, and inhibited by L-NAME (Figure 6.1.2 A). As shown in Figure 6.1.2 B, the increase in cAMP was concentration-dependent, whereby the EC₅₀ was reached at 13nM.

As the concentration of cAMP depends on its generation as well as its degradation, we tested whether the Ang-(1-7)-mediated raise in cAMP is the consequence of increased stimulation of adenylyl cyclase (AC) or decreased activity of phosphodiesterases (PDE). We used Forskolin, an activator of AC, which directly stimulates cAMP level and IBMX, a nonselective PDE inhibitor which inhibits cAMP degradation. As expected, both Forskolin and IBMX led to an increase in intracellular cAMP (Figure 6.1.2 C). However, Ang-(1-7) could increase cAMP levels stimulated by IBMX but did not further increase the levels reached by Forskolin alone. The additive effect of Ang-(1-7) and IBMX excludes the Ang-(1-7)-mediated raise in cAMP to be a result of PDE inhibition.

To finally confirm that Ang-(1-7)-mediated increase in cAMP is AC-dependent we used the specific enzyme inhibitor SQ22536. As shown in Figure 2D, the SQ22536 alone had no effect on cAMP concentration but the inhibitor blunted the Ang-(1-7)-mediated raise in cAMP linking Ang-(1-7) signalling to G_{12s}/AC/cAMP axis.

As cAMP initiates a variety of downstream signalling pathways including PKA activation, we tested whether the Ang-(1-7)-mediated increase in cAMP leads to an increased PKA activity. Stimulation of HUVEC with Ang-(1-7) for 15min resulted in a significant increase in PKA activity (Figure 6.1.2 E).

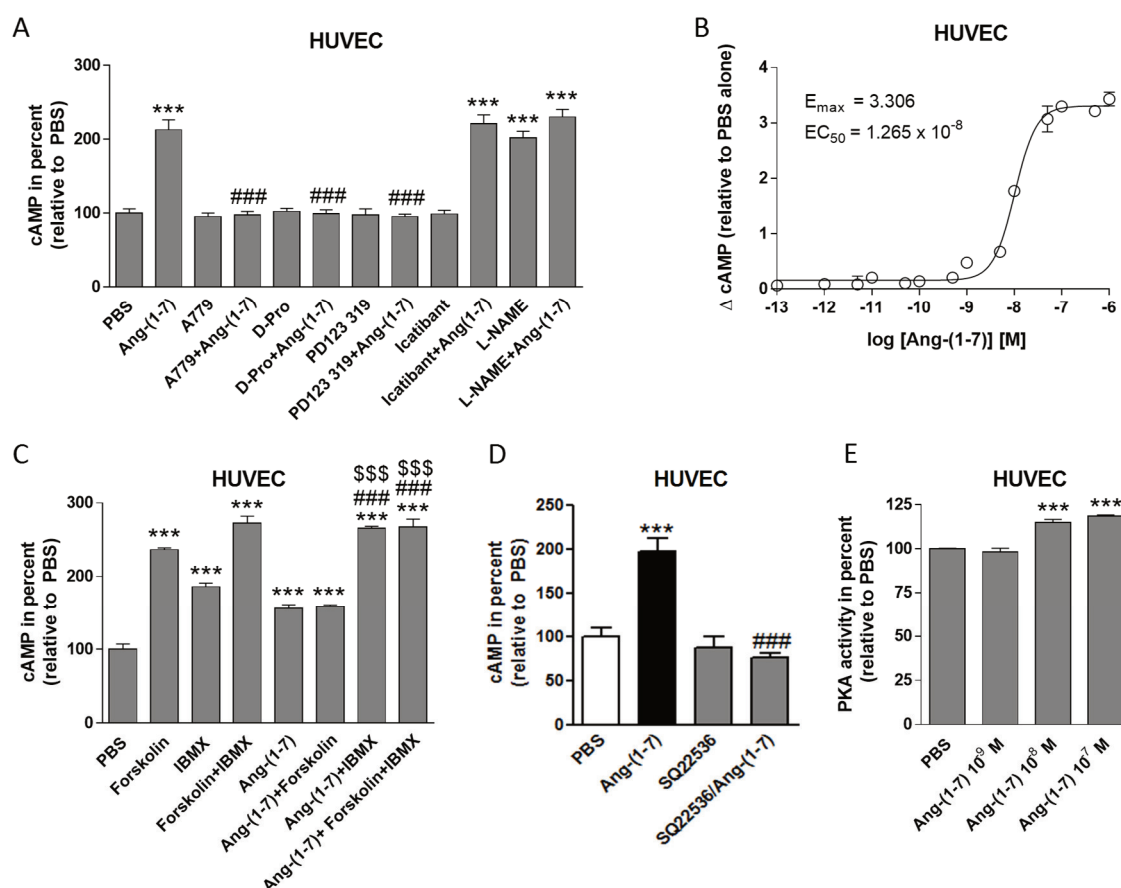


Figure 6.1.2 Ang-(1-7) increases cAMP and PKA activity in human umbilical vein endothelial cells (HUVEC).

(A) Effect of A779, D-Pro⁷-(Ang-(1-7) (D-Pro), PD123319, Icatibant, and L-NAME (all 10^{-6} M) on Ang-(1-7) (10^{-7} M)-mediated increase in cAMP, (B) concentration-dependent increase in cAMP level, (C) cAMP level stimulated with Forskolin, IBMX, Ang-(1-7) alone, or in combinations, (D) effect of the adenylyl cyclase inhibitor SQ22536 alone or in combination with Ang-(1-7) on cAMP level (E) activation of PKA by Ang-(1-7). Data are presented as mean \pm SEM. *** $P < 0.001$ vs. PBS, ### $P < 0.001$ vs. Ang-(1-7), \$\$\$ $P < 0.001$ vs. IBMX, $n = 3 \times 3$ (A-C), $n = 2 \times 3$ (D, E).

Angiotensin-(1-7) stimulates the generation of intracellular cAMP in HEK293 cells expressing either Mas or MrgD

In order to test for receptors involved in the Ang-(1-7)-mediated increase in cAMP levels, we used HEK293 cells. First, we tested untransfected cells to exclude that these cells already respond to the heptapeptide. As shown in the left panel of Figure 6.1.3 A, the heptapeptide had no effect on cAMP levels, confirming HEK293 cells as an ideal tool to measure cAMP in response to Ang-(1-7) in receptor-transfected cells.

We chose four different receptors for further tests. Firstly, we tested Mas as Ang-(1-7) has previously shown to be an endogenous ligand for this receptor [62]. Secondly, Mrg and MrgD receptors have been selected, as we showed a significant AA release in response to the heptapeptide in Mrg- and MrgD-transfected cells but not in other receptors of the Mas-like family [65]. Finally, we also tested the AT2 receptor, since PD123319 is believed to be a specific AT2 receptor blocker, and we showed that it blocks the Ang-(1-7)-mediated increase in cAMP (Figure 6.1.1 B and D, Figure 6.1.2 A). When HEK293 cells were transfected with plasmids for those four receptors, Ang-(1-7) stimulation caused a significant increase in intracellular cAMP levels in cells overexpressing Mas or MrgD but not Mrg and AT2 (Figure 6.1.3, right panel).

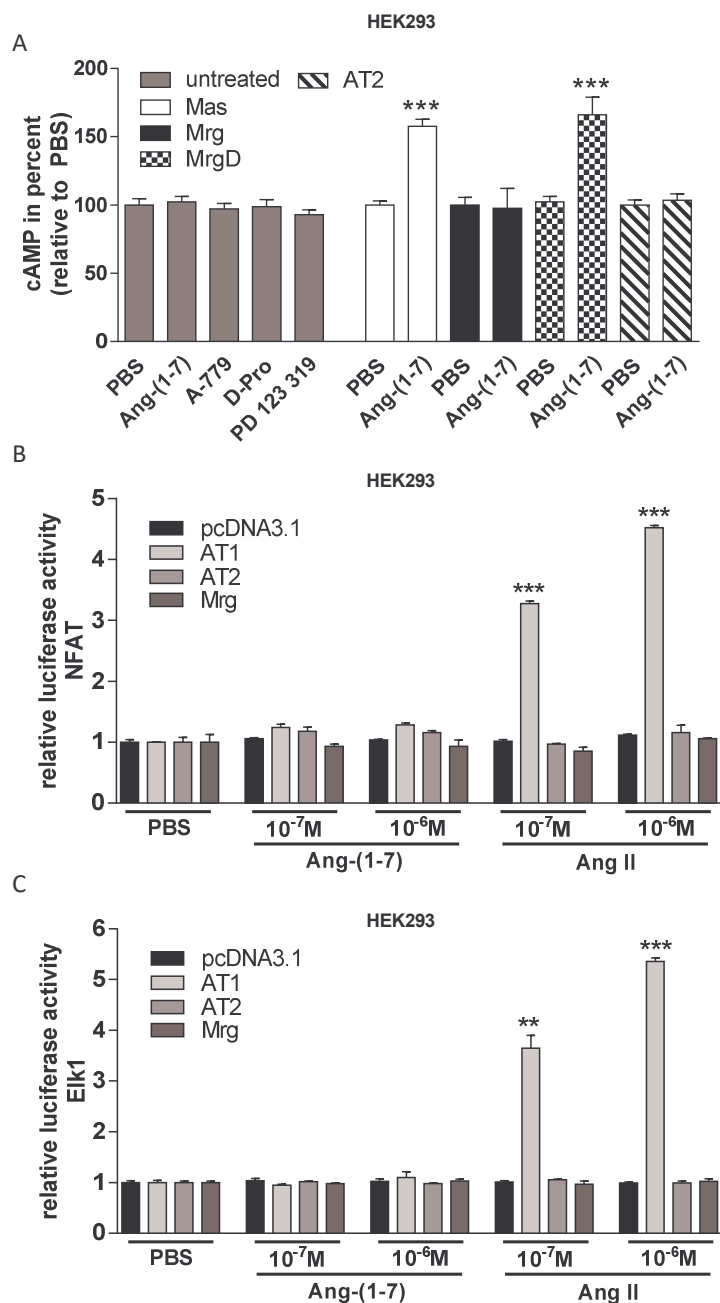


Figure 6.1.3 Ang-(1-7)-induced signalling is mediated by Mas and MrgD.

(A) cAMP concentration in untransfected HEK293 cells stimulated with either Ang-(1-7) (10^{-7} M), A779, D-Pro⁷-(Ang-(1-7) (D-Pro) and PD123319 (all 10^{-6} M) (left panel) and cAMP level in Mas, Mrg, MrgD and AT2 transfected HEK293 cells stimulated with Ang-(1-7) (right panel), (B) luciferase production in HEK293 cells transiently co-transfected with pcDNA3.1, AT1, AT2 or Mrg, and pNFAT-Luc after stimulation with PBS, Ang-(1-7), or Ang II (C) luciferase production in HEK293 cells transiently co-transfected with pcDNA3.1, AT1, AT2 or Mrg, and pElk1-Luc after stimulation with PBS, Ang-(1-7), or Ang II. Data are presented as mean \pm SEM. *** $P < 0.001$, ** $P < 0.01$ vs. related PBS control, $n = 3 \times 3$ (A), $n = 1 \times 2$ (B, C).

To exclude other main signalling pathways for AT2 and Mrg to be activated by Ang-(1-7) involving other G proteins such as $G_{\alpha q/11}$ and $G_{\alpha i}$, we tested activation of these two G proteins by measuring activation of transcription factors specifically activated by them. We have chosen nuclear factor for activated T-cells (NFAT), which is known to be coupled to $G_{\alpha q/11}$ [65] and Elk1 as indicator for $G_{\alpha i}$ activation [253]. Since AT1 receptor is known to signal through $G_{\alpha q/11}$ and $G_{\alpha i}$ after stimulation with Ang II [369], we used this receptor as the positive control. As expected, Ang II increased luciferase production in AT1 receptor expressing cells co-transfected with either NFAT or Elk1 (Figure 6.1.3 B and C, *right panels*). In contrast, Ang-(1-7) failed to stimulate any of the transcription factors in AT2- and Mrg-expressing HEK293 cells (Figure 6.1.3 B and C, *left panel*). Notably, Ang-(1-7) has been also unable to stimulate the two G proteins in AT1-transfected cells.

We used both Mas and MrgD receptors to investigate in detail their involvement in Ang-(1-7)-mediated signalling. The efficiency of the transfection in HEK293 cells was proofed by using qPCR and fluorescence microscopy (shown in Figure 10.1.1, Appendix part1). As shown on Figure 6.1.4 A, Ang-(1-7) stimulation caused a dose-dependent increase in the intracellular cAMP level in Mas-transfected cells with an EC_{50} of 5.5nM. Then, we selected the concentration of highest efficacy ($10^{-7}M$) for further tests with the previously effective blockers. Figure 6.1.4 B shows that none of the 3 blockers had an effect on cAMP levels in pcDNA3.1- or Mas-transfected cells. However, the increase in cAMP concentration generated by Ang-(1-7) in Mas-transfected cells was blocked by all three blockers (Figure 6.1.4 B).

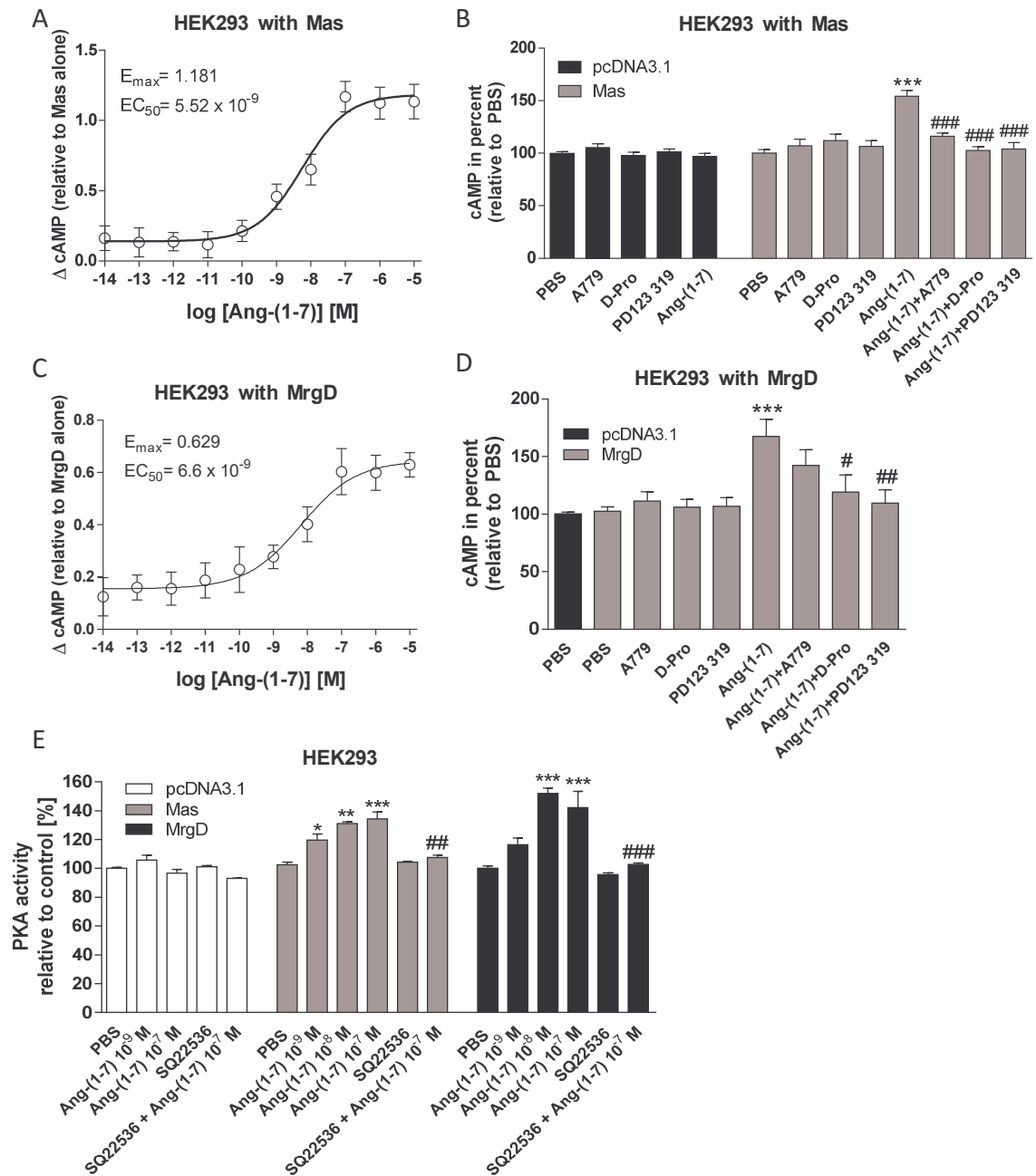


Figure 6.1.4 Ang-(1-7)-induced signalling is mediated by Mas and MrgD.

(A) concentration-dependent increase in cAMP level in Mas-transfected cells, (B) increased cAMP concentration by Ang-(1-7) is blocked by A779, D-Pro and PD123319 in Mas-transfected cells, (C) concentration-dependent increase in cAMP level in MrgD-transfected cells, (D) increased cAMP concentration by Ang-(1-7) is blocked by tested blockers in MrgD-transfected cells, (E) activation of PKA by Ang-(1-7) in Mas- or MrgD-transfected cells and the effect of the adenylyl cyclase inhibitor SQ22536. Data are presented as mean \pm SEM. * $P < 0.05$, ** $P < 0.01$, *** $P < 0.001$ vs. PBS, # $P < 0.05$, ## $P < 0.01$, ### $P < 0.001$ vs. Ang-(1-7), $n = 3 \times 3$ (A,C), $n = 8 \times 3$ (B,D), $n = 2 \times 3$ (E).

Independent experiments were carried out on HEK293 cells transfected with MrgD where Ang-(1-7) also caused a dose-dependent increase in cAMP concentration with an EC₅₀ value of 6.6nM (Figure 6.1.4 C). In contrast to Mas-transfected cells, only D-Pro and PD123319 blocked the Ang-(1-7)-mediated increase in cAMP level, while A779 had no significant effect (Figure 6.1.4 D).

To confirm that the increase in PKA activity seen in HUVEC (Figure 6.1.2 E) can be associated to Mas and MrgD signalling, we measured activity in response to Ang-(1-7) in Mas- and MrgD-transfected cells. In both receptor-overexpressing cells, the heptapeptide significantly increased PKA activity. This increase was blunted by the adenylyl cyclase inhibitor SQ22536 (Figure 6.1.4 E) confirming cAMP generation as the trigger for PKA activation.

Angiotensin-(1-7)-mediated cAMP generation is absent in mesangial cells derived from Mas/MrgD knockout animals

In order to confirm that Mas and MrgD are the two receptors used by Ang-(1-7) to generate cAMP in primary cells, we used mesangial cells derived from double knockout mice deficient in both receptors. These mice are fertile and without obvious morphological abnormalities. Initially, we examined whether the measured increase in cAMP in mesangial cells is above the threshold to initiate downstream signalling (Figure 6.1.5 A). Because one of the consequences of cAMP increase can be the activation of the transcription factor cAMP response element-binding protein (CREB) [370], we evaluated whether the Ang-(1-7) mediated increase in cAMP can also induce CREB phosphorylation. Figure 6.1.5 A and B show that CREB phosphorylation occurred 5min following Ang-(1-7)

stimulation and reached control levels within 30min. This induction was blunted by pre-treatment with SQ22536 confirming cAMP generation as initial signal for CREB phosphorylation.

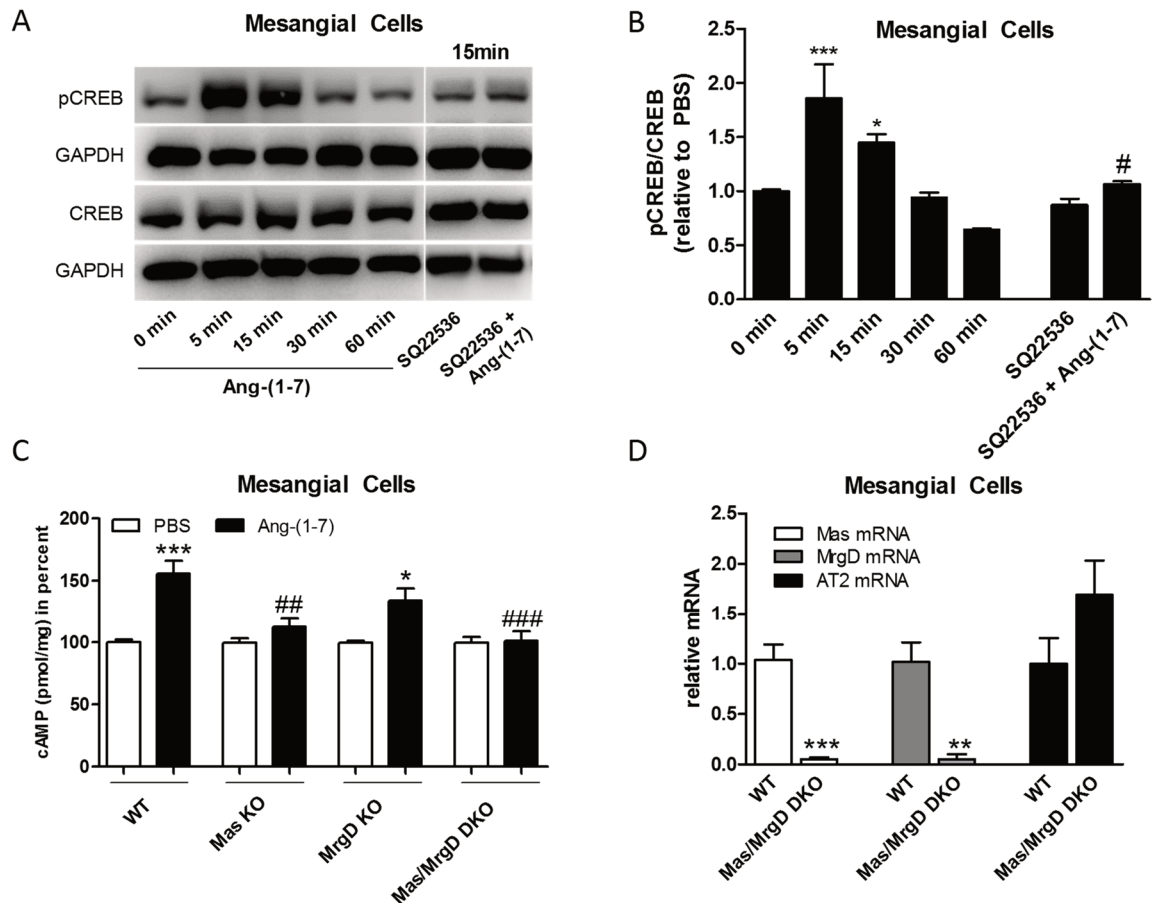


Figure 6.1.5 Ang-(1-7) induced signalling is absent in mesangial cells derived from Mas/MrgD knockout animals.

(A) Western blot of phosphorylated CREB (pCREB) and CREB and the house-keeping protein GAPDH. (B) Calculation of time-dependent CREB phosphorylation in comparison to absolute CREB protein after Ang-(1-7) stimulation and/or treatment with adenylyl cyclase inhibitor SQ22536 (15min Ang-(1-7)). (C) Effect of Ang-(1-7) in Mas knockout (KO), MrgD KO and Mas/MrgD double KO cells (PBS values of each genotype set as 100%). (D) mRNA of Mas, MrgD, and AT2 in wild-type (WT) and double KO cells. Data are presented as mean \pm SEM. * P <0.05, ** P <0.01 *** P <0.001 vs. PBS/WT, ## P <0.01, ### P <0.001 vs. Ang-(1-7) in WT. $n=2$ (A, B), $n=3 \times 3$ (C, D).

Next, we tested whether Ang-(1-7)-mediated increase in cAMP observed in wild-type mesangial cells could be abolished in Mas or MrgD deficient cells or cells isolated from Mas/MrgD double knockouts. Deficiency in one of the receptors reduced the Ang-(1-7) signal generated in wild-type cells, while the double knockout completely blunted it (Figure 6.1.5 C).

In order to exclude upregulation of the remaining receptor and also to confirm that both Mas and MrgD receptors are absent in knockout cells, we investigated the mRNA levels in mesangial cells derived from double knockouts. Figure 6.1.5 D shows that Mas and MrgD mRNA levels were barely detected in cells from double knockouts. Notably, deficiency in both receptors did not significantly alter AT2 mRNA levels.

Angiotensin-(1-7)-mediated acute hemodynamic effects are blunted in MrgD-deficient mice

As we and others showed that vasorelaxant effects of Ang-(1-7) are Mas dependent [254, 368], we finally tested whether the genetic deficiency in MrgD would also have an *in vivo* effect on the hemodynamic properties of Ang-(1-7). Acute bolus infusion of the heptapeptide led to a significant drop in mean arterial blood pressure, while no decrease was observed in MrgD knockouts (Figure 6.1.6 A).

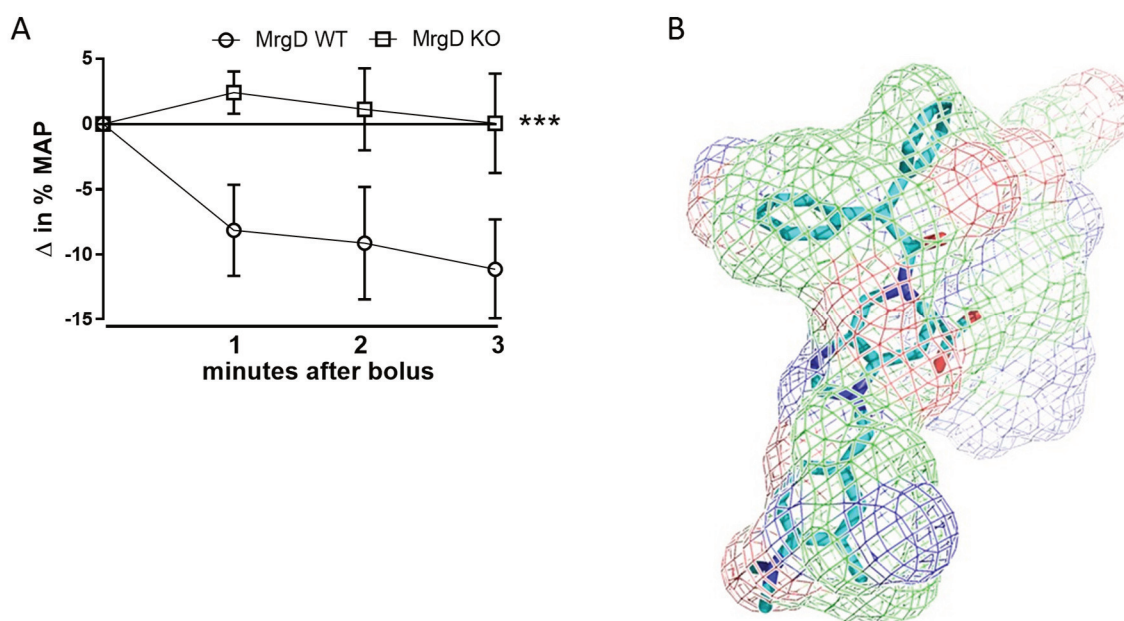


Figure 6.1.6 *Ang-(1-7) induced signalling is absent in mesangial cells derived from Mas/MrgD knockout animals.*

(A) Effect of Ang-(1-7) on mean arterial pressure (MAP) in wild-type mice and MrgD knockouts. (B) *in silico* modelling of Ang-(1-7) (mesh) and PD123119 (sticks) with the following mesh color code: blue stands for hydrogen donor chemical groups, red for hydrogen acceptor chemical groups, and green for carbon atoms. Data are presented as mean \pm SEM. *** $P < 0.001$ vs. PBS/WT, $n = 5/5(E)$.

Discussion

The lack in knowing a second messenger for Ang-(1-7) prevented not only the pharmacological confirmation of assumed receptors and the identification of further hypothesized receptors, but also the determination of efficacy and potency of a potential receptor/ligand interaction. The need of such second messenger is also illustrated by the fact that two publications over the last years intensively investigated phosphorylation of intracellular molecules [371] and quantities of intracellular proteins [372], respectively, in response to Ang-(1-7). Although aimed to identify useful molecules for receptor pharmacology, the data published failed to add useful tools to this approach.

Here, we demonstrate that a second messenger, cAMP, is an ideal tool to quantify changes in intracellular signalling mediated by Ang-(1-7). This allowed us to provide final pharmacological evidence that Mas is a functional receptor for Ang-(1-7). More importantly, the use of cAMP as a readout enabled us to screen for other receptors associated with Ang-(1-7) signalling in a hypothesis-based manner. Consequently, these results provide the first experimental proof that MrgD is a second receptor for Ang-(1-7) that has been confirmed under *in vivo* conditions. The hypothesis that MrgD acts as a receptor for the heptapeptide has been based on different findings including (1) high sequence homology between Mas and MrgD; (2) a description from a Brazilian group that Ala¹-Ang-(1-7) but not Ang-(1-7) is a ligand for MrgD [42], because unpublished modelling of both peptides excludes a decisive effect of the first amino acid on the G₁₅ activation and thus made it likely that a receptor for Ala¹-Ang-(1-7) is also a receptor for Ang-(1-7); and (3) our data that Ang-(1-7) can stimulate AA release in MrgD-transfected cells [65]. However, the experiments with Mrg might seed doubts on the latter point, as the relatively moderate AA release was not paralleled by an increase in cAMP in Mrg-transfected cells; but association between cAMP and AA release warrants further investigation.

We are the first group to establish cAMP as a readout for Ang-(1-7) receptor pharmacology, although there have been indications in the literature for such an association. Beside the work by Tallant and Clark [133] and by Liu *et al.* [141] in primary cells, a paper from 2012 showed indirect cAMP involvement in Ang-(1-7) signalling as its modulation of sympathetic activity in the paraventricular nucleus was abolished by an adenylyl cyclase inhibitor and a PKA inhibitor [373].

Furthermore, physiological effects of the heptapeptide and effects in preclinical models also implicate the involvement of cAMP. For example, we demonstrated the dominant effect of Ang-(1-7) on hematopoietic stem cells/progenitors [374], and there is significant evidence that cAMP stimulates such processes [375].

Although Mas-deficient animals showed significant effects in preclinical disease models, they do not show a strong phenotype (healthy, fertile, normal growth, normal development, and normal plasma Ang II levels) [120], except endothelial dysfunction [368]. Based on our present data, one could argue that the lack in phenotype is a result of the heptapeptide's ability to shunt the lack of Mas by using the sequence and signalling-like receptor MrgD. However, although not intensively phenotyped yet, the double-knockouts look normal, are fertile, and show no increased mortality within 12 months. This further supports the hypothesis that Ang-(1-7) is affective especially under disease conditions.

One of the key findings of this study is the exclusion of AT₂ as a functional Ang-(1-7) receptor. Our experiments excluded not only activation of G_qs by the heptapeptide in AT₂-transfected cells and thus an increase in cAMP concentration, but also coupling to two other major G proteins activated by G protein-coupled receptors (GPCRs).

Furthermore, our data also provides the identification of the reason for the controversial discussion on Ang-(1-7)/AT₂ over the last years. There are only few published experiments using AT₂ knockouts for the evaluation of an AT₂-mediated part of Ang-(1-7) action showing either no effect or only partial effects [376]. However, there are many papers concluding that Ang-(1-7) acts via AT₂, because of the blocking effect of PD123319. Based on our findings that PD123319 can also block Mas and MrgD, such a

conclusion could be wrong as the blocking effect of PD123319 is not based on AT2 but on both Ang-(1-7) receptors.

This unspecific receptor profile of PD123319 might not be surprising, if we compare its structure with Ang-(1-7). PD123319 structure can be embedded in the molecular volume of the predicted bioactive conformation of Ang-(1-7) bound to Mas and displays chemical similarities to Ang-(1-7), implicating that both molecules fit into the two Ang-(1-7) receptors, whereby PD123319 may fail to stimulate intracellular signalling (Figure 6.1.6 B).

However, identifying PD123319 as a non-specific AT2 receptor blocker, also requires a careful re-evaluation of papers, which conclude that the effects blocked by PD123319 are mediated via AT2, as we now know that it could also relate to Mas and MrgD.

Taken together, our results correct the view on the RAS (AT2 is not an Ang-(1-7) receptor), expand our understanding of the beneficial ACE2/Ang-(1-7)/Mas axis to a two-receptor axis (Mas and MrgD), identify the primary intracellular signalling cascade for the heptapeptide when interacting with its receptors (G_{12s} /AC/cAMP leading to an increase in PKA activity and CREB phosphorylation), and force a re-evaluation of more than thousand publications concluding that effects blocked by PD123319 are AT2-specific.

Perspectives

As Ang-(1-7) has been identified as a protective peptide in cardiovascular diseases, the identification of a second receptor for the peptide allows for the development of tailored drugs (non-peptidic agonists) stimulating either Mas or MrgD or both receptors depending on their expression/importance in diseases of different aetiology.

Source of Funding

The work was supported by grants of the Deutsche Forschungsgemeinschaft (WA1441/22-1 and 2; SFB TRR57).

Disclosures

TW is inventor of the patent "Use of an Ang-(1-7) receptor agonist in acute lung injury" (Application No: 08016142.5-2107). TW is scientific advisor of Tarix (Boston, USA).

Novelty and Significance**What is new?**

We discovered MrgD as the second receptor for Ang-(1-7) an. Both Mas and MrgD activate adenylyl cyclase initiating an increase in cAMP, consequently activating PKA, and leading to CREB phosphorylation. We also generated double knockout mice deficient in both Ang-(1-7) receptors, Mas and MrgD. We describe them as not having an obvious anatomical/morphological phenotype, being fertile, and not showing increased mortality until one year of age.

By identifying PD123319 as a non-specific AT₂ receptor blocker which also blocks Mas and MrgD, we now know that effects of the blocker assigned to its interaction with the AT₂ receptor could also relate to the two Ang-(1-7) receptors Mas and MrgD.

What is relevant?

We demonstrate the in vivo relevance of our findings by showing that the lack in Ang-(1-7)/MrgD interaction leads to a much less pronounced vasorelaxant response to Ang-(1-7) in mice deficient in MrgD.

Summary

Our results lead to an expansion and partial revision of the renin-angiotensin system, by identifying a second receptor for Ang-(1-7). We also solved the decade-long controversial discussion of whether AT₂ is a receptor for Ang-(1-7) by excluding this with our experiments and by providing the explanation for the recent confusion.

6.2 Decarboxylation of Ang-(1-7) to Ala¹-Ang-(1-7) leads to significant changes in pharmacodynamics

Anja Tetzner, MSc^{a,b}; Maura Naughton, MSc^a; Kinga Gebolys, PhD^a; Esther Sala, PhD^d; Óscar Villacañas, PhD^d; Thomas Walther, PhD^{a,b,c}

^aDept. Pharmacology and Therapeutics, School of Medicine and School of Pharmacy, University College Cork (UCC), Cork, Ireland;

^bDepartments Obstetrics and Paediatric Surgery, University of Leipzig, Leipzig, Germany;

^cInstitute of Medical Biochemistry and Molecular Biology, University Medicine Greifswald, Greifswald, Germany;

^dIntelligent Pharma, Barcelona, Spain.

Corresponding Author: Prof. Thomas Walther, Department Pharmacology & Therapeutics, School of Medicine and School of Pharmacy, Western Gateway Building, Western Road, University College Cork, Cork, Ireland; Phone: +353-21-420-5973, fax: +353-21-4205471, E-mail: t.walther@ucc.ie

Published in European Journal of Pharmacology, 2018 Aug 15;833:116-123

Hypothesis

Ala¹-Ang-(1-7) does not just stimulate MrgD, but also the Mas receptor. Additionally, the lack of the carboxylate group at position one might result in a change of pharmacodynamics compared to Ang-(1-7).

Aim of the study:

The aim of the study was not just to proof that MrgD, but also Mas is a functional receptor for Ala¹-Ang-(1-7). Furthermore, using various cell types (receptor-transfected HEK293 cells, human endothelial cells, receptor-deficient primary mesangial cells), and a variety of receptor blockers and enzyme inhibitors together with the recent identified cAMP assay as a readout, the ligand/receptor pharmacology for Ala¹-Ang-(1-7) was aimed to be examined.

Author Contributions

Anja Tetzner performed part of experiments for Figure 1-4, developed the images for the figures and worked on the manuscript.

Maura Naughton performed part of experiments for Figure 1B, 3 and 4, and worked on the manuscript.

Kinga Gebolys performed part of the experiments for Figure 1A and 1B.

Esther Sala computed and analysed the electrostatic potential.

Óscar Villacañas analysed the ligand-protein interactions and supervised the modelling part.

Thomas Walther initiated the work, coordinated the experiments, advised, drafted the main text body, and finalized the manuscript.

Abstract

Within the renin-angiotensin system, angiotensin (Ang)-(1-7) is cardiovascular protective, stimulates regeneration, and opposes the often detrimental effects of Ang II. We identified two receptors for the heptapeptide; the G protein-coupled receptors Mas and MrgD. Recently, a decarboxylated form of Ang-(1-7), Ala¹-Ang-(1-7) (Alamandine), has been described as having similar vasorelaxant effects as Ang-(1-7), but distinctively stimulating the MrgD receptor. The aim of this study was to elucidate the consequences of the lack of the carboxyl group in amino acid one on intracellular signalling, to discover the receptor fingerprint for Ala¹-Ang-(1-7), and to characterize the consequences for pharmacodynamics. Ala¹-Ang-(1-7) elevated cAMP concentrations in primary endothelial and mesangial cells. However, the dose-response curves clearly discriminated from the curves generated with Ang-(1-7), with a much lower EC₅₀ and a bell-shape curve for Ala¹-Ang-(1-7). We provided pharmacological proof that both, Mas and MrgD, are functional receptors for Ala¹-Ang-(1-7). Consequently, the heptapeptide failed to increase cAMP concentration in primary mesangial cells with genetic deficiency in both receptors. As previously described for Ang-(1-7), the Ala¹-Ang-(1-7) effects on Mas/MrgD-transfected HEK293 cells and on primary cells were blocked by the AT₂ receptor blocker, PD123319. The very distinct dose-response curves for both heptapeptides could be explained by *in silico* modelling, electrostatic potential calculations, and an involvement of G_{α_{hi}} for higher concentrations of Ala¹-Ang-(1-7). Our results identify Ala¹-Ang-(1-7) as

a peptide with specific pharmacodynamic properties and build the basis for the design of more potent and efficient Ang-(1-7) analogues for therapeutic interventions in a rapidly growing number of diseases.

Keywords : Ala¹-Angiotensin-(1-7), dose-response curve, G-proteins, Mas receptor, MrgD receptor, renin-angiotensin system

Introduction

The renin-angiotensin system consists of an increasing number of angiotensin (Ang) peptides which play an important role in the regulation of arterial blood pressure, electrolyte homeostasis, and water and sodium intake [353], as well as in processes like tissue regeneration [354, 377]. The renin-angiotensin system is a complex cascade in which precursor peptides are processed by specific enzymes to their active forms. In the past few years especially, Ang-(1-7) has become a peptide of interest, because of its beneficial actions in cardiovascular and renal diseases, counter-regulating the adverse effects of AngII [58]. Ang-(1-7) is mainly produced from AngII by Ang converting enzyme 2 (ACE2) [58].

In previous work, we identified the G protein-coupled receptor Mas to be associated with Ang-(1-7)-induced signalling which could be blocked by D-Ala⁷-Ang-(1-7), also named A779, a specific Ang-(1-7) antagonist [62]. Very recently, we also discovered a second receptor for the heptapeptide, the Mas-related G protein-coupled receptor MrgD [378]. In that study, we also showed that the primary intracellular pathway

activated by Ang-(1-7) interactions with either Mas or MrgD involves adenylyl cyclase, cAMP and phosphokinase A [378].

A decade ago, Jankowski *et al.* identified a modified analogue of AngII in human plasma [40]. This Ala¹-AngII, the authors named AngA, can be generated by the decarboxylation of the amino acid aspartate on position one to alanine. AngA interacts with the AT1 receptor [379] and its physiological effects can be blocked by the AT1 receptor blocker candesartan [380]. Based on such findings, an international team hypothesized the existence of Ala¹-Ang-(1-7) as a product of Ala¹-AngII through conversion by ACE2 [42]. Indeed, Ala¹-Ang-(1-7) has been identified and named alamandine. As Kupchan *et al.* used similar terminology, Allamandin, for a completely different molecule, we will use the original term, Ala¹-Ang-(1-7), describing the amino acid change in Ang-(1-7), to prevent confusion [381]. Lautner *et al.* characterized Ala¹-Ang-(1-7) as the target peptide for the MrgD receptor but not for the Mas receptor [42]. However, as we could show that Ang-(1-7) can stimulate both Mas and MrgD, we aimed to test whether Ala¹-Ang-(1-7) targets the same receptors as Ang-(1-7), or shows a distinct receptor fingerprint. In particular, we focused on the characterisation of the ligand/receptor pharmacology, by determining efficiency and potency using receptor-transfected HEK293 cells, human endothelial cells, receptor-deficient primary mesangial cells, and a variety of receptor blockers and enzyme inhibitors.

Materials and Methods

Materials

Angiotensin (Ang)-(1-7), Ala¹-Ang-(1-7), D-Ala⁷-Ang-(1-7), and D-Pro⁷-Ang-(1-7) were synthesized from Biosyntan (Berlin, Germany). HEK293, Forskolin, RPMI-1640, HEPES solution, Sodium pyruvate, Triton X-100 and trypsin/EDTA were purchased from Sigma Aldrich (St. Louise, Missouri, USA). DMEM, Fetal Bovine Serum (FBS) and L-glutamine were purchased from GIBCO (Life Technologies, Carlsbad, California, USA). PD123319 was from Parke-Davis Pharmaceutical Research (Detroit, Michigan, USA), PTX was from EMD Millipore (Billerica, MA, USA), Polyfect transfection reagent from Qiagen (Venlo, Limburg, Netherlands), and Pierce BCA Protein Assay Kit from Thermo Fisher Scientific (Waltham, Massachusetts, USA). Direct cAMP ELISA kit was from Enzo Life Sciences Ltd. (Exeter, United Kingdom). HUVEC were purchased from LONZA (Basel, Switzerland).

Animals

Mice deficient in Mas [120, 359] and both Mas and MrgD (double knockout) [378] have been bred and housed in the animal facilities at UCC, Cork, Ireland. Animal studies are reported in compliance with the ARRIVE guidelines [382, 383]. Experiments performed conformed with the guidelines from Directive 2010/63/EU of the European Parliament on the protection of animals used for scientific purposes. Experiments involving animals have been approved by the Irish HPRA and also by the Animal Experimentation Ethics Committee (AEEC) in UCC.

Cell culture conditions, transfection and stimulation

Human embryonic kidney (HEK-293) cells were cultured in DMEM medium supplemented with FBS (10%), HEPES buffer (1%), sodium pyruvate (1%), and L-glutamine (1%) and maintained under standard conditions (5% CO₂, 95% humidity and 37°C). Cells were cultured in 100mm cell culture dishes and seeded in 48-well plates at a density of 75,000 cells per well. The next day, HEK-293 cells were transfected using a transient transfection procedure following the manufacturer's instructions. Briefly, 150ng of control plasmid pcDNA3.1 or a combination of 50ng of pcDNA3.1 and 100ng of expression vectors containing the cDNA for Mas or MrgD were mixed with serum-free medium and PolyFect transfection reagent. After 10min incubation at room temperature, which allowed the complex formation, complete medium was added and the total volume was transferred into appropriate wells of the 48-well plate. The cells were incubated for 16-20hrs. The next day, the medium was replaced by serum-free medium 1hr before stimulation. After stimulation with A779, D-Pro, PD123319, forskolin (all 10⁻⁶M), or PTX (50ng/ml) for 15min, the solvent, Ala¹-Ang-(1-7) or Ang-(1-7) (all in the mentioned concentrations) were added for 15min. Then, the cells were lysed by adding 180 µl/well of 0.1M hydrochloric acid with 0.1% TritonX-100, and the lysates were stored at -80°C until cAMP measurement. The protein concentration was determined using Pierce BCA Protein Assay Kit according to the manufacturer's protocol (Thermo Fisher Scientific, Waltham, Massachusetts, USA).

Isolation and culture of primary cells and their stimulation

Kidney mesangial cells (MC) were isolated from 10-12-week old mice deficient in Mas and MrgD, and from their age- and gender-matched C57/BL6 control, according to the protocol previously described [384]. MC were cultured in 75cm² tissue culture flasks and seeded at passage 2 for stimulation in 24-well plates at a density of 100,000 cells per well. Primary human umbilical vein endothelial cells (HUVEC) were purchased from LONZA (Basel, Switzerland). HUVEC were cultured in 100mm cell culture dishes and were seeded at 75,000 per well in 24-well plates at passage 5-7, for stimulation. Stimulation with Ala¹-Ang-(1-7) and the blockers was carried out as described above.

Measurement of cAMP in cell lysates

cAMP concentration in cell lysates was determined using Direct cAMP ELISA kit (Enzo Life Sciences Ltd., Exeter, United Kingdom). Briefly, wells of 96-well plate (Goat Anti-Rabbit IgG pre-coated) were neutralized with 50µl of Neutralizing Reagent. Next, 100µl of acetylated cAMP standard or cell lysate was added, followed by 50µl of blue cAMP-Alkaline Phosphatase Conjugate and 50µl of yellow EIA Rabbit Anti-cAMP antibody. The plate was then incubated on a shaker (~ 400rpm) at room temperature for 2h. Next, the wells were aspirated and rinsed three times with Wash Buffer (1:10, Tris buffered saline containing detergents and sodium azide in deionized water). After the final wash, the plate was tapped against clean paper towel to remove any remaining Wash Buffer. To each well, 200µl p-Nitrophenyl Phosphate Substrate Solution was added, and the plate was incubated for 1h at room temperature. The enzymatic reaction was stopped by adding 50µl of Stop Solution, and the absorbance at 405nm was measured immediately.

The cAMP concentration was determined from non-linear standard curve using GraphPad Prism 6.0 software.

mRNA isolation and Real-time PCR

Total cellular RNA was isolated using the NucleoSpin RNA isolation kit (MACHEREY-NAGEL, Düren, Germany) according to the manufacturer's protocol. After isolation, 2,000ng total RNA was transcribed into cDNA using the RevertAid H Minus First Strand cDNA Synthesis kit (MBI Fermentas, Hanover, MD, USA) and oligo(dT)18 primer according to the manufacturer's guidelines. After synthesis, RNase free water was added to the single cDNA to a final volume of 100µl. Quantification of mRNA levels was performed by real-time quantitative PCR (RT-PCR) on the StepOne™ Real-Time PCR System (Thermo Fisher Scientific, Waltham, Massachusetts, USA) employing the Platinum SYBR Green qPCR SuperMix-UDG (Invitrogen) and gene specific primers (Mas forward: TTTATAGCCATCCTGAGCTTCC, Mas reverse: AATGTGGTGTAGGTCCCAAAG, MrgD forward: AAACCTATTCCAGAGGGAGCACA, MrgD reverse: TGGACCTTGTCAGTGGTATTGA). The amplifications were performed in a final volume of 20µl using the following PCR cycle: 95°C for 15min followed by 40 cycles with denaturation at 95°C for 30sec, annealing at 58°C for 30sec and elongation at 72°C for 30sec. PCR products were finally subjected to a melting curve analysis. The mRNA levels were quantified with the StepOne™ analysis software in comparative quantitation mode and normalized to beta-Actin expression levels. All quantitative RT-PCRs were done at least three times in duplicate using RNA from independent experiments.

***In silico* modelling**

The 3-dimensional structure of Ang-(1–7) was prepared by minimizing their nuclear magnetic resonance experimental structures (PDB:2JP8) with Schrödinger MacroModel (MacroModel, version 9.7, Schrödinger, LLC, New York, NY), using AMBER94 force field and water solvent. It was further docked (keeping the backbone rigid) with Autodock 4.2.3 [362] into a modeled structure of the Mas receptor [385], in which the F112 side chain conformation was further modified to create a larger binding site and to expose specific binding residues [364, 365]. The complex was minimized as before. Surface areas and electrostatic potentials were computed with Schrödinger Maestro (Maestro, version 11.3.016, Release 2017-3, Platform Linux-x86_64, Schrödinger, LLC, New York, NY).

Statistical Analyses

To ensure reproducibility of the results and to minimize bias, HEK293 cells, MC, and HUVECs were used at comparable passage numbers. The same kits and reagents were used for the experiments wherever possible. Data presented are mean \pm SEM where n denotes the number of experiments in triplicates. A *P*-value of <0.05 was considered statistically significant. Data were analysed using GraphPad Prism 6.0 (GraphPad Software Inc., San Diego, CA, USA). Statistical tests performed were a Student's *t*-test or a one-way analysis of variance (ANOVA) tests accompanied by Bonferroni post hoc test.

Results

Ala¹-Angiotensin-(1-7) stimulates the generation of intracellular cAMP in endothelial cells

As we previously demonstrated that Ang-(1-7) can increase intracellular cAMP in a dose-dependent manner [378], we first tested whether Ala¹-Ang-(1-7) can act in a similar manner using the most commonly characterized endothelial cell-line, human umbilical vein endothelial cells (HUVEC). Although Ala¹-Ang-(1-7) was comparably as efficient as Ang-(1-7), the dose-response curve showed a completely different appearance (Figure 6.2.1 A). Not only is the curve bell-shaped in contrast to the one generated by Ang-(1-7) which runs into a plateau with increasing concentrations, the increase in cAMP occurs much earlier with a leftward shift of almost 3 magnitudes of order (EC₅₀ was reached at 3.6×10^{-11} M with Ala¹-Ang-(1-7) and at 1.1×10^{-8} M with Ang-(1-7)).

To investigate whether this effect on cAMP is mediated by receptors that are sensitive to the two Ang-(1-7) antagonists, A779 and D-Pro, and to the unspecific AT₂ receptor blocker PD123319, which we identified as also blocking the Ang-(1-7) receptors Mas and MrgD [378], we used Ala¹-Ang-(1-7) in the concentration of highest efficacy (10^{-9} M) without and with the 3 receptor blockers. As shown in Figure 6.2.1 B, the three compounds did not affect base-line cAMP concentrations, but all three blockers significantly reduced the increase in intracellular cAMP in response to Ala¹-Ang-(1-7).

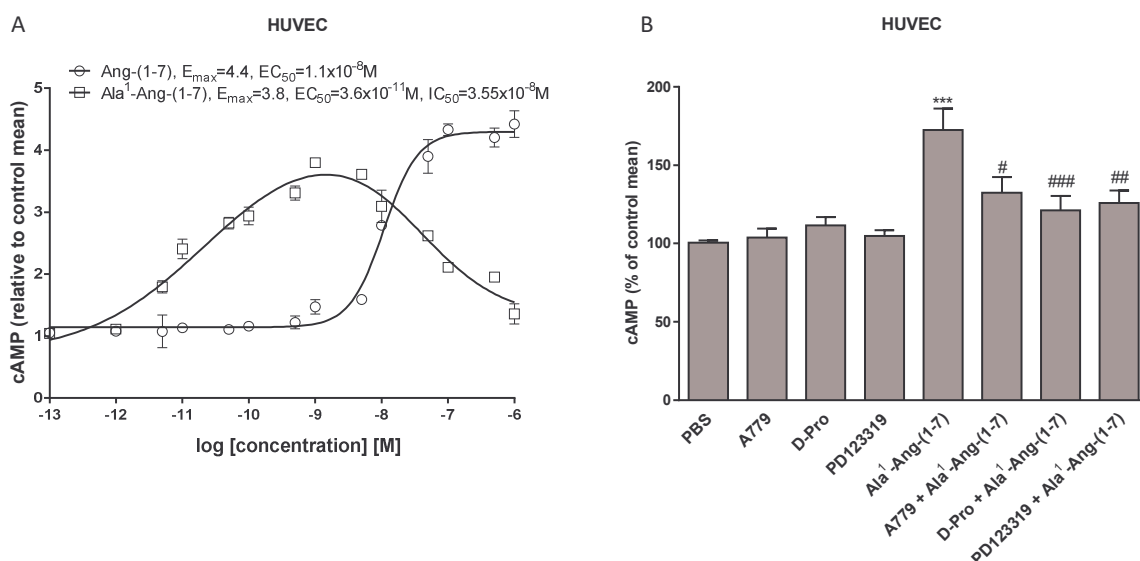


Figure 6.2.1 Intracellular cAMP is increased by Ala¹-Angiotensin-(1-7) in human umbilical vein endothelial cells (HUVEC).

(A) HUVEC were stimulated for 15min with a range of concentrations (10^{-6} to $10^{-13} M$) of Ala¹-Ang-(1-7) before analysis of cAMP concentration. (B) HUVEC were stimulated for 15min with blockers (A779, D-Pro⁷-Ang-(1-7) (D-Pro) and PD123319 (all $10^{-6} M$)), followed by 15min stimulation with Ala¹-Ang-(1-7) ($10^{-9} M$). Results are expressed as mean \pm SEM; (A) $n=3$, (B) $n=4$. Data was reported as a fold change or percentage of the untreated control mean. *** $P<0.001$, significantly different from control; ### $P<0.001$, ## $P<0.01$ or # $P<0.05$, significantly different from Ala¹-Ang-(1-7); ANOVA with Bonferoni post-hoc test.

Ala¹-Angiotensin-(1-7) stimulates the generation of intracellular cAMP in HEK293 cells expressing MrgD

Based on our work with Ang-(1-7) [378] and the results published by Lautner *et al.*, [42], we then tested Mas- and MrgD-transfected cells. As shown in Figure 6.2.2 A, Ala¹-Ang-(1-7) stimulation caused a dose-dependent increase in the intracellular cAMP level in MrgD-transfected cells with an EC₅₀ of 3.98×10^{-13} M. Since in HUVEC the dose-response curve peaked at 10^{-9} M of Ala¹-Ang-(1-7) but in MrgD-transfected cells at 10^{-11} M, we selected 10^{-11} M for further tests with the previously effective blockers. Figure 6.2.2 B shows that none of the 3 blockers had a baseline effect on cAMP levels in the pcDNA3.1 control or in MrgD-transfected cells. However, the increase in cAMP concentration generated by Ala¹-Ang-(1-7) in MrgD-transfected cells was blocked by D-Pro and PD123319, but not by A779 (Figure 6.2.2 B).

Ala¹-Ang-(1-7) in higher concentrations activates G_{αi} reducing the generation of cAMP

As cAMP is generated by the enzyme adenylyl cyclase which can be activated by G_{αs} but also inhibited by G_{αi} signalling, we hypothesised that the bell-shaped curve could be the result of a G_{αi} activation due to higher concentrations of Ala¹-Ang-(1-7). We used MrgD receptor-transfected cells and generated dose-response curves for Ala¹-Ang-(1-7) with and without pre-treatment with pertussis toxin (PTX), a G_{αi} inhibitor, which prevents the G_{αi} proteins from interacting with the receptor. Since the G_{αi} subunits remain locked in their inactive state, they are unable to inhibit adenylylase activity. As shown in Figure 6.2.2 C, the parallel treatment with PTX prevented the decline in intracellular cAMP concentrations with increasing concentrations of Ala¹-Ang-(1-7).

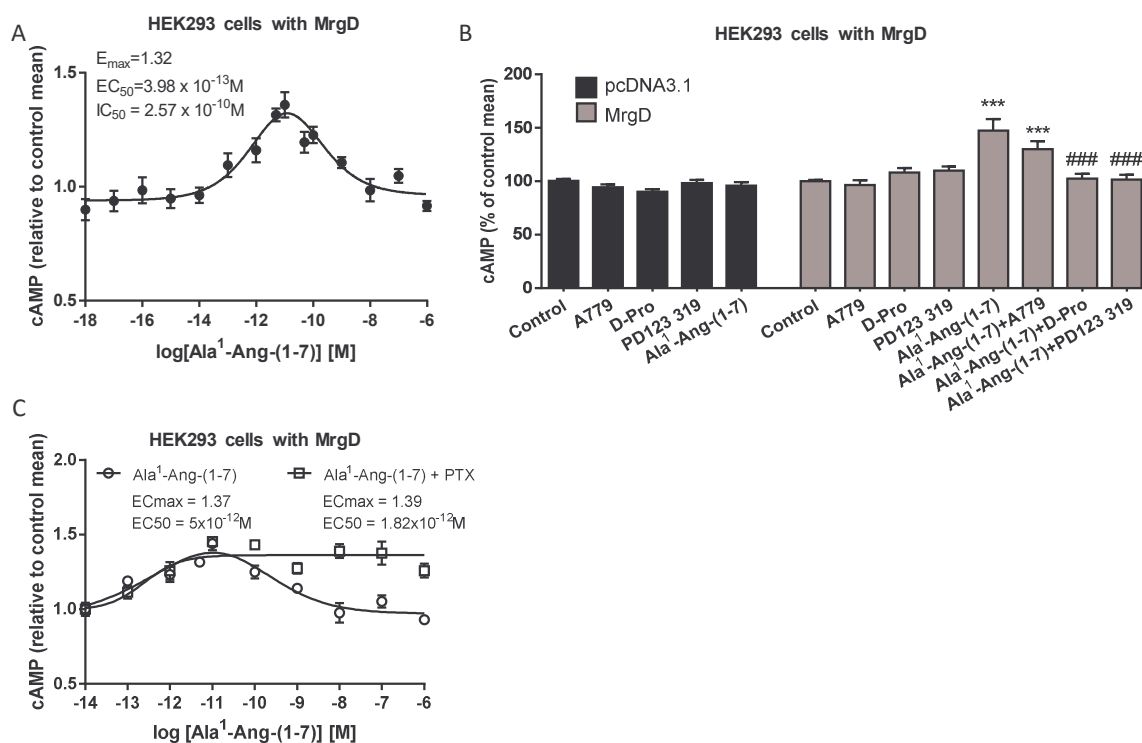


Figure 6.2.2 Ala¹-Ang-(1-7) signals through the MrgD receptor.

(A) MrgD-transfected HEK293 cells were stimulated for 15min with a range of concentrations (10^{-6} to $10^{-18}M$) of Ala¹-Ang-(1-7) before analysis of cAMP concentration. (B) Cells were stimulated for 15min with blockers (A779, D-Pro⁷-Ang-(1-7) (D-Pro) and PD123319 (all $10^{-6}M$)), followed by 15min stimulation with Ala¹-Ang-(1-7) ($10^{-11}M$). (C) Cells were stimulated for 15min with PTX (50ng/ml) followed by stimulation with Ala¹-Ang-(1-7) ($10^{-11}M$) for a further 15min. Results are expressed as mean \pm SEM; (A) $n=5$, (B) $n=4$ and (C) $n=3$. Data was reported as a fold change or percentage of the untreated control mean. *** $P<0.001$, significantly different from the MrgD control; ### $P<0.001$, significantly different from Ala¹-Ang-(1-7); ANOVA with Bonferoni post-hoc test.

Ala¹-Angiotensin-(1-7) stimulates the generation of intracellular cAMP in HEK293 cells expressing Mas

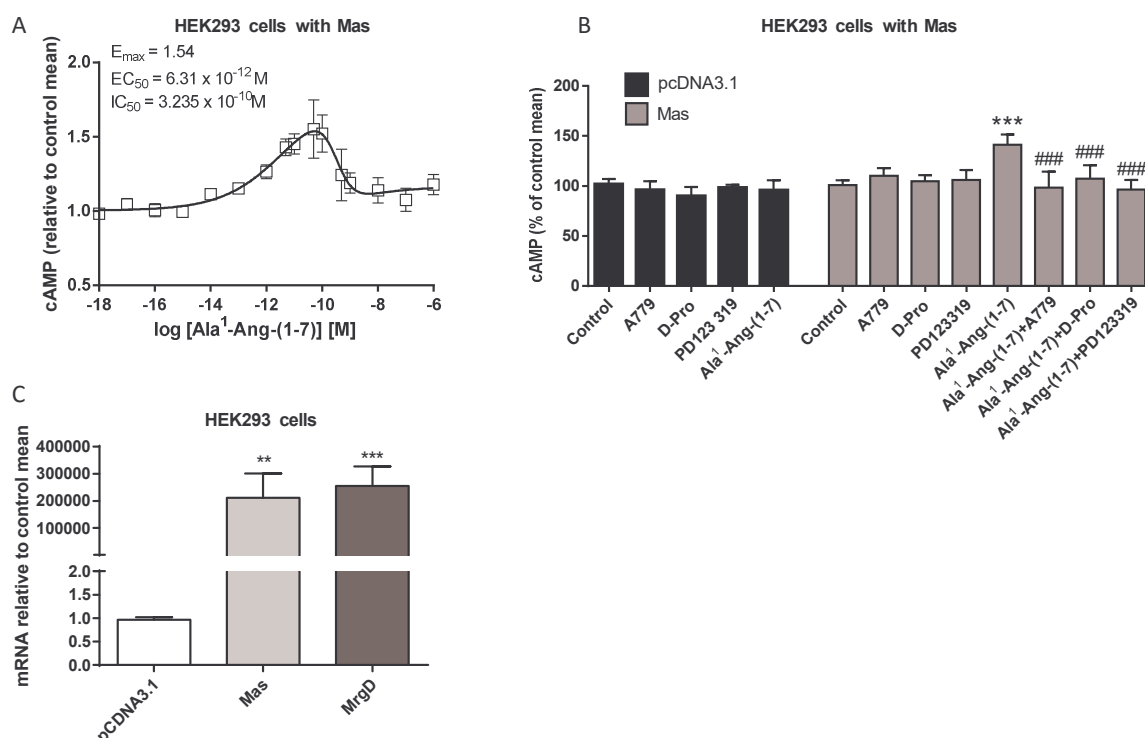


Figure 6.2.3 *Ala¹-Ang-(1-7) can also signal via the Mas receptor.*

(A) *Mas*-transfected HEK293 cells were stimulated for 15min with a range of concentrations (10^{-6} to $10^{-18}M$) of *Ala¹-Ang-(1-7)* before analysis of cAMP concentration, (B) Cells were stimulated for 15min with blockers (A779, D-Pro7-Ang-(1-7) (D-Pro) and PD123319 (all $10^{-6}M$)), followed by 15min stimulation with *Ala¹-Ang-(1-7)* ($10^{-11}M$). (C) mRNA of *Mas* and *MrgD*-transfected HEK293 cells (pcDNA3.1 values are set as 1). Results are expressed as mean \pm SEM; (A) $n=4$, (B) $n=3$ and (C) $n=8$. Data was reported as a fold change or percentage of the untreated control. *** $P<0.001$, ** $P<0.01$, significantly different from the *Mas* control; ### $P<0.001$, significantly different from *Ala¹-Ang-(1-7)*; ANOVA with Bonferoni post-hoc test and Students T-test (C).

In experiments with HEK293 cells transfected with the Mas receptor, Ala¹-Ang-(1-7) also caused a dose-dependent increase in cAMP concentration with an EC₅₀ value of 6.3pM reaching highest efficacy at 5 x 10⁻¹¹M (Figure 6.2.3 A). In contrast to MrgD-transfected cells, D-Pro, PD123319 and A779 all blocked the Ala¹-Ang-(1-7)-mediated increase in cAMP level in Mas-transfected cells (Figure 6.2.3 B).

To confirm specific overexpression of mRNA for both receptors, we measured expression of receptor mRNA in MrgD and Mas-transfected cells to confirm transfection efficacy. As shown in Figure 6.2.3 C, transfection with Mas- or MrgD- plasmids led to a significant overexpression of the receptor mRNA.

To visualise the transfection efficacy on protein level, HEK293 cells were transfected with Mas-mCherry or MrgD-GFP. As shown in Figure 10.1.1 B (Appendix part 1), transfected cells carrying not just the receptor cDNA, but both receptors are expressed in the cytoplasmic membranes of these cells.

Absence of Ala¹-Angiotensin-(1-7)-mediated cAMP generation in mesangial cells derived from Mas/MrgD knockout animals

To test whether the lack of Mas and MrgD blunts the ability of Ala¹-Ang-(1-7) to generate cAMP in primary mesangial cells, as previously examined in Ang-(1-7), we used mesangial cells derived from double knockout mice deficient in both receptors, a strain introduced recently [378]. Ala¹-Ang-(1-7) increased cAMP dose-dependently in wild-type mesangial cells, with a typical bell-shape curve as shown before in endothelial cells and Mas or MrgD-transfected HEK cells. (Figure 6.2.4 A).

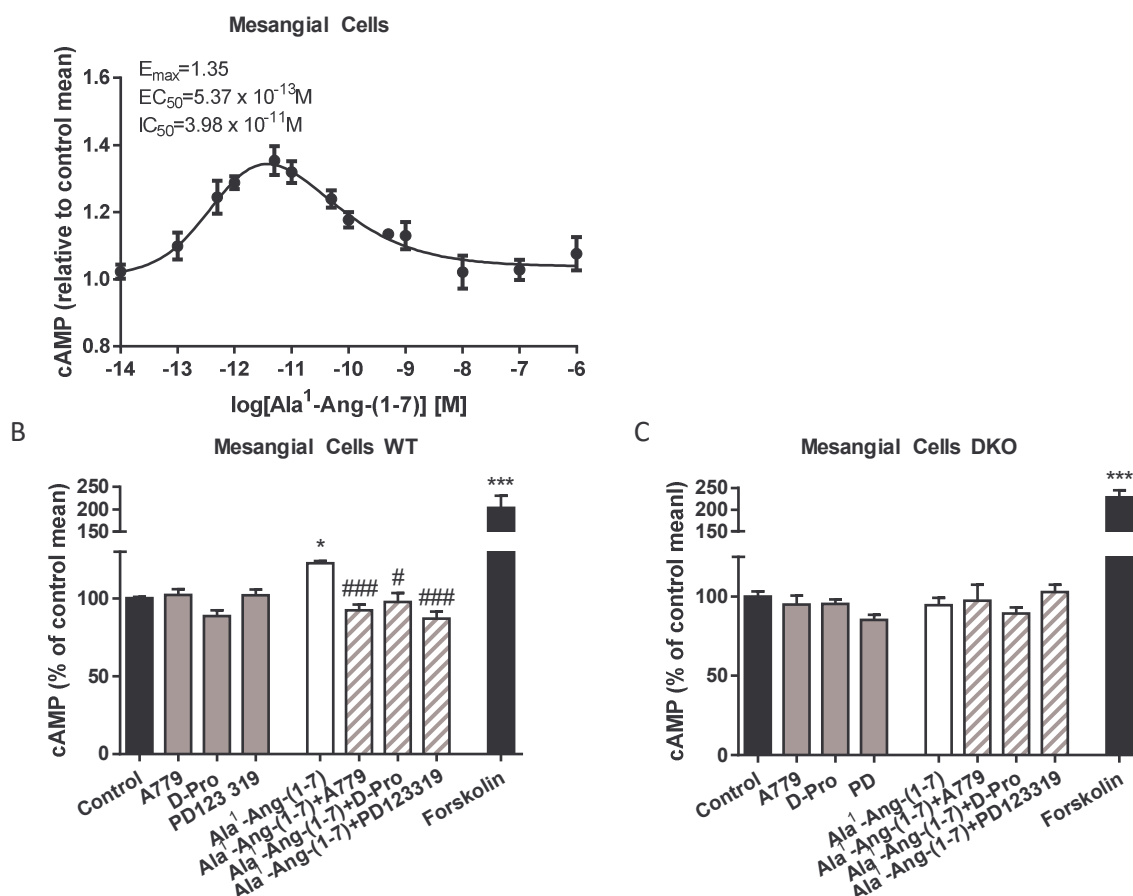


Figure 6.2.4 Ala¹-Ang-(1-7) induced signalling is absent in mesangial cells derived from Mas/MrgD double-knockout animals.

(A) WT C57BL/6 mesangial cells were stimulated for 15min with a range of concentrations (10^{-6} to $10^{-14}M$) of Ala¹-Ang-(1-7) before analysis of cAMP concentration. (B) WT C57BL/6 mesangial cells were stimulated for 15min with blockers (A779, D-Pro⁷-Ang-(1-7) (D-Pro) and PD123319 (all $10^{-6}M$)), followed by 15min stimulation with Ala¹-Ang-(1-7) ($10^{-11}M$). (C) Mas/MrgD knockout (DKO) mesangial cells were stimulated for 15min with blockers (A779, D-Pro⁷-Ang-(1-7) (D-Pro) and PD123319 (all $10^{-6}M$)), followed by 15min stimulation with Ala¹-Ang-(1-7) ($10^{-11}M$). Results are expressed as mean \pm SEM; (A) $n=6$, (B) $n=5$ & (C) $n=2$. Untreated control values of each genotype is set as 100%. *** $P<0.001$, * $P<0.05$, significantly different from WT control mean; ### $P<0.001$, # $P<0.05$, significantly different from Ala¹-Ang-(1-7); ANOVA with Bonferoni post-hoc test.

While D-Pro, PD123319 and A779 did not affect base-line cAMP concentrations in mesangial cells, all three compounds blocked the Ala¹-Ang-(1-7)-mediated increase in

cAMP level in these wild-type cells (Figure 6.2.4 B). This cAMP increase observed in wild-type mesangial cells was completely blunted in mesangial cells isolated from double-knockout mice (Figure 6.2.4 C), but still remaining in the single knockouts (see appendix Figure 10.2.1). In addition, Forskolin, a direct adenylyl cyclase activator, increased cAMP concentration in DKO mesangial cells, illustrating that the lack of stimulation by Ala¹-Ang-(1-7) is not based on a general inefficacy of the cells to generate cAMP in response to stimulation.

Discussion

Here, we demonstrate that Ala¹-Ang-(1-7), like Ang-(1-7), stimulates the generation of the second messenger, cAMP, and cAMP is thus an ideal tool to quantify changes in intracellular signalling mediated by Ala¹-Ang-(1-7). Using this readout allowed us to provide final pharmacological evidence that MrgD is a functional receptor for Ala¹-Ang-(1-7). More importantly, the use of cAMP as a readout enabled us to generate results providing the first experimental proof that Mas is the second receptor for Ala¹-Ang-(1-7). Furthermore, our data confirm findings with Ang-(1-7) [378], that A779 fails to significantly reduce the stimulation of cAMP production by Ala¹-Ang-(1-7) in MrgD-transfected cells. This may be due to the D-orientation of alanine in position 7, which might prevent the peptide fitting into the MrgD receptor, while it still fits into Mas and thus, can block the agonist effects there.

Previous work by other groups implicated that the two Ang peptides, Ang-(1-7) and Ala¹-Ang-(1-7) target different receptors, with Ala¹-Ang-(1-7) stimulating MrgD but not Mas [42]. Our data shows that not only can Ang-(1-7) can signal via Mas and MrgD, but

also the decarboxylated version of the heptapeptide, Ala¹-Ang-(1-7). One of the reasons for this discrepancy might be due to our finding that Ala¹-Ang-(1-7) generates a bell-shaped dose response curve and is much more potent than Ang-(1-7). Consequently, at concentrations where Ang-(1-7) is most efficient, Ala¹-Ang-(1-7) might have little effect as it is back to base-line levels of cAMP. However, since we measured cAMP, while others looked at NO release, it would be interesting to see whether increasing concentrations of Ala¹-Ang-(1-7) would also generate a dose-response curve for NO, with highest efficiency similar to the EC₅₀ described here for receptor-transfected cells and primary kidney and endothelial cells. Nevertheless, our findings are also supported by modelling of Ang-(1-7) in the Mas receptor binding site, in which the decarboxylation of the first residue could lead to a more favorable electrostatic complementary with the receptor surface and thus, making it likely that the Mas receptor could also be a receptor for Ala¹-Ang-(1-7).

While our data excludes a receptor fingerprint discriminating between both peptides, one of the key findings of our experiments is that Ala¹-Ang-(1-7) is much more potent than Ang-(1-7), although the difference between both peptides seems marginal, with only a lack of the carboxylate group in Ala¹-Ang-(1-7).

To better understand the reason for improved potency, we investigated the potential binding mode of the N-terminal segment of Ang-(1-7), as well as the electrostatic potential of the binding site and its complementarity to both Ang-(1-7) and Ala¹-Ang-(1-7). The proposed binding mode of Ang-(1-7) places Arg² establishing a salt bridge with Glu¹⁶⁷ and a cation- π interaction with Tyr²⁴⁸ of the Mas receptor. These interactions constrain the mobility of the N-terminal part of Ang-(1-7) and prevent the negatively charged carboxylate in Asp¹ side chain from interacting with a positive chemical group in

the protein (see Figure 6.2.5). Actually, the surface of the binding site is estimated with a positive surface area value of 5 Å² and a much greater negative surface area value of 109 Å² (considering residues within 5 Å of Ang-(1-7)). This predominance of a negatively charged protein surface is more stressed on the extracellular side (where the N-terminal Ang-(1-7) is predicted to bind), as seen in Figure 6.2.5. Thus, the Asp¹ side chain may not be stabilised according to the proposed model due to charge repulsion, although the water accessibility of this area could screen this effect.

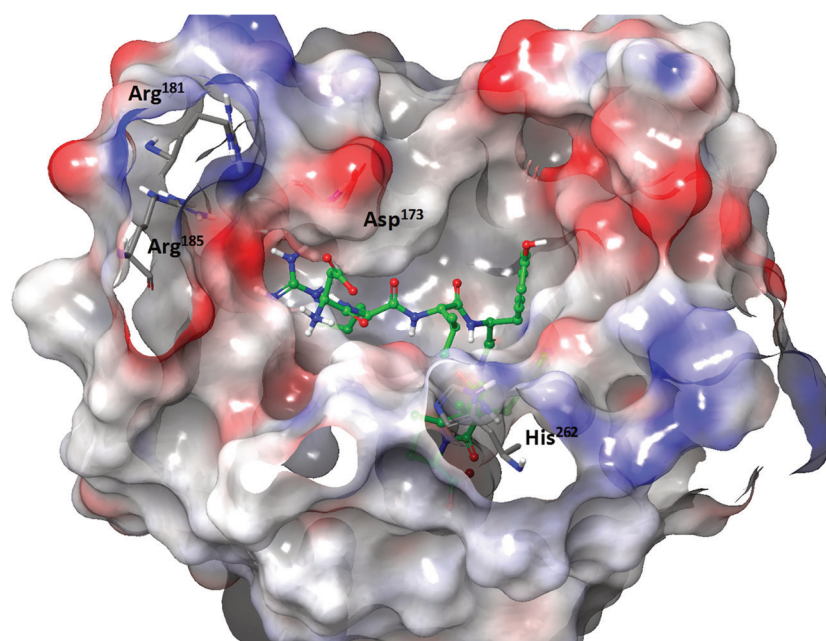


Figure 6.2.5 Electrostatic potential of Mas receptor model in the predicted Ang-(1-7) binding site (considering residues within 10 Å of Ang-(1-7)).

Red areas are favourable to interact with positively charged groups and blue with negatively charged groups. Predicted binding pose of Ang-(1-7) is depicted in green-coloured carbon atoms.

These predictions are in agreement with the increased potency observed for Ala¹-Ang-(1-7) because: i) it does not have the carboxylate group in the first residue, thus avoiding a charge repulsion with the predominant negatively charged area; and ii) this same absence may favour a salt bridge between the N-terminal amino group and the Mas receptor,

particularly with Asp¹⁷³. Thus, the interactions extracted from this model might build the base for a screening program to identify agonists stimulating Mas and MrgD.

Another very dominant pharmacodynamic difference between the two peptides is the bell-shaped dose-response curve for Ala¹-Ang-(1-7). There are hints in the literature, which might explain this bell-shaped dose-response curve. Since the late nineties, different groups have shown the β 2-adrenergic receptor to couple not only to $G_{\alpha s}$, but also to $G_{\alpha i}$ proteins in the heart [386, 387] and in receptor-transfected HEK293 cells [388], whereby the degree of activation of the two G proteins would define the agonist effect on intracellular cAMP concentrations. Interestingly, it has been also shown that this dual activation is not specific for the β 2-adrenergic receptor but has also been seen in histamine, serotonin, and glucagon receptors [389].

A decade ago, Beyermann *et al.* [390] confirmed this model by using the corticotropin-releasing factor receptor type 1. They demonstrated that native ligands stimulated $G_{\alpha i}$ and $G_{\alpha s}$ proteins, whereby in all cases, $G_{\alpha i}$ has been activated approx. two magnitudes of order to the right. Therefore, we tested whether Ala¹-Ang-(1-7) could also lead to an $G_{\alpha i}$ activation in higher concentrations, reducing the $G_{\alpha s}$ -mediated increase in cAMP. By using PTX, a substance that prevents $G_{\alpha i}$ -associated inhibition of adenylyl synthase leading to a reduction in intracellular cAMP, the decline in the dose response curve observed with Ala¹-Ang-(1-7) alone, disappeared. The curve runs in a plateau following PTX treatment and looked similar to the Ang-(1-7) curve, although with a significant leftward shift. Thus, it looks like Ala¹-Ang-(1-7), but not Ang-(1-7) can activate two G proteins, and thus, similar to a car, by pressing the gas and brake pedal, it brings the speed (an increase in cAMP) to zero.

The authors are aware that limitations of our study include the lack of knowledge in whether the decarboxylation of Ang-(1-7) to Ala¹-Ang-(1-7) results in any loss or gain of function *in vivo*, which can only be evaluated by animal and human studies. However, the enzyme being responsible for the reaction is still unidentified and thus, its inhibition / knockout *in vivo* can still not be experimentally realized.

Taken together, our results change the view on Ala¹-Ang-(1-7) as a peptide exclusively activating MrgD but not Mas, illustrate that minor changes in Ang-(1-7) (decarboxylation on amino acid 1) can lead to major changes in the pharmacodynamics of both receptors and provide a mechanistic explanation for such differences. Thus, our data lays the foundation for the development of new Ang-(1-7) analogues which may generate a more potent stimulation of the receptors and hence, leading to safer and more efficient treatment options for a growing number of diseases in which Ang-(1-7) might be beneficial, based on its success in preclinical disease models.

Financial Support

The work was supported by grants of the Deutsche Forschungsgemeinschaft (WA1441/22-1 and 2).

Disclosures

TW is inventor of the patent "Use of an Ang-(1-7) receptor agonist in acute lung injury" (Application No: 08016142.5-2107). TW is scientific advisor of Tarix Pharmaceuticals LTD (Boston, USA).

6.3 The AT2 receptor agonist, C21, also stimulates the Mas and MrgD receptor

Anja Tetzner, MSc^{1*}; Maura Naughton, MSc^{1*}; Kinga Gebolys, PhD¹; Susana Vallejo^{2,3}; Esther Sala, PhD⁴; Concepcion Peiró, PhD^{2,3}; Óscar Villacañas, PhD⁴; Thomas Walther, PhD^{1,5}

¹Dept. Pharmacology and Therapeutics, School of Medicine and School of Pharmacy, University College Cork (UCC), Cork, Ireland;

²Department of Pharmacology, Facultad de Medicina, Universidad Autonoma, Madrid, Spain

³Instituto de Investigación Sanitaria Hospital Universitario La Paz (IdiPAZ), Madrid, Spain

⁴Intelligent Pharma, Barcelona, Spain;

⁵Institute of Medical Biochemistry and Molecular Biology, University Medicine Greifswald, Greifswald, Germany.

*Equally contributing first authors

Address for correspondence: Prof. Thomas Walther, Department Pharmacology & Therapeutics, Western Gateway Building, Western Road, University College Cork, Cork, Ireland; Phone: +353-21-420-5973, Fax: +353-21-4205471, E-mail: t.walther@ucc.ie

Submitted: 25.03.2018 to Hypertension

Current State: under revision

Hypothesis:

C21 is not an AT2 specific agonist, but also interacts with other receptors such as Mas and MrgD.

Aim of the study:

Previous experiments indicated that PD123319 is not an AT2 specific antagonist, therefore the aim of the study was to test whether the AT2 receptor agonist, C21, is specific. Using receptor-transfected HEK293 cells, human endothelial cells, receptor-deficient primary mesangial cells, isolated mesenteric microvessels, and a variety of receptor blockers the interaction with the two Ang-(1-7) receptors, Mas and MrgD (ligand/receptor pharmacology), was determined.

Author contributions

Anja Tetzner performed experiments for Figure 1-4, developed the images for the figures and worked on the manuscript.

Maura Naughton performed part of experiments for Figure 1-4, and worked on the manuscript.

Kinga Gebolys performed experiments for Figure 1 A and B.

Óscar Villacañas analysed the ligand-protein interactions and supervised the modelling part.

Susana Vallejo and Concepcion Peiró performed the experiments for Figure 4 E.

Thomas Walther initiated the work, coordinated the experiments, advised, drafted the main text body, and finalized the manuscript.

Abstract

Compound 21 (C21) is a highly selective non-peptidic AT₂ receptor agonist. C21, like angiotensin (Ang)-(1-7), has cardiovascular protective effects. Since the chemical structure of C21 is similar to the Mas receptor-specific non-peptidic agonist AVE0991, and we recently showed that the AT₂ blocker, PD123319, can also block the effects of Ang-(1-7) at its natural receptors, Mas and MrgD, we tested whether C21 is really AT₂-specific or can also stimulate the Ang-(1-7) receptors.

Using cAMP as a readout in receptor-transfected HEK293 cells, we generated pharmacological proof that Mas ($EC_{50}=1.99 \times 10^{-12}$ mol/L) and MrgD ($EC_{50}=2.96 \times 10^{-9}$ mol/L) are functional receptors for C21, whereby the three receptor blockers, A779, D-Pro⁷-Ang-(1-7), and PD123319 showed receptor-specific effects towards C21. Furthermore, C21 elevated the cAMP concentration in primary mesangial cells ($EC_{50}=1.12 \times 10^{-6}$ mol/L). However, increases in cAMP levels and in CREB phosphorylation were still detectable in cells isolated from AT₂-deficient mice, but completely blunted in Mas/MrgD-double knockouts. In addition, C21-stimulated relaxation of isolated mesenteric arteries was abolished by Mas/MrgD blockers. Finally, *in silico* modelling illustrated the structural similarities and differences between C21, AVE0991, and Ang-(1-7).

Our results identify C21 as not being a specific AT₂ receptor agonist but also interacting with the two Ang-(1-7) receptors, Mas and MrgD. Therefore, the overlap in beneficial

effects of Ang-(1-7) and C21 might be based on the stimulation of the same receptors under specific pathophysiological circumstances. This also enforces the revisit of publications, which concluded on AT2 function by only using C21.

Key words: AT2 receptor, C21, dose-response curve, Mas receptor, MrgD receptor, renin-angiotensin system.

Introduction

The renin-angiotensin system (RAS) is an important regulator of arterial blood pressure, electrolyte homeostasis, and water and sodium intake [353], but is also involved in other processes like tissue regeneration [354]. Activation of the detrimental angiotensin (Ang) II type 1 (AT1) receptor leads to the pathogenesis of hypertension via vasoconstriction and sodium retention [14]. It is now widely known that the RAS includes further receptor subtypes opposing the actions of the AT1 receptor [14]. The Ang II type 2 (AT2) receptor and the Mas receptor are the best characterised protective receptors in the RAS, whereby they mediate tissue protective and regenerative actions, such as anti-fibrotic and anti-inflammatory actions [355].

AT2 or Mas receptor deficiency does not lead to a critical phenotype, however, if knockout animals are exposed to myocardial infarction [391], stroke [392], chronic kidney disease [393], or atherosclerosis [394], symptoms are substantially more severe than in healthy controls, indicating both receptors are protective in cardiovascular diseases.

It is well accepted that Compound 21 (C21) is a highly selective non-peptide AT2 receptor agonist [185], which has been shown to reduce blood pressure [187], and improve cardiac function following myocardial infarction [186]. As the AT2 receptor mediates beneficial

effects, C21 has been and is currently being studied in a variety of disease models, such as stroke [395], and heart failure [396].

During the past few years, also Ang-(1-7) has become a key peptide within the RAS due to its cardiovascular and renal protective effects, which often counteract the adverse actions of AngII [42]. Previously, we identified the G protein-coupled receptor Mas to be associated with Ang-(1-7)-induced signalling, which was found to be blocked by D-Ala⁷-Ang-(1-7), named A779, a specific Ang-(1-7) antagonist [397]. We also very recently discovered a second receptor for Ang-(1-7), the Mas-related G protein-coupled receptor MrgD [378]. Furthermore, we showed in that study that the primary intracellular pathway which is activated by Ang-(1-7) upon interaction with Mas or MrgD, involves adenylyl cyclase, cAMP, and phosphokinase A [378].

The interaction of Ang-(1-7) with the AT₂ receptor has been intensively discussed for almost two decades, mainly based on pharmacological studies using AT₂ blockers [355]. However, we recently showed that the AT₂ receptor blocker, PD123319, can also block the effects of Ang-(1-7) at its natural receptors, Mas and MrgD [378].

Furthermore, since other studies have shown that the Mas receptor blocker A779 can prevent the protective C21 effects in an ischemic stroke model [398], and the chemical structures of C21 and the Mas-specific agonist AVE0991 are very similar, interaction of C21 with Mas seems likely.

Therefore, we aimed to test whether the AT₂ receptor agonist C21 is, similar to the AT₂ blocker PD123319, not specific and can interact with the two Ang-(1-7) receptors Mas and MrgD. In particular, we focused on the characterisation of the ligand/receptor pharmacology, by determining efficiency and potency using receptor-

transfected HEK293 cells, human endothelial cells, receptor-deficient primary mesangial cells, isolated mesenteric microvessels, and a variety of receptor blockers.

Methods

Chemicals and reagents

Ang-(1-7), D-Ala⁷-Ang-(1-7) and D-Pro⁷-Ang-(1-7) were synthesized by Biosyntan (Berlin, Germany). HEK-293, Forskolin, RPMI-1640, trypsin/EDTA, Irbesartan, SQ22536, HEPES solution, penicillin-streptomycin, noradrenaline and sodium pyruvate were purchased from Sigma Aldrich (St. Louise, Missouri, USA). C21 was purchased from AXON Medchem B.V. (Groningen, The Netherlands). DMEM, GlutaMax and Fetal Bovine Serum (FBS) were purchased from BioScience (Dun Laoghaire, Dublin, Ireland). PD123319 was from Parke-Davis Pharmaceutical Research (Detroit, Michigan, USA). PTX was bought from EMD Millipore (Billerica, MA, USA). Polyfect transfection reagent was purchased from Qiagen (Crawley, U.K.). HUVEC and EBM-2 media were purchased from PromoCell (Heidelberg, Germany).

Animals

Mice deficient in both Mas and MrgD (double knockout) [378] or deficient in AT2 [399, 400] have been bred and housed in the animal facilities at UCC, Cork, Ireland. Animal studies are reported in compliance with the ARRIVE guidelines.[382] Experiments performed conformed with the guidelines from Directive 2010/63/EU of the European Parliament on the protection of animals used for scientific purposes.

Cell culture conditions, transfection and stimulation

Human embryonic kidney (HEK293) and Balb/c-3T3 cells were cultured in DMEM medium supplemented with FBS (10%), HEPES buffer (1%), sodium pyruvate (1%), and L-glutamine (1 %) and maintained under standard conditions (5% CO₂, 95% humidity and 37°C). Cells were cultured and transfected as described previously [378]. After pre-incubation with A779, D-Pro or PD123319 (10⁻⁶mol/L) or PTX (50ng/ml) for 15min, the solvent, C21 (10⁻⁷mol/L) was added for 15min and cells were lysed immediately after [378].

Isolation and culture of primary cells and their stimulation

Kidney mesangial cells (MC) were isolated from 9-11 week old mice deficient in Mas and MrgD (double knockout) [378], or deficient in AT2 [399, 400] and also from their age- and gender-matched C57/BL6 controls, according to the protocol previously described [384].

Primary human umbilical vein endothelial cells (HUVEC) were purchased from PromoCell (Heidelberg, Germany). Primary cells were cultured and stimulated as described by Tetzner & Gebolys *et al* [378]. For the test of the adenylyl cyclase inhibitor (SQ22536), cells were pre-stimulated with 2x10⁻⁶mol/L for 15min, followed by stimulation with C21 at 10⁻⁷mol/L for another 15min.

Measurement of cAMP in cell lysates

cAMP concentration in cell lysates was determined using Direct cAMP ELISA kit (Enzo Life Sciences Ltd., Exeter, United Kingdom), as previously described [378]. The cAMP

concentration of the samples was determined from the non-linear standard curve using GraphPad Prism 6.0 software.

Dual luciferase assay (DLR)

The protocol for Dual-Luciferase reporter assays has been described in detail previously [65]. In brief, HEK293 cells were seeded in 48-well plates (75,000 cells/well). About 24h later, cells were transiently transfected with 100 ng eukaryotic expression vectors of AT1 or Mas, together with 25ng pELK-Luc Reporter Vector (Signosis, Santa Clara, California, USA) luciferase reporter plasmids and 25ng pRL-TK (Promega GmbH, Mannheim, Germany). After 6h of stimulation with C21 (10^{-14} mol/L to 10^{-6} mol/L or AngII (10^{-6} mol /L), cells were lysed and incubated on a shaker for 15min at RT [378].

Western blot analyses

The protocol has been described in detail previously [378]. In short, twenty five µg protein were separated on 10 % SDS-polyacrylamide gels. PVDF membrane was incubated with the primary antibodies: CREB, pCREB, (1:1,000 dilution in 5% BSA/TBS-T) purchased from Cell Signalling Technology (Danvers, MA, USA) or the anti-GAPDH antibody (1:5,000 in 5% milk/TBS-T) from Sigma Aldrich (St. Louise, Missouri, USA), at 4°C overnight. Blots were incubated with the appropriate horseradish peroxidase (HRP)-conjugated secondary antibodies: anti-rabbit IgG in the dilution of 1:2,000 in 5% milk/ TBS-T (Cell Signalling Technology) or 1:1,000 in 5% milk/TBS-T (Sigma Aldrich) at room temperature for 2h. The membranes were developed using the enhanced chemiluminescence (ECL)-based system

(Roche Holding AG, Basel, Switzerland). Densitometric evaluation was performed with ImageJ software (National Institute of Health, USA).

Vascular reactivity in mesenteric microvessels

Three-month-old male C57BL6 mice were used for analysing vascular reactivity. Prior to the experiments, the animals were briefly exposed to carbon dioxide in a chamber until they fell unconscious and were then immediately culled by cervical dislocation. Third-branch mesenteric arteries (mean internal diameter ranging between 150 and 200 μ m) were mounted as ring preparations on a small-vessel myograph to measure isometric tension as described before [109]. Arteries were contracted with 10 μ mol l⁻¹ noradrenaline, and then the vasoactive response to C21 (1pmol l⁻¹ to 1 μ mol l⁻¹) was tested by adding increasing concentrations of the drug. In some cases, the mesenteric segments were preincubated for 15min with the D-Pro-Ang-(1-7) (1 μ mol l⁻¹) or PD123319 (1 μ mol l⁻¹), before addition of NA.

***In silico* modelling**

Ang-(1-7)-Mas complex was modelled as described previously [378]. The resulting Mas structure was used in the docking calculation. Docking of C21 was performed with Glide version 74011 (Schrödinger LCC, New York, NY), setting the center of the grid box to the centroid of Ang-(1-7) as modelled and scaling the vdW radii of ligand atoms with a charge value lower than 0.15 with a factor of 0.80. C21 was prepared with LigPrep version 41011 coupled with Epik version 39011 (Schrödinger LCC, New York, NY), setting pH to 7.4 \pm 2.

AVE0991 was prepared equivalently with LigPrep and superposed to the resulting docked pose of C21 with the flexible alignment option in Maestro (Schrödinger LCC, New York, NY).

Statistical Analyses

Data presented are mean \pm SEM, where n denotes the number of experiments in triplicates. A *P*-value of <0.05 was considered statistically significant. To ensure reproducibility and to minimize bias, HEK293 cells, MC, and HUVECs were used at comparable passage numbers throughout the repeated experiments. The same kits and reagents were used for the experiments wherever possible. Data were analysed by Student's *t*-test or one-way analysis of variance (ANOVA) tests accompanied by Bonferroni post hoc test using GraphPad Prism 6.0 (GraphPad Software Inc., San Diego, CA, USA).

Results

C21 stimulates the generation of intracellular cAMP in HEK293 cells expressing Mas

Since C21 has structural similarities to the Masagonist AVE0991 [398], we first tested in experiments with Mas-transfected HEK293 cells, whether C21 can also stimulate the Ang-(1-7) receptor. The successful overexpression of Mas was demonstrated using qPCR analysis and fluorescence microscopy as shown in Figure 10.1.1 of the supplemental data provided in Appendix part 1. As shown in Figure 6.3.1A, C21 caused a dose-dependent increase in cAMP concentration with an EC₅₀ value of 1.995 pmol/L reaching highest efficacy at 10⁻¹⁰ mol/L. Using the concentration of highest efficacy, we investigated the effect of blockers which have been shown to target the Mas receptor, D-Pro, PD123319, and A779 [378]. None of the 3 blockers had a baseline effect on cAMP levels in cells transfected with the control plasmid, pcDNA3.1, or in Mas-transfected cells. However, the increase in cAMP concentration generated by C21 in Mas-transfected cells was fully blocked by D-Pro and PD123319, but only partially by A779 (Figure 6.3.1 B).

We then tested whether the increase in cAMP was adenylyl cyclase dependent. SQ22536 blunted the C21 effect but had no significant effect on baseline cAMP levels (Figure 6.3.1 C). To exclude that the C21 induced increase of cAMP is mediated by less G_{αi} activity and thus higher adenylyl cyclase activity, Mas-transfected HEK cells were stimulated with C21 and co-treated with PTX, a G_{αi} inhibitor, whereby PTX failed to reduce the C21-mediated increase in intracellular cAMP (Figure 6.3.1 D).

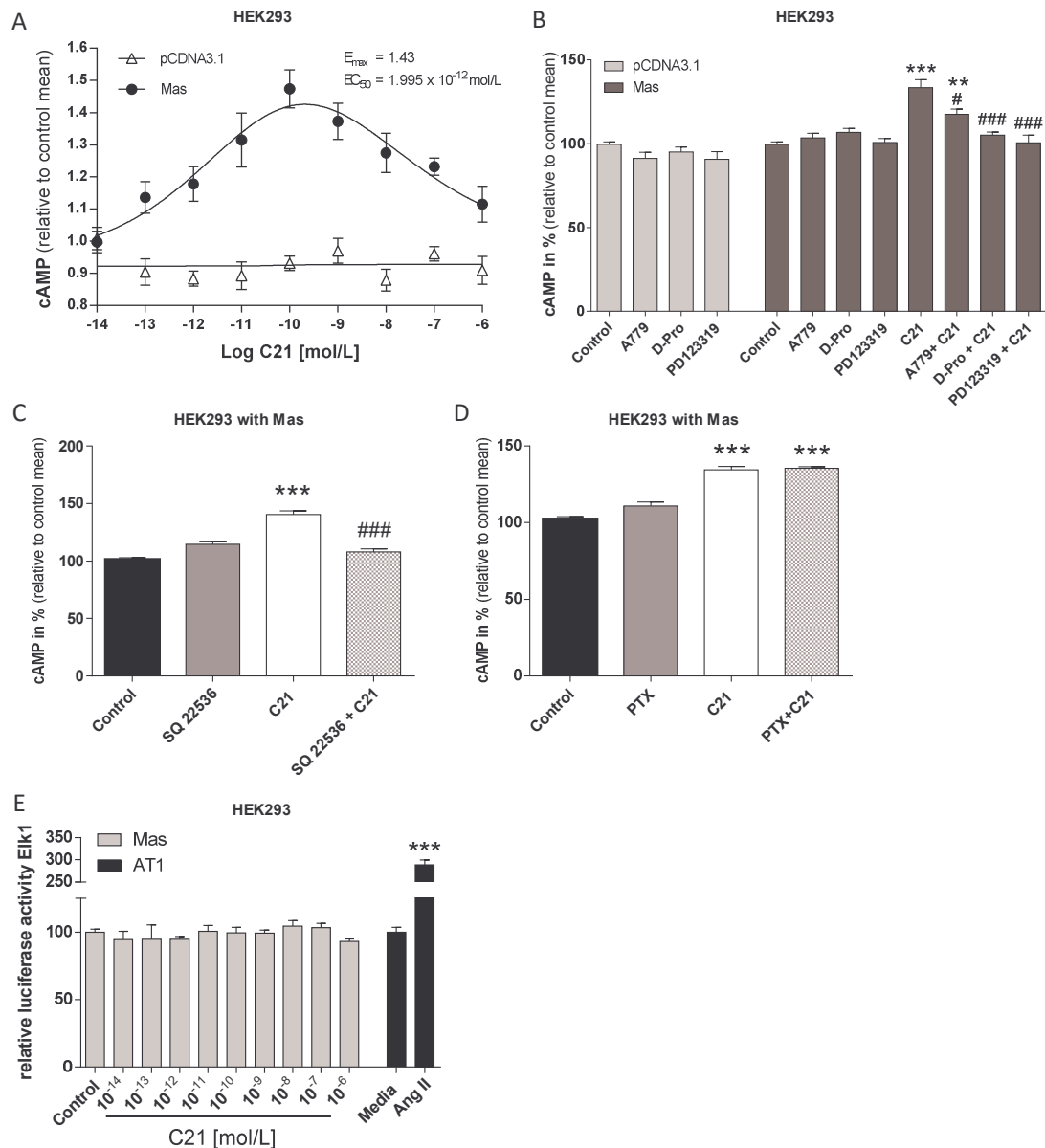


Figure 6.3.1 C21 signals via the Mas receptor.

(A) Mas or pcDNA-transfected HEK293 cells were stimulated for 15min with a range of concentrations of C21 before analysis of cAMP concentration. (B) Effect of blockers A779, D- D-Pro and PD123319, (all 10^{-6} mol/L) on C21 (10^{-10} mol/L)-mediated increase in cAMP.

(C) Effect of adenylyl cyclase inhibitor SQ22536, alone or in combination C21 (10^{-10} mol/L), on cAMP level. (D) Effect of $G_{\alpha i}$ inhibitor PTX, alone or in combination with C21 (10^{-10} mol/L), on cAMP level. (E) Luciferase production in HEK293 cells transiently co-transfected with pcDNA3.1, AT1, or Mas, and pElk1-Luc after stimulation with PBS, C21 or Ang II. Results are expressed as mean \pm SEM. Data was reported as a fold change or percentage of the untreated control. * $P < 0.05$, ** $P < 0.01$ *** $P < 0.001$ vs. Mas control mean, # $P < 0.05$, ## $P < 0.01$, ### $P < 0.001$ vs. C21; ONE WAY ANOVA with Bonferoni post-hoc test. $n=4$ (A,D,E), $n=6$ (B,C).

C21 effects were $G_{\alpha i}$ independent, which was further confirmed by investigating the activation of the $G_{\alpha i}$ -dependent transcription factor, Elk1. While the positive control AngII induced a significant increase in Elk1-stimulated transcription in AT1(a $G_{\alpha q/11}$ and $G_{\alpha i}$ coupled receptor)-transfected cells, C21 did not stimulate Elk1 in Mas-transfected cells (Figure 6.3.1 E).

C21 stimulates the generation of intracellular cAMP in HEK293 cells expressing MrgD

Based on our work with Ang-(1-7) showing that the heptapeptide stimulates not only Mas, but also the sequence-similar receptor MrgD [378], we then tested for effects of C21 in MrgD-transfected cells. Like for Mas, the successful overexpression of MrgD was demonstrated using qPCR analysis and fluorescence microscopy as shown in Figure 10.1.1 of the supplemental data provided in Appendix part 1. As shown in Figure 6.3.2 A, C21 stimulation caused a dose-dependent increase in the intracellular cAMP level in MrgD-transfected cells with an EC_{50} of 2.96×10^{-9} mol/L. In contrast to Mas-transfected cells, D-Pro, PD123319, and A779 all blocked the C21 (10^{-7} mol/L)-mediated increase in intracellular cAMP in MrgD-transfected cells (Figure 6.3.2 B).

To exclude that the receptor-mediated effects are only cell-type specific for HEK293, we transfected another cell type, Balb/c-3T3 cells with Mas (Figure 6.3.2 C) and MrgD (Figure 6.3.2 D). Also, in this fully independent cell type, C21 generated a dose-dependent increase in intracellular cAMP.

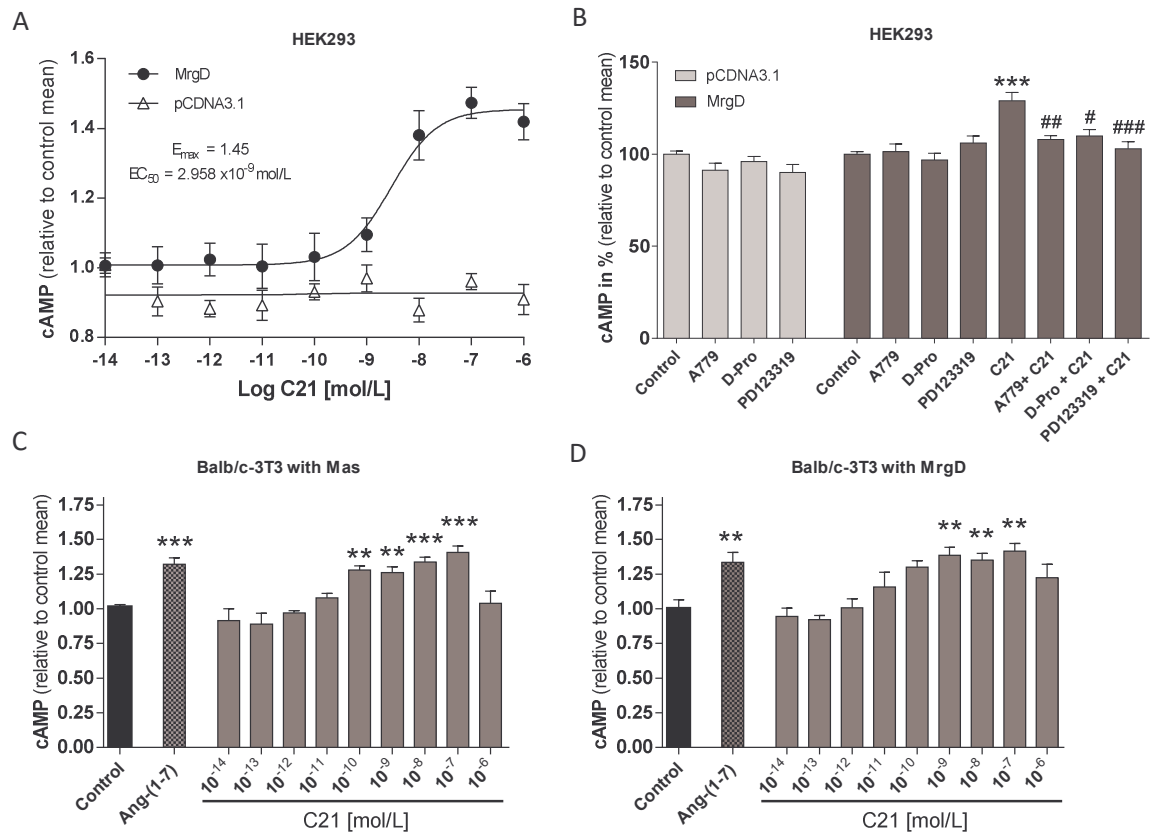


Figure 6.3.2 C21 can also signal through the MrgD receptor.

(A) MrgD or pcDNA-transfected HEK293 cells were stimulated for 15min with a range of concentrations (10^{-14} to 10^{-6} mol/L) of C21 before analysis of cAMP concentration. (B) Effect of blockers A779, D-Pro⁷-(Ang-(1-7) (D-Pro) and PD123319, (all 10^{-6} mol/L) on C21 (10^{-7} mol/L)-mediated increase in cAMP. (C) Mas-transfected Balb/c-3T3 cells were stimulated for 15min with a range of concentrations (10^{-14} to 10^{-6} mol/L) of C21 before analysis of cAMP concentration. (D) Effect of C21 in MrgD-transfected Balb/c-3T3 cells on cAMP level. Results are expressed as mean \pm SEM. Data was reported as a fold change or percentage of the untreated control mean. * $P < 0.05$, ** $P < 0.01$ *** $P < 0.001$ vs. MrgD control mean, # $P < 0.05$, ## $P < 0.01$, ### $P < 0.001$ vs. C21; ONE WAY ANOVA with Bonferoni post-hoc test. $n = 5$ (A), $n = 6$ (B), $n = 2$ (C, D).

Absence of C21-mediated cAMP generation in mesangial cells derived from Mas/MrgD knockout animals

To test whether the lack of Mas and MrgD blunts the ability of C21 to generate cAMP in primary MC, we used mesangial cells derived from double knockout mice deficient in both receptors, a transgenic strain introduced very recently [378]. C21 increased cAMP dose-dependently in wild-type MC with an EC_{50} of 1.12×10^{-10} mol/L (Figure 6.3.3 A). While D-Pro, PD123319, and A779 did not affect base-line cAMP concentrations in mesangial cells, all three compounds blocked the C21-mediated increase in intracellular cAMP in these wild-type cells (Figure 6.3.3 B). Importantly, the cAMP increase observed in wild-type mesangial cells was completely blunted in mesangial cells isolated from double-knockout mice (Figure 6.3.3 C). These cells still had a functional adenylyl cyclase and downstream signalling, as shown by normal responsiveness to the positive control Forskolin.

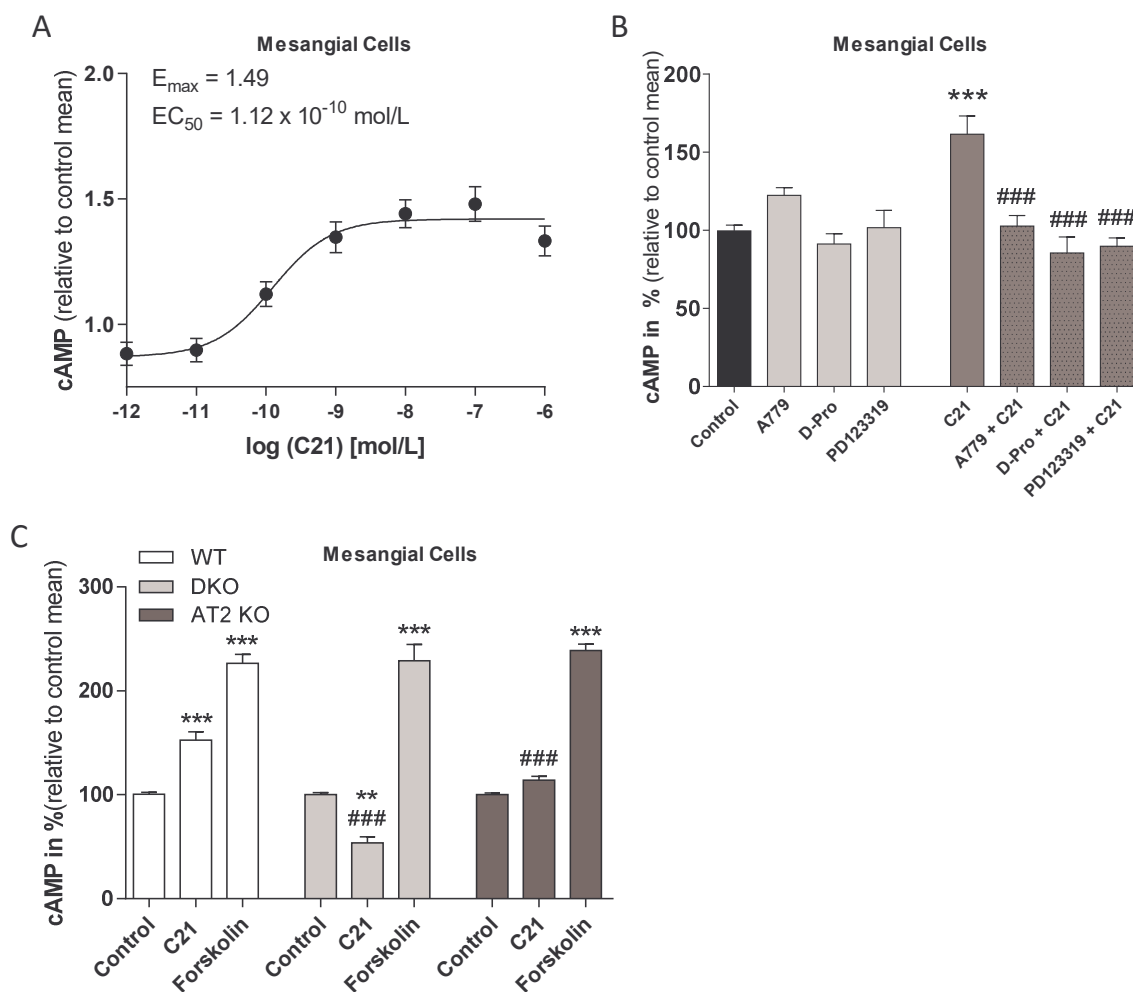


Figure 6.3.3 C21 induced signalling is absent in mesangial cells derived from *Mas/MrgD* double-knockout animals.

(A) WT C57BL/6 mesangial cells were stimulated for 15min with a range of concentrations (10^{-12} to 10^{-6} mol/L) of C21 before analysis of cAMP concentration. (B) Effect of blockers A779, D-Pro⁷-(Ang-(1-7) (D-Pro) and PD123319, (all 10^{-6} mol/L) on C21 (10^{-7} mol/L)-mediated increase in cAMP in WT C57BL/6 mesangial cells. (C) *Mas/MrgD* knockout (DKO) or AT2 knockout mesangial cells were stimulated for 15min with C21 (10^{-7} mol/L). Results are expressed as mean \pm SEM. Untreated control values of each genotype is set as 100%. ** $P < 0.01$ *** $P < 0.001$ vs. WT control mean, # $P < 0.05$, ## $P < 0.01$, ### $P < 0.001$ vs. C21; ANOVA with Bonferoni post-hoc test. $n=6$ (A), $n=4$ (B), $n=3$ (C).

C21 still mediates cAMP generation in mesangial cells derived from AT2 knockout mice

As C21 is advertised as a specific AT2 receptor agonist, we investigated the remaining C21 effects in mesangial cells deficient in AT2. As illustrated in Figure 6.3.3 C, the efficacy in stimulating an increase in intracellular cAMP was reduced, but not blunted.

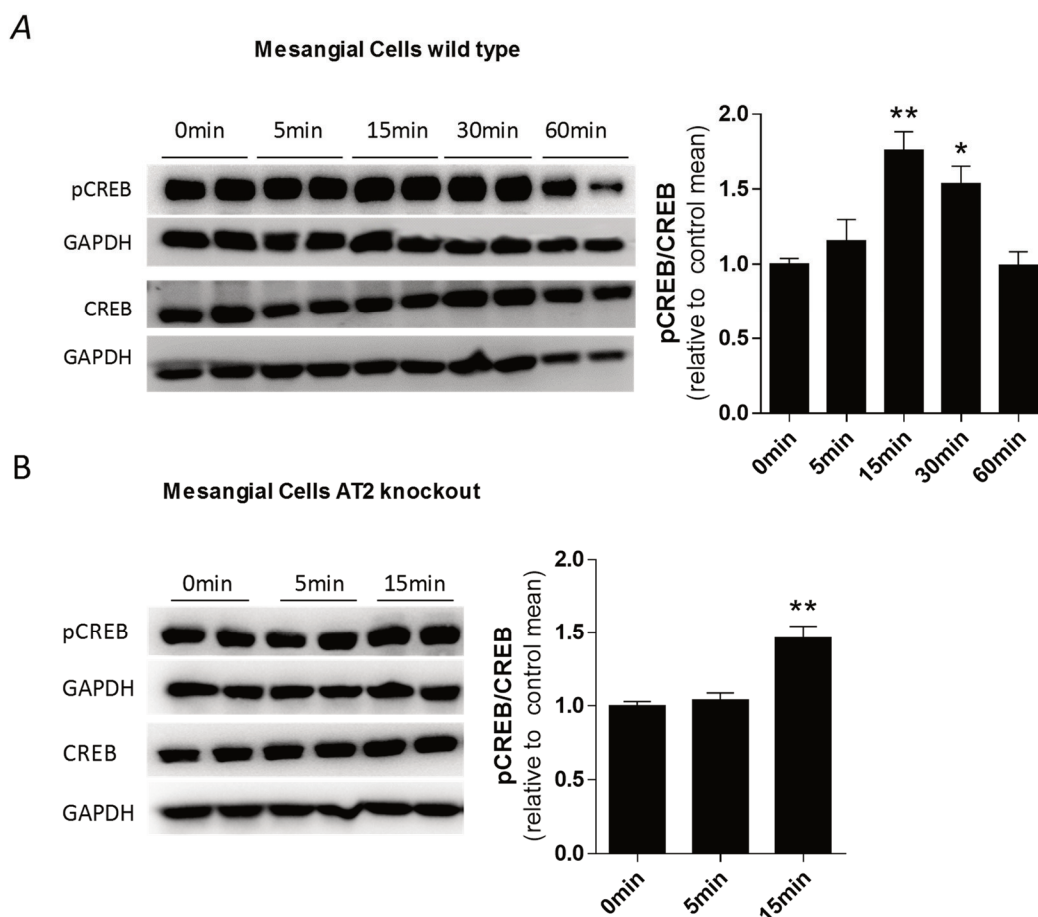


Figure 6.3.4 C21 induced signalling is absent in mesangial cells derived from *Mas/MrgD* double-knockout animals.

(A) Western blot of phosphorylated CREB (pCREB) and CREB and the housekeeping protein GAPDH and calculation of time-dependent CREB phosphorylation in comparison to absolute CREB protein after C21 stimulation in wildtype (WT) mesangial cells. (B) Western blot of phosphorylated CREB (pCREB) and CREB after C21 stimulation in AT2 knockout mesangial cells. Results are expressed as mean \pm SEM. Untreated control values of each genotype is set as 100%. * $P < 0.05$, ** $P < 0.01$ *** $P < 0.001$ vs. WT control mean; ONE WAY ANOVA with Bonferoni post-hoc test. $n=2$ (A), $n=3$ (B).

Since cAMP leads to an increase in pCREB phosphorylation downstream, we measured whether the remaining increase in cAMP after stimulation with C21 in AT2-deficient mesangial cells was still sufficient in phosphorylating CREB. C21 increased pCREB in wild-type MC in a time-dependent manner (Figure 6.3.4 A), and was still able to promote such phosphorylation at the timepoint of highest efficacy (15min) in AT2-deficient cells (Figure 6.3.4 B).

C21 stimulates the generation of intracellular cAMP in endothelial cells via Mas/MrgD but not AT2

Next, we tested whether C21 can also increase intracellular cAMP, comparable to Ang-(1-7), in endothelial cells, using the most commonly characterized endothelial cell-line, human umbilical vein endothelial cells (HUVEC). C21 nicely stimulated cAMP generation as shown in Figure 6.3.5 A. Notably, the increase in cAMP occurs much earlier with a leftward shift of almost 3 magnitudes of order with C21, in comparison to Ang-(1-7) where we have previously reported an EC₅₀ of 1.2×10^{-8} mol/L [378].

To investigate whether the effect on cAMP is mediated by receptors that are sensitive to the two Ang-(1-7) antagonists, A779 and D-Pro, and to the unspecific receptor blocker PD123319 (blocks Mas/MrgD, and AT2), we used C21 in the concentration of highest efficacy (10^{-7} mol/L) without and with the 3 receptor blockers. As shown in Figure 6.3.5 B, the three compounds did not affect base-line cAMP concentrations, but all three blockers significantly reduced the increase in intracellular cAMP in response to C21.

As shown in receptor-transfected cells for C21 in Figure 6.3.1 C, the increase in intracellular cAMP mediated by C21 could be inhibited by SQ22536. The increase mediated by our positive control Ang-(1-7) could also be inhibited, as shown before [378].

Since Ang-(1-7) and C21 behave similarly in HUVEC, this implies that both agonists stimulate Mas and MrgD but not AT2. To confirm that HUVEC do not have functional AT2 receptors, we stimulated the cells with Ang II, with and without the AT1 receptor blocker Irbesartan (Figure 6.3.5 D). While C21 stimulated the increase in intracellular cAMP, AngII failed to do so, even when blocking the AT1 receptor and thus, allowing Ang II only to interact with AT2 (Figure 6.3.5 D).

To confirm our cell culture findings under *ex vivo* conditions, precontracted–isolated mesenteric arteries responded with a significant vasorelaxation to increasing concentrations of C21. However, this relaxation could not only be blocked by PD123319, but also the Mas/MrgD-specific antagonist, D-Pro, to levels of the spontaneous relaxation over time, illustrating that the relaxation is Mas/MrgD- but not AT2-dependent (Figure 6.3.5 E).

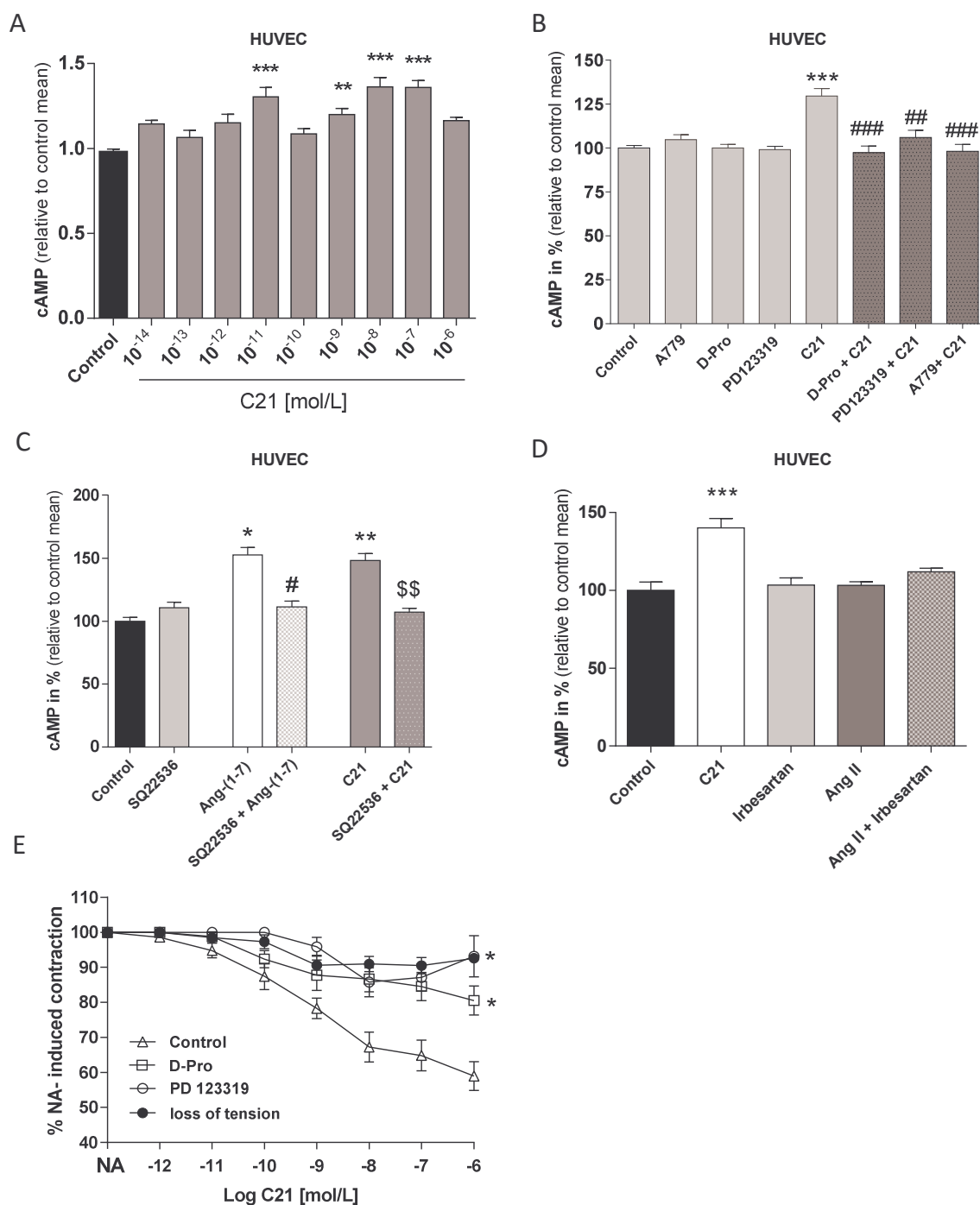


Figure 6.3.5 Intracellular cAMP is increased by C21 in human umbilical vein endothelial cells (HUVEC).

(A) HUVEC were stimulated for 15min with a range of concentrations (10^{-13} to 10^{-6} mol/L) of C21 before analysis of cAMP concentration. (B) Effect of blockers A779, D-Pro⁷-(Ang(1-7) (D-Pro) and PD123319, (all 10^{-6} mol/L) on C21 (10^{-7} mol/L)-mediated increase in cAMP in HUVEC. (C) Effect of adenylyl cyclase inhibitor SQ22536, alone or in combination with Ang(1-7) (10^{-7} mol/L) or C21

(10^{-7} mol/L), on cAMP level. (D) Effect of Ang II (10^{-7} mol/L), with and without the AT1 receptor blocker Irbesartan (10^{-6} mol/L), on cAMP level. (E) Effect of D-Pro and PD123319 (1μ M) on the endothelium-dependent relaxations induced by C21 (0.1 nmol/L to 10μ mol/L) in isolated mesenteric arteries from control C57BL/6 mice. Data are expressed (mean \pm SEM) as the percentage of the previous contraction induced with 3μ mol/L noradrenaline (NA). The number of segments used for every curve, which were obtained from 4 to 6 animals, are in parenthesis. Results are expressed as mean \pm SEM. Data was reported as a fold change or percentage of the untreated control mean. * $P < 0.05$, ** $P < 0.01$ *** $P < 0.001$ vs. control mean, # $P < 0.05$, ## $P < 0.01$, ### $P < 0.001$ vs. C21; ONE WAY ANOVA with Bonferoni post-hoc test. $n=4$ (A, D), $n=5$ (B), $n=6$ (C,E).

In silico modelling shows the structures of C21 and AVE0991 are similar

Figure 6.3.6 A shows the very similar structures of C21 and AVE0991. The superposition of both structures also shows high three-dimensional resemblance, although some differences stand out (Figure 6.3.6 B). In addition to having a sulfonylurea instead of a sulfonylcarbamate, AVE0991 is a larger compound with three chemical groups, which fall outside the volume of C21, all of them attached to the imidazole ring (phenyl, methoxy and formyl groups). Finally and interestingly, the estimation of the ionisation states gives a protonated imidazole ring in C21, while it is neutral in the case of AVE0991.

Docking of C21 into the Mas receptor (Figure 6.3.6 C) displays a hydrogen bond, cation- π and π - π directional interactions in the imidazol-1-ylmethylphenyl group. No other polar groups are observed in direct interaction with the receptor, although water-mediated interactions could be possible. In addition, the isobutyl group is observed to establish favourable contacts with Leu⁸⁰, Leu⁸¹ and Ile⁸⁴.

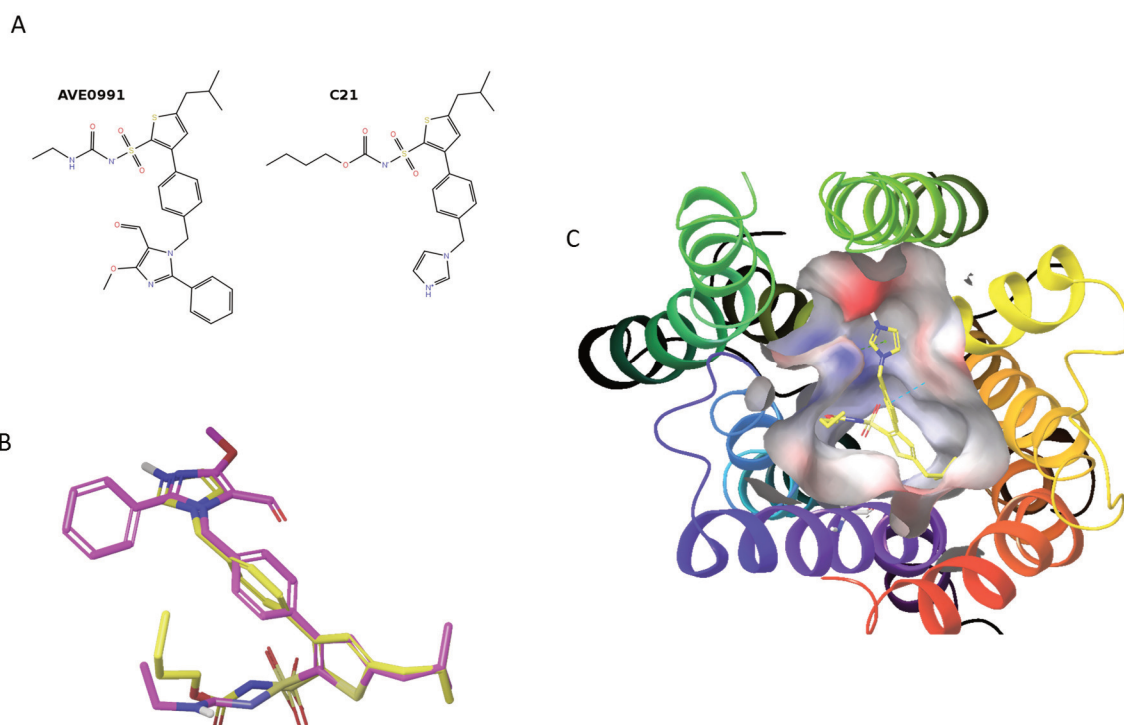


Figure 6.3.6 *In silico* modelling and structure of AVE0991 and C21 compounds

(A) 2D structure of AVE0991 and C21, (B) 3D superposition of AVE0991 (purple-coloured carbon atoms) over C21 (yellow-coloured carbon atoms), (C) Docking pose of C21 compound in the proposed Ang-(1-7) binding site of Mas receptor. Dashed lines show π - π (blue) and cation- π (green) interactions.

Discussion

Recently, we provided experimental proof that PD123319, which served as a specific AT₂ receptor blocker for two decades, also prevents the beneficial effects of Ang-(1-7) by blocking the two heptapeptide receptors, Mas and MrgD. Here we identify C21, the most popular AT₂ receptor agonist, which has been shown to be beneficial in preclinical models of cardiovascular diseases [185, 401], as an agonist for Mas and MrgD.

This supports our hypothesis that AT₂, although without significant sequence homology to Mas/MrgD, except within the transmembrane domains where all GPCRs share a

common sequence pattern, has very similar properties in its ligand-binding site to the two receptors of the Mas-like family.

Our *in silico* modelling illustrates both similarities and differences between C21 and AVE0991, the first non-peptidic agonist for the Mas receptor [232]. The main common features between C21 and AVE0991 include the imidazole ring, the isobutyl chain and the sulfonamide group, which are all attached to a 3-phenylthiophene bicyclic scaffold. On the other hand, C21 presents a protonated imidazole, a sulfonylurea and three extra fragments attached to the imidazole ring with no equivalence in the AVE0991 structure. The differences between C21 and AVE0991 could lead to distinct differences in their affinity and intrinsic activity [398]. Therefore, it was important to generate the experimental proof that C21, like AVE0991, can stimulate the Mas receptor. It might be interesting to investigate in follow-up experiments, whether AVE0991 is not Mas-specific, but can, similar to C21 also stimulate MrgD and AT2.

From a perspective of drug development for cardiovascular diseases, it might be important to merge the information on C21/AVE0991 and Ang-(1-7) to develop a pharmacophore. A pharmacophore is a model of molecular features which are necessary for molecular recognition of a ligand by a receptor [402]. This can explain how structurally diverse ligands can bind to a common receptor site and it can also be used to identify novel agonists through de novo design or virtual screening. This can be used to distinguish between the three receptors, leading to the discovery of agonists with specific receptor fingerprints, (stimulating either all three, or only one or two of the receptors), allowing for use depending on the receptor profile in various cardiovascular and neurodegenerative diseases.

Our data also illustrates that the use of Mas/MrgD blockers or animals with Mas/MrgD or AT2 deficiency, will make it possible in upcoming preclinical experiments to distinguish the receptor which C21 acts through, in specific pathophysiological circumstances. Using this approach in primary mesenteric arteries, we established first data indicating an undiscovered receptor stimulated by C21. Since the lack of Mas and MrgD does not only blunt the C21 effect observed in wild-type cells, but even attenuates the intracellular cAMP levels (Figure 6.3.3 C, middle panel), this may be explained by a 4th receptor stimulated by C21, which is $G_{\alpha i}$ coupled and thus, reduces adenylyl cyclase activity and consequently, cAMP generation. This drop in Mas/MrgD-deficient cells allows us to correctly read the data in AT2-deficient mesangial cells. The increase by C21, which is slightly above the control level, is in reality much higher, starting from a negative value based on the cAMP-lowering effect of the hypothetical $G_{\alpha i}$ coupled receptor also stimulated by C21. Final proof of this hypothesis could be generated with cells deficient in Mas/MrgD and AT2, where any drop in intracellular cAMP after C21 stimulation would relate to such a postulated receptor.

C21 stimulates different receptors in primary cells, which is also illustrated in the second cell type we used, HUVEC. Figure 6.3.5 A shows a biphasic dose-response curve, whereby its two peaks nicely correspond to the peaks in Mas and MrgD-transfected cells.

There is a significant overlap of cardiovascular protective effects of C21 and Ang-(1-7), which we and others have explained previously with two beneficial arms of the RAS: the AngII/AT2 axis and the Ang-(1-7)/Mas & MrgD axis. While this might still be correct, our results provide a new explanation, by showing that both compounds share, at least in part, the same receptors.

It will be interesting to identify diseases, where C21 is beneficial, independent of Mas/MrgD stimulation, as these diseases would benefit from an AT2-specific agonist.

Taken together, our results provide the groundwork for a better understanding of the function of the AT2 receptor under physiological and pathophysiological circumstances, as we demonstrate that conclusions based on only C21s effects might be incorrect. This also forces the revisit of such publications, which conclude on AT2 receptor effects using only C21. Furthermore, the identification of the second messenger, cAMP, being regulated by C21, will allow for the focused identification of intracellular networks in response to C21 treatment and the prediction of potential applications of this drug by identifying diseases where elevation of cAMP is assumed to be beneficial, and where target organs express either Mas, MrgD or AT2.

Perspectives

While Ang-(1-7) only stimulates Mas and MrgD, C21 also acts through the AT2 receptor. The molecular understanding of the common structural pattern required to stimulate all three receptors, or only one or two of them, opens the avenue for the development of tailored drugs (non-peptidic agonists) for cardiovascular and neurodegenerative diseases, based on the specific receptor fingerprint in target organs associated with the treatment of such diseases.

Source of Funding

The work was supported by grants of the Deutsche Forschungsgemeinschaft (WA1441/22-1 and 2) and Plan Nacional I+D+i (SAF2017-84776-R).

Disclosures

TW is inventor of the patent "Use of an Ang-(1-7) receptor agonist in acute lung injury" (Application No: 08016142.5-2107). TW is scientific advisor of Tarix Pharmaceutical (Boston, USA).

Novelty and Significance***What is new?***

We demonstrate that C21 is not an AT2-specific agonist, as it also interacts with both Ang-(1-7) receptors, Mas and MrgD. Consequently, C21 still has biological effects in AT2-deficient tissue, as long as it expresses one of the heptapeptide receptors.

What is relevant?

The understanding of structural similarities of receptor agonists will lay the ground for the design of tailored non-peptidic agonists stimulating all three, two or only one of the receptors.

Summary

C21 can stimulate both Mas and MrgD, explaining similar beneficial effects as Ang-(1-7), also enforcing the revisit of such publications, which concluded on AT2 function by only using C21.

6.4 The Angiotensin-(1-7)/Mas axis improves pancreatic β -cell function in vitro and in vivo

Anika Sahr¹, Carmen Wolke¹, Jonas Maczewsky², Peter Krippeit-Drews², Anja Tetzner^{3,4}, Gisela Drews², Simone Venz¹, Sarah Gürtler¹, Jens van den Brandt⁵, Sabine Berg⁵, Paula Döring⁶, Frank Dombrowski⁶, Thomas Walther^{3,4}, Uwe Lendeckel¹

¹Institute of Medical Biochemistry and Molecular Biology, University Medicine Greifswald, Ferdinand-Sauerbruch-Straße, D-17475 Greifswald, Germany;

²Department of Pharmacology, Institute of Pharmacy, University of Tübingen, Auf der Morgenstelle 8, D-72076, Tübingen, Germany;

³Department of Pharmacology and Therapeutics, University College Cork, Western Gateway Building, Western Road, Cork, Ireland

⁴Clinic for Pediatric Surgery and Department of Obstetrics, University Medical Centre Leipzig, Liebigstraße 20a, D-04103 Leipzig, Germany;

⁵Central Core & Research Facility of Laboratory Animals, University Medicine Greifswald, Walther-Rathenau-Straße 49a, D-17489 Greifswald, Germany;

⁶Institute of Pathology, University Medicine Greifswald, Friedrich-Loeffler-Straße 23e, D-17475 Greifswald, Germany

Key terms: renin-angiotensin system, angiotensin-(1-7), receptor Mas, β -cell function, insulin secretion, cAMP

Corresponding author: Thomas Walther; e-mail: t.walther@ucc.ie; Phone: +353-(0)21-420-5973; Department of Pharmacology and Therapeutics, School of Medicine & School of Pharmacy, University College Cork, Cork, Ireland

Published in Endocrinology, 2016 December, 157(12):4677-4690.

Hypothesis:

Ang-(1-7)/Mas axis is a potential therapeutic target for diabetic disorders (type 1 and type 2 diabetes).

Aim of the study:

The aim of the study was to investigate the positive effects of Ang-(1-7) on the regulation of insulin secretion in pancreatic β -cells. Therefore, *in vitro*, *ex vivo*, and *in vivo* experiments were used to examine the responsible processes and mechanisms of the Ang-(1-7) related effects on insulin secretion.

Disclosure statement: The authors have nothing to disclose.

Author contributions:

Anja Tetzner performed the experiments for Figure 4C and the STZ-induced diabetes study (Chapter 10.3)

Abbreviations

ACE2	angiotensin-converting enzyme 2
Ang	angiotensin
AT1	Ang II type 1 receptor
[Ca ²⁺] _c	cytosolic calcium concentration
cAMP	cyclic adenosine monophosphate
EPAC 2	exchange protein directly activated by cAMP 2

GLP-1	glucagon-like peptide-1
GSIS	glucose-stimulated insulin secretion
KO	knockout
Mas	receptor Mas
NEP	neprilysin
PKA	cAMP-dependent protein kinase
RAS	renin-angiotensin system
RT-qPCR	reverse transcription and quantitative polymerase chain reaction
WT	wild-type

Abstract

The ACE2/angiotensin (Ang)-(1-7)/Mas axis of the renin-angiotensin system (RAS) often opposes the detrimental effects of the ACE/AngII/AT1 axis and has been associated with beneficial effects on glucose homeostasis, while underlying mechanisms are mostly unknown. Here, we investigate the effects of Ang-(1-7) and its receptor Mas on β -cell function.

Isolated islets from Mas-deficient and wild-type mice were stimulated with Ang-(1-7) or its antagonists and effects on insulin secretion determined. Islets' cytoplasmic calcium and cAMP concentrations, mRNA amounts of Ins1, Ins2, Pdx1, and Mafa, and effects of inhibitors of cAMP downstream signaling were determined. Ang-(1-7) was also applied to mice by osmotic pumps for 14 days and effects on glucose tolerance and on insulin secretion were assessed.

Ang-(1-7) increased insulin secretion from wild-type islets whereas antagonists and genetic Mas-deficiency led to reduced insulin secretion. The Mas-dependent effects of Ang-(1-7) on insulin secretion did not result from changes in insulin gene expression or changes in the excitation-secretion coupling, but from increased intracellular cAMP involving exchange protein activated directly by cyclic AMP (EPAC). Administration of Ang-(1-7) in vivo had only marginal effects on glucose-tolerance in wild-type mice, but still resulted in improved insulin secretion from islets isolated of these mice. Interestingly, although less pronounced than in wild-types, Ang-(1-7) still affected insulin secretion in Mas-deficient islets.

The data indicates a significant function of Ang-(1-7) in regulation of insulin secretion from mouse islets in vitro and in vivo, mainly, but not exclusively, by Mas-dependent signaling, modulating the accessory pathway of insulin secretion via increased cAMP.

Introduction

The renin-angiotensin system (RAS) is an important regulator of blood pressure and is activated in a number of pathophysiological conditions (such as hypertension, hyperglycaemia, and cardiac insufficiency) triggering pathogenesis and progression of these diseases. In addition to inducing insulin resistance, the activation of RAS and in particular the effect of increased angiotensin (Ang) II levels hyper-stimulating the Ang II type 1 receptor (AT1) are also associated with the deterioration of β -cell function and thus the adequate production and secretion of insulin [403].

The angiotensin-converting enzyme 2 (ACE2, EC 3.4.17.23) metabolises Ang II into Ang-(1-7) by splitting off the C-terminal amino acid. This enzyme has a protective role in general and for the cardiovascular system in particular [404]. These positive effects are attributable both to the fact that ACE2 reduces Ang II concentration, which in turn reduces the activation of AT1, and that more beneficial Ang-(1-7) can stimulate its receptor Mas [62], counteracting the AT1 signalling [51].

The beneficial effects of Ang-(1-7) with respect to glucose homoeostasis have been described, but mainly concern the improvement of insulin sensitivity and thus the glucose uptake in peripheral tissues (muscle, fat). Exemplarily, in a rat model of metabolic syndrome, chronic infusion of Ang-(1-7) resulted in the normalization of insulin sensitivity/signal transduction of skeletal muscle, liver, and adipose tissue and of

hyperglycaemia, hyperinsulinaemia, and hypertriglyceridaemia [73]. In primary epididymal adipocytes of mice and in 3T3-L1 adipocytes, Ang-(1-7) resulted in an increase in glucose uptake, coupled with reduced production of reactive oxygen species due to an Ang-(1-7)-mediated inhibition of NADPH oxidase subunit expression [349]. An increase in glucose uptake in the adipocytes of transgenic rats with Ang-(1-7) overexpression was also observed, with improved insulin sensitivity and glucose tolerance and reduced triglyceride and cholesterol serum levels [125]. Furthermore, it has been shown that the oral administration of Ang-(1-7) counteracts hyperglycaemia in a rat model of inducible diabetes mellitus type 2 [348].

Initial work on the role of the ACE2/Ang-(1-7)/Mas axis and in particular the effect of Ang-(1-7) on insulin production and secretion showed that Ang-(1-7) can prevent the marked shrinkage of the cytoplasm and condensation of nuclear chromatin and significantly facilitated insulin production in pancreatic β -cells of rats with streptozotocin (STZ)-induced diabetes mellitus [350]. Thus, it was the aim of the study to explore the processes and mechanisms that result in the positive effects of Ang-(1-7) on the regulation of insulin secretion in pancreatic β -cells. Moreover, it was intended to conduct *in vitro*, *ex vivo*, and *in vivo* experiments designed to lay the foundations that will establish Ang-(1-7) as a new medication in diabetic disorders (both type 1 and type 2).

Materials and Methods

Mice

The protocol of the study was approved by the Veterinary and Food Control Office, State Department of Agriculture, Food Safety and Fisheries Mecklenburg-Vorpommern, Germany (Permit Number: 7221.3-1.1-097/12). Animals were housed at 21°C, exposed to a 12-h light and darkness cycle with access to food and water, *ad libitum*. For all experiments, 11- to 14-week old mice deficient in the receptor Mas ($Mas^{-/-}$; $-/-$) [120] and their age- and sex-matched wild-type (WT; $+/+$) controls were used (all on C57Bl/6J background) whereby knockouts and wild-types have been generated from heterozygous mice and housed under identical conditions.

Immunofluorescence microscopy

Formalin-fixed paraffin sections (5 μm) of mice pancreases were deparaffinised and rehydrated using standard methods. Antigen retrieval and immunostaining were performed as previously described [405] using primary and Alexa 488- and Cy3-conjugated secondary antibodies (listed in the Antibody table). Sections were covered with Roti®-Mount FluorCare DAPI (Roth, Karlsruhe, Germany) and images acquired using a Leica TCS SP5 confocal microscope (Leica Microsystems, Wetzlar, Germany).

Histochemistry, immunohistochemistry, and determination of beta cell volume fraction

Pancreatic tissue was fixed in 4% neutral buffered formalin, dehydrated and embedded in paraffin. Staining of slides (2 μm) with either hematoxylin and eosin or by immunohistochemistry was performed as followed: Slides were deparaffinised and treated with primary antibodies against insulin (Santa Cruz Biotechnology, Dallas, USA) or

CD34 (Dako, Glostrup, Denmark) (for details see Antibody table). Stainings were performed on automated immunohistochemistry stainers: insulin on Leica Bond using Bond Polymer Refine Detection kit (Leica Biosystems, Newcastle, UK, no. DS9800); CD34 on Roche Ventana using OptiView DAB IHC Detection kit (Ventana Medical Systems, Oro Valley, USA, no. 760-700). Volume fractions of insulin positive islet cells were estimated by the stereological point counting method described by Weibel [406] using Nikon NIS Elements software 4.30. 585 points were counted per animal.

Isolation of mouse islets of Langerhans

One ml collagenase P (2mg/ml) (Roche) was injected into the mouse pancreas through the common bile duct. After resection, the whole pancreas was digested in 2ml collagenase P solution for 6min at 37°C with gentle shaking. Ice-cold islet isolation buffer (135mmol/l NaCl, 5.6mmol/l KCl, 1.28mmol/l CaCl₂, 1.2mmol/l MgCl₂, 10mmol/l HEPES, 0.1% BSA, 100U/ml penicillin, 100µg/ml streptomycin, 3mmol/l glucose, pH7.4) was added, samples were shaken vigorously for 15s and centrifuged (500×g, 2min, 4°C). Pellets were resuspended in islet isolation buffer and islets hand-picked and collected in RPMI 1640 (PAN Biotech, Aidenbach, Germany) supplemented with 10% FBS (Thermo Fisher Scientific, Waltham, USA), 100 U/ml penicillin and 100µg/ml streptomycin (PAN Biotech). Unless otherwise stated, islets pooled from at least 5 animals (250 islets per mouse, approximately) were used for each set of experiments, and this was regarded as one biological replicate (*n* indicated in the Figure legends).

Glucose-stimulated insulin secretion (GSIS)

Five islets per well were cultured in 12-well plates (Greiner bio-one cell star®, Frickenhausen, Germany) with 500µl RPMI 1640 (supplemented as described above) at 37°C with 5% CO₂. After 24h, islets were incubated in KRB (123mmol/l NaCl, 4.7mmol/l KCl, 1.2mmol/l KH₂PO₄, 2.6mmol/l CaCl₂, 1.2mmol/l MgSO₄, 10mmol/l HEPES, 20mmol/l NaHCO₃, 0.5% BSA, pH7.4) with 2.8mmol/l glucose for 90 min, with buffer exchanged once after 30min. Islets were exposed to either 2.8mmol/l glucose, 2.8mmol/l glucose + 40mmol/l KCl, or 20mmol/l glucose, for 2h. For the treatments, Ang-(1-7) (0.2µmol/l), A779 (1µmol/l), D-Pro⁷-Ang-(1-7) (1µmol/l) (all from Bachem, Bubendorf, Switzerland), HJC 0350 (50µmol/l; Tocris Bioscience, Avonmouth, Bristol, UK), or H89 (20µmol/l; Cell Signaling, Frankfurt aM, Germany) were added. Supernatants were collected, centrifuged at 100×g for 2min at 4°C and insulin concentrations in the supernatants determined by ELISA (Mercodia, Uppsala, Sweden).

Intra-islet insulin content

Single islets were collected in 50µl lysis buffer (50mmol/l Tris-HCl (pH8.0), 5mmol/l EDTA, 150mmol/l NaCl, 10% glycerol, 0.5% NP-40, 2mmol/l Na₃VO₄, 1mmol/l NaF, 0.1mmol/l PMSF, and cOmplete™ protease inhibitor cocktail (Roche)). After 30min incubation on ice, samples were shock-frozen in liquid nitrogen and the intra-islet insulin contents determined by ELISA.

RNA isolation and quality control. Total RNA was extracted from isolated islets by performing a modified phenol extraction [407]. RNA integrity was validated by means of the lab-on-chip capillary electrophoresis technology (Bioanalyzer 2100, Agilent

Technologies, Santa Clara, USA). Only RNA samples with a RNA Integrity Number (RIN) > 7.5 [408] and absorption quotients of A260nm/A280nm \geq 1.8, A260nm/A230nm \geq 1.9 were used for subsequent experiments.

Reverse transcription and quantitative PCR (RT-qPCR)

Five hundred ng of total islet RNA were reverse-transcribed into cDNA using a RevertAid First Strand cDNA Synthesis Kit (Thermo Fisher Scientific). qPCR was performed in a CFX96 thermocycler (Bio-Rad, Munich, Germany). The 20 μ l reaction mixture consisted of 1 \times SensiMix [™] SYBR Hi-ROX Mastermix (Bioline, Luckenwalde, Germany), 0.25 μ mol/l of specific primers (Life Technologies GmbH, Darmstadt, Germany; detailed primer information is shown Table 1) and 1 μ l cDNA. Initial denaturation at 95°C for 10min was followed by 40 cycles at 95°C for 15s, annealing at 58 - 64°C for 15s and elongation at 72°C for 20sec. Data were normalised to *Rplp0*. PCR products were separated in agarose gels and visualised by RedSafe[™] (iNtRON Biotechnology, Summit, USA), using Quick-Load[®] 100 bp DNA ladder (New England Biolabs, Frankfurt, Germany) as molecular weight marker.

Determination of cytosolic calcium concentrations [Ca²⁺]_c

[Ca²⁺]_c was measured in β -cell clusters in a bath-solution (140mmol/l NaCl, 5mmol/l KCl, 1.2mmol/l MgCl₂, 2.5mmol/l CaCl₂, 10mmol/l HEPES, pH7.4, and glucose as indicated). Ang-(1-7) (1 μ mol/l) and A779 (1 μ mol/l) were present during the pre-incubation (24h) and the whole measurement. Control experiments were performed without compounds. [Ca²⁺]_c was measured by the fura-2 method according to Grynkiewicz *et al.* [409] using equipment and software from TILL photonics (Gräfelfing, Germany). Cells were loaded

with fura-2-AM (5 μ mol/l) (Biotrend, Köln, Germany) for 35min at 37°C. Intracellular fura-2 was excited alternately at 340 or 380nm by means of an oscillating diffraction grating. The emitted light was filtered (LP515nm) and measured by a digital camera. The ratio of the emitted light intensity at 340nm/380nm excitation was used to calculate $[Ca^{2+}]_c$ according to an *in vitro* calibration with fura-2 K⁺-salt.

Determination of cyclic AMP (cAMP) concentrations

Twenty islets per well isolated from wild-type or Mas-deficient mice were cultured for 24h and incubated in KRB as described for the GSIS. Islets were stimulated with or without 0.1 μ mol/l Ang-(1-7) and/or the two antagonists, D-Ala⁷-Ang-(1-7) (A779) and D-Pro⁷-Ang-(1-7) (D-Pro) for 15min and lysed in 150 μ l lysis buffer (0.1mol/l HCl, 0.1% Tween-20). Concentrations of cAMP were determined using the Direct cAMP ELISA kit (Enzo Life Sciences Ltd., Exeter, United Kingdom) following manufacturer's instructions.

Immunoblot analysis

300-400 islets were treated with Ang-(1-7) (0.2 μ mol/l) or A779 (1 μ mol/l) for 24h, washed twice with ice-cold PBS and lysed in 30 μ l lysis buffer (as shown for intra-islet insulin). After centrifugation (17,000 $\times g$, 30min, 4°C) the supernatant was used. For each condition 10 μ g of total islet protein was separated in Mini-PROTEAN® TGX Stain-Free™ Precast Gels (Bio-Rad, Munich, Germany) using Tris/glycine/SDS running buffer (25mmol/l Tris-HCl, 129mmol/l glycine, 0.1% SDS) under standard conditions according to the manufacturer's instructions. Proteins were transferred to polyvinylidene fluoride (PVDF) membranes using the Trans-Blot® Turbo™ RTA Mini PVDF Transfer Kit and the Trans-Blot® Turbo™ System (Bio-Rad). Membranes were blocked in TBST (138mmol/l NaCl, 20mmol/l Tris,

0.1% Tween 20, pH7.6) with 5% low fat powdered milk and incubated with p-PKA and total PKA primary antibodies (Cell signaling; for details see Antibody table). Using a HRP-linked secondary antibody and SuperSignal™ West Dura Extended Duration Substrate (Thermo Fisher Scientific) the signals were detected in a ChemiDoc™ Imaging System (Bio-Rad). Signal intensities were analysed using ImageJ software (ImageJ, Bethesda, USA) and the p-PKA to total PKA ratio calculated.

Continuous administration of Ang-(1-7) in vivo

ALZET® osmotic pumps [model 1002; 0.25µl/h] (Charles River Laboratories, Sulzfeld, Germany) were loaded with 0.9% saline as control solution or Ang-(1-7) dissolved in 0.9% saline. After priming for 1 h at 37°C, pumps were implanted into a subcutaneous pocket between the scapulae of isoflurane-anesthetised mice. The wound was closed with a wound clip. The pumps remained in the mice for 14 days with a calculated infusion rate of 2.47 mg kg⁻¹ d⁻¹ of Ang-(1-7).

Oral glucose tolerance test (OGTT)

Ten days after pump implantation an OGTT was performed with the mice. After 6h fasting, plasma insulin concentration and blood glucose were determined 15min before OGTT. Glucose was orally administered by gavage (2g/kg body weight). Blood samples were taken from the tail vein for blood glucose and plasma insulin analysis thereafter. Blood glucose concentrations were measured using a commercial blood glucose meter (sample volume 0.3µl; FreeStyle Lite, Abbott, USA) and plasma insulin was determined by ELISA (20µl blood).

Statistical analysis

Statistical analyses were performed using GraphPad Prism 6 software (GraphPad, La Jolla, USA). *P*-values <0.05 were considered to indicate statistically significant differences. Non-parametric data are illustrated as boxplots with medians, quartiles and an interquartile range (IQR) $\pm 1.5 \times$ IQR with outliers as indicated (Tukey method). Parametric data are shown as bars with means and standard error of mean (SEM).

Results

Islets of Langerhans express components of the alternative ACE2/Ang-(1-7)/Mas axis of the RAS

The expression of components of the ACE2/Ang-(1-7)/Mas axis of the RAS and of neprilysin (NEP, neutral endopeptidase, EC 3.4.24.11), a peptidase generating Ang-(1-7) directly out of the Ang precursor Ang I, were verified by RT-qPCR using RNA from isolated islets. The analysis revealed the existence of abundant mRNA amounts of *Ace2*, *NEP* (approx. 10% of the amounts of insulin 1 mRNA), and *Mas* (approx. 2% of insulin 1 mRNA) in murine islets. Figure 6.4.1 A shows the corresponding amplification products of the expected size. Immunofluorescence analyses of pancreatic tissue sections (Figure 6.4.1 B) indicated predominant detection of ACE2 and Mas in the β -cell population as concluded from the co-localization of Mas and ACE2 with insulin-positive rather than with glucagon-positive cells. NEP appeared to be ubiquitously expressed in all endocrine as well as exocrine cells of the pancreas.

Phenotypical analysis of islets from wild-type (+/+) or Mas-deficient mice (-/-) revealed no histological or cytological differences. Explicitly, there were no differences in gross islet architecture, vascular density, or β -cell volume fraction (Figure 6.4.2). In detail, pancreatic islets of Mas-deficient mice were well circumscribed and mean islet diameter as well as the volume fraction of islet tissue on total pancreatic tissue were similar to the wild-type mice. Islet cells showed pale cytoplasm and round, uniform nuclei with granular chromatin and no nuclear atypia. Composition of pancreatic islets was similar, too, islets consisted mainly (> 95%) of insulin-expressing β -cells. Vascularization of pancreatic islets was evaluated by histologic presentation of CD34 positive endothelial cells. Islets of wild-type as well as Mas-deficient mice showed dense capillarization of sinusoidal vessels

(Figure 6.4.2). Furthermore, the average number of islets isolated from mouse pancreata was not different between wild-type (258.3 ± 79.8 ; $n=134$) and Mas-deficient mice (280 ± 107 ; $n=181$).

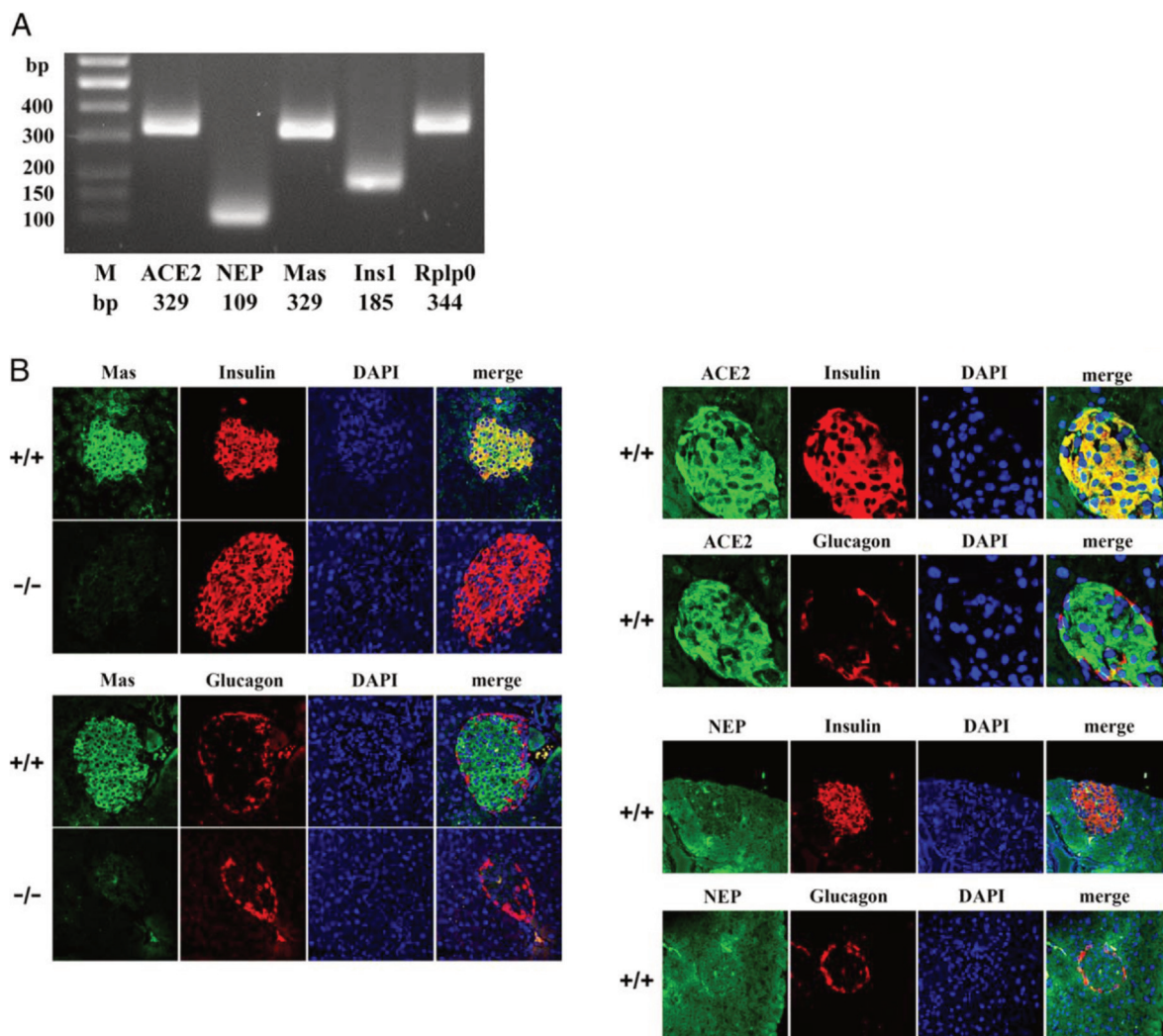


Figure 6.4.1 Detection of components of the alternative ACE2/Ang-(1-7)/Mas axis of the RAS in murine islets of Langerhans

(A) mRNA amounts of *Ace2*, *NEP*, and *Mas*. Amplificate sizes are given in bp. M=DNA Ladder. (B) Specificity of the *Mas* antibody in WT (+/+) mice was approved by immunostaining of pancreatic tissue sections from *Mas*-deficient (-/-). Insulin and glucagon immunostaining identified the islet distribution of β - and α -cells (upper panels). ACE2 and *Mas* were predominantly detected in β -cells, while NEP could be detected in endocrine and exocrine cells in WT islets (lower panels). Length of lower border of *Mas* and NEP images: 0.25 mm; lower border of ACE2 images: 0.085 mm. ACE2, angiotensin-converting enzyme 2; NEP, neprilysin.

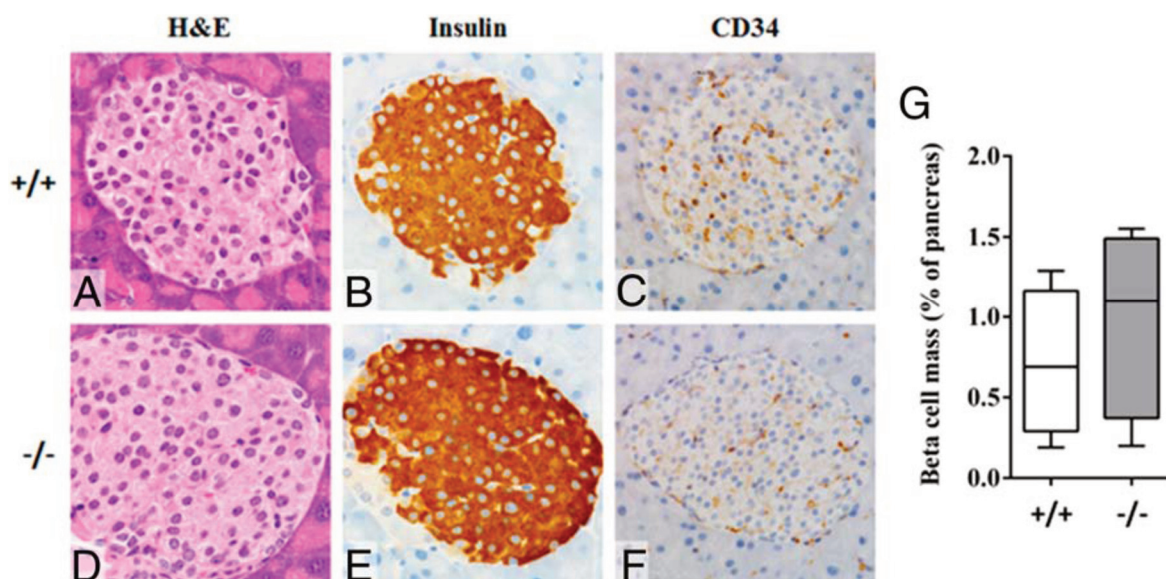


Figure 6.4.2 Phenotypic description of islets from wild-type and *Mas*-deficient mice. Islets of Langerhans in pancreatic tissue in WT (+/+; upper line) and *Mas* KO mice (-/-; lower line):

(A, D) Islets presented as sharply circumscribed nests with uniform cells containing round nuclei with granular chromatin and abundant pale cytoplasm. (B, E) In both groups islets consisted mainly of insulin expressing β -cells. (C, F) Capillary density of islets of Langerhans shown by CD34 immunostains was similar. Length of lower image border A, B, D, E: 0.16 mm; C, F: 0.23mm. (G) Calculated β -cell volume fraction as percentage of pancreas in wild-type mice (set 100%).

Pharmacological modulation of the receptor *Mas* affects insulin secretion

Exposure of isolated wild-type (WT; +/+) islets to Ang-(1-7) increased GSIS but did not significantly increase the KCl-mediated insulin secretion ($P = .466$ vs KCl-treatment without Ang-(1-7)) probably due to the wide scattering of the individual data, but the augmentation up to 259% and the 75th percentile of 168.5 could indicate an increase in KCl-induced insulin secretion with Ang-(1-7). Administration of the *Mas*-specific Ang-(1-7) antagonist, A779, respectively, provoked a significant decrease in insulin secretion with

20mmol/l glucose (-1.5-fold) and KCl treatment (-1.4-fold) (Figure 3A, left part). However, Ang-(1-7) led to a 1.4-fold increase at low (5.5mmol/l) and to a 1.4-fold increase at high (20mmol/l) glucose concentrations (Figure 6.4.3 A; middle and right part). Consequently, pretreatment with A779 was performed to test for its effect on the significant Ang-(1-7) effect on glucose-stimulated insulin secretion. For both glucose concentrations, A779 failed to block the Ang-(1-7)-mediated increase. Therefore, also the second Ang-(1-7) antagonist, D-Pro, was used. In contrast to A779, D-Pro significantly blocked the effect of Ang-(1-7) (Figure 6.4.3 A, middle and right part).

Pharmacological modulation of the receptor Mas affects neither insulin, Pdx1 or Mafa mRNA amounts nor intra-islet insulin content

To examine whether the observed changes in insulin secretion are a result of alterations in mRNA amounts of insulin or the main insulin-gene regulating transcription factors PDX-1 and MafA, islets were treated with Ang-(1-7) or A779 and mRNA amounts and intra-islet insulin content determined. No significant changes in mRNA amounts of *Ins1*, *Ins2*, *Pdx1*, or *Mafa* were observed (Figure 6.4.3 B). Furthermore, administration of Ang-(1-7) or A779 for 24h did not alter the intra-islet insulin content (Figure 6.4.3 C).

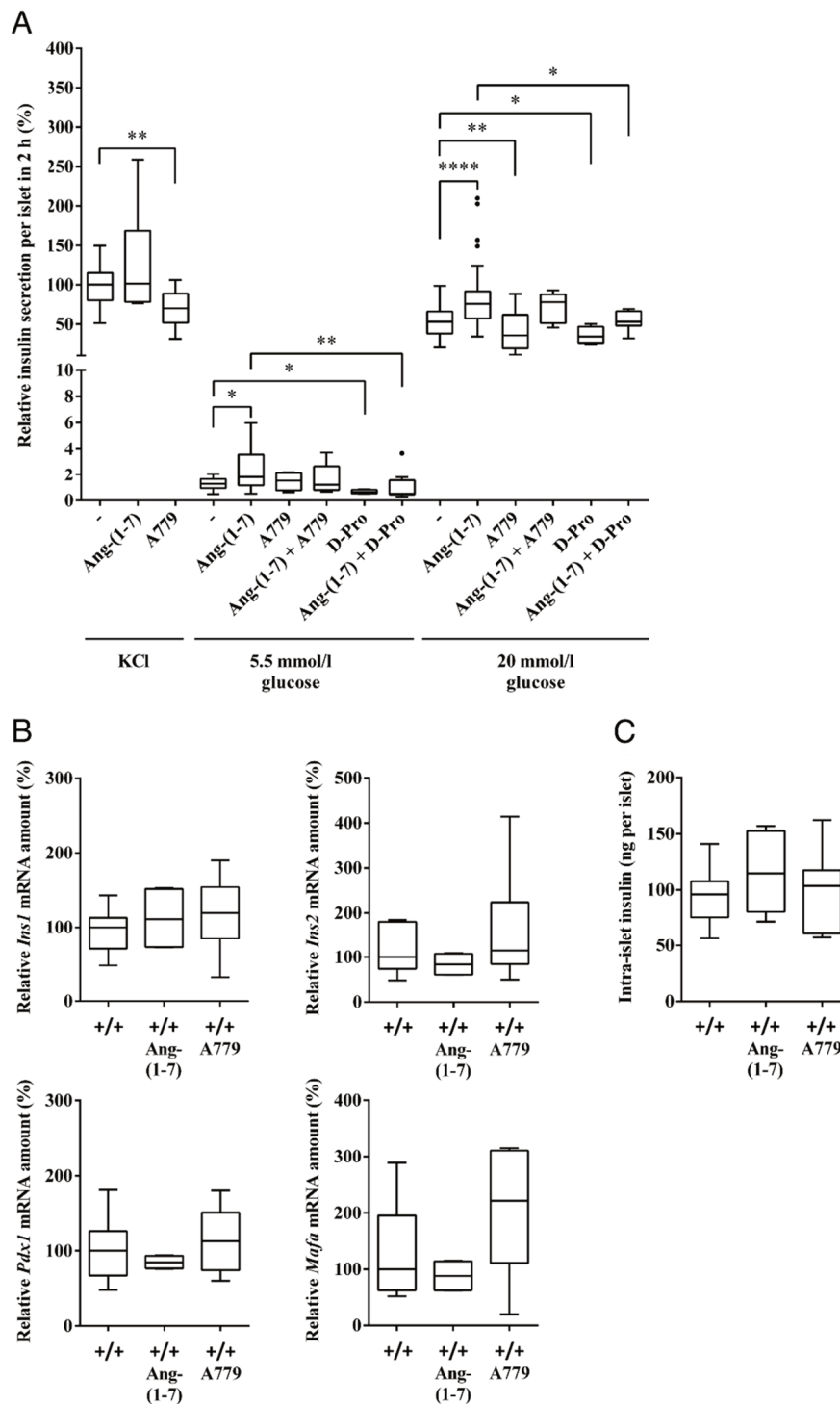


Figure 6.4.3 Pharmacological modulation of the receptor Mas ex vivo in WT islets

A) KCl- and glucose-stimulated insulin secretion in presence of Ang-(1-7), A779, or D-Pro⁷-Ang-(1-7) (D-Pro) in WT islets ($n \geq 10$; $n \geq 4$ for all D-Pro experiments). (B) mRNA amounts of *Ins1*, *Ins2*, *Pdx1* and *Mafa* in Ang-(1-7)- or A779-treated WT (+/+) islets ($n \geq 4$). (C) Intra-islet insulin concentrations in Ang-(1-7)- or A779-treated WT (+/+) islets ($n \geq 13$). (Mann–Whitney U test; *. $P < .05$; **, $P < .01$; ***, $P < .001$).

Pharmacological modulation of the receptor Mas does not lead to alterations in cytosolic calcium concentrations

To further investigate the mechanism underlying the effects of receptor Mas modulation on insulin secretion, $[Ca^{2+}]_c$ was determined in islet cell clusters exposed to Ang-(1-7) or A779, respectively. Depending on the glucose concentration, pancreatic β -cells exhibit fluctuations of the membrane potential (V_m) where burst phases with action potentials alternate with silent interburst phases generating so-called slow waves [410]. The slow waves drive oscillations of the $[Ca^{2+}]_c$ and insulin secretion. The fraction of plateau phase (FOPP; percentage of summed burst-times) correlates with the amount of insulin release. As shown in Figure 6.4.4 A, exposure of β -cells to a high glucose concentration (20mmol/l) led to significantly increased $[Ca^{2+}]_c$ when compared to 10mmol/l glucose. However, exposure of β -cells to Ang-(1-7) or A779 did not result in any changes of $[Ca^{2+}]_c$ or the pattern of Ca^{2+} oscillations at 20mmol/l glucose (Figure 6.4.4 B).

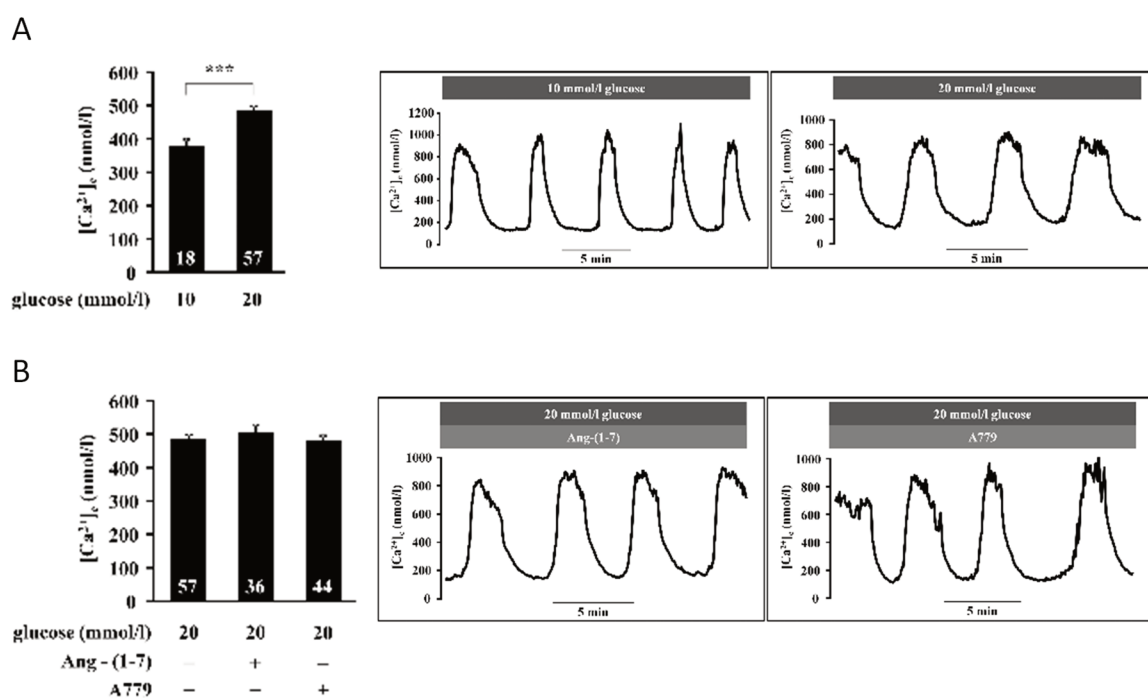
In additional experiments Mas-deficient islets showed no differences in the $[Ca^{2+}]_c$ in response to glucose or KCl compared to islets from wild-type mice (data not shown).

Administration of Ang-(1-7) increases intracellular cAMP concentrations

The fact that pharmacological modulation of Mas provoked changes in insulin secretion in the absence of any changes in $[Ca^{2+}]_c$ raised the hypothesis that Mas-dependent alteration of β -cells' Ca^{2+} -sensitivity contribute as an underlying mechanism. Previous work identified cAMP as an effective Ca^{2+} sensitizer and stimulus of insulin exocytosis in pancreatic β -cells [411, 412]. As shown in Figure 6.4.4 C, exposure of isolated WT islets to

Ang-(1-7) led to a significant 1.6-fold increase in their cAMP contents. This Ang-(1-7)-mediated increase could be abolished by the simultaneous administration of A779.

To test for the critical role of increased cAMP levels for the Ang-(1-7)-mediated stimulation of insulin secretion, the two downstream effectors of cAMP, EPAC 2 and PKA, have been inhibited under high glucose conditions. While the EPAC 2-inhibitor, HJC 0350, completely abolished the Ang-(1-7) effect on insulin secretion, no such effect could be detected for the inhibitor of PKA, H89, which suggests that activation of PKA does not contribute much to the Ang-(1-7)-mediated increase in insulin secretion (Figure 6.4.4 D). To confirm that administration of Ang-(1-7) has an effect on PKA, Western blots have been performed showing indeed increased phosphorylation state of PKA in WT islets after 24 hours, while the total PKA protein amount was not altered. The A779 treatment did not result in significant changes in total PKA amounts or phosphorylation state (Figure 6.4.4 E).



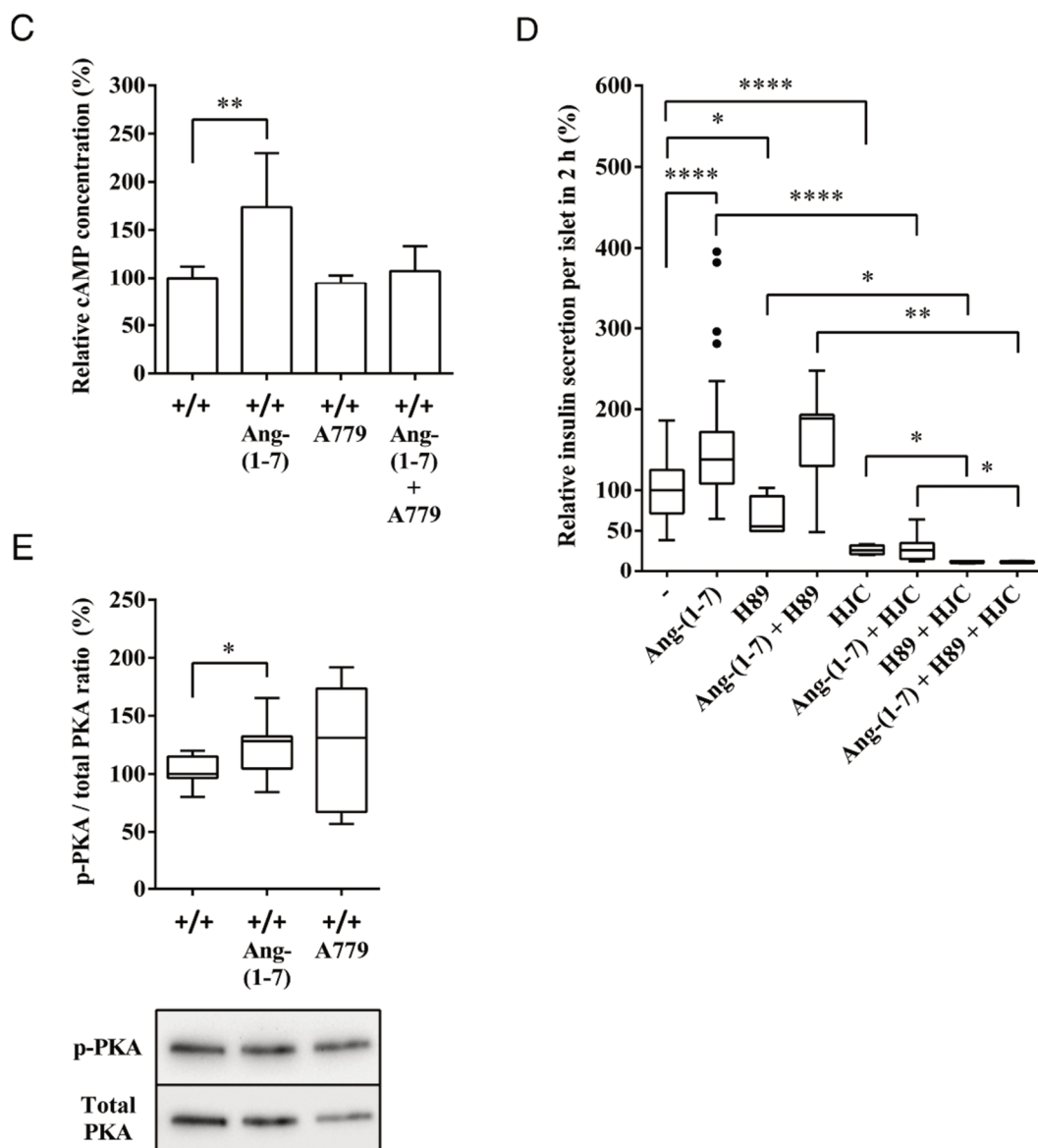


Figure 6.4.4 Effects of pharmacological modulation of the receptor Mas on cytosolic calcium concentrations ($[Ca^{2+}]_c$) in β -cells and cAMP contents, cAMP-dependent signalling, and PKA phosphorylation state in mouse islets

(A) $[Ca^{2+}]_c$ and the pattern of Ca^{2+} oscillations at 10 and 20mmol/l glucose in β -cells using the fura-2 method. Data are averaged values over 10min intervals. One representative experiment out of each group is shown. The n -values within the columns indicate the number of analysed cells (t test; ***, $P < .001$). (B) $[Ca^{2+}]_c$ and Ca^{2+} oscillation pattern in β -cells at 20mmol/l glucose in the presence of Ang-(1-7) or A779. (C) Intracellular cAMP concentrations in WT (+/+) islets with Ang-(1-7) or A779 treatment (mean \pm SEM, Mann–Whitney U test; **, $P < .01$; $n = 5$; $n = 2$ for A779). (D) Glucose-stimulated (20mmol/l) insulin secretion in presence of H89 or HJC 0350 ($n \geq 4$). (E) WT

islets were exposed to Ang-(1-7) or A779 for 24h and amounts of p-PKA and PKA were determined by immunoblot analysis with intensities analysed using ImageJ software. Calculated p-PKA/PKA ratios are presented together with one representative western blot image (Mann–Whitney U test; * $P < .05$; $n = 7$).

Mas-deficiency decreases insulin secretion from isolated islets without affecting insulin mRNA amounts or intra-islet insulin content

As already shown for the pharmacological blockade of Mas by A779 (Figure 6.4.3 A), genetic Mas-deficiency (-/-) resulted in a similar decrease in GSIS from islets under low (5.5mmol/l) as well as high (20mmol/l) glucose conditions (-1.6-fold and -2.1-fold, respectively) (Figure 6.4.5 A). Also the KCl-dependent insulin release was diminished (-2.4-fold) in these Mas-deficient islets. Furthermore, mRNA amounts of *Ins1*, *Ins2*, *Pdx1*, and *Mafa* of such islets lacking Mas were not significantly altered compared to islets isolated from WT mice (Figure 6.4.5 B).

In accordance with these findings, Mas-deficiency did not lead to changes in intra-islet insulin content when compared to wild-type islets (Figure 6.4.5 C).

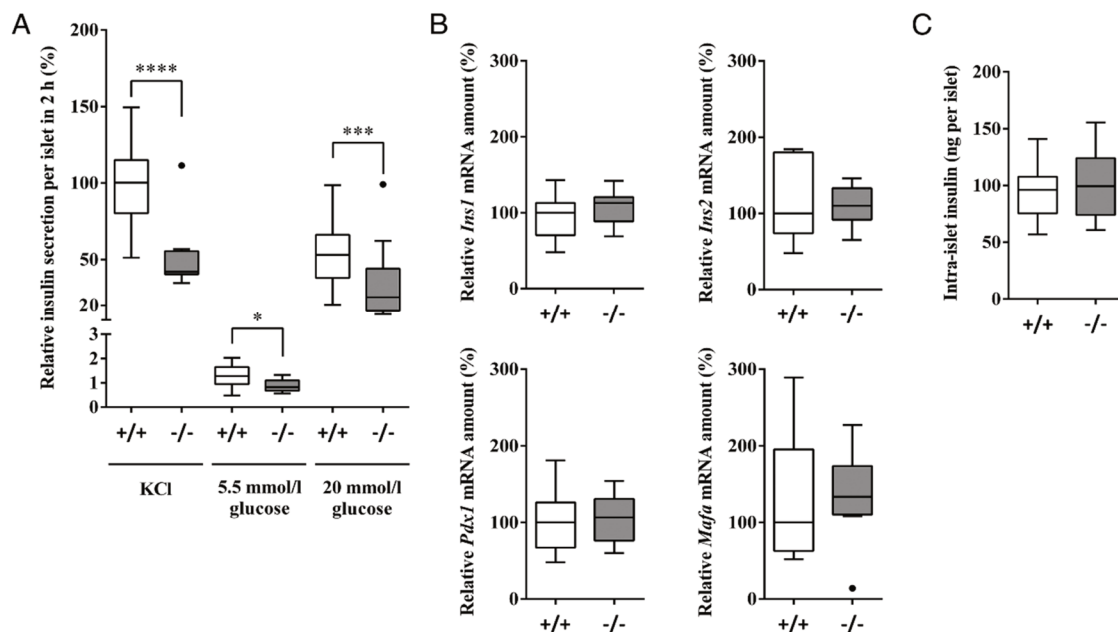


Figure 6.4.5 Effects of Mas-deficiency on

(A) KCl- and glucose-stimulated insulin secretion comparing WT (+/+) and Mas-deficient (-/-) islets (Mann–Whitney U test; **, $P < .01$; ***, $P < .001$; $n \geq 6$), (B) mRNA amounts of *Ins1*, *Ins2*, and insulin-regulating transcription factors *Pdx1* and *Mafa* in WT (+/+) and Mas-deficient (-/-) islets ($n \geq 8$), and (C) intra-islet insulin concentrations in WT (+/+) and in Mas-deficient (-/-) islets ($n \geq 13$).

Long-term Ang-(1-7) administration in vivo has minor effects on glucose tolerance

To determine long-term effects of Mas modulation on glucose tolerance and plasma insulin concentrations, Ang-(1-7) or control solution (\emptyset) were administered to wild-type and Mas-deficient mice by osmotic mini-pumps.

After 10 days, no differences in fasting blood glucose concentrations were detected between all groups of mice (Figure 6.4.6 A). The fasting plasma insulin concentrations of part of the wild-type mice treated with Ang-(1-7) showed a strong elevation, but did not reach significance compared to wild-type controls (Figure 6.4.6 B). While the fasting plasma insulin of Mas-deficient control mice was not altered in comparison to wild-type

controls, there was a significant reduction in fasting plasma insulin concentrations induced by Ang-(1-7) treatment in Mas-deficient mice (42.9pmol/l in knockout controls vs 33.2pmol/l when treated with Ang-(1-7)). Notably, this reduction in plasma insulin did not result in increased blood glucose concentration.

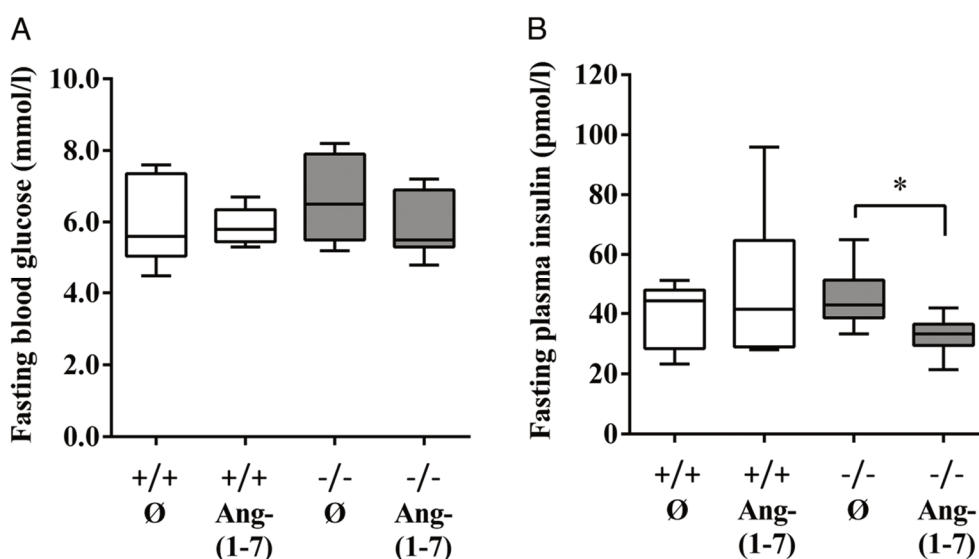


Figure 6.4.6 Effects of continuous Ang-(1-7) administration in vivo on fasting blood glucose and fasting plasma insulin concentrations of WT (+/+) and Mas-deficient (-/-) mice compared to controls (Ø)

(A) Blood glucose concentrations ($n \geq 5$) and (B) plasma insulin concentrations after 6h of fasting (Mann–Whitney U test; *. $P < .05$; $n \geq 5$).

After 10 days of continuous administration of Ang-(1-7), the rise in blood glucose during OGTT identified slightly, but not significantly higher blood glucose values in Mas-deficient compared to wild-type mice (Figure 6.4.7 A). Ang-(1-7) was not capable of significantly decreasing blood glucose concentrations in WT mice (Figure 6.4.7 B) or in Mas-deficient

mice (Figure 6.4.7 C). The influence of a 10-day Ang-(1-7) treatment on blood glucose during OGTT became apparent in Figure 6.4.7 D, where differences in blood glucose concentrations between Ang-(1-7)-treated wild-type and Ang-(1-7)-treated Mas-deficient mice reached nearly significance at 30 ($P = .064$) and 60 min ($P = .068$). This resulted in a significantly ($P = .011$) increased reactive G-AUC_{0–60 min} in Ang-(1-7)-treated Mas-deficient mice (reactive G-AUC_{0–60}: 540.4 ± 105.5 (mmol/l min)) compared to Ang-(1-7)-treated wild-type mice (reactive G-AUC_{0–60}: 388.0 ± 84.4 (mmol/l min)).

Relative changes of blood glucose concentrations during the first 15min after glucose administration (0min to 15min) were not significantly different between WT controls (+/+), Ang-(1-7)-treated WT and Mas-deficient (-/-) mice (Figure 6.4.7 E). Unexpectedly, Ang-(1-7)-treated Mas-deficient mice showed the strongest increase in blood glucose during the first 15min (2.8-fold increase), reaching significance when compared to Ang-(1-7)-treated wild-type mice (*, $P = .038$) (Figure 6.4.7 E). Congruent to the *ex vivo* data, plasma insulin concentrations increased 2.5-fold in WT mice treated with Ang-(1-7) within 15min after glucose administration, but did not reach significance ($P = .089$ vs solvent-treated WT mice) (Figure 6.4.7 F). This Ang-(1-7)-mediated increase in plasma insulin completely disappeared in Mas-deficient mice treated with the heptapeptide. Comparing the Ang-(1-7)-treated groups, there was a higher increase of blood glucose and a lower change in plasma insulin within 15min after glucose administration in Mas-deficient compared to wild-type mice (Figure 6.4.7 E, F).

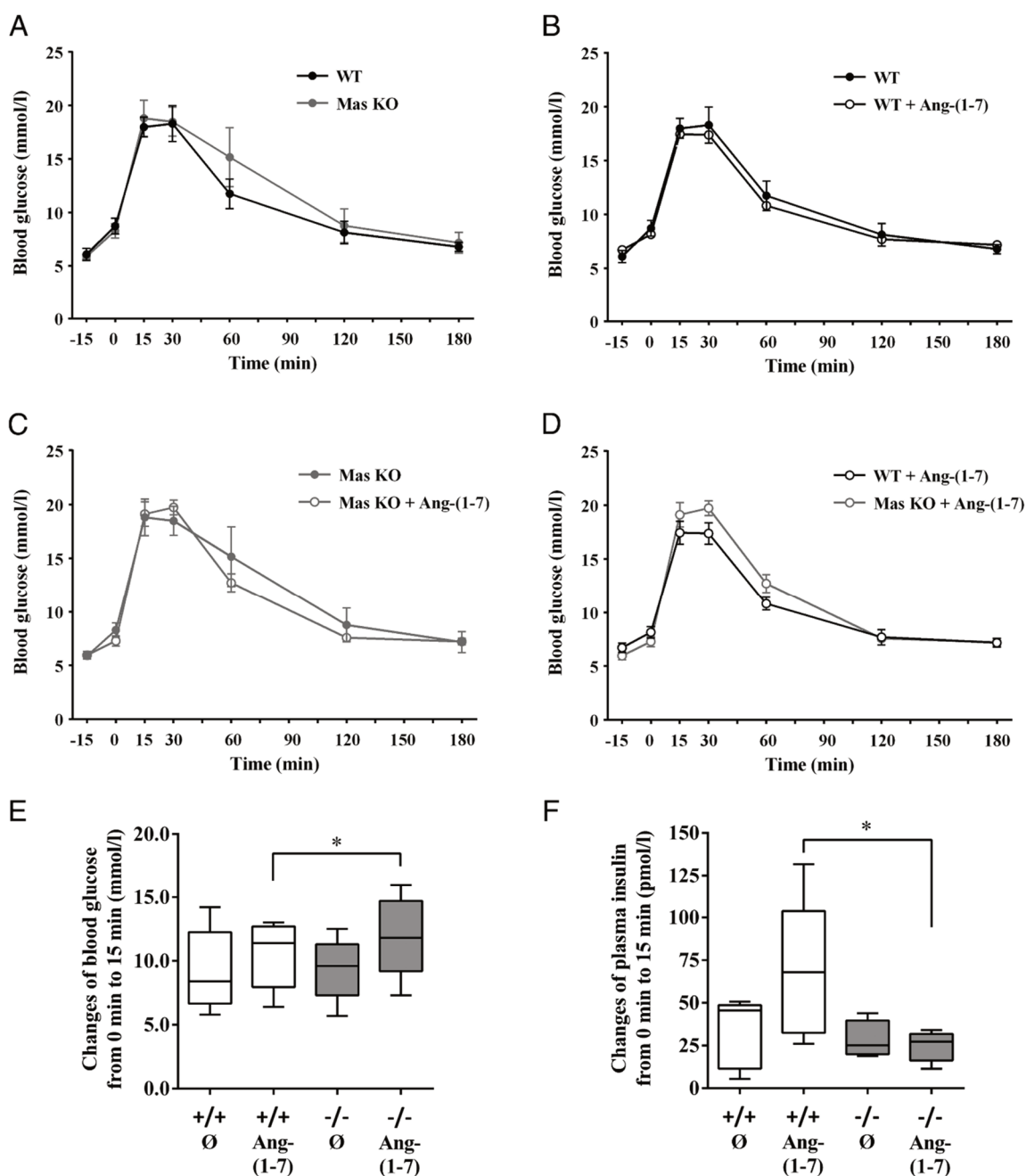


Figure 6.4.7 Effects of continuous Ang-(1-7) administration in vivo on glucose tolerance.

Blood glucose concentrations during OGTT comparing (A) WT (+/+) (black circles, $n = 5$) and Mas KO (-/-) control mice (gray circles, $n = 7$), (B) WT (+/+) control (black circles, $n = 5$) and Ang-(1-7)-treated WT (+/+) mice (white circles with black border, $n = 5$), (C) Mas KO (-/-) control mice (gray circles, $n = 7$) and Ang-(1-7)-treated Mas KO (-/-) mice (white circles with gray border, $n = 7$) and (D) Ang-(1-7) treated WT (+/+) (white circles with black border, $n = 5$) and Ang-(1-7)-treated Mas KO (-/-) mice (white circles with gray border, $n = 7$). Data are means with SEM. Changes in (E) blood glucose and (F) plasma insulin concentrations during the first 15min after glucose administration (Mann–Whitney U test; *. $P < .05$, $n \geq 4$).

Long-term Ang-(1-7) administration in vivo affects insulin secretion from isolated islets

To determine long-term effects of Mas stimulation on insulin secretion, islets from the WT and Mas-deficient mice treated 14 days with Ang-(1-7) or solvent alone were used.

Isolated islets from WT mice exposed *in vivo* to Ang-(1-7) exhibited a significant increase in insulin secretion in response to KCl (1.8-fold) and 20mmol/l glucose (1.3-fold) when compared to islets from solvent-treated mice (Figure 6.4.8 A). Of note, this effect was observed when islets were kept in culture for 24 h without further addition of Ang-(1-7).

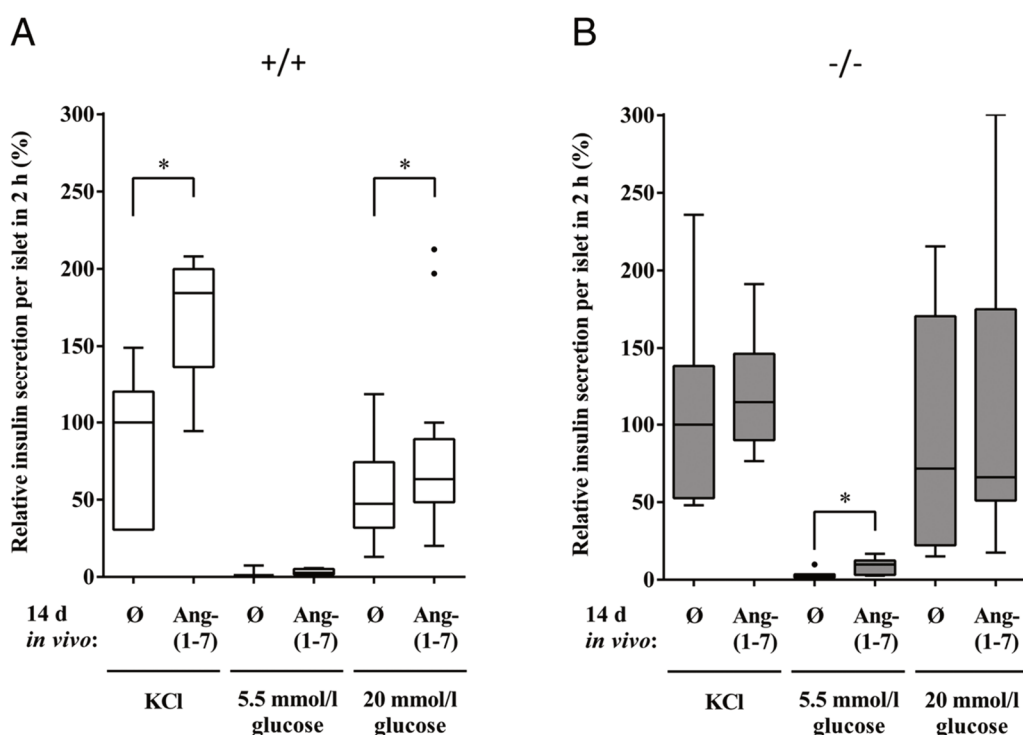


Figure 6.4.8 Effects of continuous Ang-(1-7) administration in vivo on insulin secretion of isolated islets.

KCl- and glucose-stimulated insulin secretion from isolated islets out of Ang-(1-7)-treated (A) WT (+/+) or (B) Mas-deficient (-/-) mice compared to their controls (Ø). (Mann–Whitney U test; *. $P < .05$; $n \geq 14$).

In islets from Mas-deficient mice, previously exposed to Ang-(1-7), no such changes in the KCl- or 20mmol/l glucose-induced insulin secretion could be observed (Figure 6.4.8 B) in comparison to the saline-exposed knockouts. Nevertheless, islets from these Ang-(1-7)-treated Mas-deficient mice showed a significantly increased basal secretion (3.6-fold) at low glucose conditions (5.5mmol/l) compared to islets from Mas-deficient control mice.

Discussion

The classical RAS with its ACE/Ang II/AT1 axis is a key trigger in the aetiology and severity of type 2 diabetes (2). It has been shown that increased Ang II levels are associated with the deterioration of β -cell function and adequate production and secretion of insulin [413, 414]. Nowadays, it is well accepted that the effects of the detrimental Ang II/AT1 axis can be blunted or even opposed by the Ang metabolite Ang-(1-7). Therefore, it was implicated to investigate, whether there is, besides the fairly well established role of Ang-(1-7) and its receptor Mas in the improvement of peripheral glucose uptake and insulin resistance [73, 125, 349], a considerable effect of this alternative RAS axis on the function of and, in particular, on insulin secretion from pancreatic β -cells.

Using cell biological, immunohistochemical, pharmacological, and biochemical approaches, and also genetically modified animal models, we discovered that Ang-(1-7) is capable of increasing insulin release from isolated mouse islets, despite the fact that it lacks any effects on mRNA amounts of *Ins1* and *Ins2* or transcription factors which are crucially involved in regulating insulin gene expression. This finding together with the unchanged islet insulin content strongly suggests that Ang-(1-7) exerts its effects on insulin secretion at a post-transcriptional/post-translational level. The observation that

Ca^{2+} oscillations of isolated islets are not altered in response to Ang-(1-7) further supports this finding and makes the secretory machinery a likely and reasonable target of Ang-(1-7)/Mas-dependent signalling. Our observation that even the KCl-induced insulin secretion is affected by A779 or Ang-(1-7) strongly supports the hypothesis of exocytosis being among the processes targeted by Mas ligands.

Our finding that Ang-(1-7) augments glucose-induced insulin secretion without affecting glucose-induced Ca^{2+} oscillations strongly suggests that the heptapeptide influences processes downstream to Ca^{2+} influx. The observation that insulin secretion induced by KCl depolarisation of the plasma membrane is decreased in islets from Mas-deficient mice compared to WT further supports the hypothesis of exocytosis being among the processes targeted by Mas ligands. Collectively, the data suggests that Mas ligands primarily influence the amplifying and not the triggering pathway of the regulation of insulin secretion [415]. Nenquin & Henquin showed that cAMP amplifies insulin secretion in islets lacking functional K_{ATP} channels via direct activation of EPAC [416]. Thus, amplification of insulin secretion by a cAMP-dependent mechanism may also play a crucial role for Mas receptor-mediated augmentation of hormone release.

In accordance with this assumption, Ang-(1-7) increased intracellular concentrations of cAMP in isolated islets. cAMP is a well-established key regulator of insulin secretion which acts via activation of cAMP-activated protein kinase (PKA) and/or exchange proteins activated directly by cyclic AMP 2 (EPAC 2) [417-419]. Besides regulating expression of target genes by modulating transcription factor activity, PKA and EPAC 2 proteins regulate exocytosis in various cell types, including insulin secretion from pancreatic β -cells [155]. In addition, cAMP-dependent phosphorylation by PKA contributes to the regulation of calcium-triggered exocytosis by e.g. phosphorylation of the SNARE (soluble NSF

attachment protein receptor) protein, SNAP-25, [420] or of the SNARE-binding protein, snapin [421]. Insulin exocytosis, thus, is augmented by both increased islet activity of PKA and by EPAC 2 signalling via mobilising insulin granules towards the plasma membrane of β -cells [422, 423]. However, our data implicate that the Ang-(1-7)-mediated increase in insulin secretion in response to high glucose concentration requires EPAC 2 activation but not PKA activation. Of note, that Ang-(1-7) acts via increased cAMP formation, as is the case with a number of the newer glucose-lowering drug classes (e.g. glucagon-like peptide-1 GLP-1 and its analogues), and thus in a glucose-dependent manner, would suggest it could be a better drug candidate than the previously used sulfonylureas.

Interestingly, the stimulatory effects of a 14-day *in vivo* administration of Ang-(1-7) on stimulated insulin secretion (glucose- or KCl-stimulated) of isolated islets were maintained *ex vivo* even when islets were cultured without further addition of Ang-(1-7). Thus, Ang-(1-7)-mediated effects can be “memorised” by the islets for at least 24 hours.

Despite the clear effects of Ang-(1-7) on stimulated insulin secretion of isolated islets, the observed effects *in vivo* on glucose homeostasis and plasma insulin concentrations remained marginal. This might be partly explained by the dose of Ang-(1-7) used based on literature data. It might not be the most effective dose and perhaps lower or higher concentrations may lead to more pronounced signals. Finally, the *in vivo* experiments were performed in healthy animals with naturally well-balanced glucose homeostasis. It can be thus hypothesised that the beneficial effects of Ang-(1-7) become more obvious in preclinical models of diabetes mellitus (data see Chapter 10.3). This idea is also supported indirectly by findings that tissue-nonspecific overexpression of ACE2 led to a slight reduction in blood glucose concentration in db/db mice, a model of type 2 diabetes, whereby ACE2 did not improve the glucose uptake in these mice, but instead led to an

increase in insulin concentration in the blood after glucose administration [424]. The ACE2 effect is also supported by our immunohistochemical data showing that ACE2 is predominantly expressed on β -cells. It might thus influence insulin secretion by generating locally Ang-(1-7) that can stimulate Mas there, as its expression on β -cells has been demonstrated, too.

It should be also stated that the potential Ang-(1-7) effects on the process of insulin secretion will be accompanied in the long-term by other beneficial effects of the heptapeptide on islet function. Exemplarily, Ang-(1-7) improved the intra-islet microvascular density, reduces apoptotic islet cells and increased iNOS expression and NO release in a rat model of type 2 diabetes [413, 425].

Furthermore, as a substantial number of studies over the past five decades have clearly demonstrated that β -cell mass is reduced in patients with type 2 diabetes [426], the possibility that Ang-(1-7) therapy may not only improve pancreatic cell function but also increase cell mass in patients with type 2 diabetes might therefore generate even more excitement. This is supported by data showing substantial effects of Ang-(1-7) on stem and progenitor cells [374], and immuno-histochemical images indicating an increase in the proliferation of β -cells and an increase in the cell surface per islet in ACE2-overexpressing mice [424]. Furthermore, bone marrow and circulating endothelial progenitors, as well as bone marrow mesenchymal stem cells, were increased in db/db mice treated with Ang-(1-7) [427].

One of the most interesting findings presented in the present study is the identification of Mas-independent Ang-(1-7) function as illustrated by effects of the heptapeptide in Mas-deficient mice and on islets isolated from such animals. Although there are already indications for further Ang-(1-7) receptors based on pharmacological approaches using

either different Ang-(1-7) antagonists [357] or receptor transfected cells [65], it remains a very interesting challenge to identify the second receptor Ang-(1-7) can act through when affecting β -cell function. Very recently, the authors identified a second receptor for Ang-(1-7), MrgD [378], which could be a potential candidate for mediating the Mas-independent effects of the heptapeptide. This hypothesis is also supported by the finding that the Ang-(1-7) antagonist, D-Pro⁷-Ang-(1-7), which has been shown to block both, Mas and MrgD, can abolish the Ang-(1-7)-mediated stimulation of insulin secretion, while the more Mas-specific antagonist, A779, was much less efficient. This deserves to be extensively studied in future work.

Taken together, clinically established glucose-lowering medications act either via increased insulin sensitivity and thus more efficient uptake of glucose (insulin sensitisers such as metformin and thiazolidinediones) or by increasing insulin secretion from pancreatic β -cells (insulin secretagogues such as sulfonylurea). Our data identify Ang-(1-7) as a molecule that can act via both mechanisms, representing a new and promising strategy for the treatment of diabetes mellitus, not only improving peripheral insulin resistance but also the β -cell function in the form of an adequate glucose-stimulated insulin secretion.

Acknowledgments

We thank Manja Möller, Ines Schultz, Rebecca Lancaster, Carmen Härdtner, Bärbel Miehe, and Sindy Schröder for their kind support.

7 General discussion

Over the past decades, the knowledge about the RAS has substantially improved. However, there are still biological effects of the peptides that cannot be explained with the existing knowledge about the structure of the RAS. It is clear that our current understanding of the RAS is still incomplete. Complex signalling pathways and the continued increase of members (peptidases, peptides, receptors) within the RAS is complicating the research. Additionally, the RAS activates pathways with opposing biological actions. On the one side we have the often detrimental ACE/ Ang II/ AT1 axis, and on the other side the protective ACE2/ Ang-(1-7)/ Mas axis.

7.1 cAMP is the primary second messenger activated by Ang-(1-7)

Ang-(1-7) is a heptapeptide with a lot of beneficial effects, such as vasorelaxation [104-109], anti-fibrosis [78, 95], neuro protection [111, 119] and anti-proliferation [133-135, 137-139]. The lack of knowledge about a second messenger stimulated by Ang-(1-7) hindered the confirmation of the Ang-(1-7) receptor and investigations of receptor pharmacology. Until now, specific blockers such as A779, D-Pro and PD123319, have been used to define the receptors through which Ang-(1-7) mediates its effects. Therefore I aimed to identify a second messenger to better investigate the receptor targeted by Ang-(1-7).

In recent studies, Liu *et al.*, and Tallant and Clark described that Ang-(1-7) is able to stimulate the increase of intracellular cAMP in rat MC [141] and VSMC [133], respectively, suggesting cAMP as a potential second messenger. This work (published July 2016) confirms that Ang-(1-7) can indeed increase cAMP in several cell types such as MC, VSMC (Figure 6.1.1 A and D) and HUVEC (Figure 6.1.2 A). This increase in intracellular cAMP was not mediated by the inhibition of PDE activity, which is responsible for cAMP degradation, since the treatment with IBMX (PDE inhibitor) had no effect on the intracellular cAMP levels (Figure 6.1.2 C) stimulated by Ang-(1-7). The AC inhibitor, SQ22536, inhibited the increase in cAMP (Figure 6.1.2 D), also confirming that the cAMP increase is mediated by AC and not by PDE inhibition. Furthermore, the increase in intracellular cAMP levels also mediated further downstream signalling. PKA activity (Figure 6.1.2 E) and CREB phosphorylation (Figure 6.1.5 A and B) were increased after Ang-(1-7) stimulation, confirming that the cAMP signalling pathway leads to further intracellular responses.

Besides the PDEs, intracellular cAMP concentrations are also regulated by the transport of cAMP into the extracellular space through a specific transport system, which belongs to the ATP-binding cassette (ABC) transporter superfamily [428]. The existence of extracellular cAMP could be shown for several cell types such as vascular smooth muscle cells [429], pulmonary arteries [430] and cardiac myocytes [431]. Extracellular cAMP might be able to act as an extracellular signalling molecule [432]. Thus, the level of cAMP efflux in the cell types used in this study should be investigated, as cell type specific alteration of the cAMP efflux might interfere with the intracellular cAMP concentrations.

Despite this, the identification of cAMP as a second messenger activated by the heptapeptide will be a helpful tool for further investigations regarding Ang-(1-7) and its receptors.

7.2 Mas is a functional receptor for Ang-(1-7)

For more than a decade, the receptor for Ang-(1-7) remained undiscovered. Initially, AT₂ had been thought to be an Ang-(1-7) receptor. However, the heptapeptide has only low affinity to the AT₂ receptor [64], but there were reports that Ang-(1-7) effects could be blocked by PD123319, a compound which has been assumed to be AT₂ specific [433, 434]. First it was believed that Mas is a receptor for Ang II, but neither binding nor signalling could be shown [61]. In 2003, Santos *et al.* were able to demonstrate that Mas is the receptor for Ang-(1-7). They showed that the Ang-(1-7) mediated effects could be blocked by A779, a Mas specific antagonist, while Ibersartan (AT₁ blocker) or PD123319 (AT₂ blocker) failed to block the Ang-(1-7) mediated effects, indicating that AT₁ or AT₂ were not involved in such processes. In addition, aortic rings isolated from animals lacking the Mas receptor did not show any response towards stimulation with the heptapeptide peptide, which was able to generate vasorelaxation in wild-type aortas [62].

However, the detailed molecular mechanism behind the Mas signalling mediated by Ang-(1-7) remained unknown. Most of the studies from the past years were focused on the analysis of *in vivo*/*ex vivo* function (e.g. vasorelaxation, fibrosis, endothelial function) [99, 100, 114] or downstream signalling like AA release and Ca²⁺-independent activation of NOS via PI3K. [62, 65, 232]. Therefore, the aim of this study was to investigate if Mas is a

functional receptor for Ang-(1-7) and if cAMP is the secondary messenger activated by stimulation with the heptapeptide. It was possible to confirm that Mas is indeed a functional receptor for the heptapeptide, as Ang-(1-7) was able to increase intracellular cAMP in a dose depended matter (Figure 6.1.4 A). This also illustrates that Mas couples not just to $G_{\alpha q/11}$ [240], but also $G_{\alpha s}$.

7.3 MrgD is a receptor for Ang-(1-7)

Interestingly, in contrast to the work performed by Santos *et al.* in 2003, the increase in cAMP in MC, HUVEC and VSMC was not just blocked by A779, but also PD123319 and D-Pro (Figure 6.1.1 B, D and Figure 6.1.2 A). Since PD123319 is assumed to be an AT₂ specific blocker [190-192] and D-Pro is known to block MrgD [42] and Mas [65, 254], I raised the hypothesis that the increase in cAMP in MC, HUVEC and VSMC was not just Mas related, but might also involve other receptors. Thus, the aim was to identify if Ang-(1-7) can also activate other G-protein coupled receptors.

Gembardt *at al.* were previously able to show that Ang-(1-7) could increase AA release not just in Mas-transfected, but also in Mrg and MrgD-transfected cells [65]. This finding confirms that the high similarity between the Mas like family [65, 215], makes it very likely that not just Mas, but also other members of this family might be receptors for Ang-(1-7). These two facts and my previous finding that D-Pro can block the Ang-(1-7) mediated cAMP increase in MC, HUVEC and VSMC led to the conclusion that MrgD might be another candidate as an Ang-(1-7) receptor.

Indeed, this study was able to demonstrate that not just Mas, but also MrgD is a receptor for Ang-(1-7). Using HEK293 cells transfected with the receptors of interest (Mas, MrgD, Mrg and AT2), it was possible to demonstrate that Ang-(1-7) is able to increase intracellular cAMP, not just in cells expressing Mas, but also MrgD (Figure 6.2.3 A). Both Mas and MrgD, had a comparable dose dependent increase in cAMP after Ang-(1-7) stimulation (Figure 6.1.4 A and C).

The fact that the AA release was increased in Mrg-transfected cells [65], but not cAMP (Figure 6.2.3 A) confirms that both pathways do not necessarily correlate with each other, as AA release PLA2 mediated and G_{α_s} independent [435]. Consequently, other members of the Mas family, which did not respond to the heptapeptide with an increase in AA release, might still respond with an increase in intracellular cAMP. Additionally, considering the high homology between the Mas-like receptors, the possibility is high that other members might also be functional Ang-(1-7) receptors. Therefore, the next step would be to screen other receptors of the Mas like family for a response to Ang-(1-7).

7.4 Ala¹-Ang-(1-7) can also act through the Mas receptor

Like Ang-(1-7), Ala¹-Ang-(1-7) is able to counteract effects mediated by Ang II and has beneficial effects such as vasorelaxation, being anti-hypertrophic, anti-hypertensive and anti-fibrotic [42, 246, 250]. Lautner *et al.* were the first who described and characterised Ala¹-Ang-(1-7) in 2013 [42]. They were able to demonstrate that this heptapeptide acts through the Mas-like receptor MrgD, but not Mas [42]. Compared to Ang-(1-7), the number of publications on Ala¹-Ang-(1-7) over the past 5 years is very small, indicating

that still very little is known about the peptide that has been described as endogenously occurring in human plasma [42]. Furthermore, the existing publications on Ala¹-Ang-(1-7) focus on the physiological function of the peptide (*in vivo*, *ex vivo*) [42, 249-251], for example vasorelaxation. Just very few publications dealt with the intracellular effects (for example NO, and AA release) [42, 251].

However, the fact that MrgD, and not Mas, is the receptor for Ala¹-Ang-(1-7) was accepted and never questioned over the past years. With the recent identification of cAMP as a second messenger increased by activation of Mas and MrgD, a potential tool was given to further investigate the receptors for Ala¹-Ang-(1-7). The previous finding that Ang-(1-7) can also stimulate MrgD, and the fact that both peptides interact with their C-terminal ends with the receptor, and with that should have comparable interactions, rose the hypothesis that Ala¹-Ang-(1-7) might also stimulate Mas. Therefore, the aim of the study was to investigate, whether Ala¹-Ang-(1-7) is also able to stimulate the Mas receptor. Firstly, I needed confirmation that MrgD is a functional receptor for Ala¹-Ang-(1-7). Consequently, I also aimed to investigate if Ala¹-Ang-(1-7) is able to increase intracellular cAMP levels in MrgD transfected cells. It was possible to confirm that MrgD indeed is a functional receptor for Ala¹-Ang-(1-7). The peptide increased intracellular cAMP and this effect was dose dependent (Figure 6.2.2 A). More importantly, Mas could be identified as a second functional receptor for the heptapeptide (Figure 6.2.3 A), disproving the findings made by Lautner *et al.* that Ala¹-Ang-(1-7) is not able to target both receptors [42]. Using MC derived from animals lacking Mas or MrgD, or both receptors, the final proof that both Mas and MrgD are important for Ala¹-Ang-(1-7) mediated effects was received. The MC derived from single knockout animals still showed a significant increase in cAMP, which was, however, lower compared to the WT signalling

(Appendix part 1: Figure 10.2.1). This confirmed that Mas and MrgD are important for the Ala¹-Ang-(1-7) mediated cAMP increase in MC. Furthermore, the MC derived from the double knockout animals have not been able to respond to Ala¹-Ang-(1-7) stimulation (Figure 6.2.4 C), confirming the previous finding. The finding that Ala¹-Ang-(1-7) is not MrgD specific interferes with the therapeutic options, as Lautner *et al.* described the increase of Ala¹-Ang-(1-7) under pathophysiological conditions [42].

The effects on cAMP generation mediated by Ala¹-Ang-(1-7) in Mas and MrgD transfected cells is comparable. Both dose response curves are bell shaped and the EC₅₀ values are comparable (Figure 6.2.2 A and Figure 6.2.3 A). Lautner *et al.* described in their experiments that the vasodilatory effect of Ala¹-Ang-(1-7) could not be blocked by A779 [42]. However, in our experiments, it was possible to block the Ala¹-Ang-(1-7) mediated cAMP increase in MC and HUVEC with A779, D-Pro and PD123319 (Figure 6.2.1 B and Figure 6.2.4 B), further indicating that other receptors, apart from MrgD, are involved in the Ala¹-Ang-(1-7) mediated cAMP increase.

As for Ang-(1-7), the next step would be to screen the Mas like family, as also other members might be functional receptors for Ala¹-Ang-(1-7).

7.5 Ang-(1-7) and Ala¹-Ang-(1-7) possess different pharmacodynamics

Besides the very similar physiological effects of Ang-(1-7) and Ala¹-Ang-(1-7) [42, 246, 250], the results demonstrate that the pharmacological properties are different. The dose

response curve generated with Ala¹-Ang-(1-7) is shifted leftwards (lower EC₅₀) compared to the one from Ang-(1-7) (Figure 6.2.1 A), indicating a better potency of Ala¹-Ang-(1-7). Furthermore, the shape of the dose response curves are significantly different (Figure 6.2.1 A). The bell shaped curve generated by Ala¹-Ang-(1-7) indicates the peptide has an optimum range of concentration where it shows its being most effective. However, what causes this shape of the curve? The G-protein responsible for inhibiting cAMP is G_{αi}, and MrgD is known to couple to G_{αi} [253]. Therefore, it was hypothesised that G_{αi} might be activated when higher concentrations of Ala¹-Ang-(1-7) are used. It is not uncommon, that one compound can activate different G-proteins. Beyermann *et al.* [390] confirmed this model by using the corticotropin-releasing factor receptor type 1. They demonstrated that native ligands stimulated G_{αi} and G_{αs} proteins. Indeed, PTX, a potent G_{αi} inhibitor, was able to prevent the reduction of cAMP at higher concentrations of Ala¹-Ang-(1-7) (Figure 6.2.2 C and Figure 6.2.3 C), confirming that G_{αi} is involved in the signalling mediated by this peptide. The discovery that one compound can activate two different G-proteins in both receptors is very important, as future non-peptidic agonists should be designed in a way that G_{αi} activation is avoided.

As Ang-(1-7) and Ala¹-Ang-(1-7) are very similar, another question arose: how can the difference in potency be explained? First, it was thought that the lack of the carboxylate group might releases more energy during interaction with the receptor, but our computer model could not confirm this. However, the computer analyses performed by collaborators showed, that the missing carboxylate group can stabilize the binding to the receptor and that this the reason that Ala¹-Ang-(1-7) is more potent than Ang-(1-7). While, the negatively charged carboxylate in Asp¹ of Ang-(1-7) prevents the interaction with a positive chemical group in the receptor (see Figure 6.2.5). Consequently, this

knowledge about the interactions of both peptides with the Mas receptor gained from this model, will lay a foundation for a screening program to identify agonists stimulating either one or both of the receptors.

7.6 The AT₂ specific blocker, PD123319, also blocks Mas and MrgD

In AT₂ transfected HEK293 cells, Ang-(1-7) failed to increase cAMP (Figure 6.1.3). Nevertheless, PD12219 was able to block the effects in MC and HUVEC cells, indicating an involvement of AT₂. However, if AT₂ is not responsible for the cAMP increase in those cell types, why does PD123319 block the Ang-(1-7) mediated cAMP increase? Additionally, other researchers described that under certain circumstances, PD123319 is able to block Ang-(1-7) mediated effects [433, 434]. Might PD123319 be not AT₂ specific, as it has been claimed all the years [190-192]? Indeed, it was possible to demonstrate that this is the case. In HEK293 cells expressing Mas or MrgD, PD123319 was able to block the Ang-(1-7) mediated cAMP increase (Figure 6.1.4 B and D). Furthermore, PD1222139 cannot just block Ang-(1-7) mediated cAMP, but also Ala¹-Ang-(1-7) mediated effects on cAMP levels in Mas or MrgD transfected HEK293 cells (Figure 6.2.2 B and Figure 6.2.3 B). This unspecific receptor profile of PD123319 is not surprising anymore, if its structure is compared to Ang-(1-7). PD123319 can be embedded in bioactive conformation of Ang-(1-7) when it is bound to the Mas receptor (Figure 6.1.6 F). It displays chemical similarities to Ang-(1-7), implicating that both molecules fit into the two Ang-(1-7) receptors, whereby PD123319 fails to stimulate intracellular signalling.

However, the identification of PD123319 being not AT2 specific has further consequences. Papers, which conclude on AT2 function by just using PD123319, might need to be re-evaluated, as Mas and MrgD might also be involved in the observed effects. But it also might give an explanation for cases where PD123319 was not able to block Ang-(1-7) mediated effects.

7.7 The AT2 specific compound C21 also stimulates Mas and MrgD

Since its discovery in 2004 by Wan *et al.* [185], C21 is widely used to identify and define the *in vivo* function of the AT2 receptor. C21 is claimed to be a highly specific AT2 receptor agonist and is already used in a wide range of preclinical trials [186-188]. Furthermore, this small non-peptidic molecule has a good oral availability, and was very well tolerated in phase I studies performed by Vicore-Pharma, the company owning the patent for C21 [436].

Since studies have shown that the Mas receptor blocker A779 can prevent the protective C21 effects in an ischemic stroke model [398], and the previous finding that PD123319 was not AT2 specific, the specificity of this compound is also questionable. Furthermore, the chemical structures of C21 and the Mas-specific agonist AVE0991 are very similar as Villela *et al.* [398] and we could demonstrate. The *in silico* modelling (Figure 6.3.6 A and B) in collaboration with Intelligent Pharma illustrates the similarities and differences between C21 and AVE0991, the first non-peptidic agonist for the Mas receptor [65],

which is another point to speculate that C21 is also able to stimulate the Mas receptor. Therefore, it was hypothesised that C21 might be also able to stimulate Mas and MrgD.

Indeed, in this study it was possible to show that Mas and MrgD are both functional receptors for C21. The compound stimulated an increase in intracellular cAMP in MC and this effect was abolished by A779, D-Pro and PD123319, indicating that not just AT₂, but also Mas and MrgD were involved (Figure 6.3.3 A and B). HEK293 cells transfected with Mas or MrgD (Figure 6.3.1 A and Figure 6.3.2 A) also showed an increase in intracellular cAMP, confirming that both receptors are stimulated by C21. Interestingly, the dose response curves observed in Mas and MrgD were different. Mas showed a bell shaped dose response curve (Figure 6.3.1 A), like for Ala¹-Ang-(1-7), whereas the dose response curve in MrgD transfected cells was sigmoidal (Figure 6.3.2 A), like for Ang-(1-7). There is no distinct explanation for this behaviour so far. One reason might be that beside the structural similarities of both receptors, C21 interacts slightly different with MrgD than with Mas. The involvement of G_{αi} was excluded, as C21 failed to increase the luciferase signal in HEK293 cells co-transfected with Mas and an Elk1-promotor, a downstream effector of G_{αi} (Figure 6.3.1 E). However, the observed intracellular cAMP increase was AC mediated, as it could be blunted by the AC inhibitor, SQ22536 (Figure 6.3.1 C). C21 stimulates different receptors in primary cells, which was further confirmed by using a second cell type, HUVEC. Figure 6.3.5 A shows a biphasic dose-response curve. The two maximum peaks correspond to the peaks in Mas (10⁻¹⁰ M) and MrgD (10⁻⁷ M)-transfected cells (Figure 6.3.1 A and Figure 6.3.2 A). There is no pharmacological proof existing that this is really Mas and MrgD mediated, as no specific blocker for the C21 mediated effect exists.

Using mesangial cells derived from animals not expressing AT2, the final proof that C21 is not AT2 specific was obtained. The cells were still able to respond to C21 stimulation with an increase in cAMP (Figure 6.3.3 C). This was confirmed using western blot analysis. AT2 KO cells still showed an increased CREB phosphorylation after 15min of stimulation with C21 (Figure 6.3.4 B). This was also confirmed by using western blots analysing the phosphorylation of PKA substrates (Figure 10.2.2 A and B), as AT2 KO cells still showed an increase in the phosphorylation of PKA substrates. Interestingly, in double knockout mesangial cells, lacking Mas and MrgD, the signal was not completely blunted, but lower than in untreated cells (Figure 6.3.3 C). This drop in Mas/ MrgD-deficient cells allows the interpretation of the observation made in AT2-deficient mesangial cells. The increase by C21, which is slightly above the level from the untreated cells, might be in reality much higher, considering the negative value from the DKO cells. The cAMP-lowering effect might be caused by a $G_{\alpha i}$ coupled receptor, which is also stimulated by C21. Because of the structural similarity, one possibility is that a member from the Mas like family also responds to C21. Final proof of this fascinating hypothesis could be generated with cells deficient in Mas/MrgD and AT2, where any drop in intracellular cAMP after C21 stimulation would relate to such a postulated unknown receptor.

Furthermore, it might also be interesting to investigate in follow-up experiments, whether in reverse conclusion AVE0991 is not Mas-specific, but can, similar to C21, also stimulate MrgD and AT2.

Taken together, these results improve the understanding of the function of the AT2 receptor under physiological and pathophysiological circumstances. Concluding on AT2 function by just using C21 might be incorrect. Publications, which conclude on AT2

receptor effects using only C21 need to be re-evaluated, like with PD123319, Mas and MrgD might also be involved. Furthermore, the identification of cAMP being regulated by C21 will help with the prediction of potential applications of C21 by identifying diseases where elevation of cAMP is assumed to be beneficial, and where target organs express either Mas, MrgD or AT2.

7.8 Ang-(1-7) improves beta cell function

It is well known that the RAS and blood glucose are highly connected. As increased blood glucose levels can activate the RAS through several mechanisms [325-331] (Chapter 4.3.7), it is no surprise that the manipulation of the RAS might be a useful tool to treat DM. Many studies could already demonstrate that the blockage of the ACE/ Ang II/ AT1 axis and the activation of the ACE2/ Ang-(1-7)/ Mas has beneficial effects on glucose homeostasis and other DM related symptoms (Chapter 4.3.7). However, many of the molecular mechanisms remained unclear. Therefore the aim of this study was to examine which molecular mechanism might be involved in the Ang-(1-7) mediated effects in DM.

Together with our collaborators, we were able to show that Ang-(1-7) can improve the insulin secretion in β -cells (Figure 6.4.3 A). Furthermore, this effect was mainly Mas dependent, as animals lacking the Mas receptor had a decreased insulin secretion (Figure 6.4.5 A).

In addition, cAMP was shown to be the primary secondary messenger responsible for Ang-(1-7) mediated insulin secretion (Figure 6.4.4 C). Like in our MC the downstream signalling resulted in an activation of PKA, as the increase in PKA phosphorylation

confirms (Figure 6.4.4 E). However, as the increase in insulin secretion in islets isolated from WT mice could be blocked by an EPAC inhibitor (HJC), but not by a PKA inhibitor (H89) (Figure 6.4.4 D and E), indicating that EPAC activation is necessary for insulin secretion and not PKA activation. With that, we not only confirmed that Ang-(1-7) has beneficial influence on Mas, as other groups already reported [340], but we also demonstrated that Mas is involved, and that cAMP is the major second messenger activated.

Although the effects observed in the *in vivo* studies remained marginal (Figure 6.4.6 A), it was possible to show that Ang-(1-7) has beneficial effects on the insulin secretion in β -cells (Figure 6.4.6 B). Furthermore, this effect showed to be Mas specific, as there was no change of insulin secretion in Ang-(1-7) treated animals lacking the Mas receptor (Figure 6.4.6 B). This *in vivo* results might be partly explained by the dose of Ang-(1-7) used based on literature data. It might not be the most effective dose and perhaps higher concentrations may lead to more pronounced signals. Additionally, the *in vivo* experiments were performed in healthy animals with a well-balanced glucose homeostasis. It may be hypothesised that the beneficial effects of Ang-(1-7) become more obvious in preclinical models of DM (data see Chapter 10.3).

7.9 Ang-(1-7) does not improve the blood glucose levels in STZ induced diabetic animals

Many studies could show that the ACE2/Ang-(1-7)/Mas Axis counteracts Ang II/ AT1 mediated effects, and also has beneficial effects on DM and associated symptoms as described in Chapter 4.3.7. As there was no effect on the basic blood glucose levels in healthy animals (Figure 6.4.6), it was concluded that Ang-(1-7) mediated effect on insulin secretion might just be occur under pathophysiological conditions. For this purpose, STZ-induced diabetic mice were used for further investigations. This model was chosen because 1) data provided by Invitek (Figure 10.3.1) and 2) we could use our knockout animals.

The *in vivo* experiments failed to confirm findings from other researchers, which demonstrated that Ang-(1-7) has positive effects on BG levels [73, 349, 350]. There was no significant effect on BG levels in animals expressing the Ang-(1-7) receptors, or those which lack Mas, MrgD or both receptors (Appendix Part 1: Figure 10.3.2 and Figure 10.3.3 A-D). Higher concentrations of Ang-(1-7) (2 mg/kg) showed also no beneficial effect, in fact they significantly worsened the BG levels (Appendix part 1: Figure 10.3.5). Furthermore, 0.5 mg/kg Ang-(1-7) treatment also resulted in an increase in BG levels compared to WT, over the whole time of treatment, which is contradictory to the results shown in Figure 10.3.3 A. In addition, the spleen and the heart were affected by the high glycaemic conditions. The weight of the organs from the high dose Ang-(1-7) treated group was significantly lower compared to the control group (Appendix part 1: Figure 10.3.6). It is well known that high BG levels cause long-term damage of end-organs.

Diabetic cardiomyopathy is one example [336, 337], but the spleen also can be affected. A study in STZ-induced diabetic rats described that the hyperglycaemia resulted in a decrease in the weight of the spleen [437]. Thus, the observed decrease in the weight of the heart and the spleen might be a result of the more severe diabetes those animals developed compared to the untreated group.

These findings are contrary to the ones reported in the literature, where mainly beneficial effects of Ang-(1-7) on the glucose homeostasis could be described [73, 349, 350], but also to the results from the preliminary study performed by Invitek, which showed that Ang-(1-7) significantly reduces BG levels (Appendix Part 1: Figure 10.3.1). Besides using finally the same standardised protocol in our study and the study performed by our collaborator in America used before, we still did not see the same beneficial effects of Ang-(1-7) as they described (Figure 10.3.1). This might be explained with the conditions the animals were held. Our facility might have used a different food, or exposure to pathogens happened (animals were not held behind completely sterile barrier), which could have led to different results, as those animals are very sensitive to external factors. On the other hand, other publications also reported that Ang-(1-7) did not affect the BG levels in STZ-induced diabetic rats [438, 439], but still was beneficial against diabetic renal injury [439].

Additionally, the data also indicates that endogenous Ang-(1-7) has also no important effect in the aetiology of T1DM, as there was no detrimental effect on the BG levels in animals lacking Mas, MrgD or both receptors. If Ang-(1-7) would play a role in the development of DM, at least the animals lacking both receptors should show a higher increase in BG levels compared to WT animals. Taken together, the results from this study

confirm, that Ang-(1-7) mediates beneficial effect under high glycaemic conditions, without affecting BG levels.

However, also other reasons might have caused contradictive results to the Invitek-study. If we compare the maximum of BG levels reached in our animals with those of the animals from the Invitek-study, we see that they are higher in the Cork-setting. This more severe diabetic stage might have prevented that Ang-(1-7) treatment was effective. In the future, lower dose of STZ should be tested to prevent the strong increase in BG levels. Another reason might be the concentration of Ang-(1-7) used. As higher concentrations of the heptapeptide worsened the BG levels (Appendix part 1: Figure 10.3.5), lower concentrations should be tested as well in the future. It could be that higher concentrations of Ang-(1-7) activate other receptors, which counteract the beneficial effects mediated by Ang-(1-7)/ Mas/ MrgD. Furthermore, fasted BG levels were not measured, the animals had always access to food. Thus, more variation was generated, because the weaker mice could not drink or eat, which resulted in lower BG caused by the lack in food intake, while the less sick animals could still eat, resulting in higher BG levels. In the future, fasted BG should be measured to exclude those variations. In addition, compounds such as C21 and Ala¹-Ang-(1-7) should be investigated in the future, as they might be more potent than Ang-(1-7).

8 Conclusion

This study, significantly contributed to an expansion and refining of the RAS (Figure 7.9.1).

It was possible to demonstrate that:

- 1) Mas is a functional receptor for Ang-(1-7)
- 2) cAMP is the primary second messenger
- 3) MrgD is also stimulated by Ang-(1-7)
- 4) Ala¹-Ang-(1-7) also stimulates the Mas receptor
- 5) The AT2 specific antagonist, PD123319, also blocks Mas and MrgD
- 6) The AT2 specific agonist C21 also interacts with Mas and MrgD

The experiments with Ala¹Ang-(1-7) makes it clear that even a tiny change in the molecular structure of an agonist (here Ang-(1-7)) can create a significant change of its pharmacological properties. The gained understanding of the interaction of compounds like PD123319, C21, Ala¹-Ang-(1-7), and Ang-(1-7) with AT2, Mas and MrgD, can be used as a foundation for the development of further agonists, especially non-peptidic small molecules, with better potency and specificity. This will lead to the development of pharmaceutical compounds with less side effects, caused by unwanted activation or inactivation of other receptors. Furthermore, our findings enforce the revisit of such publications, which concluded on AT2 function by only using C21 or PD123319, or both.

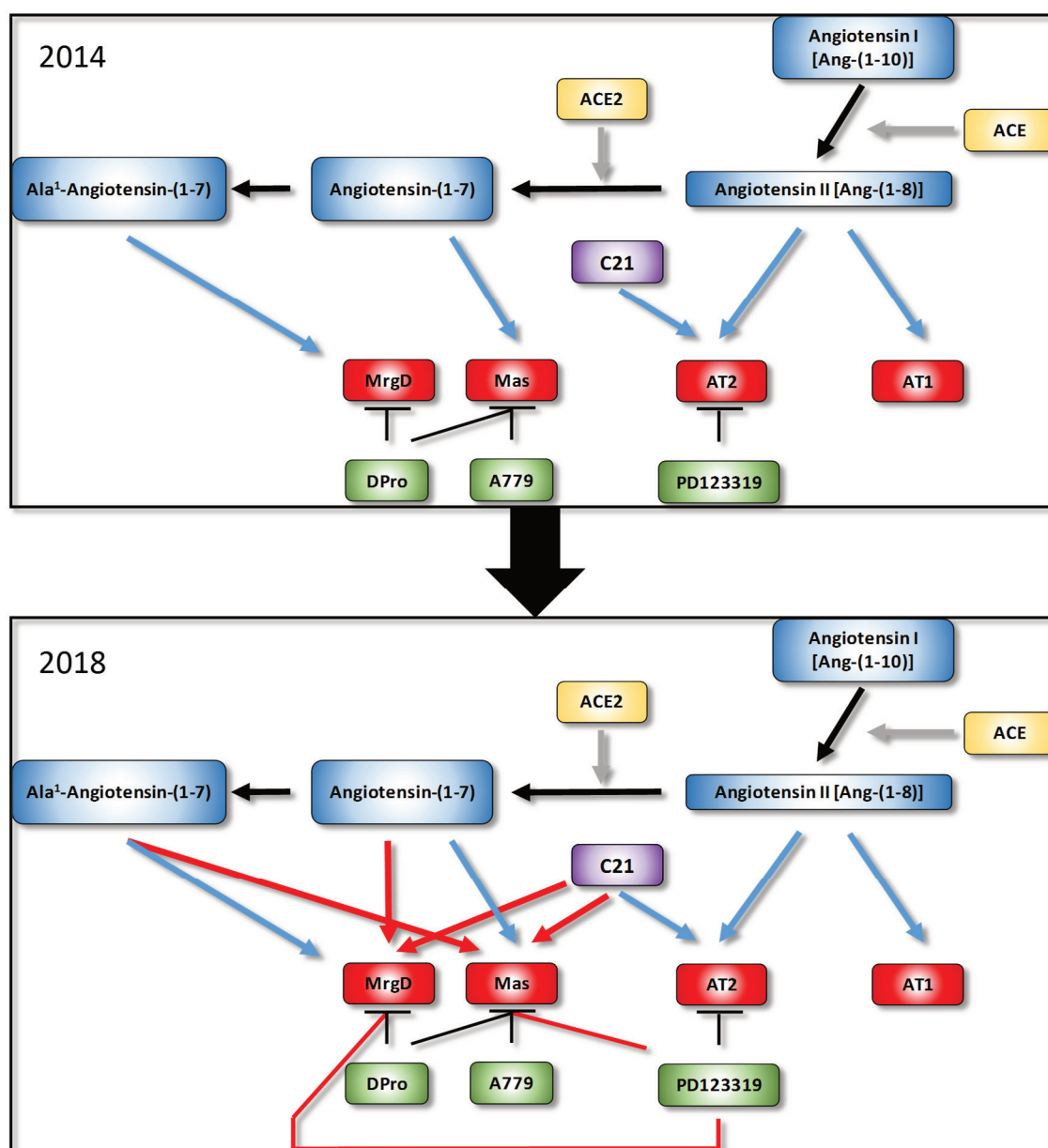


Figure 7.9.1 The renin-angiotensin system before 2014 and now

Schematic overview of the RAS before 2014 to now. The blue, black and grey lines show the connections, how they were known. Red lines and arrows indicate the new findings.

Additionally, it was not just able to revise the RAS as shown in Figure 7.9.1 and it was also possible to improve the understanding of the mechanism of the beneficial effects of Ang-(1-7) on blood glucose regulation. Although the effects observed in the *in vivo* studies

remained marginal and contradictive, it was possible to show that Ang-(1-7) has beneficial effects on the insulin secretion from β -cells. Furthermore, we demonstrated that this was mediated through Mas and cAMP and the downstream activation of EPAC and not PKA.

9 Perspectives

The discovery of cAMP as the primary second messenger will be a useful tool to screen for further receptors involved in the Ang-(1-7) mediated signalling, and will also help to identify compounds, which might be able to stimulate the same signalling as the heptapeptide. The data, which will be collected from those experiments, will help in the future to create *in silico* models to identify non-peptidic, small molecules with high efficacy and potency, which can be tested using cAMP as a readout.

The finding that Ang-(1-7) and Ala¹-Ang-(1-7) stimulate both Mas and MrgD, but have different pharmacodynamics, illustrates that minor changes in Ang-(1-7) (decarboxylation on amino acid 1) can lead to major changes in the agonist-receptor interaction. Additionally, the finding that C21 can stimulate all three receptors (Mas, MrgD and AT₂), while Ang-(1-7) and Ala¹-Ang-(1-7) just stimulate two of them (Mas and MrgD), will help to understand what structural pattern is required to stimulate all three receptors, or only one or two of them. Mutagenesis studies might also be helpful to refine the understanding of the interaction of the compounds (agonists and antagonists) with the receptors, and also for the screening of non-peptidic compounds. The *in silico* and *in vitro* studies lay the foundation for the development of new non-peptidic analogues, which can generate a more potent and selective stimulation of any of the three receptors. That will lead to safer and more efficient treatment options for an increasing number of diseases in which Ang-(1-7) and potential analogues might be beneficial. Furthermore, the identification of receptor-specific analogues will also allow a more specific treatment strategy in diseases where only one of the receptors is expressed in the tissue of interest.

Future experiments should also focus on the screening of the Mas like receptor family, as the structural similarity increases the possibility that also other members might be functional receptors for Ang-(1-7) and/ or other angiotensin peptides and non-peptidic agonists such as C21. The involvement of one of these receptors might be an explanation, why especially in the kidney contradictory effects have been observed.

Although Ang-(1-7) appears to have beneficial effects on diabetes mellitus (insulin secretion and β -cell function), many questions remain open due to the discrepancy between the data provided by Invitek and the results obtained in this study. There is no doubt that the significant effects of Ang-(1-7) on the hyperglycaemic status in STZ-induced diabetic mice described by Invitek are real. However, that this could not be confirmed in Cork, points to upcoming work, identifying the reason for the efficacy of the heptapeptide only under certain experimental conditions and the conditions in the animal facility. This will help to set treatment regimes in the future to maximise the Ang-(1-7) effects. Furthermore, the evaluation of the study needs to be extended. As the treatment with the heptapeptide might have protective effects against diabetic related end organ damage. Therefore, the functional analysis of those organs should be included. One possibility would be using non-invasive methods such as measuring the blood pressure or the glomerular filtration rate. Additionally blood and urine could be examined considering albuminuria (albumin-creatinine ration in the urine), blood-urea-nitrogen and blood cholesterol (elevated if the kidney is damaged). Moreover, qPCR analysis regarding renin expression in kidney tissue, and fibrosis marker for heart/ kidney tissue will be helpful to determine the grade of organ damage. In addition, plasma insulin levels should be measured, as the *ex vivo* experiments could show that Ang-(1-7) had beneficial effects on insulin secretion itself. Finally using histological methods, organs such as pancreas (β -cell

damage) heart (regarding fibrosis), kidneys (diabetic nephropathy) and eyes (diabetic retinopathy) need to be further investigated. The choice of model may be re-evaluated, as there might be a better model available to investigate the effect of Ang-(1-7) on blood glucose levels (diabetes induced via high fat diet, genetic models, VOD mouse).

10 Appendix part 1: Supplemental data

10.1 Proof of successful overexpression of Mas and MrgD in HEK293 cells

To confirm the overexpression of both receptors and to illustrate transfection efficacy, qPCR analysis was performed for all experiments to measure the amount of receptor mRNA in MrgD and Mas-transfected cells. As shown in Figure 10.1.1 A, transfection with Mas or MrgD plasmids led to a significant overexpression of the receptor mRNA.

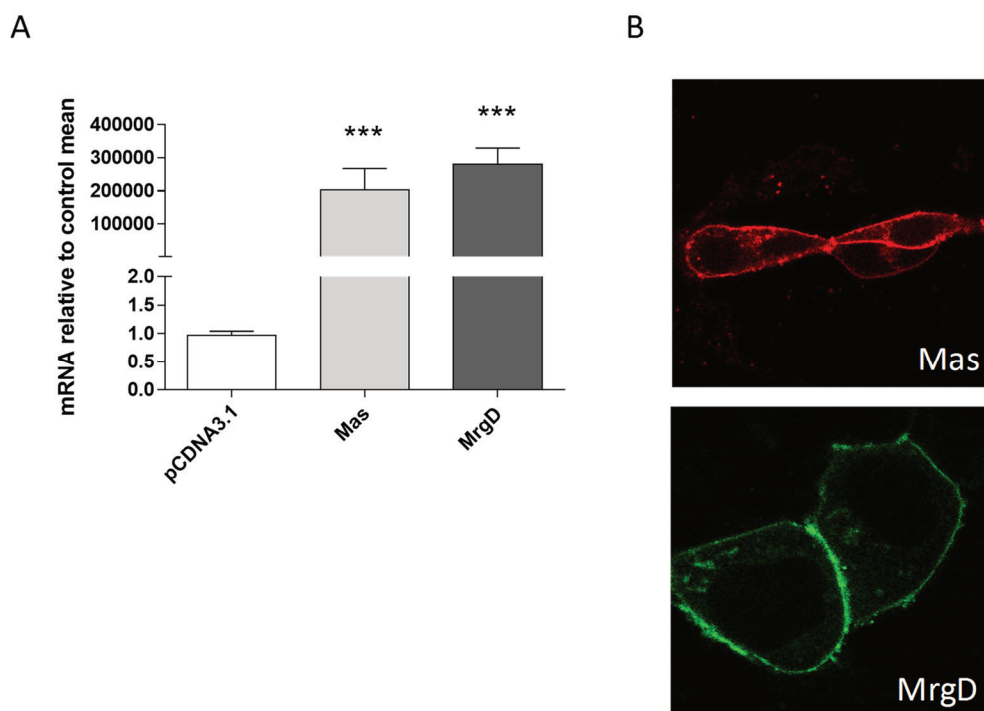


Figure 10.1.1 Successful overexpression of Mas and MrgD in HEK293 cells

(A) Average of mRNA amounts from all experiments of Mas and MrgD-transfected HEK293 cells (pcDNA3.1 values are set as 1). (B) Fluorescence microscopy of HEK293 cells transfected with Mas-mCherry (red) and MrgD-GFP (green).

The analysis of protein levels of both receptors using western blot analysis failed, as none of the commercially available antibodies worked (still signals generated in samples derived from receptor deficient mice). To finally visualise the transfection efficacy on protein level, HEK293 cells were transfected with Mas-mCherry or MrgD-GFP as seen in Figure 10.1.1 B. In transfected cells carrying the receptor cDNA, both receptors are expressed in the cytoplasmic membranes of these cells.

10.2 Preliminary data for mesangial cells derived from single knockout mice

10.2.1 Ala¹-Ang-(1-7) stimulates cAMP in single receptor knockout cells mesangial cells

We tested whether the Ala¹-Ang-(1-7)-mediated increase in cAMP we observed in wild-type mesangial cells and which was completely blunted in DKO cells (Figure 6.2.4), was already abolished in Mas or MrgD deficient cells.

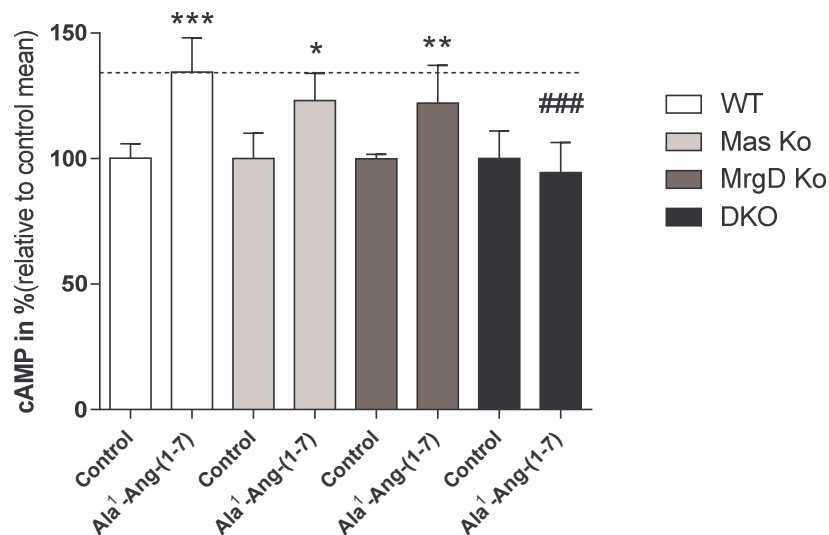


Figure 10.2.1 Ala¹-Ang-(1-7) induced signalling is absent in mesangial cells derived from Mas/MrgD knockout animals but not in single knockouts.

WT, Mas KO, MrgD KO and DKO C57BL/6 mesangial cells were stimulated for 15min with Ala¹-Ang-(1-7) (10^{-11} M). Results are expressed as mean \pm SEM; Untreated control values of each genotype is set as 100%. *** $P < 0.001$, ** $P < 0.01$, * $P < 0.05$, significantly different from control mean; ### $P < 0.001$, significantly different from WT Ala¹-Ang-(1-7); ANOVA with Bonferoni post-hoc test.

Deficiency in one of the receptors (Mas KO or MrgD KO), only reduced the Ala¹Ang-(1-7) signal compared to wild-type cells (WT) (Figure 10.2.1), implicating that the other receptor covers the lack of the knockout receptor.

10.2.2 C21 still stimulates PKA activity in mesangial cells derived from AT2

knockout mice

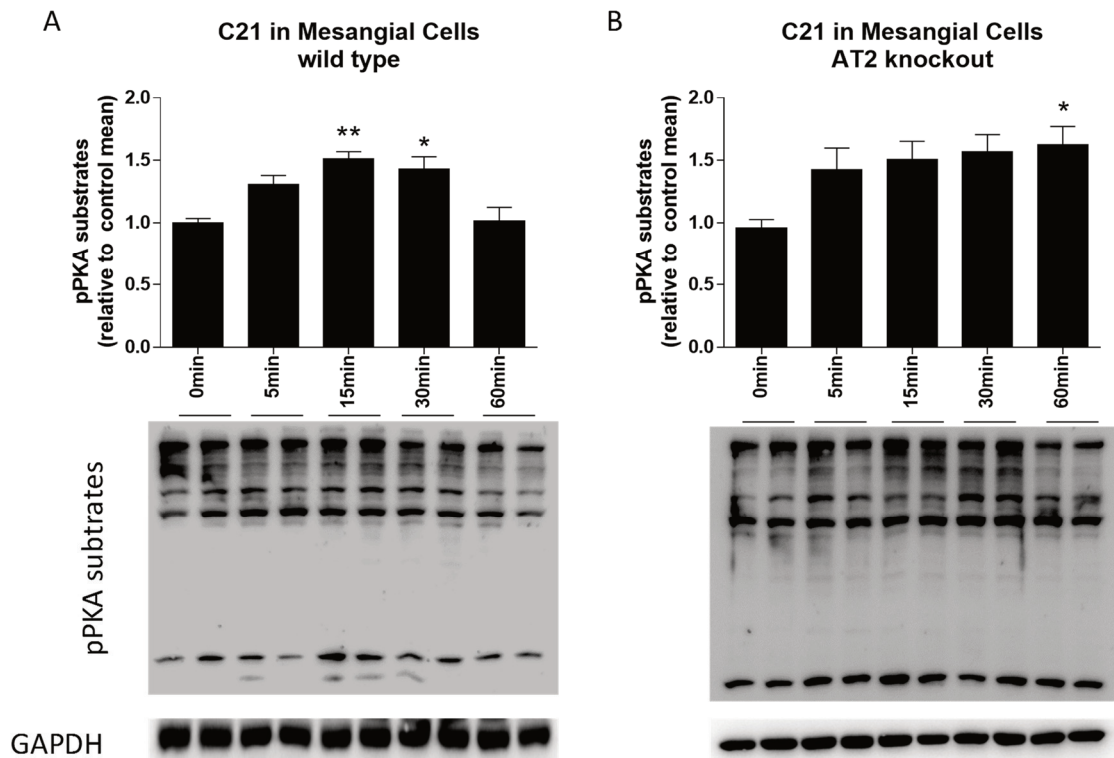


Figure 10.2.2 pPKA substrates levels in WT and AT2 KO mesangial cells

Western blot of phosphorylated PKA substrates and the housekeeping protein GAPDH and calculation of time-dependent phosphorylation of the PKA substrates after C21 stimulation in wild-type (WT) mesangial cells (A) and in AT2 knockout (AT2 KO) mesangial cells (B). Results are expressed as mean \pm SEM. Untreated control values of each genotype are set as 100 %. * $P < 0.05$, ** $P < 0.01$ vs. WT control; ANOVA with Bonferroni post-hoc test. $n=2$ (A), $n=3$ (B).

As cAMP initiates a variety of downstream signalling pathways including PKA activation, we tested whether the Ala1-Ang-(1-7)-mediated increase in cAMP leads to an increased PKA activity.

Stimulation of HUVEC with Ang-(1-7) for 15min resulted in a significant increase in the phosphorylation of PKA substrates, indicating an increase in PKA activity. This effect was still present in cells derived from AT2 KO cells, confirming the results seen for CREB phosphorylation and the cAMP (shown in Figure 6.3.4).

10.3 Effects of angiotensin-(1-7) administration on blood glucose levels in STZ induced diabetic mice

10.3.1 STZ-study performed by Invitek

Since there was no significant effect of Ang-(1-7) on blood glucose (BG) concentrations in healthy wild-type animals with naturally well-balanced glucose homeostasis, it was hypothesised that the beneficial effects of Ang-(1-7) become more obvious in preclinical models of diabetes mellitus. The model of STZ (multiple low dose) induced diabetes was chosen as β -cell damage is not just a characteristic for T1DM, but also for a late stage T2DM (glucose toxicity). The previous experiments performed in chapter 6.4, indicate that Ang-(1-7) improves β -cell function, which would be beneficial in both, T1DM and T2DM, therefore this model was the best choice to investigate the beneficial effects of Ang-(1-7). For this purpose, our collaborator (Invitek, USA) performed a study using Ang-(1-7) and analogues in STZ-induced diabetic mice. They were able to demonstrate that Ang-(1-7) and analogous were able to improve significantly the BG levels in STZ-induced mice (Figure 10.3.1).

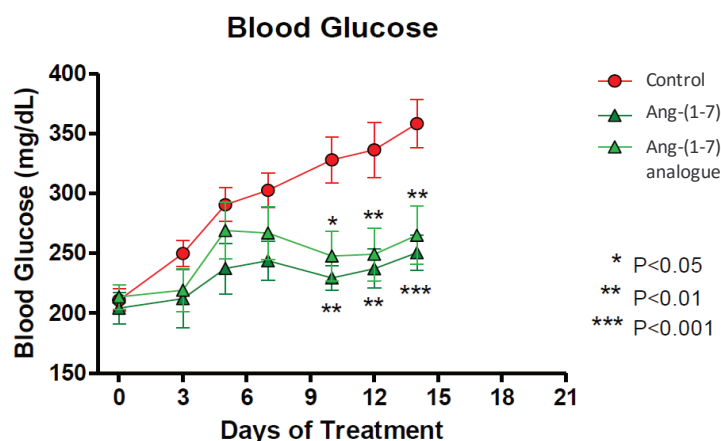


Figure 10.3.1 Preliminary data from the STZ study performed by Invitek

*Blood glucose concentrations in STZ induced diabetic mice; * $P < 0.05$, ** $P < 0.01$ vs Control, TWO WAY ANOVA.*

10.3.2 No significant difference in blood glucose concentrations between the Ang-(1-7) receptor knockouts and wild-type animals

Since Invitek could show an effect of Ang-(1-7) on BG levels it was decided to further investigate this in our own facilities, using the protocol provided by Invitek (for the exact description of the protocol used, see Chapter 11.6.1.). For this purpose, diabetes was induced using a multiple dose administration of STZ (50mg/kg), in 12-week-old male mice expressing all receptors (WT), lacking Mas (Mas KO), MrgD (MrgD KO), or both receptors (DKO), and treated them with either NaCl (control) or 0.5mg/kg Ang-(1-7).

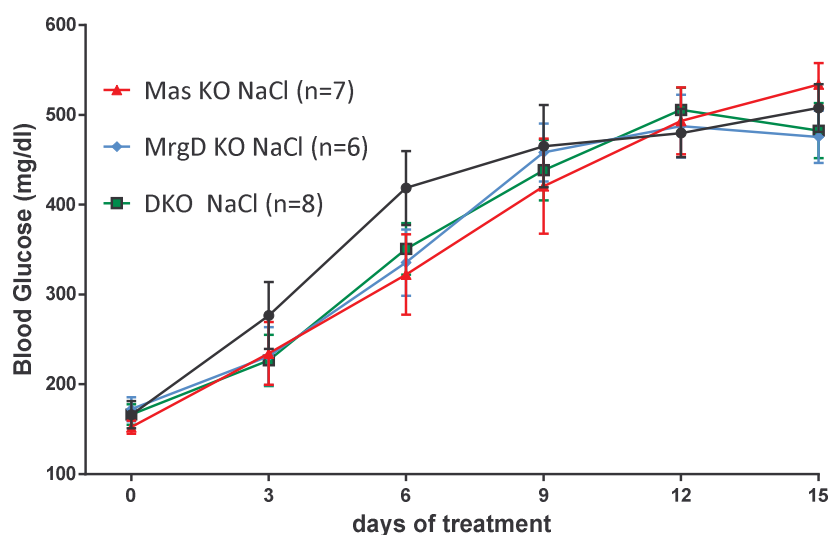


Figure 10.3.2 Effect of the receptor knockout on blood glucose in STZ induced diabetic animals

Blood glucose concentrations of STZ induced diabetic mice (male, 12-week old), comparing wild-type (WT, n=6), Mas knockout (Mas KO, n=7), MrgD knockout (MrgD KO, n=6), and double knockouts (DKO, n=8).

After 5 days of STZ administration, the BG levels showed a strong elevation in all groups, indicating the effectiveness of the STZ injections. The groups were randomly selected, and on day 6, the daily administration of Ang-(1-7) (0.5mg/kg) was started. After 15 days of Ang-(1-7) administration, no differences in BG concentrations were detected between all groups of mice (Figure 10.3.2).

10.3.3 No significant effect of Ang-(1-7) administration on the hyperglycaemic status

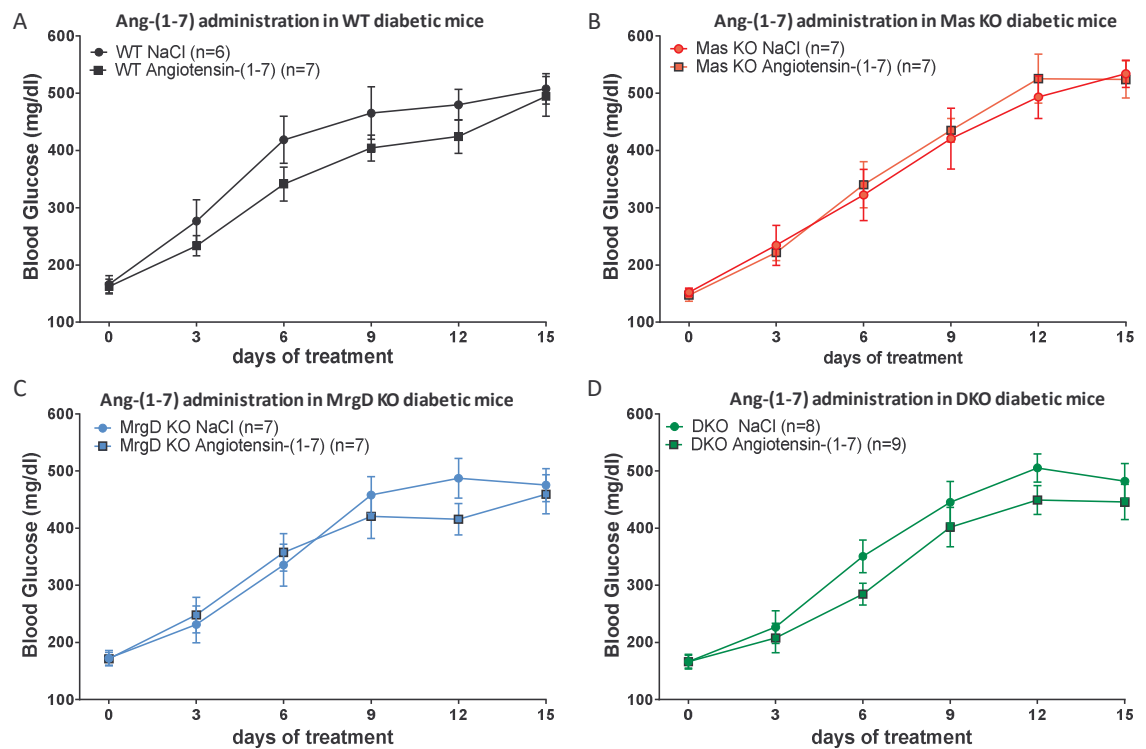


Figure 10.3.3 Effects of Ang-(1-7) administration in vivo on blood glucose

Blood glucose concentrations in STZ induced diabetic mice (male, 12 weeks old), with and without Ang-(1-7) administration versus control (NaCl) in A) wildtype (WT, NaCl: $n = 6$, Ang-(1-7): $n = 7$), B) Mas knockout (Mas KO, NaCl: $n = 7$, Ang-(1-7): $n = 7$), C) MrgD knockout (MrgD KO, NaCl: $n = 7$, Ang-(1-7): $n = 7$) and D) double knockouts (DKO, NaCl: $n = 8$, Ang-(1-7): $n = 9$).

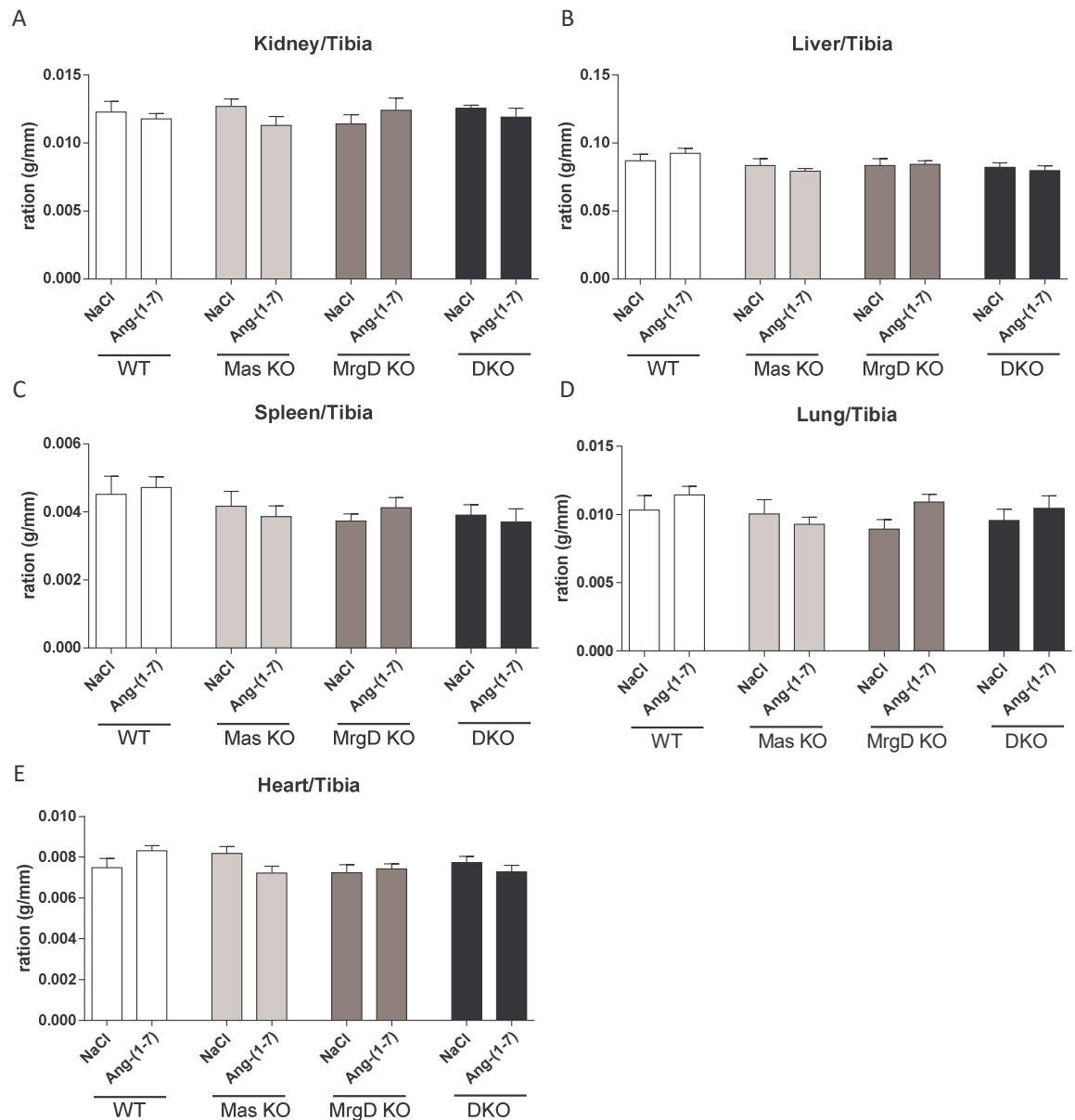


Figure 10.3.4 Effect of Ang-(1-7) administration in vivo on organ weights

Weight of kidney (A), liver (B), spleen (C), lung (D), and the heart (E) from STZ induced diabetic mice (male, 12 weeks old), with and without Ang-(1-7) administration versus control (NaCl) in A) wildtype (WT, NaCl: n=6, Ang-(1-7): n=7), B) Mas knockout (Mas KO, NaCl: n=7, Ang-(1-7): n=7), C) MrgD knockout (MrgD KO, NaCl: n=7, Ang-(1-7): n=7) and D) double knockouts (DKO, NaCl: n=8, Ang-(1-7): n=9). All weights were corrected against tibia length.

No significant differences in BG concentrations were detected between NaCl and Ang-(1-7) treated mice in all groups. (Figure 10.3.3 A-D). Furthermore, heart, lung, kidney, liver and spleen were dissected to evaluate any changes in organ weight. There was no significant difference in the weights of kidney, liver, spleen, heart and lung between the most of the groups (Figure 10.3.4).

10.3.4 Negative effects of high concentrations of Ang-(1-7) on blood glucose concentration in wild-type mice

As there was no significant effect with 0.5mg/kg Ang-(1-7), it was hypothesised that this might not be the effective dose. To test whether higher concentrations of the heptapeptide might have beneficial effects we treated STZ induced diabetic animals (male, 12 weeks old) for 13 days with 2mg/kg Ang-(1-7) and compared with 0.5mg/kg Ang-(1-7) and the NaCl control (Figure 10.3.5).

Surprisingly, the 2mg/kg significantly, and 0.5mg/kg of Ang-(1-7) worsened the diabetes and further increased the BG concentration in those animals compared to the control. That also 0.5mg/kg Ang-(1-7) treatment resulted in an increase in BG compared to WT is contradictory to the results shown in Figure 10.3.3 A.

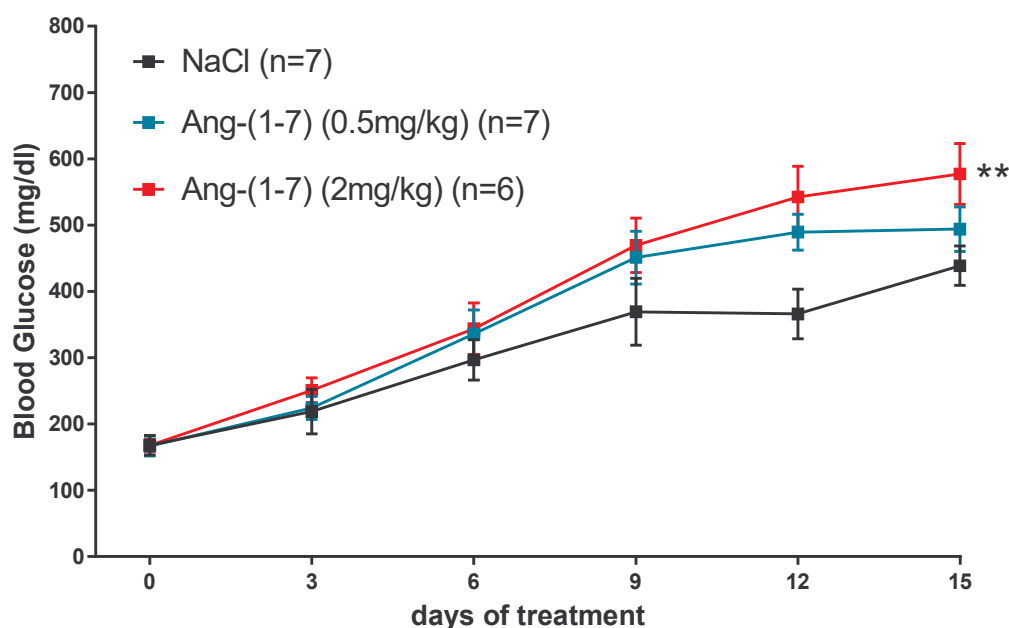


Figure 10.3.5 Effect of different Ang-(1-7) concentrations in vivo on blood glucose

Blood glucose concentrations in STZ induced diabetic mice (male, 12 weeks old), comparing 0.5 mg/kg Ang-(1-7), 2.0 mg/kg Ang-(1-7) administration to control (NaCl) in wild-type animals (WT, NaCl: n=7, 0.5 mg/kg Ang-(1-7): n=7, 2 mg/kg Ang-(1-7): n=6); ** $P < 0.01$ vs NaCl, TWO WAY ANOVA.

10.3.5 Effects of high concentrations of Ang-(1-7) on organ weights

The animals treated with the high concentration of Ang-(1-7) showed a significant reduction of the heart weight (Figure 10.3.6 E) and a reduction of the weight of the spleen (Figure 10.3.6 C), which was not significant. There was no significant effect on the other organs (Figure 10.3.6 B, C, D).

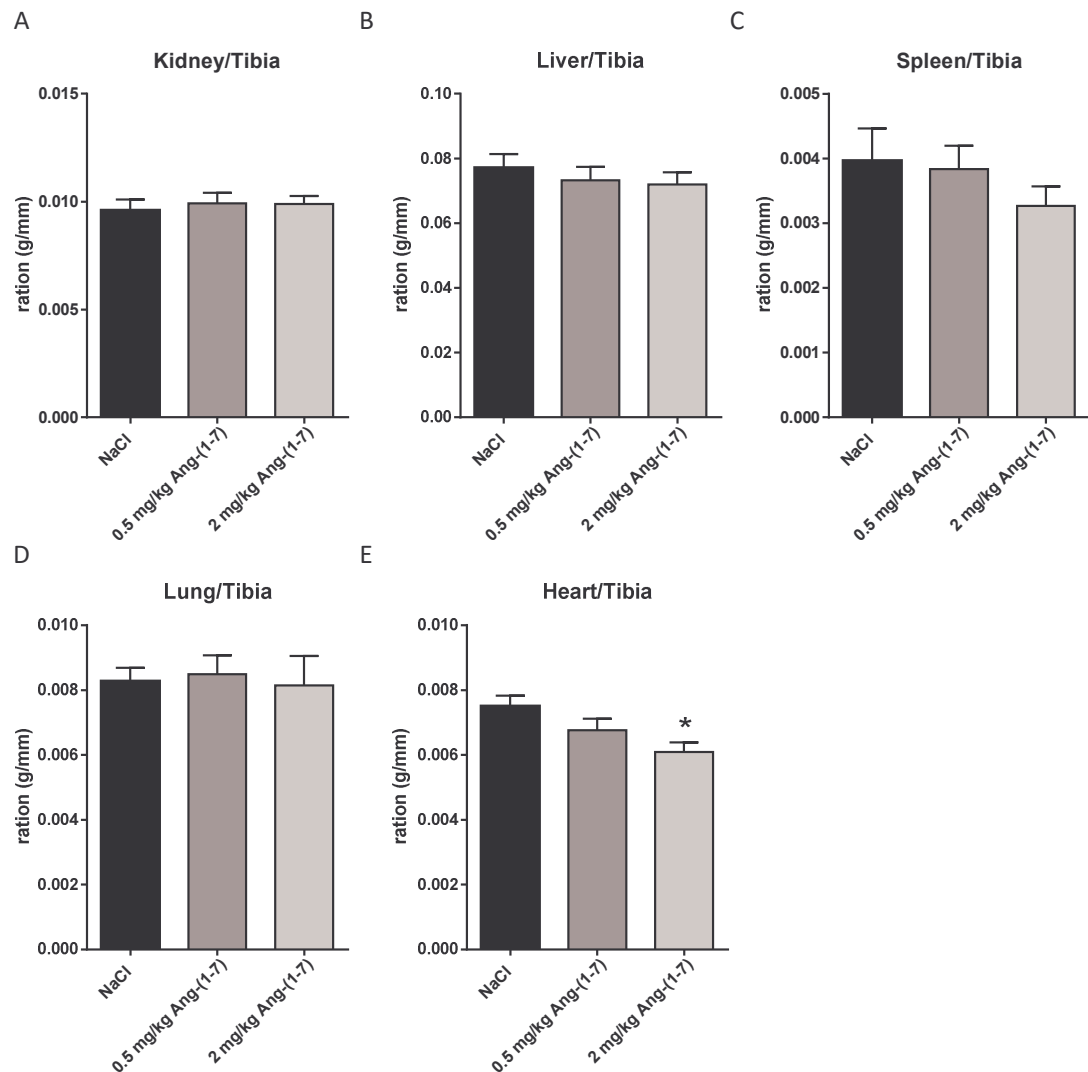


Figure 10.3.6 Effect of different Ang-(1-7) concentrations in vivo on organ weights

Weight of kidney (A), liver (B), spleen (C), lung (D), and the heart (A) from STZ induced diabetic mice (male, 12 weeks old), comparing 0.5mg/kg Ang-(1-7), 2.0mg/kg Ang-(1-7) administration and control (NaCl) in wild-type animals (WT, NaCl: n=7, 0.5mg/kg Ang-(1-7): n=7, 2mg/kg Ang-(1-7): n=6). All weights are corrected against tibia length; * $P < 0.05$, vs control, ONE WAY ANOVA.

10.3.6 Gender depending effects of Ang-(1-7) on blood glucose concentration in wild-type mice

As higher concentrations of Ang-(1-7) had rather negative effects on the BG, we went back to using the lower concentration of the heptapeptide (0.5mg/kg), which also Invitek used. After consulting Invitek again, it turned out that they used 6-7 week old females for the study shown in Figure 10.3.1. To have a better comparison to their preliminary data it was decided to use 6-7 week old female animals. Additionally, it is known the vasodilatory effect of the heptapeptide is gender specific [110]. Consequently, it was hypothesised that this might also be the case for the effects on BG regulation under diabetic conditions. For this purpose, we induced diabetes in 12-week-old male and female mice and compared the basic BG, and also the effect of Ang-(1-7) administration in both genders.

Male mice showed a significant stronger increase in BG level than female mice (Figure 10.3.7 A), indicating that female animals less affected by the STZ treatment than the male mice. However, in female animals the Ang-(1-7) administration showed beneficial effects on the BG concentration after 14 days, although this effect was not significant (Figure 10.3.7 B). In contrast, there was no noticeable effect observed in male mice (Figure 10.3.7 C), indicating a gender dependent effect of Ang-(1-7) on BG concentration. There was no significant difference in the organ weights between NaCl and Ang-(1-7) treated mice (Figure 10.3.8).

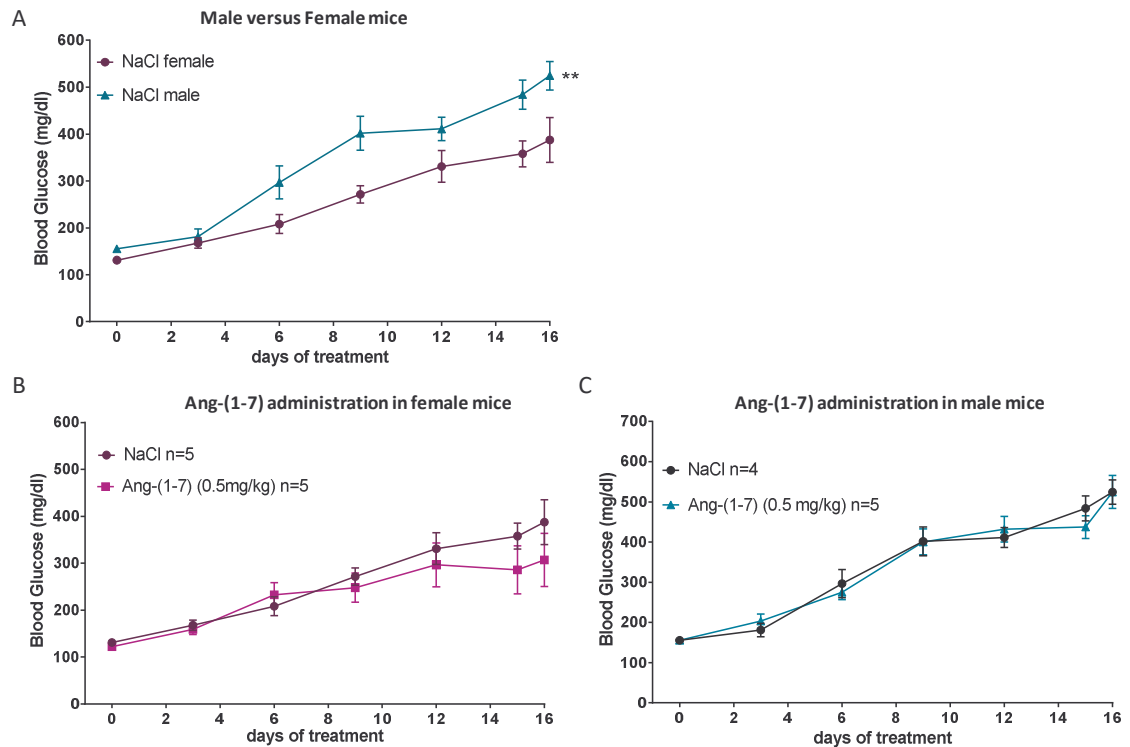


Figure 10.3.7 Gender specific effects in vivo on blood glucose with and without Ang-(1-7) administration

A) Blood glucose concentrations in STZ induced diabetic mice (12 weeks old), comparing male and female wild-type (WT) animals with NaCl. B) Blood glucose concentrations in female STZ induced diabetic mice (12 weeks old), comparing 0.5mg/kg Ang-(1-7) and control (NaCl) (NaCl: n=5, 0.5mg/kg Ang-(1-7): n=5). C) Blood glucose concentrations in male STZ induced diabetic mice (12 weeks old), comparing 0.5mg/kg Ang-(1-7) and control (NaCl) (NaCl: n=4, 0.5mg/kg Ang-(1-7): n=5); ** $P < 0.01$ vs NaCl female, TWO WAY ANOVA.

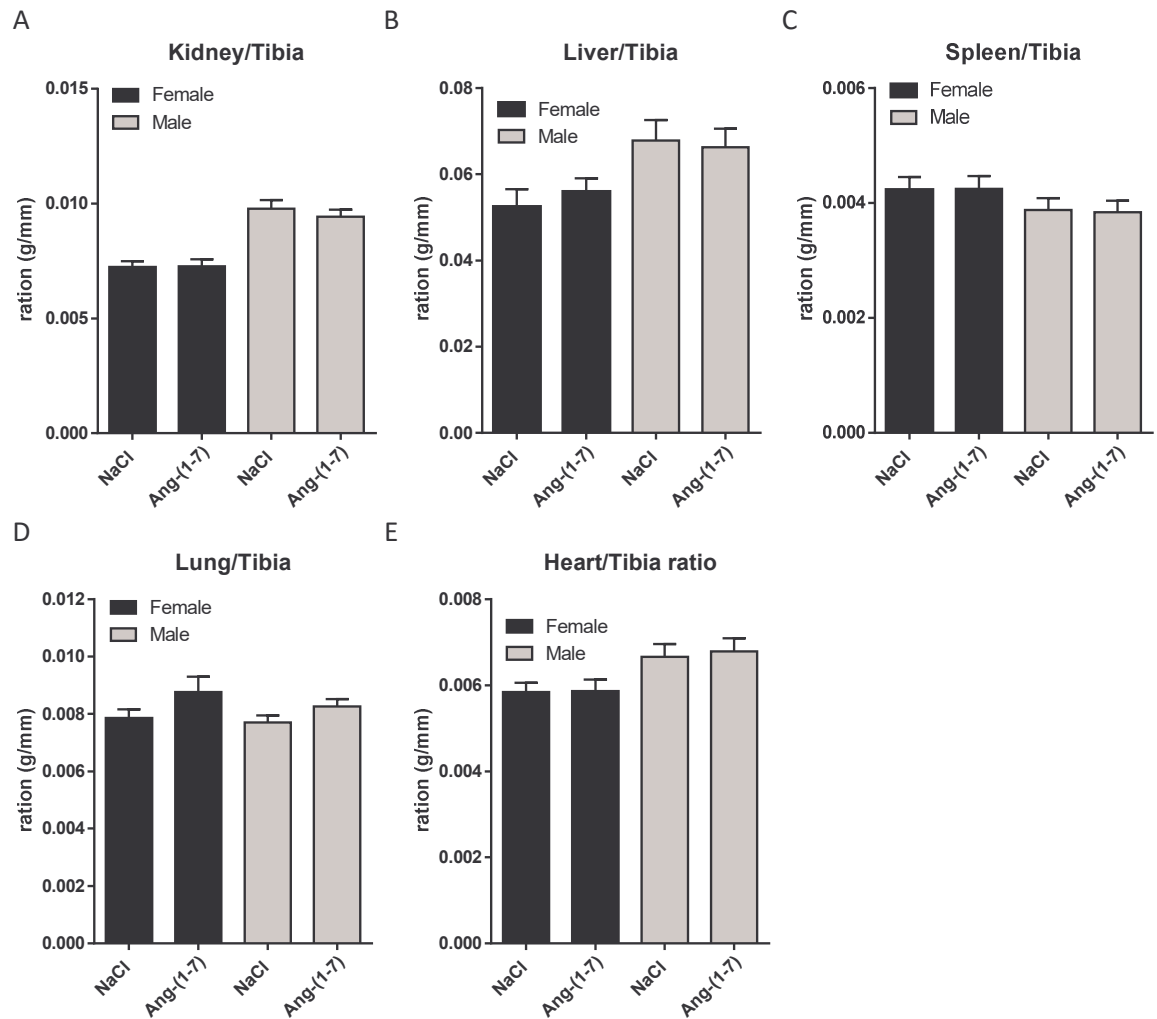


Figure 10.3.8 Effect of Ang-(1-7) administration in vivo on organ weights of female and male mice

Weight from kidney (A), liver (B), spleen (C), lung (D), and the heart (A) from STZ induced diabetic mice (male, 12 weeks old), comparing 0.5mg/kg Ang-(1-7), administration and control (NaCl) in female and male wild-type animals (12 weeks old). (NaCl: n=4, 0.5mg/kg Ang-(1-7): n=5). All weights are corrected against tibia length.

11 Appendix part 2: Materials and methods

11.1 Materials

11.1.1 Special equipment

Machine	Manufacturer
Cryo freezing container	Nalgene (Nalge Nunc, Rochester, NY, USA)
Electrophoresis chamber	Mini-PROTEAN Tetra Cell (Bio Rad Laboratories, Hercules, California, USA)
Luminometer	Orion L Microplate Luminometer (Berthold Detection Systems GmbH, Pforzheim, Germany)
Luminescence and UV detection system	Syngene GBox - EF Gel Documentation System (Syngene UK, Cambridge, United Kingdom)
Microscope	CKX41 inverted microscope (Olympus europe Se & Co. KG, Hamburg, Germany)
Nano Drop	Nano Drop 2000 Spectrophotometer (Thermo Fisher Scientific, Waltham, Massachusetts, USA)
Plate reader	Tecan Sunrise 96 well Microplate Readers (Tecan Group Ltd., Männedorf, Switzerland)
qPCR-cycler	StepOne™ Real-Time PCR System (Thermo Fisher Scientific, Waltham, Massachusetts, USA)
Semidry blot chamber	PEGASUS (PHASE Gesell. für Phorese, Analytik und Separation mbH, Luebeck, Germany)
Thermocycler	Pro Flex Pcr-System (Thermo Fisher Scientific, Waltham, Massachusetts, USA)
Ultrasound homogeninator	Ultrasonic homogeniser 470 series (Cole-Parmer, St. Neots, United Kingdom)

11.1.2 Complete systems (kits)

System	Application	Manufacturer
BCA Protein Assay Kit	Determination of protein concentration	Thermo Fisher Scientific (Waltham, Massachusetts, USA)
PKA activity kit	Determination of PKA activity	Arbor Assays (Michigan, USA)
Direct cAMP elisa kit	cAMP measurement	Enzo Life Sciences Ltd. (Exeter, United Kingdom)
Polyfect	Transfection	Qiagen (Venlo, Limburg, Netherlands)
PureYield™ Plasmid Maxiprep System	Plasmid isolation	Promega (Madison, Wisconsin, USA)
NucleoBond Xtra Midi RNA Purification Kit	RNA-Isolation	Macherey-Nagel (Dueren, Germany)
SYBR Green qPCR SuperMix Kit	qPCR	Invitrogen (Carlsbad, California, USA)
RevertAid H Minus First Strand cDNA Synthesis Kit	cDNA-Synthese	Fermentas (St. Leon-Rot, Germany)
ECL Western Blot-Substrate	Immunodetection	Thermo Fisher Scientific (Waltham, Massachusetts, USA)

11.1.3 Oligonucleotides

Gene	Ref-Nr.	Forward primer	Reverse primer
A) qPCR			
mmMas	NM_008552.5	CCTCCCATTCTTCGAAGCTGTA	GCCTGGGTTGC-ATTTTCATCTTT
mmMrgD	NM_203490.3	TCTACTGGGTGGATGTGAAACG	TCATTAGTACACGTGGATGGCG
mmAT2	NM_000686.4	GAATTACCCGTGACCAAGTCCT	GGAACCTAAACACACTGCGGA
hMas	NM_002377.2	TTTATAGCCATCCTGAGCTTCC	AATGTGGTGTAGGTTCCCAAAG
hMrgD	NM_198923.2	AAACTATTCCAGAGGGAGCACCA	TGGACCTTGTCAGTGGTATTGA
hAT2	NM_000686.4	CATCATTTGCTGGCTTCCCTTC	ATTGGAACCCTAAACACACTGC
GAPDH	NM_002046	GGACTCATGACCACAGTCCAT	AGGTCCACCACTGACACGTT
HPRT	NM_000194	GCTGGATTACATCAAAGCACTG	CTGACCAAGGAAAGCAAAGTCT
β-Aktin	NM_001101	TCCTGTGGCATCCACGAAACT	GAAGCATTTCGGTGGACGAT
B) Genotyping			
Mas wt	-	CTGGTTCCTCTGCTTCCGGATGAGG (Mas11)	GCCGTTGCCCTCCTGGCGCCTGGG (Mas12)
Mas ko	-	GCCGTTGCCCTCCTGGCGCCTGGG (Mas12)	GGCAGCGCGGCTATCGTGG (NeoPVU)
MrgD wt	-	CTGCTCATAGTCAACATTTCTGC (MrgD1)	CATGAGATGCTCTATCCATTGGG (MrgD8)
MrgD ko	-	CATGAGATGCTCTATCCATTGGG (MrgD8)	GGAGAAACAGCTAAAGTGCG (rtTA1)
AT2 wt	-	CCACCAGCAGAAACATTACC (AT2 5)	GAACTACATAAGATGCTTGCCAGG (AT2 3)
AT2 ko	-	GAACTACATAAGATGCTTGCCAGG (AT2 3)	GGCAGCGCGGCTATCGTGG (NeoPVU)

11.1.4 Antibodies

Antibody	Manufacturer	M _w	Source	Dilution	5 % Milk/ 5 % BSA
A) Primary antibody					
Akt	Cell Signaling (Beverly, MA, USA)	60 kDa	Rabbit	1:1000	BSA
Erk1/2	Cell Signaling	42/44 kDa	Rabbit	1:1000	BSA
CREB	Cell Signaling	43 kDa	Rabbit	1:1000	BSA
GAPDH	Sigma Aldrich (St. Louis, Missouri, United States	40 kDa	Rabbit	1:10000	Milk
pAkt (Ser473)	Cell Signaling	60 kDa	Rabbit	1:1000	BSA
pErk1/2	Cell Signaling	42/44 kDa	Rabbit	1:1000	BSA
pCREB	Cell Signaling	43 kDa	Rabbit	1:1000	BSA
PKA	Chemicon	68 kDa	Rabbit	1:1000	BSA
pPKA	Cell Signaling	20 kDa	Rabbit	1:1000	BSA
PKA substrate	Cell Signaling	-	Rabbit	1:1000	BSA
B) Secondary antibody					
Anti-Rabbit*	Sigma Aldrich			1:2000	Milk
Anti-Rabbit*	Cell Signaling			1:2000	Milk

* immunoglobulin G (IgG), horseradish peroxidase (HRP)-coupled

11.1.5 Chemicals

Chemical	Manufacturer
Acrylamid-Solution	Sigma-Aldrich (St. Louis, MO, USA)
Agarose	Sigma-Aldrich
Bacteriological agar	Sigma-Aldrich
Bromphenolblue	Sigma-Aldrich
Bovine serum albumin (BSA)	Sigma-Aldrich
Calcium chloride (CaCl ₂)	Sigma-Aldrich
Citric acid monohydrate	Merck-Millipore (Darmstadt, Germany)
Compound 21 (C21)	Axon Medchem (Groningen, Netherlands)
DMSO (Dimethylsulfoxid)	Sigma-Aldrich
DMEM (cell culture media)	Lonza (Basel, Switzerland)
DTT (Dithiothreitol)	Sigma-Aldrich
EDTA (Ethylenediaminetetraacetat)	Sigma-Aldrich
EGM-2 (cell culture media)	PromoCell (Heidelberg, Germany)
Ethanol	-
Fetal calf serum (FCS)	GIBCO (Thermo Fisher Scientific, Waltham, Massachusetts, USA)
Forskolin	Sigma-Aldrich
Gel Red (Nucleic acid stain)	Cambridge Bioscience (Cambridge, UK)
Glucose	Sigma-Aldrich
GlutaMax (L-Glutamine, L-Alanine)	Lonza
Glycerol	Roth (Karlsruhe, Germany)
Glycin	Sigma-Aldrich
HEPES (4-(2-hydroxyethyl)-1-piperazineethanesulfonic acid)	Sigma-Aldrich
HEPES (for cell culture)	Sigma-Aldrich
IBMX (3-isobutyl-1-methylxanthine)	Sigma-Aldrich
Isopropanol	Roth
L-Alanyl-L-Glutamine (GlutaMax)	GIBCO
LB-Broth (Miller)	Sigma-Aldrich
Magnesium chloride (MgCl ₂)	Sigma-Aldrich
Magnesium sulfate (MgSO ₄)	Merck-Millipore
Methanol	Sigma-Aldrich
Milk powder	Roth
Paraformaldehyde	Merck-Millipore
PD123319	Parke-Davis Pharmaceutical Research (Detroit, Michigan, USA)
Penicillin/ Streptomycin (100x)	Sigma-Aldrich
Peptides and A779 and D-Pro	Biosynthon (Berlin, Germany)
Pertussis toxin (PTX)	Merck-Millipore
Phenylmethylsulfonyl fluoride (PMSF)	Sigma-Aldrich
Phosphate buffered saline	PAA (Pasching, Austria)
Phosphatase inhibitor cocktail 2 and 3	Sigma-Aldrich
Ponceau S	Sigma-Aldrich
Potassium chloride (KCL)	Merck-Millipore
Potassium dihydrogen phosphate (KH ₂ PO ₄)	Sigma-Aldrich
Protease inhibitor cocktail	Sigma-Aldrich
RPMI (cell culture media)	Sigma-Aldrich
SDS (Sodium dodecylsulfat)	Sigma-Aldrich
Sodium chloride	Sigma-Aldrich
Sodium hydroxide	Sigma-Aldrich
Sodium hydrogen carbonate (NaHCO ₃)	Sigma-Aldrich
Sodium pyruvate	Lonza
SQ22536	Sigma-Aldrich
TEMED (Tetramethylethylenediamin)	Sigma-Aldrich
Tris (Tris(hydroxymethyl)-aminomethan) (HCL and Base)	Sigma-Aldrich
Trisodium citrate, dehydrate	Sigma-Aldrich
Triton-X	Sigma-Aldrich
Trypsin/EDTA (0,5 % (w/v))	Sigma-Aldrich
Tween 20	Sigma-Aldrich
β-Mercaptoethanol	Sigma-Aldrich

11.1.6 Buffer

4x DNA loading buffer

Concentration	Chemical
40 % (v/v)	Glycerol
1 x	Tris-Acetate-EDTA-(TAE)-Buffer
Spatula tip	Bromphenolblue
add 50 ml	H ₂ O

50x Tris-Acetate-EDTA-(TAE)-buffer (pH 8.0):

Concentration	Chemical
2 M	Tris (Tris(hydroxymethyl)-aminomethane)
1 M	Acetic acid
50 mM	EDTA
add 1 l	H ₂ O

Laemmli-sample buffer (pH 6.8)

Concentration	Chemical
0.5 M	Tris
10 % (v/v)	Glycerol
2 % (w/v)	SDS
0.1 M	DTT (Dithiothreitol)
Spatula tip	Bromphenolblue
add 50 ml	H ₂ O

10 x SDS-Tris-Glycine running buffer

Concentration	Chemical
25 mM	Tris (Tris(hydroxymethyl)-aminomethane)
250 mM	Glycine
1 % (w/v)	SDS (Natriumdodecylsulfate)
add 2 l	H ₂ O

20 x Tris buffert saline (TBS) (pH 7.5)

Concentration	Chemical
2 M	NaCl
400 mM	Tris
add 1 l	H ₂ O

TBS-Tween-20

Concentration	Chemical
1 x	TBS
0.1 % (v/v)	Tween-20
add 1 l	H ₂ O

Anode buffer I (pH 10.4):

Concentration	Chemical
0.3 M	Tris (Tris(hydroxymethyl)-aminomethane)
20 % (v/v)	Methanol
add 1 l	H ₂ O

Cathode buffer II (pH 10.4):

Concentration	Chemical
0.3 M	Tris (Tris(hydroxymethyl)-aminomethane) base
20 % (v/v)	Methanol
add 1 l	H ₂ O

Cathode buffer III (pH 7.6):

Concentration	Chemical
40 mM	ϵ -aminocaproic acid
20 % (v/v)	Methanol
add 1 l	H ₂ O

Ponceau S solution:

Concentration	Chemical
0.3 % (w/v)	Ponceau S
30 % (v/v)	trichloroacetic acid
add 1 l	H ₂ O

Islet isolation buffer (pH 7.4)

Concentration	Chemical
135 mM	NaCl
5.6 mM	KCl
1.28 mM	CaCl ₂
1.3 mM	MgCl ₂
10 mM	HEPES
0.1 % (w/ v)	BSA
1x	PenStrep (10x)
3 mM	Glucose
add 1 l	H ₂ O

Krebs Ringer buffer (pH 7.4)

Concentration	Chemical
123 mM	NaCl
4.7 mM	KCl
2.6 mM	CaCl ₂
1.2 mM	KH ₂ PO ₄
1.2 mM	MgSO ₄
10 mM	HEPES
20 mM	NaHCO ₃
0.5 % (w/ v)	BSA
add 1 l	H ₂ O

Citrate buffer (pH 4.5)

Concentration	Chemical
0.1 M	Citric acid monohydrate (Solution A)
0.1 M	trisodium citrate, dehydrate (Solution B)
Mix 47 ml of A and 53 ml of B and adjust pH	

11.2 Cell biological methods

11.2.1 Cultivation of eukaryotic cells

Eukaryotic cells (Table 7.1) were cultivated in an incubator at 37°C and 5% CO₂. Every two to three days the cell culture medium was changed (cell line and corresponding media see table 3). At about 90% confluence, the cells were passaged. For this purpose, the culture medium was completely removed, the cells were washed with PBS to remove remaining cell culture medium, and incubated with trypsin for 5min at 37°C. The trypsin reaction was stopped by adding a ten-fold volume of cell culture medium to the dish. The cell suspension was centrifuged at 1100rpm at room temperature and the pellet re-suspended in complete media. The suspension was placed in a cell depending ratio into new cell culture dishes or flasks.

11.2.2 Isolation of mesangial cells from mouse kidney

In order to obtain murine glomerular mesangial cells (MC), kidneys from two mice were dissected. Subsequently, the organ capsule was removed and the kidney homogenised. Fifteen ml of pure cold RPMI media was added to the homogenate and filtered using a cell strainer (100µm). The remaining kidney fragments in the cell strainer were rinsed with 15ml cold RPMI media. The filtered homogenate (now in 30ml media) was again filtered using a cell strainer (75µm). Subsequently, the filtrate was suspended 3 times using a 21G needle. Afterwards the solution was centrifuged at RT at 1100rpm for 10min. The pellet was re-suspended in a solution of 4mg/ml collagenase type II in pure RPMI. The cell suspension was incubated for 30min at 37°C. After incubation, the digestion was

stopped by adding 30ml complete RPMI (Table 7.2) and the solution was centrifuged for 10min at 1100rpm at RT. The supernatant was discarded and the pellet re-suspended in complete RPMI medium. The cells were plated in one 75cm² flask and cultivated in an incubator at 37°C and 5% CO₂.

No media was changed during the first three days. At the end of the three days, the glomeruli were differentiated into mesangial cells. The media was removed, the cells washed with PBS and new media was added. The MCs were passaged as soon as the cells reached 90 % confluence. In order to prevent the negative influence of low cell density on cell growth, the cells were split at a maximum ratio of 1:5. The MCs were used between passage numbers P2 and P3 for the experiments to ensure the functionality of the cells.

Table 11.1 Cell lines

Cell line	Species	Description	Adhesion	Origin
HEK293	human	human embryonic kidney cells	semi-adherent	Sigma-Aldrich (St. Louis, MO, USA)
BALB/3T3	mouse	embryonic fibroblast cells	adherent	LGC Standards (ATCC), (Teddington, UK)
HUVEC	human	human umbilical cord (primary cells)	adherent	PromoCell (Heidelberg, Germany)
Mesangial Cells	mouse	glomerular mesangial cell (primary cells)	adherent	isolated from mouse tissue

Table 11.2 Cell culture media

Media	Concentration	Add ins	Cell line
DMEM	10 % (v/v)	FCS	HEK293 and BALB/3T3
	1x	HEPES (100x)	
	1x	Glutamax (100x)	
	1x	Penicillin/Streptomycin (100x)	
RPMI	16% (v/v)	FCS	Mesangial Cells
	1x	HEPES (100x)	
	1x	Sodium Pyruvat (100x)	
	1x	Glutamax (100x)	
EGM-2	1x	Penicillin/Streptomycin (100x)	HUVEC
	2% (v/v)	FCS	
	5 ng / ml	Epidermal Growth Factor	
	10 ng / ml	Basic Fibroblast Growth Factor	
	20 ng / ml	Insulin-like Growth Factor (Long R3 IGF)	
	0.5 ng / ml	Vascular Endothelial Growth Factor 165	
	1 µg / ml	Ascorbic Acid	
	22.5 µg / ml	Heparin	
	0.2 µg / ml	Hydrocortisone	

11.2.3 Cell count

The cell count was carried out using a “Neubauer counting chamber” (Neubauer improved, LO-Laboroptik, Friedrichsdorf, D). First, the cells were trypsinised (as described in Chapter 11.2.1) and centrifuged for 5min at 1100 rpm. The cell pellet was re-suspended in 5-10mL complete media. Next, 10µl of a 1:20 dilution of this cell suspension was pipetted into the counting chamber and the cell number was determined at 10x magnification in four large squares. Since the dimensions of the counting chamber (the volume between the cover glass and the object carrier) are firmly defined, the cell number per ml can be calculated using following formula.

$$\text{cells per ml} = \text{sum of cells in 4 quadrants} \times \frac{\text{dilution factor}}{4 \times \text{depth} \times \text{area}}$$

For example:

$$\text{cells per ml} = 42+45+38+41 \times \frac{1:20}{4 \times 0.1\text{mm} \times 0.0025\text{mm}^2} = 8,300 \text{ cells per ml}$$

11.2.4 Cryopreservation and reactivation of eukaryotic cells

For permanent storage, the cells were cryopreserved in liquid nitrogen. For this purpose, 90 % confluent cells were trypsinated like previously described. The pellet was re-suspended in 10% (v/v) dimethylsulfoxide (DMSO) and complete media (2ml per 100mm dish), and 1ml was transferred in to each cryogenic tubes (Nalgene, Rochester, NY, USA). After transferring the cryogenic tubes into a freezing vessel filled with isopropanol, the cells were frozen at -80°C for at least 24h. The isopropanol ensures a continuous lowering of the temperature by 1°C per hour. For long-term storage, the frozen cells were transferred to liquid nitrogen the next day. To revitalize the cells, they were re-suspended in 10ml of warm cell culture medium and centrifuged at 1100rpm for 5min. Afterwards the cell pellet was resuspended in 5ml of culture medium and the mixture was transferred to a 100mm cell culture dish. To remove dead cells, the media was changed the next morning.

11.2.5 Transfection of eukaryotic cells

Transfection is a method of introducing foreign DNA into eukaryotic cells. Various methods are known. For example, calcium phosphate precipitation [440, 441],

electroporation [442] or viral transfection [443]. Within the scope of this study, lipofection was carried out exclusively. The liposome-forming reagent PolyFect (Qiagen, Limburg, Netherlands) was used for the DNA transfer into the cells. PolyFect contains a mixture of activated-dendrimers. Those dendrimers build a spherical architecture with branches radiating from a central core. The branches are positively charged and can interact with the negatively charged phosphate groups of the DNA. After the addition of the mixture to the cells, the formed complexes bind to the cell surface, and get absorbed by the cell through endocytosis [444].

For the lipofection, 75,000 cells (HEK293) were seeded into the cavity of a 48-well plate and left over night. The next day the transfection was carried out. For this purpose, the reaction mixture was prepared as shown in Table 11.3 and incubated for 10min at room temperature and complete media was then added. Next, 70µl of the reaction mix was pipetted into each well. After 18-20h the cells were stimulated as described in Chapter 11.2.6.

Table 11.3 Transfection mix

add in	amount
pure DMEM	10ul
plasmid DNA	150ng *
PolyFect	2ul
10min incubation at RT	
complete DMEM	60ul

* cAMP-Assay: 100ng receptor and 50ng pCDNA3.1

* Dual Luciferase Assay: 25ng Reporter-Firefly luciferase construct, 25ng Renilla,

11.2.6 Stimulation and treatment of eukaryotic cells

To investigate the effect of certain compounds, the transfected cells were treated 18-20h after transfection (Chapter 11.2.5). HUVEC and MC were treated the day after seeding. For this purpose, the cell culture media was removed and pure media was added. After 1h of starving, the treatment took place. For cAMP-assay (Chapter 11.5.5), the cells were treated for 15min with the compound of interest. If blockers were used, a 15min pre-treatment took place followed by a 15min stimulation. For the dual luciferase assay the cells were treated 6h with the compound of interest. After treatment, the cells were harvested depending on the assay used.

To examine the effect of the compounds on intracellular signalling in HUVEC and mesangial cells using immunoblot analysis, the cells were seeded in to 60mm dishes. The next day the cells were starved for 1h and treated for 15min, or certain time points, with the compound of interest. If needed a 15min pre-incubation with blockers took place. After treatment the cells were harvested like described in Chapter 11.5.1.

11.2.7 Isolation and stimulation of mouse islets of Langerhans

The islets of Langerhans are located within the pancreas. They consist the insulin-producing beta cells, the glucagon-producing alpha cells and somatostatin-producing delta cells. Their isolation requires the gentle enzymatic and mechanical digestion of the exocrine tissue without causing damage to the islets. Depending on the mouse, 200-400 islets can be isolated. For this purpose, all media and solvents were warmed up to 37°C. One ml collagenase P (2mg/ml) (Roche, Basel, Switzerland) in Krebs Ringer buffer was injected into the mouse pancreas through the common bile duct. The whole pancreas

was removed and digested in 2 ml collagenase P solution for 6 min at 37 °C with continuous, gentle shaking. Ice-cold islet isolation buffer (Chapter 11.1.6) was added, samples were shaken vigorously for 15 s and centrifuged (500×*g*, 2min, 4°C). Pellets were resuspended in islet isolation buffer and islets were hand-picked and collected in RPMI1640 (Sigma-Aldrich, St. Louis, MO, USA) supplemented with 10% FBS, and 1x penicillin/streptomycin (Sigma-Aldrich, St. Louis, MO, USA). Twenty islets per well isolated from wild-type or Mas-deficient mice were cultured for 24h in 12 well plates with 500µl RPMI1640 (supplemented as described above) at 37°C with 5% CO₂. After 24h, islets were incubated in Krebs Ringer buffer (Chapter 11.1.6) with 2.8mmol/l glucose for 90min, with buffer exchanged once after 30min. Islets were exposed to different glucose concentrations (2.8mmol/l glucose, 2.8mmol/l glucose + 40mmol/l KCl, or 20mmol/l KCl) for 2h. For the treatments, Ang-(1-7) (0.2µmol/l), A779 (1µmol/l), and D-Pro (1µmol/l) were added. Supernatants were collected, centrifuged at 100xg for 2min at 4°C and insulin concentrations in the supernatants determined by ELISA (Mercodia, Uppsala, Sweden).

For cAMP analysis, islets were treated as described in Chapter 11.2.6.

11.3 Microbiological methods

11.3.1 Transformation of prokaryotic cells

The bacterial strain used in this work was *Escherichia Coli* (*E. Coli*) DH5α. These cells are engineered in order to maximize the transformation efficiency. They are defined by 3 mutations ([The Coli Genetic Stock Center](#)). Those mutations are recA1, endA1 and

lacZM15. The first two mutations help with plasmid insertion, while the other mutation enables the blue white screening [445].

For the transformation of *E.coli*, the heat shock method was used [446]. For this purpose, 100µl of chemo competent *E. coli DH5a* were thawed on ice and then incubated with 400 ng of plasmid DNA for 30min, allowing the precipitation of the DNA due to the high salt concentration. A heat shock for 45s at 42°C causes pores in the bacterial membrane, where the plasmid DNA can enter the cells. After two-minutes incubation on ice, 1000µl of LB medium was added to the cells and the mixture was left shaking for one hour at 37°C on a thermo-block (Eppendorf, Hamburg, Germany). After centrifugation at 110rpm for 5min the supernatant was decanted. The bacteria pellet was resuspended in 50µl LB-Media. The suspension was plated on antibiotic containing agar plates using a Drygalski spatula and left overnight at 37°C in an incubator. The choice of antibiotic was based on the resistance contained in the vector backbone used (indicated in the vector card). The plasmids used in this work (pcDNA3.1, Mas-pcDNA3.1, MrgD-pcDNA3.1, AT2-pcDNA3.1, or Mrg-pcDNA3.1) were provided by the group [65].

11.3.2 Multiplication of prokaryotic cells

After transformation and selection on antibiotic-containing agar plates, a single cell colony was picked and added to 200ml Lysogeny broth (LB) media, supplemented with 100µg/ml antibiotics. The bacterial culture was incubated for 16-18h overnight with shaking at 37°C. After centrifugation for 20min at 14000rpm, the bacterial pellet was stored at -20°C until plasmid purification.

11.3.3 Isolation of plasmid DNA

The plasmid DNA from *E. Coli DH5a* was prepared from a 5ml pre-culture with the QIAprep Spin Miniprep Kit (Qiagen, Hilden, Germany) and from a 200ml bacteria culture with the PureYield™ Plasmid Maxiprep System (Promega GmbH, Mannheim, Germany) according to manufacturer's instructions. The preparation took place according to the manufacturer's protocol after the principle of alkaline lysis [447].

Briefly, the cell pellet was resuspended in 12ml of "Cell Resuspension Solution" (provided in kit) by vortexing or pipetting. Then, 12ml of "Cell Lysis Solution" (included in kit) was added and the vial was gently inverted 3–5 times to mix. After 3min incubation at room temperature, 12ml of "Neutralization Solution" (included in kit) was added and the mix gently inverted 10–15 times to mix. Subsequently, the lysate was centrifuged at maximum speed for 30min at room temperature.

For the next steps the blue PureYield™ Clearing Column and the white PureYield™ Maxi Binding Column were assembled in a stack, with the clearing column on top. This column stack was then placed on the vacuum manifold. The lysate was poured on to the column and vacuum maintained until the liquid had cleared both columns. Then, the blue PureYield™ Clearing Column was discarded and the PureYield™ Maxi Binding Column was left on the vacuum manifold. Next, 5ml of Endotoxin Removal Wash was added to the PureYield™ Maxi Binding Column, vacuum was applied and the solution was allowed to be pulled through the column. After that, 20ml of Column Wash was added to the binding column, and the vacuum was applied to pull the solution through the column. Next, the membrane was dried by applying the vacuum for 10minutes. The PureYield™ Maxi

Binding Column was removed from the vacuum manifold and the tip of the column was tapped on a paper towel to remove any remaining ethanol.

For the elution, the column and a 1.5 ml micro-centrifuge tube were placed into the base of the Eluator™ Vacuum Elution Device. Next, this Device was placed on to the vacuum manifold and 1ml of Nuclease-Free Water was added to the DNA binding membrane in the binding column. After 1min incubation the maximum vacuum was applied until all liquid had passed through the column.

The concentration of the plasmid DNA was determined by using the Nano-Drop (Thermo Fisher Scientific, Waltham, Massachusetts, USA)

11.4 Molecular biological methods

11.4.1 Genotyping mice

11.4.1.1 Preparation of ear biopsies

The animals were marked on the ears for later identification. The generated ear biopsies were used for the isolation of genomic DNA. For this purpose the ear pieces were transferred into a 1.5ml reaction tube and incubated with 100µl earhole buffer and 12µl proteinase K solution at 37°C overnight with gentle shaking. The next day, the proteinase K was inactivated by heating the samples at 95°C for 10min. After short centrifuging, 400µl of TE buffer and 13µl of RNase A solution were added to the samples. The prepared samples were directly used for PCR or stored at -20°C.

11.4.1.2 Polymerase chain reaction (PCR) for genotyping

The genotyping of the animals was carried out by using PCR [448]. Specific sections of the target gene in the genomic DNA were amplified by PCR and separated on an agarose gel. The first PCR was used to amplify the sequence in the natural, unaltered target gene. The second PCR was used to amplify the change in the DNA sequence of the target gene, which leads to its elimination (knockout). In this way, the genotype of the animals was clearly determined. The general reaction mixtures used for each PCR is listed in Table 11.4.

Table 11.4 Reaction mix for Genotype PCR

PCR reaction mix genotyping

Reagent	Volume					
	Mas WT	Mas KO	MrgD WT	MrgD KO	AT2 WT	AT2 KO
H ² O	30.45	30.45	29.95	30.25	30.25	30.45
NH ₄	4.5	4.5	4.5	4.5	4.5	4.5
MgCl ₂	1.8	1.8	2.3	2	2	1.8
dNTPs	2.4	2.4	2.4	2.4	2.4	2.4
Forward primer*	1.8	1.8	1.8	1.8	1.8	1.8
Reverse Primer*	1.8	1.8	1.8	1.8	1.8	1.8
Taq	0.25	0.25	0.25	0.25	0.25	0.25

* Primer were diluted 1:10 before used for PCR

Table 11.5 PCR conditions

Mas WT PCR				Mas KO PCR			
Temperature	Time	Step	Cycles	Temperature	Time	Step	Cycles
94 °C	5 min	initial denaturation	1 x	94 °C	5 min	initial denaturation	1 x
94 °C	30 s	denaturation	34 x	94 °C	30 sec	denaturation	34 x
59 °C	30 s	annealing		62 °C	30 sec	annealing	
72 °C	1 min 5sec	amplification		72 °C	1 min 5sec	amplification	
72 °C	7 min	final amplification	1x	72 °C	7min	final amplification	1x
4 °C	unlimited	end		4 °C		end	

MrgD WT PCR				MrgD KO PCR			
Temperature	Time	Step	Cycles	Temperature	Time	Step	Cycles
94 °C	5 min	initial denaturation	1 x	94 °C	5 min	initial denaturation	1 x
94 °C	30 sec	denaturation	34 x	94 °C	30 sec	denaturation	34 x
54.6 °C	30 sec	annealing		60 °C	30 sec	annealing	
72 °C	59 sec	amplification		72 °C	1 min 5 sec	amplification	
72 °C	7min	final amplification	1x	72 °C	7min	final amplification	1x
4 °C		end		4 °C		end	

AT2 WT PCR				AT2 KO PCR			
Temperature	Time	Step	Cycles	Temperature	Time	Step	Cycles
94 °C	5 min	initial denaturation	1 x	94 °C	5 min	initial denaturation	1 x
94 °C	30 sec	denaturation	34 x	94 °C	30 sec	denaturation	34 x
51.3 °C	30 sec	annealing		51.3 °C	30 sec	annealing	
72 °C	27 sec	amplification		72 °C	35 sec	amplification	
72 °C	10 min	final amplification	1x	72 °C	10 min	final amplification	1x
4 °C		end		4 °C		end	

11.4.1.3 Agarose gel electrophoresis

The gel electrophoretic separation of PCR products was carried out in horizontal running chambers. For PCR products generated in the PCRs for Mas (WT/ KO), MrgD (WT/ KO) and AT2 (WT/ KO), 1.5% (w/v), agarose gels were used. For this purpose, the agarose (Sigma-Aldrich, St. Louis, MO, USA) was dissolved in TAE buffer (1x) under heat using a microwave. After cooling down to about 50°C, 0.5µl/ml Gel Red (Cambridge Bioscience, Camebridge, UK) was added and the mixture poured into the gel carrier. Gel Red is a DNA intercalating dye, which can be detected using ultraviolet light. The loading of the

samples and a corresponding molecular weight marker (lambda marker) was carried out after the addition of ¼ volume of DNA loading buffer. The gel electrophoresis was performed at 100V. The visualization/digitization was carried out using the Syngene GBox - EF Gel Documentation System (Syngene UK, Cambridge, United Kingdom). Figure 11.4.1 shows an example of the expected signal combinations and their interpretation.

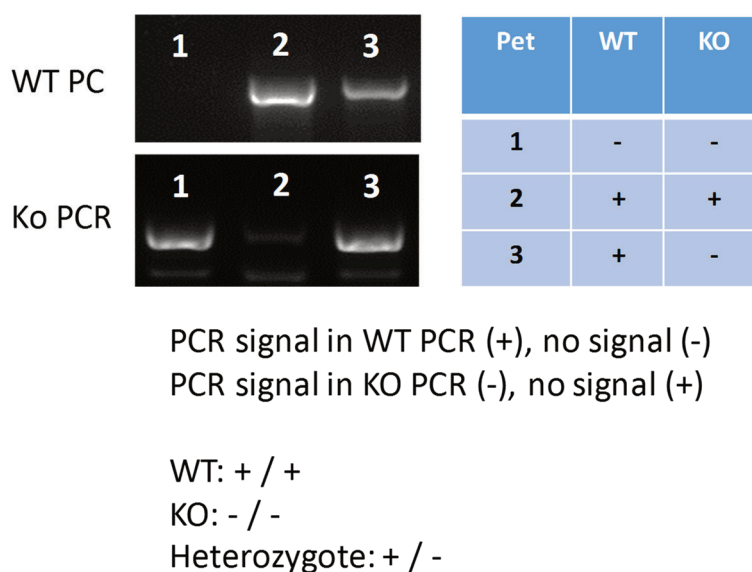


Figure 11.4.1 Example for genotyping PCR

Example of the combination of results that can be expected.

11.4.2 Isolation of RNA

RNA was isolated using the NucleoSpin RNA Kit (Macherey-Nagel, Dueren, Germany). The following steps were carried out according to the manufacturer's protocol. Cells were lysed in 350µl of lysis buffer (RA1) supplemented with 1% (v/v) of β-mercaptoethanol. The lysate was transferred to the filtration column and centrifuged for 1min at 10000×g, to remove cell debris. The supernatant was collected and the filter discarded. In order to achieve optimal binding to the affinity column, the RNA was pre-precipitated by the

addition of 350µl of 70% (v/v) ethanol to the column, and centrifugation at 10000×g for 30s at RT. After desalination of the column with 350µl of Membrane Desalting Buffer (MDB) and subsequent centrifugation at 10000×g for 1min, genomic DNA was degraded by the addition of 95µl of prepared DNase solution and incubation for 15min. Subsequently, the column was washed three times and the RNA eluted in 40µl of water by centrifugation at 10000×g for 2min. The RNA was either immediately quantified or stored at -80°C.

11.4.3 Quantification of nucleic acids

For the determination of the concentrations, 1µl of the isolated RNA or DNA was applied to the NanoDrop (Thermo Fisher Scientific, Waltham, Massachusetts, USA) and quantified at a wavelength of 260nm (absorption maximum of the nucleic acids). At the same time, a measurement was carried out at 280nm (absorption of aromatic amino acids). The quotient of the absorbance at 260nm and 280nm gives an indication of the purity of the preparation. For pure DNA/RNA, the quotient is between 1.7 and 2.0, and below 1.6 when protein impurities are in the sample. For each sample, the concentration was determined in duplicates, from which the mean value was calculated.

11.4.4 Synthesis of complementary DNA (cDNA)

The reverse transcription of mRNA into cDNA was carried out using the RevertAid H Minus First Strand cDNA Synthesis Kit (Thermo Fisher Scientific, Waltham, Massachusetts, USA) according to the manufacturer's instructions. Two µg of isolated RNA was mixed with 1µl oligo-(dT)18 primer in a final volume of 12µl. The use of these primers allowed

the transcription of biologically active mRNA species possessing a corresponding poly (A) tail. After incubation at 65°C for 5min, a mix of 4µl of 5× reaction buffer, 2µl of deoxyribonucleoside triphosphate (dNTP) mix, and 1µl of ribonuclease inhibitor and reverse transcriptase were added from the kit for each reaction.

Table 11.6 cDNA synthesis mix

Amount	reagent	
1 µl	Oligo-d(T) ₁₈ -Primer	Reaction 1
2 µg	RNA	
add 12µl	ddH ₂ O	
2 µl	10 mM dNTPs	stock mix
4 µl	5x Reaction buffer	
1 µl	Reverse Transcriptase (200 U/µl)	
1 µl	RNase-Inhibitor (20 U/µl)	
8 µl	stock mix to reaction 1	

The reverse transcription was carried out in a thermocycler using the following program: 37°C for 5min, 42°C for 1h and 70°C for 10min. Subsequently, the cDNA was diluted 1: 5 in water.

11.4.5 Quantitative real time PCR (qRT-PCR)

The qPCR allows the relative quantification of mRNA levels using DNA intercalating dyes like SybrGreen. The more DNA is synthesized during the PCR the more dye is deposited in it. By measuring the fluorescence intensity after each PCR cycle, the amount of the amplification product can thus be measured and quantified by means of special analysis

programs compared to other PCR [148]. The complete system Platinum SYBR Green qPCR SuperMix-UDG Kit (Invitrogen, Carlsbad, California, United States) was used for the qPCR experiments. The corresponding primer sequences are summarized in Chapter 11.1.3. A reaction approach included:

Table 11.7 qPCR reaction mix

Reagent	volume [μl]
SYBR Green qPCR Mix	10.0
H ₂ O	8.5
Forward primer (100 pmol/μl)	0.25
Reverse primer (100 pmol/μl)	0.25
cDNA	1.0

The PCR was performed in a StepOne qPCR cycler (Thermo Fisher Scientific, Waltham, Massachusetts, USA). The determination of the melting point was used to check whether the PCR product was synthesized and to see if other nonspecific PCR products or primer dimers were generated. The evaluation was carried out using the raw data exported from the StepOne software. The raw data shows the threshold cycle (Ct), which represents the transition of the PCR into the exponential phase and is a measure of the mRNA quantity. The PCR efficiency (E), was assumed to be 1.8 as the machine doesn't give this information. In theory this value is 2 as with each cycle the amount of DNA gets duplicated. In the past it was shown, that this value usually is between 1.7 and 1.9. The ΔC_t method was used for the calculation of normalized expression (Exp_{norm}), from the

relative expression of the control ($\text{Exp}_{\text{rel (control)}}$) and that of the target gene ($\text{Exp}_{\text{rel (target gene)}}$).

The calculation was carried out using the following formulas:

E = increase from the linear regression of the exponential phase

$$\Delta C_t = C_t(\text{control}) - C_t(\text{sample})$$

$$\text{Exp}_{\text{rel}} = (\text{Exp}_{\text{target gene/control}})^{\Delta C_t}$$

$$\text{Exp}_{\text{norm}} = \frac{\text{Exp}_{\text{rel (target gene)}}}{\text{Exp}_{\text{rel (control)}}$$

The relative expressions of the investigated genes were compared with those of constitutively expressed household genes, e.g. Hypoxanthine phosphoribosyltransferase (HPRT), glyceraldehyde-3-phosphate dehydrogenase (GAPDH) and β -actin, to reduce variance between the samples by methodological errors. Three independent biological replicates were used to analyse gene expression using qPCR.

11.4.6 Dual luciferase assay (DLR)

For the examination of receptor activity, transcription factors and intracellular signaling the Dual Luciferase Reporter (DLR) Assay kit (Promega GmbH, Mannheim, Germany) was used. The “dual” refers to the consecutive expression and measurement of two individual reporter enzymes within one system. In this DLR, the activities of Firefly (*Photinus pyralis*) and Renilla (*Renilla reniformis*, also known as sea pansy) luciferases are measured (Figure

11.4.2). Whereas the firefly luciferase is coupled to the reporter, the Renilla luciferase is used as the internal control [449].

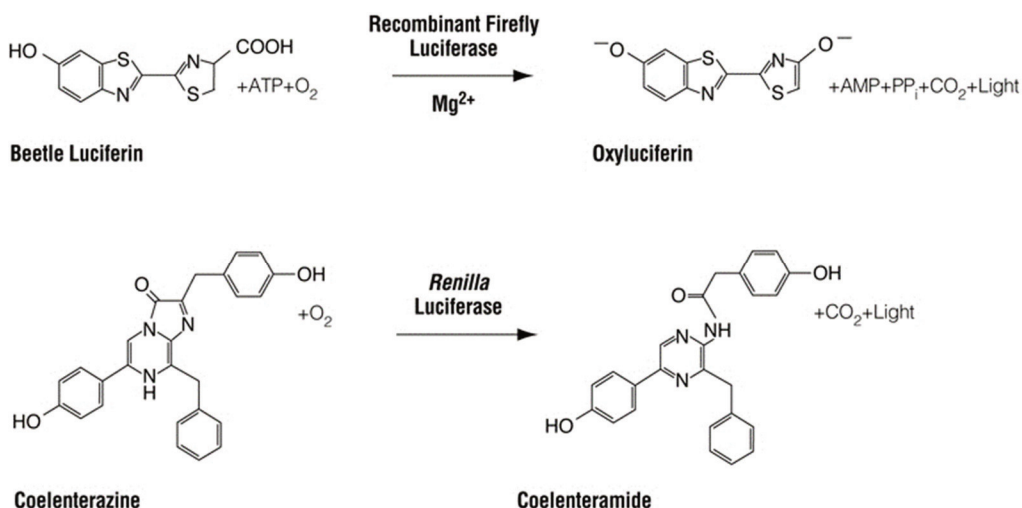


Figure 11.4.2 Light emission from firefly and Renilla luciferase

Schematic overview of the reactions of the Firefly and Renilla luciferase, which result in the emission of light.

For the DLR assay, HEK293 cells were seeded as previously described in Chapter 11.2.5. About 24h later, cells were transiently transfected (see Chapter 11.2.5) with 100ng eukaryotic expression vectors of AT1 [65], AT2, Mas, MrgD or Mrg together with 25ng pNFAT-TA-Luc-, (BD Biosciences; Heidelberg; Germany) or pELK-Luc Reporter Vector (Signosis, Santa Clara, California, USA) luciferase reporter plasmids and 25ng pRL-TK (Promega GmbH, Mannheim, Germany). Next day, the stimulation took place as described in Chapter 11.2.6. After 6 hours of stimulation, the cells were lysed with 70μL passive lysis buffer per well (provided with the kit) and incubated on a shaker for 15min at RT. The activity for Firefly and Renilla Luciferase was measured with Orion-L Microplate Luminometer (Berthold Detection Systems GmbH, Pforzheim, Germany) according to the

manufactures protocol. Briefly, 30 μ L of lysed cells were transferred into a white 96-MicroWell plate (Thermo Fisher Scientific, Waltham, Massachusetts, USA), and 100 μ L of Luciferase Assay Reagent II was added. After quantifying the Firefly luminescence, the reaction was quenched by adding 100 μ L of Stop&Glo reagent and Renilla activity was measured. For calculations, the ratio of firefly and Renilla luciferase was used.

11.5 Protein biochemical methods

11.5.1 Protein extraction

In order to examine the expression and phosphorylation of intracellular proteins, the proteins were isolated by directly lysing the cells as quickly as possible as phosphorylation is a very unstable state. For this purpose, the medium of a 100mm (HUVEC and MC) or 60mm (HEK293) cell culture dish was completely aspirated and 500 μ L/200 μ L of ice-cooled RIPA buffer (Thermo Fisher Scientific, Waltham, Massachusetts, USA) was added immediately. The buffer was mixed with 1% (v/v) phosphatase inhibitor mix 2 and 3 (Sigma Aldrich, St. Louis, MO, USA) and protease inhibitor mix (Sigma Aldrich, St. Louis, MO, USA) to prevent dephosphorylation and protein degradation. After rapid removal of the cells from the bottom of the cell culture dish with a cell scraper, the cell lysate was transferred to a pre-cooled 1.5ml reaction tube. After 20min of incubation on ice, the cell was further processed by using ultrasound (10 pulses of ultrasound at a power of 60%). After a further 10min incubation on ice, non-lysed cells or cell debris were removed by centrifugation at 13,000 \times g and 4°C for 20min. The protein lysate was transferred to a new pre-cooled reaction tube. The protein concentrations were determined by using the biuret reaction (see Chapter 11.5.2).

11.5.2 Protein concentration determination according to Biuret (BCA)

Protein determination using the biuret reaction was carried out using the BCA protein assay kit (Thermo Fisher Scientific, Waltham, Massachusetts, USA). The reduction of the Cu^{2+} ions in alkaline solution to Cu^+ ions by proteins is exploited. The resulting Cu^+ ions building complexes with two molecules of bicinchonic acid (BCA) which leads to a bathochromic shift which can be measured at 562nm [450]. Ten microliter each of a 1:10 dilution of proteins were pipetted in triplicates into a 96-well plate, and mixed with 200 μl of BCA reagent, consisting of 50 parts of solution A and 1 part of solution B. In addition, 10 μl of pure standard solutions with known concentrations of bovine serum albumin (BSA, 0 to 2mg/ml) were prepared in duplicates. After incubation at 60°C for 20min, the absorbance of each sample was determined at 562nm on a plate reader. The protein concentration of the samples was calculated by linear regression of the BSA standard with correction of the substrate blank.

11.5.3 Sodium dodecyl sulphate polyacrylamide gel electrophoresis (SDS-PAGE)

SDS-PAGE is a gel electrophoretic separation process for proteins under denaturing conditions [451]. The anionic detergent SDS binds to proteins in a ratio of approx. 1.4:1 and superimposes the charge of the proteins with its strong charge. By the addition of thiols, for example dithiothreitol (DTT), the tertiary structures are destroyed, which is caused by the disruption of disulfide bridges. In this way, the proteins are separated in the electric field only by their molecular weight and not by their charge or globularity.

In this work chemically inert acrylamide bisacrylamide gels of size 83 x 73 x 1.5mm were used. The composition of the separating and stacking gels were as follows:

Table 11.8 Acrylamide gel composition

Chemical	seperating gel 1x [ml]		stacking gel 1x [ml]
	10 %	12 %	
H ₂ O	2.95	2.45	2.06
30 % Acrylamide	2.5	3.0	0.5
1.5 M Tris (pH 8,8)	3.8	1.9	-
1.5 M Tris (pH 6,8)	-	-	0.375
10 % (w/v) SDS	0.075	0.075	0.03
10 % (w/v) APS	0.075	0.075	0.03
TEMED	0.004	0.004	0.003

For sample preparation, 20µg protein per sample was added with ¼ of the final volume 4-fold Laemmli sample buffer and 0.1M DTT. Subsequently, the proteins were denatured by incubation at 95°C for 5min. After applying the samples to the gel pockets, the proteins were electrophoresed in The Mini-PROTEAN Tetra hand cast systems in 1x SDS-Tris-Glycine running buffer. A voltage of 50V was applied until the separating gel was reached, then a voltage of 120-150V was applied. A pre-colored protein size marker (PageRuler Prestained Protein Ladder, Fermentas) was included for the purpose of later size control.

11.5.4 Immunoblot analysis

The immobilization of the proteins separated in the SDS-PAGE onto a nitrocellulose membrane (Macherey-Nagel, Dueren, Germany) was carried out by the so-called electro

blot method. The negatively charged proteins migrate in the electric field to the anode of the blotting system and bind covalently to the membrane [452].

Both a discontinuous buffer system and a semidry blotter chamber were used in this work. Three-layer filter paper were each soaked in anode solution I or II, as well as in the cathode solution. The nitrocellulose membrane was incubated for 10min in the anode solution II. The structure of the apparatus is shown in Figure 11.5.1.

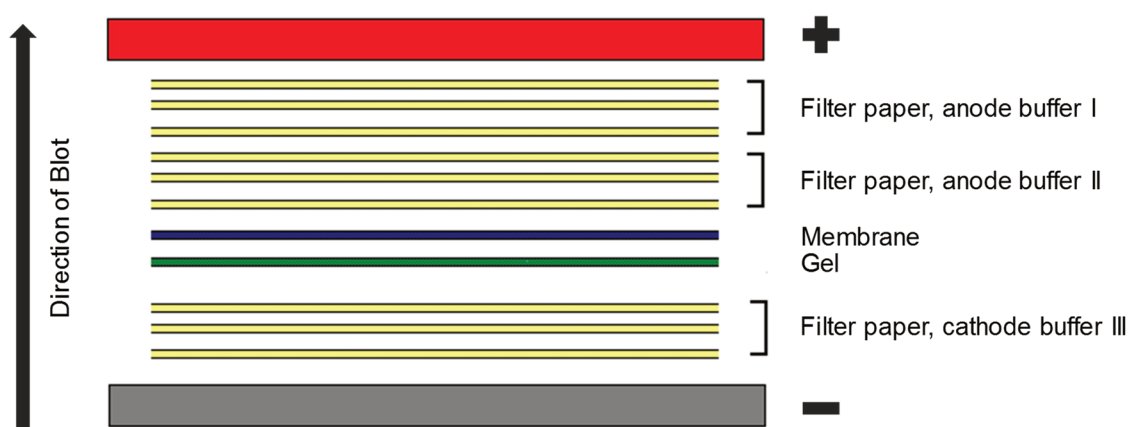


Figure 11.5.1 Application of the semi dry blot

Schematic overview of the application of the semi dry blot.

At a constant current intensity of 0.85mA per cm² of membrane area, the proteins were transferred to the membrane for 1h. The quality and efficiency of the transfer was checked with a Ponceau S staining. For this, the membrane was shaken for about 2min in the Ponceau S solution, then the excess dyeing solution was tipped off and the membrane was decolourised by washing several times in water.

The immunostaining of the protein bands was carried out by using epitope-specific primary antibodies and horseradish peroxidase (HRP) -conjugated secondary antibodies (Chapter 11.1.4) followed by chemiluminescence detection. First, free binding sites of the nitrocellulose membrane were blocked with 5% (w/v) low-fat milk powder (Roth, Karlsruhe, Germany) in TBS-T for about 1h. Subsequently, the incubation with the primary antibody (dilutions and incubation solutions are listed in Chapter 11.1.4) were performed at 4°C overnight. After washing 3 times with TBS-T for 5min each, an HRP-conjugated secondary antibody specific to the species of primary antibody was incubated for 2h at RT. Unbound antibodies were removed by washing three times for 5min each with TBS-T and twice in TBS. Subsequently, the immunoblots were analysed by means of the chemiluminescent reaction by adding a 1:1 mixture of peroxide and luminol enhancer solution of the ECL Western blot substrate (Thermo Fisher Scientific, Waltham, Massachusetts, USA). Luminol is oxidized by the HRP using hydrogen peroxide. The 3-aminonaphthalic dianion is formed as an energetic intermediate product with the emission of photons (Figure 11.5.2). The released photons were detected with the help of the luminescence detection device.

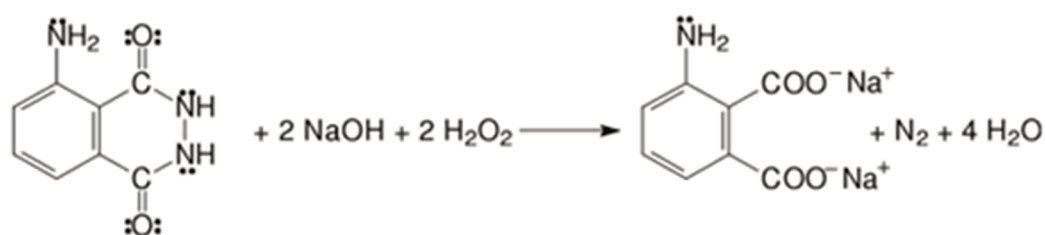


Figure 11.5.2 Luminol reaction

A subsequent quantification of the relative protein levels of five independent biological replicates was carried out using the AIDA program.

11.5.5 Cyclic Adenosine monophosphate enzyme-linked immunosorbent assay (cAMP ELISA)

Like immune blot analysis, an ELISA is an immune based assay. In general, one primary antibody is immobilised on the bottom of a well of a 96-well plate. The antigen can bind and is detected in different ways. Several types of ELISAs exist: direct, indirect, sandwich and competitive ELISA [453]. The ELISA used in this work is the competitive ELISA. In this case, no second labelled antibody is used for detection, but a labelled competitor antigen (a synthetic compound that is structurally similar to the analysed substance and also binds to the antibody) is used. Thus, the competition between the analysed substance and the competitor leads to a binding site on the antibody. The signal behaves in the opposite direction to the concentration of the analysed substance: little amount of analysed substance means that almost all antibody binding sites can be occupied by the labelled competitor, which leads to a strong colour reaction; while huge amount of analysed substance leads to weak colour reaction. The detection systems used (enzymes / substrates) are usually the same as for the ELISA.

Intracellular cAMP concentration was determined using the Direct cAMP ELISA kit (Enzo Life Sciences Ltd., Exeter, United Kingdom). This is a colorimetric competitive immunoassay. All steps were performed according to the manufacturer's protocol (Figure 11.5.3). Briefly, samples and standards (20pmol/l, 5pmol/l, 1.25pmol/l, 0.321pmol/l and 0.078pmol/L) were acetylated by adding 5µl acetylation reagent (0.5mL of

acetic anhydride to 1mL of triethylamine) to 100µl sample/ standard. The wells of 96-well plate (Goat Anti-Rabbit IgG pre-coated) were neutralized with 50µl of Neutralizing Reagent. Next, 100µl of acetylated cAMP standard or cell lysate was added, followed by

50µl of blue cAMP-Alkaline Phosphatase Conjugate and 50µl of yellow EIA Rabbit Anti-cAMP antibody. The plate was then incubated on a shaker (~ 400rpm) at RT for 2h. Next, the wells were aspirated and rinsed three times with Wash Buffer (1:10, TBS containing detergents and sodium azide in deionized water). After the final wash, the plate was tapped against clean paper towel to remove any remaining Wash Buffer. To each well 200µl p-Nitrophenyl Phosphate Substrate Solution was added, and the plate was incubated for 1h at RT. The enzymatic reaction was stopped by adding 50µl of Stop Solution, and the absorbance at 405nm was measured immediately. The cAMP concentration was determined from non-linear standard curve using GraphPad Prism 5.0 software.

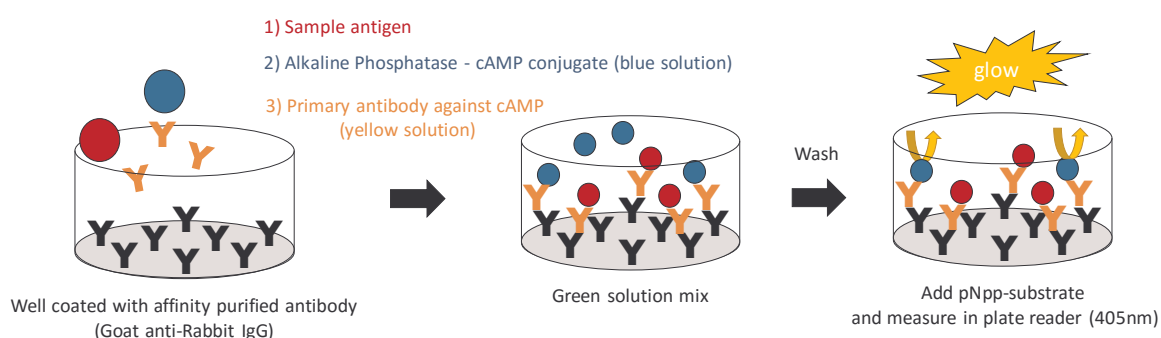


Figure 11.5.3 cAMP assay

Schematic overview of the cAMP assay. The sample antigen (cAMP) and the alkaline phosphatase (AP) ladled cAMP compete for the binding to the primary antibody. The signal behaves in the opposite direction to the concentration of the analysed substance.

11.5.6 Protein kinase A (PKA) activity analysis

The measurement of Protein Kinase A (PKA) activity was performed using the PKA Colorimetric Activity Kit (Arbor Assays Headquarters, Ann Arbor, Michigan, USA) following the manufacturer's instructions. Briefly, HEK293 cells were seeded into 48-well plates. On

the next day, cells were transiently transfected using PolyFect reagent as described in Chapter 11.2.5. For HUVEC cells, 24-well plates (75,000 per well) were used and plated overnight. Sixteen to 20h later, the stimulation took place (Chapter 11.2.6). Then, the cells were lysed in 50 μ L (HEK293) or 100 μ L (HUVEC) activated cell Lysis Buffer provided by the kit, containing 1mM PMSF (phenylmethylsulfonyl fluoride), 1 μ L/ml protease and phosphatase inhibitor cocktail (Sigma Aldrich, St. Louise, Missouri, USA) and incubated for 30min on ice. The lysates were transferred to 1.5ml reaction tubes and centrifuged at 10,000rpm at 4°C for 10min. The supernatant was directly used for the analysis or stored at -80°C until the measurement.

For measurement, all samples were diluted 1:10 in Kinase Assay Buffer provided by the Kit. For the measurement, 40 μ L of the sample (in triplicates) or standard (in duplicates) were pipetted in to each well. Afterwards, 10 μ L of ATP was added to each well and incubated for 1.5h at 30°C on a shaker. Next, the wells were aspirated and rinsed four times with Wash Buffer (1:20 in deionized water). After the final wash, the plate was tapped against clean paper towel to remove any remaining Wash Buffer. Twenty-five μ L of the Goat anti-rabbit IgG HRP and 25 μ L of the Rabbit Phospho PKA Substrate antibody were added to each well and incubated at RT for 60min with shaking. The wells were aspirated again and rinsed four times with Wash Buffer (1:20 in deionized water). After the final wash, the plate was tapped against clean paper towel to remove any remaining Wash Buffer. Next, 100 μ L of the TMB Substrate Solution were added to each well and incubated for 30min at RT. Afterwards, 50 μ L of stop solution was added to each well and the optical density was measured at 450nm using a plate reader. The PKA activity (U/ml) was determined from the linear standard curve using linear regression from Excel.

11.6 *In vivo* studies

11.6.1 STZ induced diabetes

For this purpose, 12 week old mice deficient in Mas [120], MrgD [359] (strain #36050, [B6.129S1-Mrgprd^{tm5Mjz}/Mmnc](#) The Mutant Mouse Regional Resource Center 8U42OD010924-13, Chapel Hill, NC, USA), or both receptors, and the corresponding wild-type animals were used.

The diabetes was induced by using streptozotocin (STZ). The structural similarity with glucose allows STZ to bind to the Glucose receptor (GLUT2) leading to damage of the pancreatic β -cells, which results in hypoinsulinemia and hyperglycemia [454]. Depending on the dose, STZ induces diabetes in two ways. At high doses (single dose administration), STZ destroys the β -cells through its alkylating property [455]. At low doses (multiple dose administration), STZ provokes an immune and inflammatory response. An autoimmune response like mechanism destroys the β -cells and leads to the hyperglycaemic conditions [456].

For the purpose of our studies, we used multiple dose administration of STZ. The injection of STZ took place in the first 5 days of the study. For this purpose, 50mg/kg STZ (Sigma Aldrich, St. Louis, MO, USA) dissolved in citrate buffer (Chapter 11.1.6) was injected intraperitoneal. Additionally the bodyweight from each animal was determined on day one. After five days, the body weights were determined, and blood glucose levels were measured through tail clip and by using the Contour Blood Glucose Meter (Bayer, Berlin, Germany). From day 6 on, a daily subcutaneous (neck) injection of Ang-(1-7) (relevant dose was dissolved in 0.9% NaCl solution) was performed. Every 3 days the body weight

and blood glucose was determined (day: 8, 11, 14, 17, 20). On day 20, the animals were sacrificed and organs dissected, snap frozen and stored at -80°C or fixed in paraformaldehyde (PFA).

12 Acknowledgements

I would like to thank Prof. Thomas Walther for the provision of the very interesting topic and the supervision of my dissertation, for the many inspiring discussions and the scientific suggestions and advices that made this work possible.

I thank also all members and former members of the working group for the great atmosphere, the fun and cooperation in the lab. In particular: Kinga, Franziska, Marlies, Maura, Cliona, Andrew, Ilka, and the two Anjas.

Dear Maura, big “thank you” to you for the support and the strong nerves while submitting our publications and the revisions.

My special thanks go to my mum, Holger and my grandparents, who accompanied me during my PhD and supported me in every imaginable way.

Finally, I would like to thank all the friends I made during my time here in Ireland for the awesome time, the fun nights in the pubs, the understanding, and support during all the time.

13 Publications, posters and oral presentations

13.1 Publications

Meinert C, Gembardt F, Böhme I, **Tetzner A**, Wieland T, Greenberg B, Walther T.

Identification of intracellular proteins and signaling pathways in human endothelial cells regulated by angiotensin-(1-7). J Proteomics. 2016 Jan 1;130:129-39. doi: 10.1016/j.jprot.2015.09.020. Epub 2015 Sep 24. PMID: 26388433

Tetzner A, Gebolys K, Meinert C, Klein S, Uhlich A, Trebicka J, Villacañas Ó, Walther T.

G-Protein-Coupled Receptor MrgD Is a Receptor for Angiotensin-(1-7) Involving Adenylyl Cyclase, cAMP, and Phosphokinase A. Hypertension. 2016 Jul;68(1):185-94. doi: 10.1161/HYPERTENSIONAHA.116.07572. Epub 2016 May 23. PMID: 27217404

Sahr A, Wolke C, Maczewsky J, Krippeit-Drews P, **Tetzner A**, Drews G, Venz S, Gürtler S, van den Brandt J, Berg S, Döring P, Dombrowski F, Walther T, Lendeckel U.

The Angiotensin-(1-7)/Mas Axis Improves Pancreatic β -Cell Function in Vitro and in Vivo.

Endocrinology. 2016 Dec;157(12):4677-4690. Epub 2016 Oct 7. PMID: 27715254

Meinert C, Kohse F, Böhme I, Gembardt F, **Tetzner A**, Wieland T, Greenberg B, Walther T.

Further intracellular proteins and signaling pathways regulated by angiotensin-(1-7) in human endothelial cells. Data Brief. 2016 Dec 8;10:354-363. doi: 10.1016/j.dib.2016.12.004. eCollection 2017 Feb. PMID: 28018949 September, 2015

Anja Tetzner, MSc; Maura Naughton, MSc; Kinga Gebolys, PhD; Rebecca Lancaster; Thomas Walther, PhD. (2017) *Decarboxylation of Ang-(1-7) to Ala1-Ang-(1-7) leads to significant changes in pharmacodynamics*. Eur J Pharmacol. 2018 Aug 15;833:116-123. doi: 10.1016/j.ejphar.2018.05.031. Epub 2018 May 21.

Anja Tetzner, MSc; Maura Naughton, MSc; Kinga Gebolys, PhD; Rebecca Lancaster; Thomas Walther, PhD. (2018). *The AT2 receptor agonist, C21, can also stimulate Mas and MrgD receptors*.

13.2 Posters

Anja Tetzner, Kinga Gebolys, Florian Gembardt, Thomas Wieland, Susanne Lutze, Thomas Walther.

The G protein-coupled receptor Mas encoded by the Mas proto-oncogene mediates its mitogenic properties through constitutive activity.

Signaling and GPCR- Pharmacology Deutsche Gesellschaft für Pharmakologie DGP e.V. Forum Junge Wissenschaft in der DGPT DFG Graduiertenkolleg 1873, Bonn: 27 – 29

Anja Tetzner, MSc; Kinga Gebolys, PhD; Christian Meinert, PhD; Sabine Klein, PhD; Anja Uhlich, MSc; Jonel Trebicka, MD, PhD; Óscar Villacañas Pérez, PhD; Thomas Walther, PhD. (2016)

The G protein-coupled receptor MrgD is a receptor for angiotensin-(1-7) involving GalphaS, cAMP, and phosphokinase A.

82nd Annual Meeting of the German Society for Experimental and Clinical Pharmacology and Toxicology (DGPT), 18th Annual Meeting of the Clinical Pharmacology (VKliPha) in cooperation with the AGAH, 29 February – 3 March 2016 – Berlin

And "Cutting Edges Concepts in Molecular Pharmacology" in Berlin, March 3-5, 2016

Anja Tetzner, MSc; Maura Naughton, MSc; Kinga Gebolys, PhD; Rebecca Lancaster; Thomas Walther, PhD. (2017) *Decarboxylation of Ang-(1-7) to Ala1-Ang-(1-7) leads to major changes in pharmacodynamics.*

2nd German Pharm-Tox Summit, 06–09 March 2017 at the University of Heidelberg

Anja Tetzner, MSc; Maura Naughton, MSc; Kinga Gebolys, PhD; Rebecca Lancaster; Thomas Walther, PhD. (2017) *Decarboxylation of Ang-(1-7) to Ala1-Ang-(1-7)*

ASH Hypertension 2017 – The American Society of Hypertension Annual Scientific Meeting & Exposition, 13-16 September 2017, San Francisco, USA

Anja Tetzner, MSc; Maura Naughton, MSc; Kinga Gebolys, PhD; Rebecca Lancaster; Thomas Walther, PhD. (2017)

The AT2 receptor agonist, C21, can also stimulate Mas and MrgD receptors

ASH Hypertension 2017 – The American Society of Hypertension Annual Scientific Meeting & Exposition, 13-16 September 2017, San Francisco, USA

13.3 Oral presentations

The AT2 receptor agonist, C21, is also a ligand for Mas and MrgD receptors

2017 Irish Association of Pharmacologists – Conway Institute, University College Dublin, 24th November 2017

The AT2 receptor agonist, C21, can also stimulate Mas and MrgD receptors

2nd German Pharm-Tox Summit, 06–09 March 2017 at the University of Heidelberg

The AT2 receptor agonist, C21, is also a ligand for Mas and MrgD receptors

40. Wissenschaftlicher Kongress der Deutschen Hochdruckliga e.V. DHL®

Deutsche Gesellschaft für Hypertonie und Prävention, 01.-03. Dezember 2016, Berlin

The Angiotensin-(1-7)/Mas Axis Improves Pancreatic β -Cell Function in Vitro and in Vivo.

2016 Irish Association of Pharmacologists – Trinity College Dublin, November 2016

14 Abbreviations

[Ca ²⁺] _c	Cytosolic calcium concentration
7TMR	Seven transmembrane receptors
AA	Arachidonic acid
AC	Adenylyl cyclase
ACE	Angiotensin converting enzyme
Ang	Angiotensin
AP	Aminopeptidase
AT1	Angiotensin receptor type 1
AT2	Angiotensin receptor type 1
ATP	Adenosine triphosphate
BCA	Bicinchonic acid
BCL-2	B-cell lymphoma 2
BG	Blood glucose
C21	Compound 21
CAMK	Calmodulin-dependent kinase
cAMP	Cyclic adenosine monophosphate
cGMP	Cyclic guanosine monophosphate

CML	Nepsilon-(carboxymethyl)-lysine
CRE	CREB response element
CREB	cAMP response element-binding protein
DAG	Diacylglycerol
DKO	Double knockout
DLR	Dual luciferase assay
DM	Diabetes mellitus
DMSO	Dimethyl sulfoxide
DUB-1	Dual-specificity phosphatase 1
ECL	Enhanced chemiluminescence
ELISA	Enzyme-linked immunosorbent assay
eNOS	Endothelial nitric oxide synthase
EPAC	Exchange factor directly activated by cAMP
ER	Endoplasmic reticulum
FBS	Foetal bovine serum
GABA	Gamma-aminobutyric acid
GAG	Diacylglycerol
GAPDH	Glyceraldehyde 3-phosphate dehydrogenase
GDP	Guanosine diphosphate

GEF	Guanine exchange factor
GLP-1	Glucagon-like peptide-1
Gly Phos	Glycogen phosphatase
Gly Synth	Glycogen synthase
GPCR	G-protein coupled receptor
GSIS	Glucose-stimulated insulin secretion
GTP	Guanosine triphosphate
HEK	Human embryonal kidney cells
HPRT	Hypoxanthine-guanine phosphoribosyltransferase
HRP	Horseradish peroxidase
HUVEC	Human umbilical vein endothelial cells
IFN- γ	Interferon gamma
IgG	Immunoglobulin G
IL	Interleukin
iNOS	Inducible nitric oxide synthase
IP3	Inositol trisphosphate
IRAP/ AT4	Insulin regulating amino peptidase
JNK	c-Jun n-terminal kinase
KO	Knockout

LB	Lysogenic broth
MAPK/Erk	Mitogen activated protein kinase
MC	Mesangial cells
MEK	Mitogen-activated protein kinase kinase
MKP-1	MAP kinase phosphatase-1
Mrg (Mrgpr)	Mas related G-protein coupled receptor
NADPH	Nicotinamide adenine dinucleotide phosphate
NEP	Neprilysin
NFAT	Nuclear factor of activated T-cells
NFκB	Nuclear factor kappa-light-chain-enhancer of activated B cells
nNOS	Neuronal nitric oxide synthase
NO	Nitric oxide
NOX	Nicotinamide adenine dinucleotide phosphate oxidase
pAkt	Phospho Akt
PBS	Phosphate-buffered saline
PCR	Polymerase chain reaction
PDE	Phosphodiesterase
PGE2	Prostaglandin E2
PGI2	Prostacyclin

PhosK	Phosphorylase kinase
PI3K	Phosphatidylinositide 3-kinases
PIP2	Phosphatidylinositol 4,5-bisphosphate
pJNK	Phospho JNK
PKA	Protein kinase A
PKB/Akt	Protein kinase B
PKC	Protein kinase C
PLA2	Phospholipase A2
PLC β	Phospholipase C beta
PP2A	Protein phosphatase 2A
PTX	Pertussis toxin
PYK2	Protein tyrosine kinase 2
Raf	Family of serine/threonine-specific protein kinases
RAP	GTP-binding protein or Ras-related protein
RAS	Renin-angiotensin system
Ras	Family of small GTPases
Rho	Small GTPase
ROCK	Rho-associated protein kinase
ROS	Reactive oxygen species

RT	Room temperature
RT-qPCR	Reverse transcription and quantitative polymerase chain reaction
SDS-PAGE	Sodium dodecyl sulfate polyacrylamide gel electrophoresis
SGLT2	Sodium–glucose cotransporter 2
SHP-1	Src homology region 2 domain-containing phosphatase-1
Src	Pyrosine-protein kinase
STZ	Streptozotocin
T1DM	Diabetes mellitus type 1 or Type 1 diabetes
T2DM	Diabetes mellitus type 2 or Type 2 diabetes
TAE	Tris-acetate-EDTA
TBS	Tris-buffered saline
TGF β	Transforming growth factor beta
TNF- α	Tumour necrosis factor alpha
VEGF	Vascular endothelial growth factor
VSMC	Vascular smooth muscle cells
WT	Wild-type

15 Figures

Figure 4.1.1 The general structure of the renin-angiotensin system	12
Figure 4.1.2 Biologically active angiotensin peptides and their generation.....	16
Figure 4.1.3 The receptors of the RAS	17
Figure 4.1.4 Ang-(1-7) tissue specific effects	20
Figure 4.2.1 G-Protein coupled receptor	30
Figure 4.2.2 The $G_{\alpha s}$ and $G_{\alpha i}$ pathway	31
Figure 4.2.3 The $G_{\alpha q/11}$ and $G_{\alpha 12/13}$ pathway	33
Figure 4.2.4 AT ₂ mediated intracellular signalling	37
Figure 4.2.5 Intracellular signalling pathways of Mas	42
Figure 4.2.6 Intracellular MrgD signaling pathways	46
Figure 4.3.1 Mechanism of renin release by high levels of blood glucose	58
Figure 6.1.1 Intracellular cAMP is increased in angiotensin-(1-7) in various cell types	78
Figure 6.1.2 Ang-(1-7) increases cAMP and PKA activity in human umbilical vein endothelial cells (HUVEC).....	80
Figure 6.1.3 Ang-(1-7)-induced signalling is mediated by Mas and MrgD.....	82
Figure 6.1.4 Ang-(1-7)-induced signalling is mediated by Mas and MrgD.....	84
Figure 6.1.5 Ang-(1-7) induced signalling is absent in mesangial cells derived from Mas/MrgD knockout animals.....	86
Figure 6.1.6 Ang-(1-7) induced signalling is absent in mesangial cells derived from Mas/MrgD knockout animals.....	88
Figure 6.2.1 Intracellular cAMP is increased by Ala ¹ -Angiotensin-(1-7) in human umbilical vein endothelial cells (HUVEC).....	105
Figure 6.2.2 Ala ¹ -Ang-(1-7) signals through the MrgD receptor.....	107
Figure 6.2.3 Ala ¹ -Ang-(1-7) can also signal via the Mas receptor.....	108

Figure 6.2.4 Ala ¹ -Ang-(1-7) induced signalling is absent in mesangial cells derived from Mas/MrgD double-knockout animals.	110
Figure 6.2.5 Electrostatic potential of Mas receptor model in the predicted Ang-(1-7) binding site (considering residues within 10 Å of Ang-(1-7)).....	113
Figure 6.3.1 C21 signals via the Mas receptor.	127
Figure 6.3.2 C21 can also signal through the MrgD receptor.	129
Figure 6.3.3 C21 induced signalling is absent in mesangial cells derived from Mas/MrgD double-knockout animals.....	131
Figure 6.3.4 C21 induced signalling is absent in mesangial cells derived from Mas/MrgD double-knockout animals.....	132
Figure 6.3.5 Intracellular cAMP is increased by C21 in human umbilical vein endothelial cells (HUVEC).	135
Figure 6.3.6 In silico modelling and structure of AVE0991 and C21 compounds.....	137
Figure 6.4.1 Detection of components of the alternative ACE2/Ang-(1-7)/Mas axis of the RAS in murine islets of Langerhans.....	156
Figure 6.4.2 Phenotypic description of islets from wild-type and Mas-deficient mice. Islets of Langerhans in pancreatic tissue in WT (+/+; upper line) and Mas KO mice (-/-; lower line):.....	157
Figure 6.4.3 Pharmacological modulation of the receptor Mas ex vivo in WT islets	159
Figure 6.4.4 Effects of pharmacological modulation of the receptor Mas on cytosolic calcium concentrations ([Ca ²⁺] _c) in β-cells and cAMP contents, cAMP-depending signalling, and PKA phosphorylation state in mouse islets.....	162
Figure 6.4.5 Effects of Mas-deficiency on	164
Figure 6.4.6 Effects of continuous Ang-(1-7) administration in vivo on fasting blood glucose and fasting plasma insulin concentrations of WT (+/+) and Mas-deficient (-/-) mice compared to controls (Ø)	165
Figure 6.4.7 Effects of continuous Ang-(1-7) administration in vivo on glucose tolerance.	167
Figure 6.4.8 Effects of continuous Ang-(1-7) administration in vivo on insulin secretion of isolated islets.....	168

Figure 7.9.1 The renin-angiotensin system before 2014 and now	192
Figure 10.1.1 Successful overexpression of Mas and MrgD in HEK293 cells.....	197
Figure 10.2.1 Ala ¹ -Ang-(1-7) induced signalling is absent in mesangial cells derived from Mas/MrgD knockout animals but not in single knockouts.	199
Figure 10.2.2 pPKA substrates levels in WT and AT2 KO mesangial cells.....	200
Figure 10.3.1 Preliminary data from the STZ study performed by Invitek	202
Figure 10.3.2 Effect of the receptor knockout on blood glucose in STZ induced diabetic animals	203
Figure 10.3.3 Effects of Ang-(1-7) administration in vivo on blood glucose.....	204
Figure 10.3.4 Effect of Ang-(1-7) administration in vivo on organ weights.....	205
Figure 10.3.5 Effect of different Ang-(1-7) concentrations in vivo on blood glucose	207
Figure 10.3.6 Effect of different Ang-(1-7) concentrations in vivo on organ weights.....	208
Figure 10.3.7 Gender specific effects in vivo on blood glucose with and without Ang-(1-7) administration	210
Figure 10.3.8 Effect of Ang-(1-7) administration in vivo on organ weights of female and male mice	211
Figure 11.4.1 Example for genotyping PCR.....	231
Figure 11.4.2 Light emission from firefly and Renilla luciferase.....	236
Figure 11.5.1 Application of the semi dry blot.....	240
Figure 11.5.2 Luminol reaction	241
Figure 11.5.3 cAMP assay	243

16 Tables

Table 11.1 Cell lines.....	220
Table 11.2 Cell culture media.....	221
Table 11.3 Transfection mix.....	223
Table 11.4 Reaction mix for Genotype PCR	229
Table 11.5 PCR conditions.....	230
Table 11.6 cDNA synthesis mix	233
Table 11.7 qPCR reaction mix	234
Table 11.8 Acrylamide gel composition	239

17 Literature

1. L.T. Skeggs, Jr., W.H. Marsh, J.R. Kahn, and N.P. Shumway, *The purification of hypertensin I*. J Exp Med, 1954. **100**(4): p. 363.
2. L.T. Skeggs, Jr., W.H. Marsh, J.R. Kahn, and N.P. Shumway, *The existence of two forms of hypertensin*. J Exp Med, 1954. **99**(3): p. 275.
3. M. Paul, A. Poyan Mehr, and R. Kreutz, *Physiology of local renin-angiotensin systems*. Physiol Rev, 2006. **86**(3): p. 747.
4. H. Castrop, K. Hocherl, A. Kurtz, F. Schweda, V. Todorov, and C. Wagner, *Physiology of kidney renin*. Physiol Rev, 2010. **90**(2): p. 607.
5. E. Hackenthal, M. Paul, D. Ganten, and R. Taugner, *Morphology, physiology, and molecular biology of renin secretion*. Physiol Rev, 1990. **70**(4): p. 1067.
6. L.M. Harrison-Bernard, *The renal renin-angiotensin system*. Adv Physiol Educ, 2009. **33**(4): p. 270.
7. B.I. Levy, *Can angiotensin II type 2 receptors have deleterious effects in cardiovascular disease? Implications for therapeutic blockade of the renin-angiotensin system*. Circulation, 2004. **109**(1): p. 8.
8. T. Unger, *Björn Fokow Award Lecture The angiotensin type 2 receptor: variations on an enigmatic theme*. Journal of Hypertension, 1999. **17**(12): p. 1775.
9. S.Y. Oppong and N.M. Hooper, *Characterization of a secretase activity which releases angiotensin-converting enzyme from the membrane*. Biochem J, 1993. **292 (Pt 2)**: p. 597.
10. A.J. Turner and N.M. Hooper, *The angiotensin-converting enzyme gene family: genomics and pharmacology*. Trends Pharmacol Sci, 2002. **23**(4): p. 177.

11. P. Corvol, T.A. Williams, and F. Soubrier, *Peptidyl dipeptidase A: angiotensin I-converting enzyme*. Methods Enzymol, 1995. **248**: p. 283.
12. P.M. Finnegan and B.L. Gleason, *Combination ACE Inhibitors and Angiotensin II Receptor Blockers for Hypertension*. Annals of Pharmacotherapy, 2003. **37**(6): p. 886.
13. N.K. Hollenberg and G.H. Williams, *Angiotensin as a renal, adrenal, and cardiovascular hormone: responses to saralasin in normal man and in essential and secondary hypertension*. Kidney Int Suppl, 1979(9): p. S29.
14. M. de Gasparo, K.J. Catt, T. Inagami, J.W. Wright, and T. Unger, *International union of pharmacology. XXIII. The angiotensin II receptors*. Pharmacol Rev, 2000. **52**(3): p. 415.
15. T. Unger, *The angiotensin type 2 receptor: variations on an enigmatic theme*. J Hypertens, 1999. **17**(12 Pt 2): p. 1775.
16. P.K. Mehta and K.K. Griendling, *Angiotensin II cell signaling: physiological and pathological effects in the cardiovascular system*. Am J Physiol Cell Physiol, 2007. **292**(1): p. C82.
17. T. Yamamoto, K. Hayashi, H. Matsuda, E. Kubota, H. Tanaka, Y. Ogasawara, H. Nakamoto, H. Suzuki, T. Saruta, and F. Kajiya, *In vivo visualization of angiotensin II- and tubuloglomerular feedback-mediated renal vasoconstriction*. Kidney Int, 2001. **60**(1): p. 364.
18. A. Ichihara, H. Kobori, A. Nishiyama, and L.G. Navar, *Renal Renin-Angiotensin System*. Contributions to nephrology, 2004. **143**: p. 117.
19. A. Benigni, P. Cassis, and G. Remuzzi, *Angiotensin II revisited: new roles in inflammation, immunology and aging*. EMBO Mol Med, 2010. **2**(7): p. 247.

20. R.E. Widdop, E.S. Jones, R.E. Hannan, and T.A. Gaspari, *Angiotensin AT₂ receptors: cardiovascular hope or hype?* Br J Pharmacol, 2003. **140**(5): p. 809.
21. R. Tigerstedt and P.Q. Bergman, *Niere und Kreislauf*. Skandinavisches Archiv F r Physiologie, 1898. **8**(1): p. 223.
22. J.L. Lavoie and C.D. Sigmund, *Minireview: overview of the renin-angiotensin system--an endocrine and paracrine system*. Endocrinology, 2003. **144**(6): p. 2179.
23. D.J. Campbell, *Clinical relevance of local Renin Angiotensin systems*. Front Endocrinol (Lausanne), 2014. **5**: p. 113.
24. V.J. Dzau and R. Re, *Tissue angiotensin system in cardiovascular medicine. A paradigm shift?* Circulation, 1994. **89**(1): p. 493.
25. L.J. Field, R.A. McGowan, D.P. Dickinson, and K.W. Gross, *Tissue and gene specificity of mouse renin expression*. Hypertension, 1984. **6**(4): p. 597.
26. P. Corvol, A. Michaud, F. Soubrier, and T.A. Williams, *Recent advances in knowledge of the structure and function of the angiotensin I converting enzyme*. J Hypertens Suppl, 1995. **13**(3): p. S3.
27. M. Kawamura, M. Nakamaru, and T. Inagami, *Evidence for existence of angiotensins I and II in mature renin granules from rat kidney cortex*. Biochem Biophys Res Commun, 1985. **131**(2): p. 628.
28. M.R. Celio and T. Inagami, *Angiotensin II immunoreactivity coexists with renin in the juxtaglomerular granular cells of the kidney*. Proc Natl Acad Sci U S A, 1981. **78**(6): p. 3897.
29. J.D. Swales, *Arterial wall or plasma renin in hypertension?* Clin Sci (Lond), 1979. **56**(4): p. 293.

30. J.D. Swales, A. Abramovici, F. Beck, R.F. Bing, M. Loudon, and H. Thurston, *Arterial wall renin*. J Hypertens Suppl, 1983. **1**(1): p. 17.
31. G. Aguilera, A. Schirar, A. Baukal, and K.J. Catt, *Circulating angiotensin II and adrenal receptors after nephrectomy*. Nature, 1981. **289**(5797): p. 507.
32. D. Ganten, K. Hermann, T. Unger, and R.E. Lang, *The tissue renin-angiotensin systems: focus on brain angiotensin, adrenal gland and arterial wall*. Clin Exp Hypertens A, 1983. **5**(7-8): p. 1099.
33. T. Okamura, D.L. Clemens, and T. Inagami, *Generation of angiotensins in cultured pheochromocytoma cells*. Neurosci Lett, 1984. **46**(2): p. 151.
34. D. Ganten, K. Hermann, C. Bayer, T. Unger, and R.E. Lang, *Angiotensin synthesis in the brain and increased turnover in hypertensive rats*. Science, 1983. **221**(4613): p. 869.
35. T. Inagami, *Renin in the brain and neuroblastoma cells: an endogenous and intracellular system*. Neuroendocrinology, 1982. **35**(6): p. 475.
36. K.N. Pandey, K.S. Misono, and T. Inagami, *Evidence for intracellular formation of angiotensins: coexistence of renin and angiotensin-converting enzyme in Leydig cells of rat testis*. Biochem Biophys Res Commun, 1984. **122**(3): p. 1337.
37. F. Fyhrquist and O. Saijonmaa, *Renin-angiotensin system revisited*. J Intern Med, 2008. **264**(3): p. 224.
38. K. Kramkowski, A. Mogielnicki, and W. Buczko, *The physiological significance of the alternative pathways of angiotensin II production*. J Physiol Pharmacol, 2006. **57**(4): p. 529.
39. M. Ohishi, K. Yamamoto, and H. Rakugi, *Angiotensin (1-7) and other angiotensin peptides*. Curr Pharm Des, 2013. **19**(17): p. 3060.

-
40. V. Jankowski, R. Vanholder, M. van der Giet, M. Tolle, S. Karadogan, J. Gobom, J. Furkert, A. Oksche, E. Krause, T.N. Tran, M. Tepel, M. Schuchardt, H. Schluter, A. Wiedon, M. Beyermann, M. Bader, M. Todiras, W. Zidek, and J. Jankowski, *Mass-spectrometric identification of a novel angiotensin peptide in human plasma*. *Arterioscler Thromb Vasc Biol*, 2007. **27**(2): p. 297.
41. D.C. Coutinho, G. Foureaux, K.D. Rodrigues, R.L. Salles, P.L. Moraes, T.M. Murca, M.L. De Maria, E.R. Gomes, R.A. Santos, S. Guatimosim, and A.J. Ferreira, *Cardiovascular effects of angiotensin A: a novel peptide of the renin-angiotensin system*. *J Renin Angiotensin Aldosterone Syst*, 2014. **15**(4): p. 480.
42. R.Q. Lautner, D.C. Villela, R.A. Fraga-Silva, N. Silva, T. Verano-Braga, F. Costa-Fraga, J. Jankowski, V. Jankowski, F. Sousa, A. Alzamora, E. Soares, C. Barbosa, F. Kjeldsen, A. Oliveira, J. Braga, S. Savergnini, G. Maia, A.B. Peluso, D. Passos-Silva, A. Ferreira, F. Alves, A. Martins, M. Raizada, R. Paula, D. Motta-Santos, F. Klempin, A. Pimenta, N. Alenina, R. Sinisterra, M. Bader, M.J. Campagnole-Santos, and R.A. Santos, *Discovery and characterization of alamandine: a novel component of the renin-angiotensin system*. *Circ Res*, 2013. **112**(8): p. 1104.
43. I. Haulica, W. Bild, and D.N. Serban, *Angiotensin peptides and their pleiotropic actions*. *J Renin Angiotensin Aldosterone Syst*, 2005. **6**(3): p. 121.
44. V.G. Yugandhar and M.A. Clark, *Angiotensin III: a physiological relevant peptide of the renin angiotensin system*. *Peptides*, 2013. **46**: p. 26.
45. S.Y. Chai, R. Fernando, G. Peck, S.Y. Ye, F.A. Mendelsohn, T.A. Jenkins, and A.L. Albiston, *The angiotensin IV/AT4 receptor*. *Cell Mol Life Sci*, 2004. **61**(21): p. 2728.

-
46. M.F. Sardinia, J.M. Hanesworth, F. Krishnan, and J.W. Harding, *AT4 receptor structure-binding relationship: N-terminal-modified angiotensin IV analogues*. Peptides, 1994. **15**(8): p. 1399.
47. J.D. Swindle, K.L. Santos, and R.C. Speth, *Pharmacological characterization of a novel non-AT1, non-AT2 angiotensin binding site identified as neurolysin*. Endocrine, 2013. **44**(2): p. 525.
48. A.J. Ferreira, R.A. Santos, and M.K. Raizada, *Angiotensin-(1-7)/angiotensin-converting enzyme 2/mas receptor axis and related mechanisms*. Int J Hypertens, 2012. **2012**: p. 690785.
49. R.A. Santos, A.J. Ferreira, T. Verano-Braga, and M. Bader, *Angiotensin-converting enzyme 2, angiotensin-(1-7) and Mas: new players of the renin-angiotensin system*. J Endocrinol, 2013. **216**(2): p. R1.
50. A. Nguyen Dinh Cat and R.M. Touyz, *A new look at the renin-angiotensin system--focusing on the vascular system*. Peptides, 2011. **32**(10): p. 2141.
51. E. Kostenis, G. Milligan, A. Christopoulos, C.F. Sanchez-Ferrer, S. Heringer-Walther, P.M. Sexton, F. Gembardt, E. Kellett, L. Martini, P. Vanderheyden, H.P. Schultheiss, and T. Walther, *G-protein-coupled receptor Mas is a physiological antagonist of the angiotensin II type 1 receptor*. Circulation, 2005. **111**(14): p. 1806.
52. S.R. Tipnis, N.M. Hooper, R. Hyde, E. Karran, G. Christie, and A.J. Turner, *A human homolog of angiotensin-converting enzyme. Cloning and functional expression as a captopril-insensitive carboxypeptidase*. J Biol Chem, 2000. **275**(43): p. 33238.
53. M. Donoghue, F. Hsieh, E. Baronas, K. Godbout, M. Gosselin, N. Stagliano, M. Donovan, B. Woolf, K. Robison, R. Jeyaseelan, R.E. Breitbart, and S. Acton, *A novel*

- angiotensin-converting enzyme-related carboxypeptidase (ACE2) converts angiotensin I to angiotensin 1-9*. Circ Res, 2000. **87**(5): p. E1.
54. D. Harmer, M. Gilbert, R. Borman, and K.L. Clark, *Quantitative mRNA expression profiling of ACE 2, a novel homologue of angiotensin converting enzyme*. FEBS Lett, 2002. **532**(1-2): p. 107.
55. J.L. Guy, D.W. Lambert, F.J. Warner, N.M. Hooper, and A.J. Turner, *Membrane-associated zinc peptidase families: comparing ACE and ACE2*. Biochim Biophys Acta, 2005. **1751**(1): p. 2.
56. Z.W. Lai, I. Hanchapola, D.L. Steer, and A.I. Smith, *Angiotensin-converting enzyme 2 ectodomain shedding cleavage-site identification: determinants and constraints*. Biochemistry, 2011. **50**(23): p. 5182.
57. J.L. Guy, R.M. Jackson, K.R. Acharya, E.D. Sturrock, N.M. Hooper, and A.J. Turner, *Angiotensin-converting enzyme-2 (ACE2): comparative modeling of the active site, specificity requirements, and chloride dependence*. Biochemistry, 2003. **42**(45): p. 13185.
58. C. Vickers, P. Hales, V. Kaushik, L. Dick, J. Gavin, J. Tang, K. Godbout, T. Parsons, E. Baronas, F. Hsieh, S. Acton, M. Patane, A. Nichols, and P. Tummino, *Hydrolysis of biological peptides by human angiotensin-converting enzyme-related carboxypeptidase*. J Biol Chem, 2002. **277**(17): p. 14838.
59. M.T. Schiavone, R.A. Santos, K.B. Brosnihan, M.C. Khosla, and C.M. Ferrario, *Release of vasopressin from the rat hypothalamo-neurohypophyseal system by angiotensin-(1-7) heptapeptide*. Proc Natl Acad Sci U S A, 1988. **85**(11): p. 4095.

-
60. C.M. Ferrario, K.B. Brosnihan, D.I. Diz, N. Jaiswal, M.C. Khosla, A. Milsted, and E.A. Tallant, *Angiotensin-(1-7): a new hormone of the angiotensin system*. Hypertension, 1991. **18**(5 Suppl): p. lii126.
61. T.R. Jackson, L.A. Blair, J. Marshall, M. Goedert, and M.R. Hanley, *The mas oncogene encodes an angiotensin receptor*. Nature, 1988. **335**(6189): p. 437.
62. R.A. Santos, A.C. Simoes e Silva, C. Maric, D.M. Silva, R.P. Machado, I. de Buhr, S. Heringer-Walther, S.V. Pinheiro, M.T. Lopes, M. Bader, E.P. Mendes, V.S. Lemos, M.J. Campagnole-Santos, H.P. Schultheiss, R. Speth, and T. Walther, *Angiotensin-(1-7) is an endogenous ligand for the G protein-coupled receptor Mas*. Proc Natl Acad Sci U S A, 2003. **100**(14): p. 8258.
63. M.M. Gironacci, M.P. Coba, and C. Pena, *Angiotensin-(1-7) binds at the type 1 angiotensin II receptors in rat renal cortex*. Regul Pept, 1999. **84**(1-3): p. 51.
64. S. Bosnyak, E.S. Jones, A. Christopoulos, M.I. Aguilar, W.G. Thomas, and R.E. Widdop, *Relative affinity of angiotensin peptides and novel ligands at AT1 and AT2 receptors*. Clin Sci (Lond), 2011. **121**(7): p. 297.
65. F. Gembardt, S. Grajewski, M. Vahl, H.P. Schultheiss, and T. Walther, *Angiotensin metabolites can stimulate receptors of the Mas-related genes family*. Mol Cell Biochem, 2008. **319**(1-2): p. 115.
66. C.M. Ferrario and M.C. Chappell, *Novel angiotensin peptides*. Cell Mol Life Sci, 2004. **61**(21): p. 2720.
67. A.F. Almeida-Santos, L.M. Kangussu, and M.J. Campagnole-Santos, *The Renin-Angiotensin System and the Neurodegenerative Diseases: A Brief Review*. Protein Pept Lett, 2017. **24**(9): p. 841.

-
68. P.R. Gard, S. Fidalgo, I. Lotter, C. Richardson, N. Farina, J. Rusted, and N. Tabet, *Changes of renin-angiotensin system-related aminopeptidases in early stage Alzheimer's disease*. Exp Gerontol, 2017. **89**: p. 1.
69. S. Perez-Lloret, M. Otero-Losada, J.E. Toblli, and F. Capani, *Renin-angiotensin system as a potential target for new therapeutic approaches in Parkinson's disease*. Expert Opin Investig Drugs, 2017. **26**(10): p. 1163.
70. D. Atanasova, J. Tchekalarova, N. Ivanova, Z. Nenchovska, E. Pavlova, N. Atanassova, and N. Lazarov, *Losartan suppresses the kainate-induced changes of angiotensin AT1 receptor expression in a model of comorbid hypertension and epilepsy*. Life Sci, 2018. **193**: p. 40.
71. A.S. Khudaverdiev, *[Angiotensin III participation in mechanisms of development of an alcoholism and other kinds of behavioural activity]*. Georgian Med News, 2008(164): p. 83.
72. M. Guivernau and J. Pallavicini, *[Effect of angiotensin II synthesis inhibition on alcohol consumption]*. Rev Med Chil, 2008. **136**(8): p. 968.
73. J.F. Giani, M.A. Mayer, M.C. Munoz, E.A. Silberman, C. Hocht, C.A. Taira, M.M. Gironacci, D. Turyn, and F.P. Dominici, *Chronic infusion of angiotensin-(1-7) improves insulin resistance and hypertension induced by a high-fructose diet in rats*. Am J Physiol Endocrinol Metab, 2009. **296**(2): p. E262.
74. P.R. Gard, *The role of angiotensin II in cognition and behaviour*. Eur J Pharmacol, 2002. **438**(1-2): p. 1.
75. U. Danilczyk, U. Eriksson, G.Y. Oudit, and J.M. Penninger, *Physiological roles of angiotensin-converting enzyme 2*. Cell Mol Life Sci, 2004. **61**(21): p. 2714.

-
76. J. Zhang, N.A. Noble, W.A. Border, and Y. Huang, *Infusion of angiotensin-(1-7) reduces glomerulosclerosis through counteracting angiotensin II in experimental glomerulonephritis*. Am J Physiol Renal Physiol, 2010. **298**(3): p. F579.
77. K.D. Silveira, L.C. Barroso, A.T. Vieira, D. Cisalpino, C.X. Lima, M. Bader, R.M. Arantes, R.A. Dos Santos, E.S.A.C. Simoes, and M.M. Teixeira, *Beneficial effects of the activation of the angiotensin-(1-7) MAS receptor in a murine model of adriamycin-induced nephropathy*. PLoS One, 2013. **8**(6): p. e66082.
78. J. Mori, V.B. Patel, T. Ramprasath, O.A. Alrob, J. DesAulniers, J.W. Scholey, G.D. Lopaschuk, and G.Y. Oudit, *Angiotensin 1-7 mediates renoprotection against diabetic nephropathy by reducing oxidative stress, inflammation, and lipotoxicity*. Am J Physiol Renal Physiol, 2014. **306**(8): p. F812.
79. S. Andreatta-van Leyen, M.F. Romero, M.C. Khosla, and J.G. Douglas, *Modulation of phospholipase A2 activity and sodium transport by angiotensin-(1-7)*. Kidney Int, 1993. **44**(5): p. 932.
80. Y. Shao, M. He, L. Zhou, T. Yao, Y. Huang, and L.M. Lu, *Chronic angiotensin (1-7) injection accelerates STZ-induced diabetic renal injury*. Acta Pharmacol Sin, 2008. **29**(7): p. 829.
81. V. Esteban, S. Heringer-Walther, A. Sterner-Kock, R. de Bruin, S. van den Engel, Y. Wang, S. Mezzano, J. Egido, H.P. Schultheiss, M. Ruiz-Ortega, and T. Walther, *Angiotensin-(1-7) and the G Protein-Coupled Receptor Mas Are Key Players in Renal Inflammation*. PLoS One, 2009. **4**(4).
82. Z. Su, J. Zimpelmann, and K.D. Burns, *Angiotensin-(1-7) inhibits angiotensin II-stimulated phosphorylation of MAP kinases in proximal tubular cells*. Kidney Int, 2006. **69**(12): p. 2212.
-

-
83. J.Y. Moon, M. Tanimoto, T. Gohda, S. Hagiwara, T. Yamazaki, I. Ohara, M. Murakoshi, T. Aoki, Y. Ishikawa, S.H. Lee, K.H. Jeong, T.W. Lee, C.G. Ihm, S.J. Lim, and Y. Tomino, *Attenuating effect of angiotensin-(1-7) on angiotensin II-mediated NAD(P)H oxidase activation in type 2 diabetic nephropathy of KK-A(y)/Ta mice*. *Am J Physiol Renal Physiol*, 2011. **300**(6): p. F1271.
84. J. Zimpelmann and K.D. Burns, *Angiotensin-(1-7) activates growth-stimulatory pathways in human mesangial cells*. *Am J Physiol Renal Physiol*, 2009. **296**(2): p. F337.
85. Z. Liu, X.R. Huang, H.Y. Chen, J.M. Penninger, and H.Y. Lan, *Loss of angiotensin-converting enzyme 2 enhances TGF-beta/Smad-mediated renal fibrosis and NF-kappaB-driven renal inflammation in a mouse model of obstructive nephropathy*. *Lab Invest*, 2012. **92**(5): p. 650.
86. G.Y. Oudit, G.C. Liu, J. Zhong, R. Basu, F.L. Chow, J. Zhou, H. Loibner, E. Janzek, M. Schuster, J.M. Penninger, A.M. Herzenberg, Z. Kassiri, and J.W. Scholey, *Human recombinant ACE2 reduces the progression of diabetic nephropathy*. *Diabetes*, 2010. **59**(2): p. 529.
87. S.V. Pinheiro, A.J. Ferreira, G.T. Kitten, K.D. da Silveira, D.A. da Silva, S.H. Santos, E. Gava, C.H. Castro, J.A. Magalhaes, R.K. da Mota, G.A. Botelho-Santos, M. Bader, N. Alenina, R.A. Santos, and A.C. Simoes e Silva, *Genetic deletion of the angiotensin-(1-7) receptor Mas leads to glomerular hyperfiltration and microalbuminuria*. *Kidney Int*, 2009. **75**(11): p. 1184.
88. R.A. Santos, J.M. Brum, K.B. Brosnihan, and C.M. Ferrario, *The renin-angiotensin system during acute myocardial ischemia in dogs*. *Hypertension*, 1990. **15**(2 Suppl): p. I121.
-

-
89. A. Mahmood, H.L. Jackman, L. Teplitz, and R. Igic, *Metabolism of angiotensin I in the coronary circulation of normal and diabetic rats*. Peptides, 2002. **23**(6): p. 1171.
90. A.J. Ferreira, R.A. Santos, and A.P. Almeida, *Angiotensin-(1-7) improves the post-ischemic function in isolated perfused rat hearts*. Braz J Med Biol Res, 2002. **35**(9): p. 1083.
91. Y.Y. Lu, W.S. Wu, Y.K. Lin, C.C. Cheng, Y.C. Chen, S.A. Chen, and Y.J. Chen, *Angiotensin 1-7 modulates electrophysiological characteristics and calcium homoeostasis in pulmonary veins cardiomyocytes via MAS/PI3K/eNOS signalling pathway*. Eur J Clin Invest, 2018. **48**(1).
92. P. Pachauri, D. Garabadu, A. Goyal, and P.K. Upadhyay, *Angiotensin (1-7) facilitates cardioprotection of ischemic preconditioning on ischemia-reperfusion-challenged rat heart*. Mol Cell Biochem, 2017. **430**(1-2): p. 99.
93. J. Wang, W. He, L. Guo, Y. Zhang, H. Li, S. Han, and D. Shen, *The ACE2-Ang (1-7)-Mas receptor axis attenuates cardiac remodeling and fibrosis in post-myocardial infarction*. Mol Med Rep, 2017. **16**(2): p. 1973.
94. A.E. Loot, A.J. Roks, R.H. Henning, R.A. Tio, A.J. Suurmeijer, F. Boomsma, and W.H. van Gilst, *Angiotensin-(1-7) attenuates the development of heart failure after myocardial infarction in rats*. Circulation, 2002. **105**(13): p. 1548.
95. J.F. Giani, M.C. Munoz, M.A. Mayer, L.C. Veiras, C. Arranz, C.A. Taira, D. Turyn, J.E. Toblli, and F.P. Dominici, *Angiotensin-(1-7) improves cardiac remodeling and inhibits growth-promoting pathways in the heart of fructose-fed rats*. Am J Physiol Heart Circ Physiol, 2010. **298**(3): p. H1003.
-

-
96. L.T. McCollum, P.E. Gallagher, and E. Ann Tallant, *Angiotensin-(1-7) attenuates angiotensin II-induced cardiac remodeling associated with upregulation of dual-specificity phosphatase 1*. Am J Physiol Heart Circ Physiol, 2012. **302**(3): p. H801.
97. J.L. Grobe, A.P. Mecca, M. Lingis, V. Shenoy, T.A. Bolton, J.M. Machado, R.C. Speth, M.K. Raizada, and M.J. Katovich, *Prevention of angiotensin II-induced cardiac remodeling by angiotensin-(1-7)*. Am J Physiol Heart Circ Physiol, 2007. **292**(2): p. H736.
98. A. Shah, Y.B. Oh, S.H. Lee, J.M. Lim, and S.H. Kim, *Angiotensin-(1-7) attenuates hypertension in exercise-trained renal hypertensive rats*. Am J Physiol Heart Circ Physiol, 2012. **302**(11): p. H2372.
99. R.A. Santos, C.H. Castro, E. Gava, S.V. Pinheiro, A.P. Almeida, R.D. Paula, J.S. Cruz, A.S. Ramos, K.T. Rosa, M.C. Irigoyen, M. Bader, N. Alenina, G.T. Kitten, and A.J. Ferreira, *Impairment of in vitro and in vivo heart function in angiotensin-(1-7) receptor MAS knockout mice*. Hypertension, 2006. **47**(5): p. 996.
100. E. Gava, C.H. de Castro, A.J. Ferreira, H. Colleta, M.B. Melo, N. Alenina, M. Bader, L.A. Oliveira, R.A. Santos, and G.T. Kitten, *Angiotensin-(1-7) receptor Mas is an essential modulator of extracellular matrix protein expression in the heart*. Regul Pept, 2012. **175**(1-3): p. 30.
101. T. Walther, N. Wessel, N. Kang, A. Sander, C. Tschope, H. Malberg, M. Bader, and A. Voss, *Altered heart rate and blood pressure variability in mice lacking the Mas protooncogene*. Braz J Med Biol Res, 2000. **33**(1): p. 1.
102. K.B. Brosnihan, P. Li, and C.M. Ferrario, *Angiotensin-(1-7) dilates canine coronary arteries through kinins and nitric oxide*. Hypertension, 1996. **27**(3 Pt 2): p. 523.

-
103. R.A. Santos, K.B. Brosnihan, D.W. Jacobsen, P.E. DiCorleto, and C.M. Ferrario, *Production of angiotensin-(1-7) by human vascular endothelium*. Hypertension, 1992. **19**(2 Suppl): p. li56.
104. P. Li, M.C. Chappell, C.M. Ferrario, and K.B. Brosnihan, *Angiotensin-(1-7) augments bradykinin-induced vasodilation by competing with ACE and releasing nitric oxide*. Hypertension, 1997. **29**(1 Pt 2): p. 394.
105. H. Heitsch, S. Brovkovich, T. Malinski, and G. Wiemer, *Angiotensin-(1-7)-Stimulated Nitric Oxide and Superoxide Release From Endothelial Cells*. Hypertension, 2001. **37**(1): p. 72.
106. S.N. Iyer, K. Yamada, D.I. Diz, C.M. Ferrario, and M.C. Chappell, *Evidence that prostaglandins mediate the antihypertensive actions of angiotensin-(1-7) during chronic blockade of the renin-angiotensin system*. J Cardiovasc Pharmacol, 2000. **36**(1): p. 109.
107. X. Xiao, C. Zhang, X. Ma, H. Miao, J. Wang, L. Liu, S. Chen, R. Zeng, Y. Chen, and J.C. Bihl, *Angiotensin-(1-7) counteracts angiotensin II-induced dysfunction in cerebral endothelial cells via modulating Nox2/ROS and PI3K/NO pathways*. Exp Cell Res, 2015. **336**(1): p. 58.
108. P.L. de Moraes, L.M. Kangussu, C.H. Castro, A.P. Almeida, R.A.S. Santos, and A.J. Ferreira, *Vasodilator Effect of Angiotensin-(1-7) on Vascular Coronary Bed of Rats: Role of Mas, ACE and ACE2*. Protein Pept Lett, 2017. **24**(9): p. 869.
109. C. Peiro, S. Vallejo, F. Gembardt, E. Palacios, S. Novella, V. Azcutia, L. Rodriguez-Manas, C. Hermenegildo, C.F. Sanchez-Ferrer, and T. Walther, *Complete blockade of the vasorelaxant effects of angiotensin-(1-7) and bradykinin in murine microvessels by antagonists of the receptor Mas*. J Physiol, 2013. **591**(9): p. 2275.

-
110. K.B. Brosnihan, P. Li, D. Ganten, and C.M. Ferrario, *Estrogen protects transgenic hypertensive rats by shifting the vasoconstrictor-vasodilator balance of RAS*. Am J Physiol, 1997. **273**(6 Pt 2): p. R1908.
111. M.J. Durand, G. Raffai, B.D. Weinberg, and J.H. Lombard, *Angiotensin-(1-7) and low-dose angiotensin II infusion reverse salt-induced endothelial dysfunction via different mechanisms in rat middle cerebral arteries*. Am J Physiol Heart Circ Physiol, 2010. **299**(4): p. H1024.
112. C. Peiro, S. Vallejo, F. Gembardt, V. Azcutia, S. Heringer-Walther, L. Rodriguez-Manas, H.P. Schultheiss, C.F. Sanchez-Ferrer, and T. Walther, *Endothelial dysfunction through genetic deletion or inhibition of the G protein-coupled receptor Mas: a new target to improve endothelial function*. J Hypertens, 2007. **25**(12): p. 2421.
113. C. Peiró, S. Vallejo, F. Gembardt, E. Palacios, S. Novella, V. Azcutia, L. Rodríguez-Mañas, C. Hermenegildo, C.F. Sánchez-Ferrer, and T. Walther, *Complete blockade of the vasorelaxant effects of angiotensin-(1–7) and bradykinin in murine microvessels by antagonists of the receptor Mas*. The Journal of Physiology, 2013. **591**(Pt 9): p. 2275.
114. P. Xu, A.C. Costa-Goncalves, M. Todiras, L.A. Rabelo, W.O. Sampaio, M.M. Moura, S.S. Santos, F.C. Luft, M. Bader, V. Gross, N. Alenina, and R.A. Santos, *Endothelial dysfunction and elevated blood pressure in MAS gene-deleted mice*. Hypertension, 2008. **51**(2): p. 574.
115. L.A. Rabelo, P. Xu, M. Todiras, W.O. Sampaio, J. Buttgereit, M. Bader, R.A. Santos, and N. Alenina, *Ablation of angiotensin (1-7) receptor Mas in C57Bl/6 mice causes endothelial dysfunction*. J Am Soc Hypertens, 2008. **2**(6): p. 418.
-

-
116. K. Hellner, T. Walther, M. Schubert, and D. Albrecht, *Angiotensin-(1-7) enhances LTP in the hippocampus through the G-protein-coupled receptor Mas*. Mol Cell Neurosci, 2005. **29**(3): p. 427.
117. J. Staschewski, C. Kulisch, and D. Albrecht, *Different isoforms of nitric oxide synthase are involved in angiotensin-(1-7)-mediated plasticity changes in the amygdala in a gender-dependent manner*. Neuroendocrinology, 2011. **94**(3): p. 191.
118. T.L. Lazaroni, A.C. Raslan, W.R. Fontes, M.L. de Oliveira, M. Bader, N. Alenina, M.F. Moraes, R.A. Dos Santos, and G.S. Pereira, *Angiotensin-(1-7)/Mas axis integrity is required for the expression of object recognition memory*. Neurobiol Learn Mem, 2012. **97**(1): p. 113.
119. D.M. Bennion, E.A. Haltigan, A.J. Irwin, L.L. Donnangelo, R.W. Regenhardt, D.J. Pioquinto, D.L. Purich, and C. Sumners, *Activation of the Neuroprotective Angiotensin-Converting Enzyme 2 in Rat Ischemic Stroke*. Hypertension, 2015. **66**(1): p. 141.
120. T. Walther, D. Balschun, J.P. Voigt, H. Fink, W. Zuschratter, C. Birchmeier, D. Ganten, and M. Bader, *Sustained long term potentiation and anxiety in mice lacking the Mas protooncogene*. J Biol Chem, 1998. **273**(19): p. 11867.
121. B.H. Jones, M.K. Standridge, and N. Moustaid, *Angiotensin II increases lipogenesis in 3T3-L1 and human adipose cells*. Endocrinology, 1997. **138**(4): p. 1512.
122. M.S. Coelho, K.L. Lopes, A. Freitas Rde, E.B. de Oliveira-Sales, C.T. Bergasmaschi, R.R. Campos, D.E. Casarini, A.K. Carmona, S. Araujo Mda, J.C. Heimann, and M.S. Dolnikoff, *High sucrose intake in rats is associated with increased ACE2 and angiotensin-(1-7) levels in the adipose tissue*. Regul Pept, 2010. **162**(1-3): p. 61.

-
123. Y. Marcus, G. Shefer, K. Sasson, F. Kohen, R. Limor, O. Pappo, N. Nevo, I. Biton, M. Bach, T. Berkutzki, M. Fridkin, D. Benayahu, Y. Shechter, and N. Stern, *Angiotensin 1-7 as means to prevent the metabolic syndrome: lessons from the fructose-fed rat model*. *Diabetes*, 2013. **62**(4): p. 1121.
124. S.H. Santos, J.M. Andrade, L.R. Fernandes, R.D. Sinisterra, F.B. Sousa, J.D. Feltenberger, J.I. Alvarez-Leite, and R.A. Santos, *Oral Angiotensin-(1-7) prevented obesity and hepatic inflammation by inhibition of resistin/TLR4/MAPK/NF-kappaB in rats fed with high-fat diet*. *Peptides*, 2013. **46**: p. 47.
125. S.H. Santos, J.F. Braga, E.G. Mario, L.C. Porto, G. Rodrigues-Machado Mda, A. Murari, L.M. Botion, N. Alenina, M. Bader, and R.A. Santos, *Improved lipid and glucose metabolism in transgenic rats with increased circulating angiotensin-(1-7)*. *Arterioscler Thromb Vasc Biol*, 2010. **30**(5): p. 953.
126. S.H. Santos, L.R. Fernandes, E.G. Mario, A.V. Ferreira, L.C. Porto, J.I. Alvarez-Leite, L.M. Botion, M. Bader, N. Alenina, and R.A. Santos, *Mas deficiency in FVB/N mice produces marked changes in lipid and glycemic metabolism*. *Diabetes*, 2008. **57**(2): p. 340.
127. E.G. Mario, S.H. Santos, A.V. Ferreira, M. Bader, R.A. Santos, and L.M. Botion, *Angiotensin-(1-7) Mas-receptor deficiency decreases peroxisome proliferator-activated receptor gamma expression in adipocytes*. *Peptides*, 2012. **33**(1): p. 174.
128. V. Sukumaran, P.T. Veeraveedu, N. Gurusamy, K. Yamaguchi, A.P. Lakshmanan, M. Ma, K. Suzuki, M. Kodama, and K. Watanabe, *Cardioprotective effects of telmisartan against heart failure in rats induced by experimental autoimmune myocarditis through the modulation of angiotensin-converting enzyme-2/angiotensin 1-7/mas receptor axis*. *Int J Biol Sci*, 2011. **7**(8): p. 1077.
-

-
129. V. Sukumaran, P.T. Veeraveedu, N. Gurusamy, A.P. Lakshmanan, K. Yamaguchi, M. Ma, K. Suzuki, M. Kodama, and K. Watanabe, *Telmisartan acts through the modulation of ACE-2/ANG 1-7/mas receptor in rats with dilated cardiomyopathy induced by experimental autoimmune myocarditis*. Life Sci, 2012. **90**(7-8): p. 289.
130. L.A. Villalobos, A. San Hipolito-Luengo, M. Ramos-Gonzalez, E. Cercas, S. Vallejo, A. Romero, T. Romacho, R. Carraro, C.F. Sanchez-Ferrer, and C. Peiro, *The Angiotensin-(1-7)/Mas Axis Counteracts Angiotensin II-Dependent and -Independent Pro-inflammatory Signaling in Human Vascular Smooth Muscle Cells*. Front Pharmacol, 2016. **7**: p. 482.
131. V. Esteban, S. Heringer-Walther, A. Sterner-Kock, R. de Bruin, S. van den Engel, Y. Wang, S. Mezzano, J. Egido, H.P. Schultheiss, M. Ruiz-Ortega, and T. Walther, *Angiotensin-(1-7) and the g protein-coupled receptor MAS are key players in renal inflammation*. PLoS One, 2009. **4**(4): p. e5406.
132. A. Hammer, G. Yang, J. Friedrich, A. Kovacs, D.-H. Lee, K. Grave, S. Jörg, N. Alenina, J. Grosch, J. Winkler, R. Gold, M. Bader, A. Manzel, L.C. Rump, D.N. Müller, R.A. Linker, and J. Stegbauer, *Role of the receptor Mas in macrophage-mediated inflammation in vivo*. Proceedings of the National Academy of Sciences of the United States of America, 2016. **113**(49): p. 14109.
133. E.A. Tallant and M.A. Clark, *Molecular mechanisms of inhibition of vascular growth by angiotensin-(1-7)*. Hypertension, 2003. **42**(4): p. 574.
134. E.A. Tallant, C.M. Ferrario, and P.E. Gallagher, *Angiotensin-(1-7) inhibits growth of cardiac myocytes through activation of the mas receptor*. Am J Physiol Heart Circ Physiol, 2005. **289**(4): p. H1560.

-
135. R.M. Pereira, R.A. Dos Santos, M.M. Teixeira, V.H. Leite, L.P. Costa, F.L. da Costa Dias, L.S. Barcelos, G.B. Collares, and A.C. Simoes e Silva, *The renin-angiotensin system in a rat model of hepatic fibrosis: evidence for a protective role of Angiotensin-(1-7)*. J Hepatol, 2007. **46**(4): p. 674.
136. J.S. Lubel, C.B. Herath, J. Tchongue, J. Grace, Z. Jia, K. Spencer, D. Casley, P. Crowley, W. Sievert, L.M. Burrell, and P.W. Angus, *Angiotensin-(1-7), an alternative metabolite of the renin-angiotensin system, is up-regulated in human liver disease and has antifibrotic activity in the bile-duct-ligated rat*. Clin Sci (Lond), 2009. **117**(11): p. 375.
137. Y. Liu, B. Li, X. Wang, G. Li, R. Shang, J. Yang, J. Wang, M. Zhang, Y. Chen, Y. Zhang, C. Zhang, and P. Hao, *Angiotensin-(1-7) Suppresses Hepatocellular Carcinoma Growth and Angiogenesis via Complex Interactions of Angiotensin II Type 1 Receptor, Angiotensin II Type 2 Receptor and Mas Receptor*. Mol Med, 2015. **21**: p. 626.
138. E.E. Hinsley, C.E. de Oliveira, S. Hunt, R.D. Coletta, and D.W. Lambert, *Angiotensin 1-7 inhibits angiotensin II-stimulated head and neck cancer progression*. Eur J Oral Sci, 2017. **125**(4): p. 247.
139. N. Cambados, T. Walther, K. Nahmod, J.M. Tocci, N. Rubinstein, I. Bohme, M. Simian, R. Sampayo, M. Del Valle Suberbordes, E.C. Kordon, and C. Schere-Levy, *Angiotensin-(1-7) counteracts the transforming effects triggered by angiotensin II in breast cancer cells*. Oncotarget, 2017. **8**(51): p. 88475.
140. M.A. Khajah, M.M. Fateel, K.V. Ananthalakshmi, and Y.A. Luqmani, *Anti-Inflammatory Action of Angiotensin 1-7 in Experimental Colitis*. PLoS One, 2016. **11**(3): p. e0150861.
-

-
141. G.C. Liu, G.Y. Oudit, F. Fang, J. Zhou, and J.W. Scholey, *Angiotensin-(1-7)-induced activation of ERK1/2 is cAMP/protein kinase A-dependent in glomerular mesangial cells*. Am J Physiol Renal Physiol, 2012. **302**(6): p. F784.
142. N. King, C.T. Hittinger, and S.B. Carroll, *Evolution of key cell signaling and adhesion protein families predates animal origins*. Science, 2003. **301**(5631): p. 361.
143. A.S. Hauser, M.M. Attwood, M. Rask-Andersen, H.B. Schioth, and D.E. Gloriam, *Trends in GPCR drug discovery: new agents, targets and indications*. Nat Rev Drug Discov, 2017. **16**(12): p. 829.
144. D.M. Rosenbaum, S.G.F. Rasmussen, and B.K. Kobilka, *The structure and function of G-protein-coupled receptors*. Nature, 2009. **459**(7245): p. 356.
145. A. Manglik and A.C. Kruse, *Structural Basis for G Protein-Coupled Receptor Activation*. Biochemistry, 2017. **56**(42): p. 5628.
146. M. Audet and M. Bouvier, *Restructuring G-protein- coupled receptor activation*. Cell, 2012. **151**(1): p. 14.
147. V.V. Gurevich and E.V. Gurevich, *Molecular Mechanisms of GPCR Signaling: A Structural Perspective*. Int J Mol Sci, 2017. **18**(12).
148. J. Duchene, J.P. Schanstra, C. Pecher, A. Pizard, C. Susini, J.P. Esteve, J.L. Bascands, and J.P. Girolami, *A novel protein-protein interaction between a G protein-coupled receptor and the phosphatase SHP-2 is involved in bradykinin-induced inhibition of cell proliferation*. J Biol Chem, 2002. **277**(43): p. 40375.
149. N. Wettschureck and S. Offermanns, *Mammalian G proteins and their cell type specific functions*. Physiol Rev, 2005. **85**(4): p. 1159.
150. K. Khafizov, G. Lattanzi, and P. Carloni, *G protein inactive and active forms investigated by simulation methods*. Proteins, 2009. **75**(4): p. 919.

-
151. S.R. Neves, P.T. Ram, and R. Iyengar, *G protein pathways*. Science, 2002. **296**(5573): p. 1636.
152. J.L. Bos, J. de Rooij, and K.A. Reedquist, *Rap1 signalling: adhering to new models*. Nat Rev Mol Cell Biol, 2001. **2**(5): p. 369.
153. J.M. Schmitt and P.J. Stork, *PKA phosphorylation of Src mediates cAMP's inhibition of cell growth via Rap1*. Mol Cell, 2002. **9**(1): p. 85.
154. Alcino J. Silva, Jeffrey H. Kogan, a. Paul W. Frankland, and S. Kida, *CREB AND MEMORY*. Annual Review of Neuroscience, 1998. **21**(1): p. 127.
155. Y. Kashima, T. Miki, T. Shibasaki, N. Ozaki, M. Miyazaki, H. Yano, and S. Seino, *Critical role of cAMP-GEFII--Rim2 complex in incretin-potentiated insulin secretion*. J Biol Chem, 2001. **276**(49): p. 46046.
156. T.J. Berg JM, Stryer L, *Biochemistry*. 5 ed. 2002, New York: W H Freeman.
157. Z. Xie, W.T. Ho, R. Spellman, S. Cai, and J.H. Exton, *Mechanisms of regulation of phospholipase D1 and D2 by the heterotrimeric G proteins G13 and Gq*. J Biol Chem, 2002. **277**(14): p. 11979.
158. C.S. Shi and J.H. Kehrl, *PYK2 links G(q)alpha and G(13)alpha signaling to NF-kappa B activation*. J Biol Chem, 2001. **276**(34): p. 31845.
159. G. Pearson, F. Robinson, T. Beers Gibson, B.-e. Xu, M. Karandikar, K. Berman, and M.H. Cobb, *Mitogen-Activated Protein (MAP) Kinase Pathways: Regulation and Physiological Functions**. Endocrine Reviews, 2001. **22**(2): p. 153.
160. Y. Jiang, W. Ma, Y. Wan, T. Kozasa, S. Hattori, and X.Y. Huang, *The G protein G alpha12 stimulates Bruton's tyrosine kinase and a rasGAP through a conserved PH/BM domain*. Nature, 1998. **395**(6704): p. 808.

-
161. K. Riento and A.J. Ridley, *Rocks: multifunctional kinases in cell behaviour*. Nat Rev Mol Cell Biol, 2003. **4**(6): p. 446.
162. E.F. Grady, L.A. Sechi, C.A. Griffin, M. Schambelan, and J.E. Kalinyak, *Expression of AT2 receptors in the developing rat fetus*. J Clin Invest, 1991. **88**(3): p. 921.
163. S. Shanmugam, Z.G. Lenkei, J.M. Gasc, P.L. Corvol, and C.M. Llorens-Cortes, *Ontogeny of angiotensin II type 2 (AT2) receptor mRNA in the rat*. Kidney Int, 1995. **47**(4): p. 1095.
164. P. Namsolleck, F. Boato, K. Schwengel, L. Paulis, K.S. Matho, N. Geurts, C. Thone-Reineke, K. Lucht, K. Seidel, A. Hallberg, B. Dahlof, T. Unger, S. Hendrix, and U.M. Steckelings, *AT2-receptor stimulation enhances axonal plasticity after spinal cord injury by upregulating BDNF expression*. Neurobiol Dis, 2013. **51**: p. 177.
165. U.M. Steckelings, E. Kaschina, and T. Unger, *The AT2 receptor--a matter of love and hate*. Peptides, 2005. **26**(8): p. 1401.
166. Z. Lenkei, M. Palkovits, P. Corvol, and C. Llorens-Cortes, *Expression of angiotensin type-1 (AT1) and type-2 (AT2) receptor mRNAs in the adult rat brain: a functional neuroanatomical review*. Front Neuroendocrinol, 1997. **18**(4): p. 383.
167. H. Matsubara, T. Sugaya, S. Murasawa, Y. Nozawa, Y. Mori, H. Masaki, K. Maruyama, Y. Tsutumi, Y. Shibasaki, Y. Moriguchi, Y. Tanaka, T. Iwasaka, and M. Inada, *Tissue-specific expression of human angiotensin II AT1 and AT2 receptors and cellular localization of subtype mRNAs in adult human renal cortex using in situ hybridization*. Nephron, 1998. **80**(1): p. 25.
168. N. Miyata, F. Park, X.F. Li, and A.W. Cowley, Jr., *Distribution of angiotensin AT1 and AT2 receptor subtypes in the rat kidney*. Am J Physiol, 1999. **277**(3 Pt 2): p. F437.

-
169. Z.Q. Wang, A.F. Moore, R. Ozono, H.M. Siragy, and R.M. Carey, *Immunolocalization of subtype 2 angiotensin II (AT2) receptor protein in rat heart*. Hypertension, 1998. **32**(1): p. 78.
170. T. Jing, H. Wang, K.S. Srivenugopal, G. He, J. Liu, L. Miao, and Y. He, *Conditional expression of type 2 angiotensin II receptor in rat vascular smooth muscle cells reveals the interplay of the angiotensin system in matrix metalloproteinase 2 expression and vascular remodeling*. Int J Mol Med, 2009. **24**(1): p. 103.
171. M. Nakajima, H.G. Hutchinson, M. Fujinaga, W. Hayashida, R. Morishita, L. Zhang, M. Horiuchi, R.E. Pratt, and V.J. Dzau, *The angiotensin II type 2 (AT2) receptor antagonizes the growth effects of the AT1 receptor: gain-of-function study using gene transfer*. Proc Natl Acad Sci U S A, 1995. **92**(23): p. 10663.
172. Y. Nio, H. Matsubara, S. Murasawa, M. Kanasaki, and M. Inada, *Regulation of gene transcription of angiotensin II receptor subtypes in myocardial infarction*. J Clin Invest, 1995. **95**(1): p. 46.
173. Y. Xu, V. Menon, and B.I. Jugdutt, *Cardioprotection after angiotensin II type 1 blockade involves angiotensin II type 2 receptor expression and activation of protein kinase C-epsilon in acutely reperfused myocardial infarction in the dog. Effect of UP269-6 and losartan on AT1 and AT2-receptor expression and IP3 receptor and PKCepsilon proteins*. J Renin Angiotensin Aldosterone Syst, 2000. **1**(2): p. 184.
174. N. Ohkubo, H. Matsubara, Y. Nozawa, Y. Mori, S. Murasawa, K. Kijima, K. Maruyama, H. Masaki, Y. Tsutumi, Y. Shibasaki, T. Iwasaka, and M. Inada, *Angiotensin type 2 receptors are reexpressed by cardiac fibroblasts from failing*

- myopathic hamster hearts and inhibit cell growth and fibrillar collagen metabolism*. Circulation, 1997. **96**(11): p. 3954.
175. M. Ruiz-Ortega, V. Esteban, Y. Suzuki, M. Ruperez, S. Mezzano, L. Ardiles, P. Justo, A. Ortiz, and J. Egido, *Renal expression of angiotensin type 2 (AT2) receptors during kidney damage*. Kidney Int Suppl, 2003(86): p. S21.
 176. R. Bautista, A. Sanchez, J. Hernandez, A. Oyekan, and B. Escalante, *Angiotensin II type AT(2) receptor mRNA expression and renal vasodilatation are increased in renal failure*. Hypertension, 2001. **38**(3 Pt 2): p. 669.
 177. K. Shibata, I. Makino, H. Shibaguchi, M. Niwa, Y. Ohgami, M. Fujiwara, T. Furukawa, and T. Katsuragi, *[Expression of angiotensin type-2 receptors in rat brain during the cell injury]*. Nihon Yakurigaku Zasshi, 1998. **112 Suppl 1**: p. 53p.
 178. I. Makino, K. Shibata, Y. Ohgami, M. Fujiwara, and T. Furukawa, *Transient upregulation of the AT2 receptor mRNA level after global ischemia in the rat brain*. Neuropeptides, 1996. **30**(6): p. 596.
 179. S. Gallinat, M. Yu, A. Dorst, T. Unger, and T. Herdegen, *Sciatic nerve transection evokes lasting up-regulation of angiotensin AT2 and AT1 receptor mRNA in adult rat dorsal root ganglia and sciatic nerves*. Brain Res Mol Brain Res, 1998. **57**(1): p. 111.
 180. R. Lucius, S. Gallinat, P. Rosenstiel, T. Herdegen, J. Sievers, and T. Unger, *The angiotensin II type 2 (AT2) receptor promotes axonal regeneration in the optic nerve of adult rats*. J Exp Med, 1998. **188**(4): p. 661.
 181. E. Clauser, K.M. Curnow, E. Davies, S. Conchon, B. Teutsch, B. Vianello, C. Monnot, and P. Corvol, *Angiotensin II receptors: protein and gene structures, expression and potential pathological involvements*. Eur J Endocrinol, 1996. **134**(4): p. 403.

-
182. B.A. Kemp, J.F. Bell, D.M. Rottkamp, N.L. Howell, W. Shao, L.G. Navar, S.H. Padia, and R.M. Carey, *INTRARENAL ANGIOTENSIN III IS THE PREDOMINANT AGONIST FOR PROXIMAL TUBULE AT(2) RECEPTORS*. Hypertension, 2012. **60**(2): p. 387.
183. M.P. Ocaranza, J. Moya, V. Barrientos, R. Alzamora, D. Hevia, C. Morales, M. Pinto, N. Escudero, L. Garcia, U. Novoa, P. Ayala, G. Diaz-Araya, I. Godoy, M. Chiong, S. Lavandero, J.E. Jalil, and L. Michea, *Angiotensin-(1-9) reverses experimental hypertension and cardiovascular damage by inhibition of the angiotensin converting enzyme/Ang II axis*. J Hypertens, 2014. **32**(4): p. 771.
184. S.E. Whitebread, V. Taylor, S.P. Bottari, B. Kamber, and M. de Gasparo, *Radioiodinated CGP 42112A: a novel high affinity and highly selective ligand for the characterization of angiotensin AT2 receptors*. Biochem Biophys Res Commun, 1991. **181**(3): p. 1365.
185. Y. Wan, C. Wallinder, B. Plouffe, H. Beaudry, A.K. Mahalingam, X. Wu, B. Johansson, M. Holm, M. Botoros, A. Karlen, A. Pettersson, F. Nyberg, L. Fandriks, N. Gallo-Payet, A. Hallberg, and M. Alterman, *Design, synthesis, and biological evaluation of the first selective nonpeptide AT2 receptor agonist*. J Med Chem, 2004. **47**(24): p. 5995.
186. E. Kaschina, A. Grzesiak, J. Li, A. Foryst-Ludwig, M. Timm, F. Rompe, M. Sommerfeld, U.R. Kemnitz, C. Curato, P. Namsolleck, C. Tschope, A. Hallberg, M. Alterman, T. Hucko, I. Paetsch, T. Dietrich, B. Schnackenburg, K. Graf, B. Dahlof, U. Kintscher, T. Unger, and U.M. Steckelings, *Angiotensin II type 2 receptor stimulation: a novel option of therapeutic interference with the renin-angiotensin system in myocardial infarction?* Circulation, 2008. **118**(24): p. 2523.

-
187. S. Bosnyak, I.K. Welungoda, A. Hallberg, M. Alterman, R.E. Widdop, and E.S. Jones, *Stimulation of angiotensin AT₂ receptors by the non-peptide agonist, Compound 21, evokes vasodepressor effects in conscious spontaneously hypertensive rats*. Br J Pharmacol, 2010. **159**(3): p. 709.
188. A. Rehman, A. Leibowitz, N. Yamamoto, Y. Rautureau, P. Paradis, and E.L. Schiffrin, *Angiotensin type 2 receptor agonist compound 21 reduces vascular injury and myocardial fibrosis in stroke-prone spontaneously hypertensive rats*. Hypertension, 2012. **59**(2): p. 291.
189. B.A. Kemp, N.L. Howell, J.J. Gildea, S.R. Keller, S.H. Padia, and R.M. Carey, *AT₂ receptor activation induces natriuresis and lowers blood pressure*. Circ Res, 2014. **115**(3): p. 388.
190. D.T. Dudley and R.M. Summerfelt, *Regulated expression of angiotensin II (AT₂) binding sites in R3T3 cells*. Regul Pept, 1993. **44**(2): p. 199.
191. A.T. Chiu, W.F. Herblin, D.E. McCall, R.J. Ardecky, D.J. Carini, J.V. Duncia, L.J. Pease, P.C. Wong, R.R. Wexler, A.L. Johnson, and et al., *Identification of angiotensin II receptor subtypes*. Biochem Biophys Res Commun, 1989. **165**(1): p. 196.
192. R.S. Chang and V.J. Lotti, *Two distinct angiotensin II receptor binding sites in rat adrenal revealed by new selective nonpeptide ligands*. Mol Pharmacol, 1990. **37**(3): p. 347.
193. M.T. Smith, T.M. Woodruff, B.D. Wyse, A. Muralidharan, and T. Walther, *A small molecule angiotensin II type 2 receptor (AT₂R) antagonist produces analgesia in a rat model of neuropathic pain by inhibition of p38 mitogen-activated protein kinase (MAPK) and p44/p42 MAPK activation in the dorsal root ganglia*. Pain Med, 2013. **14**(10): p. 1557.
-

-
194. A.S.C. Rice, R.H. Dworkin, T.D. McCarthy, P. Anand, C. Bountra, P.I. McCloud, J. Hill, G. Cutter, G. Kitson, N. Desem, and M. Raff, *EMA401, an orally administered highly selective angiotensin II type 2 receptor antagonist, as a novel treatment for postherpetic neuralgia: a randomised, double-blind, placebo-controlled phase 2 clinical trial*. *Lancet*, 2014. **383**(9929): p. 1637.
195. J.M. Keppel Hesselink and M.E. Schatman, *EMA401: an old antagonist of the AT2R for a new indication in neuropathic pain*. *J Pain Res*, 2017. **10**: p. 439.
196. U. Anand, P. Facer, Y. Yiangou, M. Sinisi, M. Fox, T. McCarthy, C. Bountra, Y.E. Korchev, and P. Anand, *Angiotensin II type 2 receptor (AT2 R) localization and antagonist-mediated inhibition of capsaicin responses and neurite outgrowth in human and rat sensory neurons*. *Eur J Pain*, 2013. **17**(7): p. 1012.
197. M.T. Smith, T. Lau, V.C. Wallace, B.D. Wyse, and A.S. Rice, *Analgesic efficacy of small-molecule angiotensin II type 2 receptor antagonists in a rat model of antiretroviral toxic polyneuropathy*. *Behav Pharmacol*, 2014. **25**(2): p. 137.
198. C. Nahmias and A.D. Strosberg, *The angiotensin AT2 receptor: searching for signal-transduction pathways and physiological function*. *Trends in Pharmacological Sciences*, 1995. **16**(7): p. 223.
199. J. Kang, P. Posner, and C. Sumners, *Angiotensin II type 2 receptor stimulation of neuronal K⁺ currents involves an inhibitory GTP binding protein*. *Am J Physiol*, 1994. **267**(5 Pt 1): p. C1389.
200. S. Nouet and C. Nahmias, *Signal transduction from the angiotensin II AT2 receptor*. *Trends Endocrinol Metab*, 2000. **11**(1): p. 1.

-
201. X.C. Huang, E.M. Richards, and C. Sumners, *Angiotensin II type 2 receptor-mediated stimulation of protein phosphatase 2A in rat hypothalamic/brainstem neuronal cocultures*. J Neurochem, 1995. **65**(5): p. 2131.
202. J.Y. Lehtonen, L. Daviet, C. Nahmias, M. Horiuchi, and V.J. Dzau, *Analysis of functional domains of angiotensin II type 2 receptor involved in apoptosis*. Mol Endocrinol, 1999. **13**(7): p. 1051.
203. M. Horiuchi, W. Hayashida, T. Kambe, T. Yamada, and V.J. Dzau, *Angiotensin type 2 receptor dephosphorylates Bcl-2 by activating mitogen-activated protein kinase phosphatase-1 and induces apoptosis*. J Biol Chem, 1997. **272**(30): p. 19022.
204. S. Nouet and C. Nahmias, *Signal Transduction from the Angiotensin II AT2 Receptor*. Trends in Endocrinology & Metabolism, 2000. **11**(1): p. 1.
205. U.V. Shenoy, E.M. Richards, X.C. Huang, and C. Sumners, *Angiotensin II type 2 receptor-mediated apoptosis of cultured neurons from newborn rat brain*. Endocrinology, 1999. **140**(1): p. 500.
206. G. Wiemer, B.A. Scholkens, A. Wagner, H. Heitsch, and W. Linz, *The possible role of angiotensin II subtype AT2 receptors in endothelial cells and isolated ischemic rat hearts*. J Hypertens Suppl, 1993. **11**(5): p. S234.
207. N. Seyedi, X. Xu, A. Nasjletti, and T.H. Hintze, *Coronary kinin generation mediates nitric oxide release after angiotensin receptor stimulation*. Hypertension, 1995. **26**(1): p. 164.
208. C. Thorup, M. Kornfeld, J.M. Winaver, M.S. Goligorsky, and L.C. Moore, *Angiotensin-II stimulates nitric oxide release in isolated perfused renal resistance arteries*. Pflugers Arch, 1998. **435**(3): p. 432.
-

-
209. H.M. Siragy and R.M. Carey, *Protective role of the angiotensin AT₂ receptor in a renal wrap hypertension model*. Hypertension, 1999. **33**(5): p. 1237.
210. Y. Zhao, T. Biermann, C. Luther, T. Unger, J. Culman, and P. Gohlke, *Contribution of bradykinin and nitric oxide to AT₂ receptor-mediated differentiation in PC12 W cells*. J Neurochem, 2003. **85**(3): p. 759.
211. F. Cote, L. Laflamme, M.D. Payet, and N. Gallo-Payet, *Nitric oxide, a new second messenger involved in the action of angiotensin II on neuronal differentiation of NG108-15 cells*. Endocr Res, 1998. **24**(3-4): p. 403.
212. D. Haithcock, H. Jiao, X.L. Cui, U. Hopfer, and J.G. Douglas, *Renal proximal tubular AT₂ receptor: signaling and transport*. J Am Soc Nephrol, 1999. **10 Suppl 11**: p. S69.
213. S. Sandmann, M. Yu, E. Kaschina, A. Blume, E. Bouzinova, C. Aalkjaer, and T. Unger, *Differential effects of angiotensin AT₁ and AT₂ receptors on the expression, translation and function of the Na⁺-H⁺ exchanger and Na⁺-HCO₃⁻ symporter in the rat heart after myocardial infarction*. J Am Coll Cardiol, 2001. **37**(8): p. 2154.
214. D. Young, G. Waitches, C. Birchmeier, O. Fasano, and M. Wigler, *Isolation and characterization of a new cellular oncogene encoding a protein with multiple potential transmembrane domains*. Cell, 1986. **45**(5): p. 711.
215. M. Bader, N. Alenina, M.A. Andrade-Navarro, and R.A. Santos, *MAS and its related G protein-coupled receptors, Mrgprs*. Pharmacol Rev, 2014. **66**(4): p. 1080.
216. X. Dong, S. Han, M.J. Zylka, M.I. Simon, and D.J. Anderson, *A diverse family of GPCRs expressed in specific subsets of nociceptive sensory neurons*. Cell, 2001. **106**(5): p. 619.

-
217. T. Wittenberger, H.C. Schaller, and S. Hellebrand, *An expressed sequence tag (EST) data mining strategy succeeding in the discovery of new G-protein coupled receptors*. J Mol Biol, 2001. **307**(3): p. 799.
218. P.M. Lembo, E. Grazzini, T. Groblewski, D. O'Donnell, M.O. Roy, J. Zhang, C. Hoffert, J. Cao, R. Schmidt, M. Pelletier, M. Labarre, M. Gosselin, Y. Fortin, D. Banville, S.H. Shen, P. Strom, K. Payza, A. Dray, P. Walker, and S. Ahmad, *Proenkephalin A gene products activate a new family of sensory neuron--specific GPCRs*. Nat Neurosci, 2002. **5**(3): p. 201.
219. S. Takeda, S. Kadowaki, T. Haga, H. Takaesu, and S. Mitaku, *Identification of G protein-coupled receptor genes from the human genome sequence*. FEBS Lett, 2002. **520**(1-3): p. 97.
220. L. Zhang, N. Taylor, Y. Xie, R. Ford, J. Johnson, J.E. Paulsen, and B. Bates, *Cloning and expression of MRG receptors in macaque, mouse, and human*. Brain Res Mol Brain Res, 2005. **133**(2): p. 187.
221. E.S. Burstein, T.R. Ott, M. Feddock, J.N. Ma, S. Fuhs, S. Wong, H.H. Schiffer, M.R. Brann, and N.R. Nash, *Characterization of the Mas-related gene family: structural and functional conservation of human and rhesus MrgX receptors*. Br J Pharmacol, 2006. **147**(1): p. 73.
222. M.J. Zylka, X. Dong, A.L. Southwell, and D.J. Anderson, *Atypical expansion in mice of the sensory neuron-specific Mrg G protein-coupled receptor family*. Proc Natl Acad Sci U S A, 2003. **100**(17): p. 10043.
223. N. Alenina, T. Baranova, E. Smirnow, M. Bader, A. Lippoldt, E. Patkin, and T. Walther, *Cell type-specific expression of the Mas proto-oncogene in testis*. J Histochem Cytochem, 2002. **50**(5): p. 691.
-

-
224. D. Young, K. O'Neill, T. Jessell, and M. Wigler, *Characterization of the rat mas oncogene and its high-level expression in the hippocampus and cerebral cortex of rat brain*. Proc Natl Acad Sci U S A, 1988. **85**(14): p. 5339.
225. B. Bunnemann, K. Fuxe, R. Metzger, J. Mullins, T.R. Jackson, M.R. Hanley, and D. Ganten, *Autoradiographic localization of mas proto-oncogene mRNA in adult rat brain using in situ hybridization*. Neurosci Lett, 1990. **114**(2): p. 147.
226. A.J. Villar and R.A. Pedersen, *Parental imprinting of the Mas protooncogene in mouse*. Nat Genet, 1994. **8**(4): p. 373.
227. R. Metzger, M. Bader, T. Ludwig, C. Berberich, B. Bunnemann, and D. Ganten, *Expression of the mouse and rat mas proto-oncogene in the brain and peripheral tissues*. FEBS Lett, 1995. **357**(1): p. 27.
228. N. Alenina, P. Xu, B. Rentzsch, E.L. Patkin, and M. Bader, *Genetically altered animal models for Mas and angiotensin-(1-7)*. Exp Physiol, 2008. **93**(5): p. 528.
229. M. Kumar, P. Grammas, F. Giacomelli, and J. Wiener, *Selective expression of c-mas proto-oncogene in rat cerebral endothelial cells*. Neuroreport, 1996. **8**(1): p. 93.
230. A.C.d.C. Gonçalves, R. Leite, R.A. Fraga-Silva, S.V. Pinheiro, A.B. Reis, F.M. Reis, R.M. Touyz, R.C. Webb, N. Alenina, M. Bader, and R.A.S. Santos, *Evidence that the vasodilator angiotensin-(1-7)-Mas axis plays an important role in erectile function*. American Journal of Physiology-Heart and Circulatory Physiology, 2007. **293**(4): p. H2588.
231. V. Jankowski, M. Tolle, R.A. Santos, T. Gunthner, E. Krause, M. Beyermann, P. Welker, M. Bader, S.V. Pinheiro, W.O. Sampaio, R. Lautner, A. Kretschmer, M. van der Giet, W. Zidek, and J. Jankowski, *Angioprotectin: an angiotensin II-like peptide causing vasodilatory effects*. FASEB J, 2011. **25**(9): p. 2987.

-
232. G. Wiemer, L.W. Dobrucki, F.R. Louka, T. Malinski, and H. Heitsch, *AVE 0991, a nonpeptide mimic of the effects of angiotensin-(1-7) on the endothelium*. Hypertension, 2002. **40**(6): p. 847.
233. I.F. Benter, M.H. Yousif, C. Cojocel, M. Al-Maghrebi, and D.I. Diz, *Angiotensin-(1-7) prevents diabetes-induced cardiovascular dysfunction*. Am J Physiol Heart Circ Physiol, 2007. **292**(1): p. H666.
234. Y. Ma, H. Huang, J. Jiang, L. Wu, C. Lin, A. Tang, G. Dai, J. He, and Y. Chen, *AVE 0991 attenuates cardiac hypertrophy through reducing oxidative stress*. Biochem Biophys Res Commun, 2016. **474**(4): p. 621.
235. A.J. Ferreira, B.A. Jacoby, C.A. Araujo, F.A. Macedo, G.A. Silva, A.P. Almeida, M.V. Caliari, and R.A. Santos, *The nonpeptide angiotensin-(1-7) receptor Mas agonist AVE-0991 attenuates heart failure induced by myocardial infarction*. Am J Physiol Heart Circ Physiol, 2007. **292**(2): p. H1113.
236. K.D. da Silveira, F.M. Coelho, A.T. Vieira, D. Sachs, L.C. Barroso, V.V. Costa, T.L. Bretas, M. Bader, L.P. de Sousa, T.A. da Silva, R.A. dos Santos, A.C. Simoes e Silva, and M.M. Teixeira, *Anti-inflammatory effects of the activation of the angiotensin-(1-7) receptor, MAS, in experimental models of arthritis*. J Immunol, 2010. **185**(9): p. 5569.
237. J. Toton-Zuranska, M. Gajda, G. Pyka-Fosciak, K. Kus, M. Pawlowska, A. Niepsuj, P. Wolkow, R. Olszanecki, J. Jawien, and R. Korbut, *AVE 0991-angiotensin-(1-7) receptor agonist, inhibits atherogenesis in apoE-knockout mice*. J Physiol Pharmacol, 2010. **61**(2): p. 181.
238. D.S. Skiba, R. Nosalski, T.P. Mikolajczyk, M. Siedlinski, F.J. Rios, A.C. Montezano, J. Jawien, R. Olszanecki, R. Korbut, M. Czesnikiewicz-Guzik, R.M. Touyz, and T.J.

- Guzik, *Anti-atherosclerotic effect of the angiotensin 1-7 mimetic AVE0991 is mediated by inhibition of perivascular and plaque inflammation in early atherosclerosis*. Br J Pharmacol, 2017. **174**(22): p. 4055.
239. R.A. Santos, M.J. Campagnole-Santos, N.C. Baracho, M.A. Fontes, L.C. Silva, L.A. Neves, D.R. Oliveira, S.M. Caligorne, A.R. Rodrigues, C. Gropen Junior, and et al., *Characterization of a new angiotensin antagonist selective for angiotensin-(1-7): evidence that the actions of angiotensin-(1-7) are mediated by specific angiotensin receptors*. Brain Res Bull, 1994. **35**(4): p. 293.
240. M. Canals, L. Jenkins, E. Kellett, and G. Milligan, *Up-regulation of the angiotensin II type 1 receptor by the MAS proto-oncogene is due to constitutive activation of Gq/G11 by MAS*. J Biol Chem, 2006. **281**(24): p. 16757.
241. L.D. Kluskens, S.A. Nelemans, R. Rink, L. de Vries, A. Meter-Arkema, Y. Wang, T. Walther, A. Kuipers, G.N. Moll, and M. Haas, *Angiotensin-(1-7) with thioether bridge: an angiotensin-converting enzyme-resistant, potent angiotensin-(1-7) analog*. J Pharmacol Exp Ther, 2009. **328**(3): p. 849.
242. M.A. Fontes, L.C. Silva, M.J. Campagnole-Santos, M.C. Khosla, P.G. Guertzenstein, and R.A. Santos, *Evidence that angiotensin-(1-7) plays a role in the central control of blood pressure at the ventro-lateral medulla acting through specific receptors*. Brain Res, 1994. **665**(1): p. 175.
243. T. Shinohara, M. Harada, K. Ogi, M. Maruyama, R. Fujii, H. Tanaka, S. Fukusumi, H. Komatsu, M. Hosoya, Y. Noguchi, T. Watanabe, T. Moriya, Y. Itoh, and S. Hinuma, *Identification of a G protein-coupled receptor specifically responsive to beta-alanine*. J Biol Chem, 2004. **279**(22): p. 23559.

-
244. G.M. Etelvino, A.A. Peluso, and R.A. Santos, *New components of the renin-angiotensin system: alamandine and the MAS-related G protein-coupled receptor* D. Curr Hypertens Rep, 2014. **16**(6): p. 433.
245. L.R. Avula, R. Buckinx, H. Favoreel, E. Cox, D. Adriaensen, L. Van Nassauw, and J.P. Timmermans, *Expression and distribution patterns of Mas-related gene receptor subtypes A-H in the mouse intestine: inflammation-induced changes*. Histochem Cell Biol, 2013. **139**(5): p. 639.
246. B. Habiyakare, H. Alsaadon, M.L. Mathai, A. Hayes, and A. Zulli, *Reduction of angiotensin A and alamandine vasoactivity in the rabbit model of atherogenesis: differential effects of alamandine and Ang(1-7)*. Int J Exp Pathol, 2014. **95**(4): p. 290.
247. S. Nishimura, M. Uno, Y. Kaneta, K. Fukuchi, H. Nishigohri, J. Hasegawa, H. Komori, S. Takeda, K. Enomoto, F. Nara, and T. Agatsuma, *MRGD, a MAS-related G-protein coupled receptor, promotes tumorigenesis and is highly expressed in lung cancer*. PLoS One, 2012. **7**(6): p. e38618.
248. Q. Liu, P. Sikand, C. Ma, Z. Tang, L. Han, Z. Li, S. Sun, R.H. LaMotte, and X. Dong, *Mechanisms of itch evoked by beta-alanine*. J Neurosci, 2012. **32**(42): p. 14532.
249. J. Hrenak, L. Paulis, and F. Simko, *Angiotensin A/Alamandine/MrgD Axis: Another Clue to Understanding Cardiovascular Pathophysiology*. Int J Mol Sci, 2016. **17**(7).
250. Y. le Tran and C. Forster, *Angiotensin-(1-7) and the rat aorta: modulation by the endothelium*. J Cardiovasc Pharmacol, 1997. **30**(5): p. 676.
251. D.C. Villela, D.G. Passos-Silva, and R.A. Santos, *Alamandine: a new member of the angiotensin family*. Curr Opin Nephrol Hypertens, 2014. **23**(2): p. 130.

-
252. S.K. Ajit, M.H. Pausch, J.D. Kennedy, and E.J. Kaftan, *Development of a FLIPR assay for the simultaneous identification of MrgD agonists and antagonists from a single screen*. J Biomed Biotechnol, 2010. **2010**.
253. M. Uno, S. Nishimura, K. Fukuchi, Y. Kaneta, Y. Oda, H. Komori, S. Takeda, T. Haga, T. Agatsuma, and F. Nara, *Identification of physiologically active substances as novel ligands for MRGPRD*. J Biomed Biotechnol, 2012. **2012**: p. 816159.
254. R.A. Santos, A.S. Haibara, M.J. Campagnole-Santos, A.C. Simoes e Silva, R.D. Paula, S.V. Pinheiro, M.F. Leite, V.S. Lemos, D.M. Silva, M.T. Guerra, and M.C. Khosla, *Characterization of a new selective antagonist for angiotensin-(1-7), D-pro7-angiotensin-(1-7)*. Hypertension, 2003. **41**(3 Pt 2): p. 737.
255. T. Uchiyama, F. Okajima, C. Mogi, A. Tobo, S. Tomono, and K. Sato, *Alamandine reduces leptin expression through the c-Src/p38 MAP kinase pathway in adipose tissue*. PLoS One, 2017. **12**(6): p. e0178769.
256. G. Milligan, *Constitutive activity and inverse agonists of G protein-coupled receptors: a current perspective*. Mol Pharmacol, 2003. **64**(6): p. 1271.
257. T. Zhang, Z. Li, H. Dang, R. Chen, C. Liaw, T.A. Tran, P.D. Boatman, D.T. Connolly, and J.W. Adams, *Inhibition of Mas G-protein signaling improves coronary blood flow, reduces myocardial infarct size, and provides long-term cardioprotection*. Am J Physiol Heart Circ Physiol, 2012. **302**(1): p. H299.
258. W.R. Rowley, C. Bezold, Y. Arian, E. Byrne, and S. Krohe, *Diabetes 2030: Insights from Yesterday, Today, and Future Trends*. Population Health Management, 2017. **20**(1): p. 6.

-
259. *Global, regional, and national incidence, prevalence, and years lived with disability for 310 diseases and injuries, 1990-2015: a systematic analysis for the Global Burden of Disease Study 2015*. Lancet, 2016. **388**(10053): p. 1545.
260. J.P. Boyle, A.A. Honeycutt, K.M.V. Narayan, T.J. Hoerger, L.S. Geiss, H. Chen, and T.J. Thompson, *Projection of Diabetes Burden Through 2050*. Impact of changing demography and disease prevalence in the U.S., 2001. **24**(11): p. 1936.
261. S.F. Awad, M. O'Flaherty, J. Critchley, and L.J. Abu-Raddad, *Forecasting the Burden of Type 2 Diabetes Mellitus in Qatar to 2050: A Novel Modeling Approach*. Diabetes Res Clin Pract, 2017.
262. F.J. Pasquel and G.E. Umpierrez, *Hyperosmolar hyperglycemic state: a historic review of the clinical presentation, diagnosis, and treatment*. Diabetes Care, 2014. **37**(11): p. 3124.
263. N.N. Tun, G. Arunagirinathan, S.K. Munshi, and J.M. Pappachan, *Diabetes mellitus and stroke: A clinical update*. World J Diabetes, 2017. **8**(6): p. 235.
264. M.S. Shah and M. Brownlee, *Molecular and Cellular Mechanisms of Cardiovascular Disorders in Diabetes*. Circ Res, 2016. **118**(11): p. 1808.
265. U. Alam, D.R. Riley, R.S. Jugdey, S. Azmi, S. Rajbhandari, K. D'Aout, and R.A. Malik, *Diabetic Neuropathy and Gait: A Review*. Diabetes Ther, 2017. **8**(6): p. 1253.
266. M.A. Bodman and S.C. Dulebohn. *Diabetic Neuropathy*. StatPearls 2017; Available from: <https://www.ncbi.nlm.nih.gov/books/NBK442009/>.
267. R.M. Kashim, P. Newton, and O. Ojo, *Diabetic Retinopathy Screening: A Systematic Review on Patients' Non-Attendance*. Int J Environ Res Public Health, 2018. **15**(1).
268. R.A. DeFronzo, *Pathogenesis of type 2 diabetes mellitus*. Medical Clinics. **88**(4): p. 787.

269. S.A. Paschou, N. Papadopoulou-Marketou, G.P. Chrousos, and C. Kanaka-Gantenbein, *On type 1 diabetes mellitus pathogenesis*. Endocr Connect, 2018. **7**(1): p. R38.
 270. T. Roy and C.E. Lloyd, *Epidemiology of depression and diabetes: a systematic review*. J Affect Disord, 2012. **142 Suppl**: p. S8.
 271. J.A. See, K. Kaukinen, G.K. Makharia, P.R. Gibson, and J.A. Murray, *Practical insights into gluten-free diets*. Nat Rev Gastroenterol Hepatol, 2015. **12**(10): p. 580.
 272. P. Elfstrom, J. Sundstrom, and J.F. Ludvigsson, *Systematic review with meta-analysis: associations between coeliac disease and type 1 diabetes*. Aliment Pharmacol Ther, 2014. **40**(10): p. 1123.
 273. A. Katsarou, S. Gudbjörnsdottir, A. Rawshani, D. Dabelea, E. Bonifacio, B.J. Anderson, L.M. Jacobsen, D.A. Schatz, and Å. Lernmark, *Type 1 diabetes mellitus*. Nature Reviews Disease Primers, 2017. **3**: p. 17016.
 274. J. Storling and F. Pociot, *Type 1 Diabetes Candidate Genes Linked to Pancreatic Islet Cell Inflammation and Beta-Cell Apoptosis*. Genes (Basel), 2017. **8**(2).
 275. J.A. Bluestone, K. Herold, and G. Eisenbarth, *Genetics, pathogenesis and clinical interventions in type 1 diabetes*. Nature, 2010. **464**(7293): p. 1293.
 276. J. Lucier and R.S. Weinstock, *Diabetes Mellitus, Type 1*, in *StatPearls*. 2018, StatPearls Publishing
- StatPearls Publishing LLC.: Treasure Island (FL).
277. H. Beyan, H. Riese, M.I. Hawa, G. Beretta, H.W. Davidson, J.C. Hutton, H. Burger, M. Schlosser, H. Snieder, B.O. Boehm, and R.D. Leslie, *Glycotoxin and*

- autoantibodies are additive environmentally determined predictors of type 1 diabetes: a twin and population study.* Diabetes, 2012. **61**(5): p. 1192.
278. M. Knip, R. Veijola, S.M. Virtanen, H. Hyoty, O. Vaarala, and H.K. Akerblom, *Environmental triggers and determinants of type 1 diabetes.* Diabetes, 2005. **54** **Suppl 2**: p. S125.
279. M. Knip, *Environmental triggers and determinants of beta-cell autoimmunity and type 1 diabetes.* Rev Endocr Metab Disord, 2003. **4**(3): p. 213.
280. G. Serena, S. Camhi, C. Sturgeon, S. Yan, and A. Fasano, *The Role of Gluten in Celiac Disease and Type 1 Diabetes.* Nutrients, 2015. **7**(9): p. 7143.
281. S. Bibbo, M.P. Dore, G.M. Pes, G. Delitala, and A.P. Delitala, *Is there a role for gut microbiota in type 1 diabetes pathogenesis?* Ann Med, 2017. **49**(1): p. 11.
282. M. Rewers and J. Ludvigsson, *Environmental risk factors for type 1 diabetes.* Lancet, 2016. **387**(10035): p. 2340.
283. R. Brentjens and L. Saltz, *Islet cell tumors of the pancreas: the medical oncologist's perspective.* Surg Clin North Am, 2001. **81**(3): p. 527.
284. J. Wu and L.J. Yan, *Streptozotocin-induced type 1 diabetes in rodents as a model for studying mitochondrial mechanisms of diabetic beta cell glucotoxicity.* Diabetes Metab Syndr Obes, 2015. **8**: p. 181.
285. H. Bays, L. Mandarino, and R.A. DeFronzo, *Role of the Adipocyte, Free Fatty Acids, and Ectopic Fat in Pathogenesis of Type 2 Diabetes Mellitus: Peroxisomal Proliferator-Activated Receptor Agonists Provide a Rational Therapeutic Approach.* The Journal of Clinical Endocrinology & Metabolism, 2004. **89**(2): p. 463.
286. W. Sami, T. Ansari, N.S. Butt, and M.R.A. Hamid, *Effect of diet on type 2 diabetes mellitus: A review.* Int J Health Sci (Qassim), 2017. **11**(2): p. 65.

-
287. A. Abdullah, A. Peeters, M. de Courten, and J. Stoelwinder, *The magnitude of association between overweight and obesity and the risk of diabetes: a meta-analysis of prospective cohort studies*. Diabetes Res Clin Pract, 2010. **89**(3): p. 309.
288. J. Maddatu, E. Anderson-Baucum, and C. Evans-Molina, *Smoking and the risk of type 2 diabetes*. Transl Res, 2017. **184**: p. 101.
289. A. Pan, Y. Wang, M. Talaei, F.B. Hu, and T. Wu, *Relation of active, passive, and quitting smoking with incident type 2 diabetes: a systematic review and meta-analysis*. Lancet Diabetes Endocrinol, 2015. **3**(12): p. 958.
290. C. Touma and S. Pannain, *Does lack of sleep cause diabetes?* Cleve Clin J Med, 2011. **78**(8): p. 549.
291. V.S. Malik, B.M. Popkin, G.A. Bray, J.P. Després, and F.B. Hu, *Sugar Sweetened Beverages, Obesity, Type 2 Diabetes and Cardiovascular Disease risk*. Circulation, 2010. **121**(11): p. 1356.
292. V.S. Malik, B.M. Popkin, G.A. Bray, J.P. Després, W.C. Willett, and F.B. Hu, *Sugar-Sweetened Beverages and Risk of Metabolic Syndrome and Type 2 Diabetes: A meta-analysis*. Diabetes Care, 2010. **33**(11): p. 2477.
293. U. Risérus, W.C. Willett, and F.B. Hu, *Dietary fats and prevention of type 2 diabetes*. Prog Lipid Res, 2009. **48**(1): p. 44.
294. I.M. Lee, E.J. Shiroma, F. Lobelo, P. Puska, S.N. Blair, and P.T. Katzmarzyk, *Impact of Physical Inactivity on the World's Major Non-Communicable Diseases*. Lancet, 2012. **380**(9838): p. 219.
295. C. Herder and M. Roden, *Genetics of type 2 diabetes: pathophysiologic and clinical relevance*. Eur J Clin Invest, 2011. **41**(6): p. 679.

-
296. H. Izzedine, V. Launay-Vacher, C. Deybach, E. Bourry, B. Barrou, and G. Deray, *Drug-induced diabetes mellitus*. *Expert Opin Drug Saf*, 2005. **4**(6): p. 1097.
297. U.K. Sampson, M.R.F. Linton, and S. Fazio, *Are statins diabetogenic?* *Curr Opin Cardiol*, 2011. **26**(4): p. 342.
298. E. Resmini, F. Minuto, A. Colao, and D. Ferone, *Secondary diabetes associated with principal endocrinopathies: the impact of new treatment modalities*. *Acta Diabetol*, 2009. **46**(2): p. 85.
299. J.B. Farrell, A. Deshmukh, and A.A. Baghaie, *Low testosterone and the association with type 2 diabetes*. *Diabetes Educ*, 2008. **34**(5): p. 799.
300. C. Raina Elley and T. Kenealy, *Lifestyle interventions reduced the long-term risk of diabetes in adults with impaired glucose tolerance*. *Evid Based Med*, 2008. **13**(6): p. 173.
301. L.J. Orozco, A.M. Buchleitner, G. Gimenez-Perez, I.F.M. Roque, B. Richter, and D. Mauricio, *Exercise or exercise and diet for preventing type 2 diabetes mellitus*. *Cochrane Database Syst Rev*, 2008(3): p. Cd003054.
302. G. Wilcox, *Insulin and Insulin Resistance*. *Clinical Biochemist Reviews*, 2005. **26**(2): p. 19.
303. W.T. Cefalu, *Insulin resistance: cellular and clinical concepts*. *Exp Biol Med* (Maywood), 2001. **226**(1): p. 13.
304. M.H. Shanik, Y. Xu, J. Škrha, R. Dankner, Y. Zick, and J. Roth, *Insulin Resistance and Hyperinsulinemia*. Is hyperinsulinemia the cart or the horse?, 2008. **31**(Supplement 2): p. S262.
305. S. Muntoni, S. Muntoni, and B. Draznin, *Effects of chronic hyperinsulinemia in insulin-resistant patients*. *Current Diabetes Reports*, 2008. **8**(3): p. 233.

-
306. M.J. Fowler, *Microvascular and Macrovascular Complications of Diabetes*. Clinical Diabetes, 2008. **26**(2): p. 77.
307. J.A. Beckman, M.A. Creager, and P. Libby, *Diabetes and atherosclerosis: epidemiology, pathophysiology, and management*. Jama, 2002. **287**(19): p. 2570.
308. S.P. Laing, A.J. Swerdlow, S.D. Slater, A.C. Burden, A. Morris, N.R. Waugh, W. Gatling, P.J. Bingley, and C.C. Patterson, *Mortality from heart disease in a cohort of 23,000 patients with insulin-treated diabetes*. Diabetologia, 2003. **46**(6): p. 760.
309. F.S. Sorrentino, S. Matteini, C. Bonifazzi, A. Sebastiani, and F. Parmeggiani, *Diabetic retinopathy and endothelin system: microangiopathy versus endothelial dysfunction*. Eye (Lond), 2018. **32**(7): p. 1157.
310. H. Xu, T. Curtis, and A. Stitt. *Pathophysiology and Pathogenesis of Diabetic Retinopathy [internet]*. 2014 [cited 2014 13. August]; Available from: <https://www.diapedia.org/7104343513/rev/14>.
311. Z. Cao and M.E. Cooper, *Pathogenesis of diabetic nephropathy*. Journal of Diabetes Investigation, 2011. **2**(4): p. 243.
312. S. Vijan, *In the clinic. Type 2 diabetes*. Ann Intern Med, 2010. **152**(5): p. ITC31.
313. E. Selvin, M.W. Steffes, H. Zhu, K. Matsushita, L. Wagenknecht, J. Pankow, J. Coresh, and F.L. Brancati, *Glycated hemoglobin, diabetes, and cardiovascular risk in nondiabetic adults*. N Engl J Med, 2010. **362**(9): p. 800.
314. A.K. Brinkman, *Management of Type 1 Diabetes*. Nurs Clin North Am, 2017. **52**(4): p. 499.
315. C. Lombardo, V.G. Perrone, G. Amorese, F. Vistoli, W. Baronti, P. Marchetti, and U. Boggi, *Update on pancreatic transplantation on the management of diabetes*. Minerva Med, 2017. **108**(5): p. 405.

-
316. H.C. Denroche and C.B. Verchere, *IAPP and type 1 diabetes: implications for immunity, metabolism and islet transplants*. J Mol Endocrinol, 2018. **60**(2): p. R57.
317. C.A. Chang, M.C. Lawrence, and B. Naziruddin, *Current issues in allogeneic islet transplantation*. Curr Opin Organ Transplant, 2017. **22**(5): p. 437.
318. S. Zanuso, A. Jimenez, G. Pugliese, G. Corigliano, and S. Balducci, *Exercise for the management of type 2 diabetes: a review of the evidence*. Acta Diabetol, 2010. **47**(1): p. 15.
319. R. Boussageon, I. Supper, T. Bejan-Angoulvant, N. Kellou, M. Cucherat, J.P. Boissel, B. Kassai, A. Moreau, F. Gueyffier, and C. Cornu, *Reappraisal of metformin efficacy in the treatment of type 2 diabetes: a meta-analysis of randomised controlled trials*. PLoS Med, 2012. **9**(4): p. e1001204.
320. S.E. Inzucchi, R.M. Bergenstal, J.B. Buse, M. Diamant, E. Ferrannini, M. Nauck, A.L. Peters, A. Tsapas, R. Wender, and D.R. Matthews, *Management of hyperglycaemia in type 2 diabetes, 2015: a patient-centred approach. Update to a position statement of the American Diabetes Association and the European Association for the Study of Diabetes*. Diabetologia, 2015. **58**(3): p. 429.
321. K. McBrien, D.M. Rabi, N. Campbell, L. Barnieh, F. Clement, B.R. Hemmelgarn, M. Tonelli, L.A. Leiter, S.W. Klarenbach, and B.J. Manns, *Intensive and Standard Blood Pressure Targets in Patients With Type 2 Diabetes Mellitus: Systematic Review and Meta-analysis*. Arch Intern Med, 2012. **172**(17): p. 1296.
322. B. Zinman, C. Wanner, J.M. Lachin, D. Fitchett, E. Bluhmki, S. Hantel, M. Mattheus, T. Devins, O.E. Johansen, H.J. Woerle, U.C. Broedl, and S.E. Inzucchi, *Empagliflozin, Cardiovascular Outcomes, and Mortality in Type 2 Diabetes*. New England Journal of Medicine, 2015. **373**(22): p. 2117.
-

-
323. J.L. Gross, M.J. de Azevedo, S.P. Silveiro, L.H. Canani, M.L. Caramori, and T. Zelmanovitz, *Diabetic nephropathy: diagnosis, prevention, and treatment*. Diabetes Care, 2005. **28**(1): p. 164.
324. U.N. Das, *Renin-angiotensin-aldosterone system in insulin resistance and metabolic syndrome*. J Transl Int Med, 2016. **4**(2): p. 66.
325. L. Li, L. Han, Q. Fu, Y. Li, Z. Liang, J. Su, and B. Li, *Formation and inhibition of Nepsilon-(carboxymethyl)lysine in saccharide-lysine model systems during microwave heating*. Molecules, 2012. **17**(11): p. 12758.
326. J.R. Beattie, A.M. Pawlak, M.E. Boulton, J. Zhang, V.M. Monnier, J.J. McGarvey, and A.W. Stitt, *Multiplex analysis of age-related protein and lipid modifications in human Bruch's membrane*. Faseb j, 2010. **24**(12): p. 4816.
327. P.C. Chang, T.H. Chen, C.J. Chang, C.C. Hou, P. Chan, and H.M. Lee, *Advanced glycosylation end products induce inducible nitric oxide synthase (iNOS) expression via a p38 MAPK-dependent pathway*. Kidney Int, 2004. **65**(5): p. 1664.
328. F. Schweda, U. Friis, C. Wagner, O. Skott, and A. Kurtz, *Renin release*. Physiology (Bethesda), 2007. **22**: p. 310.
329. J. Peti-Peterdi, *High glucose and renin release: the role of succinate and GPR91*. Kidney Int, 2010. **78**(12): p. 1214.
330. A.C. Ariza, P.M. Deen, and J.H. Robben, *The succinate receptor as a novel therapeutic target for oxidative and metabolic stress-related conditions*. Front Endocrinol (Lausanne), 2012. **3**: p. 22.
331. T. Li, J. Hu, S. Du, Y. Chen, S. Wang, and Q. Wu, *ERK1/2/COX-2/PGE2 signaling pathway mediates GPR91-dependent VEGF release in streptozotocin-induced diabetes*. Mol Vis, 2014. **20**: p. 1109.
-

-
332. A. Kanda and S. Ishida, *Receptor-associated prorenin system contributes to development of inflammation and angiogenesis in proliferative diabetic retinopathy*. *Inflamm Regen*, 2016. **36**: p. 22.
333. J. Wysocki, D.I. Ortiz-Melo, N.K. Mattocks, K. Xu, J. Prescott, K. Evora, M. Ye, M.A. Sparks, S.K. Haque, D. Batlle, and S.B. Gurley, *ACE2 deficiency increases NADPH-mediated oxidative stress in the kidney*. *Physiol Rep*, 2014. **2**(3): p. e00264.
334. D. Zablocki and J. Sadoshima, *Angiotensin II and oxidative stress in the failing heart*. *Antioxid Redox Signal*, 2013. **19**(10): p. 1095.
335. P. Chen, A.M. Guo, P.A. Edwards, G. Trick, and A.G. Scicli, *Role of NADPH oxidase and ANG II in diabetes-induced retinal leukostasis*. *Am J Physiol Regul Integr Comp Physiol*, 2007. **293**(4): p. R1619.
336. G. Jia, A. Whaley-Connell, and J.R. Sowers, *Diabetic cardiomyopathy: a hyperglycaemia- and insulin-resistance-induced heart disease*. *Diabetologia*, 2018. **61**(1): p. 21.
337. Y. Ozawa, K. Yuki, R. Yamagishi, K. Tsubota, and M. Aihara, *Renin-angiotensin system involvement in the oxidative stress-induced neurodegeneration of cultured retinal ganglion cells*. *Jpn J Ophthalmol*, 2013. **57**(1): p. 126.
338. R.M. Carey and H.M. Siragy, *The intrarenal renin-angiotensin system and diabetic nephropathy*. *Trends Endocrinol Metab*, 2003. **14**(6): p. 274.
339. F. Folli, M.J. Saad, L. Velloso, H. Hansen, O. Carandente, E.P. Feener, and C.R. Kahn, *Crosstalk between insulin and angiotensin II signalling systems*. *Exp Clin Endocrinol Diabetes*, 1999. **107**(2): p. 133.

-
340. S. Bernardi, A. Michelli, G. Zuolo, R. Candido, and B. Fabris, *Update on RAAS Modulation for the Treatment of Diabetic Cardiovascular Disease*. J Diabetes Res, 2016. **2016**: p. 8917578.
341. *Effects of ramipril on cardiovascular and microvascular outcomes in people with diabetes mellitus: results of the HOPE study and MICRO-HOPE substudy*. Heart Outcomes Prevention Evaluation Study Investigators. Lancet, 2000. **355**(9200): p. 253.
342. K.A. Jandeleit-Dahm, C. Tikellis, C.M. Reid, C.I. Johnston, and M.E. Cooper, *Why blockade of the renin-angiotensin system reduces the incidence of new-onset diabetes*. J Hypertens, 2005. **23**(3): p. 463.
343. M. Furuhashi, N. Ura, H. Takizawa, D. Yoshida, N. Moniwa, H. Murakami, K. Higashiura, and K. Shimamoto, *Blockade of the renin-angiotensin system decreases adipocyte size with improvement in insulin sensitivity*. J Hypertens, 2004. **22**(10): p. 1977.
344. M. Frossard, C. Joukhadar, G. Steffen, R. Schmid, H.G. Eichler, and M. Muller, *Paracrine effects of angiotensin-converting-enzyme- and angiotensin-II-receptor-inhibition on transcapillary glucose transport in humans*. Life Sci, 2000. **66**(10): p. P1147.
345. R. Lupi, S. Del Guerra, M. Bugliani, U. Boggi, F. Mosca, S. Torri, S. Del Prato, and P. Marchetti, *The direct effects of the angiotensin-converting enzyme inhibitors, zofenoprilat and enalaprilat, on isolated human pancreatic islets*. Eur J Endocrinol, 2006. **154**(2): p. 355.
346. T. Behl and A. Kotwani, *Potential of angiotensin II receptor blockers in the treatment of diabetic retinopathy*. Life Sci, 2017. **176**: p. 1.
-

-
347. L. Foggensteiner, S. Mulroy, and J. Firth, *Management of diabetic nephropathy*. J R Soc Med, 2001. **94**(5): p. 210.
348. S.H. Santos, J.F. Giani, V. Burghi, J.G. Miquet, F. Qadri, J.F. Braga, M. Todiras, K. Kotnik, N. Alenina, F.P. Dominici, R.A. Santos, and M. Bader, *Oral administration of angiotensin-(1-7) ameliorates type 2 diabetes in rats*. J Mol Med (Berl), 2014. **92**(3): p. 255.
349. C. Liu, X.H. Lv, H.X. Li, X. Cao, F. Zhang, L. Wang, M. Yu, and J.K. Yang, *Angiotensin-(1-7) suppresses oxidative stress and improves glucose uptake via Mas receptor in adipocytes*. Acta Diabetol, 2012. **49**(4): p. 291.
350. J. He, Z. Yang, H. Yang, L. Wang, H. Wu, Y. Fan, W. Wang, X. Fan, and X. Li, *Regulation of insulin sensitivity, insulin production, and pancreatic beta cell survival by angiotensin-(1-7) in a rat model of streptozotocin-induced diabetes mellitus*. Peptides, 2015. **64**: p. 49.
351. A. Verma, Z. Shan, B. Lei, L. Yuan, X. Liu, T. Nakagawa, M.B. Grant, A.S. Lewin, W.W. Hauswirth, M.K. Raizada, and Q. Li, *ACE2 and Ang-(1-7) confer protection against development of diabetic retinopathy*. Mol Ther, 2012. **20**(1): p. 28.
352. K. Zhang, X. Meng, D. Li, J. Yang, J. Kong, P. Hao, T. Guo, M. Zhang, Y. Zhang, and C. Zhang, *Angiotensin(1-7) attenuates the progression of streptozotocin-induced diabetic renal injury better than angiotensin receptor blockade*. Kidney Int, 2015. **87**(2): p. 359.
353. S.D. Crowley and T.M. Coffman, *Recent advances involving the renin-angiotensin system*. Exp Cell Res, 2012. **318**(9): p. 1049.
354. H. Takeda, Y. Katagata, Y. Hozumi, and S. Kondo, *Effects of angiotensin II receptor signaling during skin wound healing*. Am J Pathol, 2004. **165**(5): p. 1653.
-

-
355. C. Sumners, M. Horiuchi, R.E. Widdop, C. McCarthy, T. Unger, and U.M. Steckelings, *Protective arms of the renin-angiotensin-system in neurological disease*. Clin Exp Pharmacol Physiol, 2013. **40**(8): p. 580.
356. P.E. Walters, T.A. Gaspari, and R.E. Widdop, *Angiotensin-(1-7) acts as a vasodepressor agent via angiotensin II type 2 receptors in conscious rats*. Hypertension, 2005. **45**(5): p. 960.
357. N. Klein, F. Gembardt, S. Supe, S.M. Kaestle, H. Nickles, L. Erfinanda, X. Lei, J. Yin, L. Wang, M. Mertens, K. Szaszi, T. Walther, and W.M. Kuebler, *Angiotensin-(1-7) protects from experimental acute lung injury*. Crit Care Med, 2013. **41**(11): p. e334.
358. X. Zhu, Y. Wang, A. Schwiebs, and T. Walther, *Chimeric natriuretic peptide ACNP stimulates both natriuretic peptide receptors, the NPRA and NPRB*. Molecular and cellular endocrinology, 2013. **366**(1): p. 117.
359. M.J. Zylka, F.L. Rice, and D.J. Anderson, *Topographically distinct epidermal nociceptive circuits revealed by axonal tracers targeted to Mrgprd*. Neuron, 2005. **45**(1): p. 17.
360. M. Iwata, R.T. Cowling, D. Gurantz, C. Moore, S. Zhang, J.X. Yuan, and B.H. Greenberg, *Angiotensin-(1-7) binds to specific receptors on cardiac fibroblasts to initiate antifibrotic and antitrophic effects*. Am J Physiol Heart Circ Physiol, 2005. **289**(6): p. H2356.
361. G. Perez-Rivero, M.P. Ruiz-Torres, J.V. Rivas-Elena, M. Jerkic, M.L. Diez-Marques, J.M. Lopez-Novoa, M.A. Blasco, and D. Rodriguez-Puyol, *Mice deficient in telomerase activity develop hypertension because of an excess of endothelin production*. Circulation, 2006. **114**(4): p. 309.

-
362. R. Huey, G.M. Morris, A.J. Olson, and D.S. Goodsell, *A semiempirical free energy force field with charge-based desolvation*. J Comput Chem, 2007. **28**(6): p. 1145.
363. *GPCR databases (GPCRdb)*. 2018; Available from: <http://gpcrdb.org/>.
364. J. Perodin, M. Deraet, M. Auger-Messier, A.A. Boucard, L. Rihakova, M.E. Beaulieu, P. Lavigne, J.L. Parent, G. Guillemette, R. Leduc, and E. Escher, *Residues 293 and 294 are ligand contact points of the human angiotensin type 1 receptor*. Biochemistry, 2002. **41**(48): p. 14348.
365. J.W. Prokop, R.A. Santos, and A. Milsted, *Differential mechanisms of activation of the Ang peptide receptors AT1, AT2, and MAS: using in silico techniques to differentiate the three receptors*. PLoS One, 2013. **8**(6): p. e65307.
366. N.M. O'Boyle, M. Banck, C.A. James, C. Morley, T. Vandermeersch, and G.R. Hutchison, *Open Babel: An open chemical toolbox*. J Cheminform, 2011. **3**: p. 33.
367. N.M. Mordwinkin, C.J. Meeks, S.S. Jadhav, T. Espinoza, N. Roda, G.S. diZerega, S.G. Louie, and K.E. Rodgers, *Angiotensin-(1-7) Administration Reduces Oxidative Stress in Diabetic Bone Marrow*. Endocrinology, 2012. **153**(5): p. 2189.
368. C. Peiro, S. Vallejo, F. Gembardt, V. Azcutia, S. Heringer-Walther, L. Rodriguez-Manas, H.P. Schultheiss, C.F. Sanchez-Ferrer, and T. Walther, *Endothelial dysfunction through genetic deletion or inhibition of the G protein-coupled receptor Mas: a new target to improve endothelial function*. Journal of Hypertension, 2007. **25**(12): p. 2421.
369. S. Higuchi, H. Ohtsu, H. Suzuki, H. Shirai, G.D. Frank, and S. Eguchi, *Angiotensin II signal transduction through the AT1 receptor: novel insights into mechanisms and pathophysiology*. Clin Sci (Lond), 2007. **112**(8): p. 417.

-
370. B. Mayr and M. Montminy, *Transcriptional regulation by the phosphorylation-dependent factor CREB*. Nature Reviews Molecular Cell Biology, 2001. **2**(8): p. 599.
371. T. Verano-Braga, V. Schwammle, M. Sylvester, D.G. Passos-Silva, A.A.B. Peluso, G.M. Etelvino, R.A.S. Santos, and P. Roepstorff, *Time-Resolved Quantitative Phosphoproteomics: New Insights into Angiotensin-(1-7) Signaling Networks in Human Endothelial Cells*. Journal of Proteome Research, 2012. **11**(6): p. 3370.
372. C. Meinert, F. Gembardt, I. Bohme, A. Tetzner, T. Wieland, B. Greenberg, and T. Walther, *Identification of intracellular proteins and signaling pathways in human endothelial cells regulated by angiotensin-(1-7)*. J Proteomics, 2016. **130**: p. 129.
373. Y. Han, H.J. Sun, P. Li, Q. Gao, Y.B. Zhou, F. Zhang, X.Y. Gao, and G.Q. Zhu, *Angiotensin-(1-7) in paraventricular nucleus modulates sympathetic activity and cardiac sympathetic afferent reflex in renovascular hypertensive rats*. PLoS One, 2012. **7**(11): p. e48966.
374. S. Heringer-Walther, K. Eckert, S.M. Schumacher, L. Uharek, A. Wulf-Goldenberg, F. Gembardt, I. Fichtner, H.P. Schultheiss, K. Rodgers, and T. Walther, *Angiotensin-(1-7) stimulates hematopoietic progenitor cells in vitro and in vivo*. Haematologica, 2009. **94**(6): p. 857.
375. A.K. Boer, A.L. Drayer, and E. Vellenga, *cAMP/PKA-mediated regulation of erythropoiesis*. Leuk Lymphoma, 2003. **44**(11): p. 1893.
376. K. Ohshima, M. Mogi, H. Nakaoka, J. Iwanami, L.J. Min, H. Kanno, K. Tsukuda, T. Chisaka, H.Y. Bai, X.L. Wang, A. Ogimoto, J. Higaki, and M. Horiuchi, *Possible role of angiotensin-converting enzyme 2 and activation of angiotensin II type 2 receptor by angiotensin-(1-7) in improvement of vascular remodeling by angiotensin II type 1 receptor blockade*. Hypertension, 2014. **63**(3): p. e53.
-

-
377. Y. Wang, C. Qian, A.J. Roks, D. Westermann, S.M. Schumacher, F. Escher, R.G. Schoemaker, T.L. Reudelhuber, W.H. van Gilst, H.P. Schultheiss, C. Tschope, and T. Walther, *Circulating rather than cardiac angiotensin-(1-7) stimulates cardioprotection after myocardial infarction*. *Circ Heart Fail*, 2010. **3**(2): p. 286.
378. A. Tetzner, K. Gebolys, C. Meinert, S. Klein, A. Uhlich, J. Trebicka, O. Villacanas, and T. Walther, *G-Protein-Coupled Receptor MrgD Is a Receptor for Angiotensin-(1-7) Involving Adenylyl Cyclase, cAMP, and Phosphokinase A*. *Hypertension*, 2016. **68**(1): p. 185.
379. R. Yang, T. Walther, F. Gembardt, I. Smolders, P. Vanderheyden, A.L. Albiston, S.Y. Chai, and A.G. Dupont, *Renal vasoconstrictor and pressor responses to angiotensin IV in mice are AT1a-receptor mediated*. *J Hypertens*, 2010. **28**(3): p. 487.
380. R. Yang, I. Smolders, P. Vanderheyden, H. Demaegdt, A. Van Eeckhaut, G. Vauquelin, A. Lukaszuk, D. Tourwe, S.Y. Chai, A.L. Albiston, C. Nahmias, T. Walther, and A.G. Dupont, *Pressor and renal hemodynamic effects of the novel angiotensin A peptide are angiotensin II type 1A receptor dependent*. *Hypertension*, 2011. **57**(5): p. 956.
381. S.M. Kupchan, A.L. Dessertine, B.T. Blaylock, and R.F. Bryan, *Isolation and structural elucidation of allamandin, an antileukemic iridoid lactone from Allamanda cathartica*. *J Org Chem*, 1974. **39**(17): p. 2477.
382. C. Kilkeny, W. Browne, I.C. Cuthill, M. Emerson, D.G. Altman, and N.C.R.R.G.W. Group, *Animal research: reporting in vivo experiments: the ARRIVE guidelines*. *Br J Pharmacol*, 2010. **160**(7): p. 1577.

-
383. J.C. McGrath and E. Lilley, *Implementing guidelines on reporting research using animals (ARRIVE etc.): new requirements for publication in BJP*. Br J Pharmacol, 2015. **172**(13): p. 3189.
384. X. Zhu, Y. Wang, A. Schwiebs, and T. Walther, *Chimeric natriuretic peptide ACNP stimulates both natriuretic peptide receptors, the NPRA and NPRB*. Mol Cell Endocrinol, 2013. **366**(1): p. 117.
385. F. Horn, E. Bettler, L. Oliveira, F. Campagne, F.E. Cohen, and G. Vriend, *GPCRDB information system for G protein-coupled receptors*. Nucleic Acids Res, 2003. **31**(1): p. 294.
386. R.P. Xiao, X. Ji, and E.G. Lakatta, *Functional coupling of the beta 2-adrenoceptor to a pertussis toxin-sensitive G protein in cardiac myocytes*. Mol Pharmacol, 1995. **47**(2): p. 322.
387. R.P. Xiao, P. Avdonin, Y.Y. Zhou, H. Cheng, S.A. Akhter, T. Eschenhagen, R.J. Lefkowitz, W.J. Koch, and E.G. Lakatta, *Coupling of beta2-adrenoceptor to Gi proteins and its physiological relevance in murine cardiac myocytes*. Circ Res, 1999. **84**(1): p. 43.
388. Y. Daaka, L.M. Luttrell, and R.J. Lefkowitz, *Switching of the coupling of the beta2-adrenergic receptor to different G proteins by protein kinase A*. Nature, 1997. **390**(6655): p. 88.
389. J.D. Kilts, M.A. Gerhardt, M.D. Richardson, G. Sreeram, G.B. Mackensen, H.P. Grocott, W.D. White, R.D. Davis, M.F. Newman, J.G. Reves, D.A. Schwinn, and M.M. Kwatra, *Beta(2)-adrenergic and several other G protein-coupled receptors in human atrial membranes activate both G(s) and G(i)*. Circ Res, 2000. **87**(8): p. 705.
-

-
390. M. Beyermann, N. Heinrich, K. Fechner, J. Furkert, W. Zhang, O. Kraetke, M. Bienert, and H. Berger, *Achieving signalling selectivity of ligands for the corticotropin-releasing factor type 1 receptor by modifying the agonist's signalling domain*. Br J Pharmacol, 2007. **151**(6): p. 851.
391. Y. Adachi, Y. Saito, I. Kishimoto, M. Harada, K. Kuwahara, N. Takahashi, R. Kawakami, M. Nakanishi, Y. Nakagawa, K. Tanimoto, Y. Saitoh, S. Yasuno, S. Usami, M. Iwai, M. Horiuchi, and K. Nakao, *Angiotensin II type 2 receptor deficiency exacerbates heart failure and reduces survival after acute myocardial infarction in mice*. Circulation, 2003. **107**(19): p. 2406.
392. R.W. Regenhardt, F. Desland, A.P. Mecca, D.J. Pioquinto, A. Afzal, J. Mocco, and C. Sumners, *Anti-inflammatory effects of angiotensin-(1-7) in ischemic stroke*. Neuropharmacology, 2013. **71**: p. 154.
393. R.A. Benndorf, C. Krebs, B. Hirsch-Hoffmann, E. Schwedhelm, G. Cieslar, R. Schmidt-Haupt, O.M. Steinmetz, C. Meyer-Schwesinger, F. Thaiss, M. Haddad, S. Fehr, A. Heilmann, U. Helmchen, L. Hein, H. Ehmke, R.A. Stahl, R.H. Boger, and U.O. Wenzel, *Angiotensin II type 2 receptor deficiency aggravates renal injury and reduces survival in chronic kidney disease in mice*. Kidney Int, 2009. **75**(10): p. 1039.
394. A. Hammer, G. Yang, J. Friedrich, A. Kovacs, D.H. Lee, K. Grave, S. Jorg, N. Alenina, J. Grosch, J. Winkler, R. Gold, M. Bader, A. Manzel, L.C. Rump, D.N. Muller, R.A. Linker, and J. Stegbauer, *Role of the receptor Mas in macrophage-mediated inflammation in vivo*. Proc Natl Acad Sci U S A, 2016. **113**(49): p. 14109.
395. J.P. Joseph, A.P. Mecca, R.W. Regenhardt, D.M. Bennion, V. Rodriguez, F. Desland, N.A. Patel, D.J. Pioquinto, T. Unger, M.J. Katovich, U.M. Steckelings, and C.

- Sumners, *The angiotensin type 2 receptor agonist Compound 21 elicits cerebroprotection in endothelin-1 induced ischemic stroke*. *Neuropharmacology*, 2014. **81**: p. 134.
396. J. Gao, I.H. Zucker, and L. Gao, *Activation of central angiotensin type 2 receptors by compound 21 improves arterial baroreflex sensitivity in rats with heart failure*. *Am J Hypertens*, 2014. **27**(10): p. 1248.
397. R.A.S. Santos, A.C.S. e Silva, C. Maric, D.M.R. Silva, R.P. Machado, I. de Buhr, S. Heringer-Walther, S.V.B. Pinheiro, M.T. Lopes, M. Bader, E.P. Mendes, V.S. Lemos, M.J. Campagnole-Santos, H.-P. Schultheiss, R. Speth, and T. Walther, *Angiotensin-(1–7) is an endogenous ligand for the G protein-coupled receptor Mas*. *Proceedings of the National Academy of Sciences of the United States of America*, 2003. **100**(14): p. 8258.
398. D. Villela, J. Leonhardt, N. Patel, J. Joseph, S. Kirsch, A. Hallberg, T. Unger, M. Bader, R.A. Santos, C. Sumners, and U.M. Steckelings, *Angiotensin type 2 receptor (AT2R) and receptor Mas: a complex liaison*. *Clin Sci (Lond)*, 2015. **128**(4): p. 227.
399. T. Ichiki, P.A. Labosky, C. Shiota, S. Okuyama, Y. Imagawa, A. Fogo, F. Niimura, I. Ichikawa, B.L. Hogan, and T. Inagami, *Effects on blood pressure and exploratory behaviour of mice lacking angiotensin II type-2 receptor*. *Nature*, 1995. **377**(6551): p. 748.
400. B. Maul, O. von Bohlen und Halbach, A. Becker, A. Sterner-Kock, J.P. Voigt, W.E. Siems, G. Grecksch, and T. Walther, *Impaired spatial memory and altered dendritic spine morphology in angiotensin II type 2 receptor-deficient mice*. *J Mol Med (Berl)*, 2008. **86**(5): p. 563.

-
401. S. Foulquier, U.M. Steckelings, and T. Unger, *Impact of the AT(2) receptor agonist C21 on blood pressure and beyond*. Curr Hypertens Rep, 2012. **14**(5): p. 403.
402. A. Vuorinen and D. Schuster, *Methods for generating and applying pharmacophore models as virtual screening filters and for bioactivity profiling*. Methods, 2015. **71**: p. 113.
403. J.M. Luther and N.J. Brown, *The renin-angiotensin-aldosterone system and glucose homeostasis*. Trends Pharmacol Sci, 2011. **32**(12): p. 734.
404. E. Mendoza-Torres, A. Oyarzun, D. Mondaca-Ruff, A. Azocar, P.F. Castro, J.E. Jalil, M. Chiong, S. Lavandero, and M.P. Ocaranza, *ACE2 and vasoactive peptides: novel players in cardiovascular/renal remodeling and hypertension*. Ther Adv Cardiovasc Dis, 2015. **9**(4): p. 217.
405. I. Grantzдорffer, U. Lendeckel, S. Carl-McGrath, A. Roessner, and C. Rocken, *Angiotensin I-converting enzyme (CD143) is down-regulated in focal nodular hyperplasia of the liver*. Am J Surg Pathol, 2004. **28**(1): p. 84.
406. E.R. Weibel, *Stereological principles for morphometry in electron microscopic cytology*. Int Rev Cytol, 1969. **26**: p. 235.
407. J.M. Chirgwin, A.E. Przybyla, R.J. MacDonald, and W.J. Rutter, *Isolation of biologically active ribonucleic acid from sources enriched in ribonuclease*. Biochemistry, 1979. **18**(24): p. 5294.
408. A. Schroeder, O. Mueller, S. Stocker, R. Salowsky, M. Leiber, M. Gassmann, S. Lightfoot, W. Menzel, M. Granzow, and T. Ragg, *The RIN: an RNA integrity number for assigning integrity values to RNA measurements*. BMC Mol Biol, 2006. **7**: p. 3.
409. G. Grynkiewicz, M. Poenie, and R.Y. Tsien, *A new generation of Ca²⁺ indicators with greatly improved fluorescence properties*. J Biol Chem, 1985. **260**(6): p. 3440.
-

-
410. T. Pfeiffer, U. Kraushaar, M. Dufer, S. Schonecker, D. Haspel, E. Gunther, G. Drews, and P. Krippeit-Drews, *Rapid functional evaluation of beta-cells by extracellular recording of membrane potential oscillations with microelectrode arrays*. Pflugers Arch, 2011. **462**(6): p. 835.
411. Y. Yang and K.D. Gillis, *A highly Ca^{2+} -sensitive pool of granules is regulated by glucose and protein kinases in insulin-secreting INS-1 cells*. J Gen Physiol, 2004. **124**(6): p. 641.
412. Q.F. Wan, Y. Dong, H. Yang, X. Lou, J. Ding, and T. Xu, *Protein kinase activation increases insulin secretion by sensitizing the secretory machinery to Ca^{2+}* . J Gen Physiol, 2004. **124**(6): p. 653.
413. L. Yuan, X. Li, G.L. Xu, and C.J. Qi, *Effects of renin-angiotensin system blockade on islet function in diabetic rats*. J Endocrinol Invest, 2010. **33**(1): p. 13.
414. G. Lastra and C. Manrique, *The expanding role of oxidative stress, renin angiotensin system, and beta-cell dysfunction in the cardiometabolic syndrome and Type 2 diabetes mellitus*. Antioxid Redox Signal, 2007. **9**(7): p. 943.
415. J.C. Henquin, *Triggering and amplifying pathways of regulation of insulin secretion by glucose*. Diabetes, 2000. **49**(11): p. 1751.
416. M. Nenquin and J.C. Henquin, *Sulphonylurea receptor-1, sulphonylureas and amplification of insulin secretion by Epac activation in beta cells*. Diabetes Obes Metab, 2016. **18**(7): p. 698.
417. A.R. Meloni, M.B. DeYoung, C. Lowe, and D.G. Parkes, *GLP-1 receptor activated insulin secretion from pancreatic beta-cells: mechanism and glucose dependence*. Diabetes Obes Metab, 2013. **15**(1): p. 15.
-

-
418. G. Kang and G.G. Holz, *Amplification of exocytosis by Ca^{2+} -induced Ca^{2+} release in INS-1 pancreatic beta cells*. J Physiol, 2003. **546**(Pt 1): p. 175.
419. G.G. Holz, G. Kang, M. Harbeck, M.W. Roe, and O.G. Chepurny, *Cell physiology of cAMP sensor Epac*. J Physiol, 2006. **577**(Pt 1): p. 5.
420. G. Nagy, K. Reim, U. Matti, N. Brose, T. Binz, J. Rettig, E. Neher, and J.B. Sorensen, *Regulation of releasable vesicle pool sizes by protein kinase A-dependent phosphorylation of SNAP-25*. Neuron, 2004. **41**(3): p. 417.
421. M.G. Chheda, U. Ashery, P. Thakur, J. Rettig, and Z.H. Sheng, *Phosphorylation of Snapin by PKA modulates its interaction with the SNARE complex*. Nat Cell Biol, 2001. **3**(4): p. 331.
422. T. Shibasaki, H. Takahashi, T. Miki, Y. Sunaga, K. Matsumura, M. Yamanaka, C. Zhang, A. Tamamoto, T. Satoh, J. Miyazaki, and S. Seino, *Essential role of Epac2/Rap1 signaling in regulation of insulin granule dynamics by cAMP*. Proc Natl Acad Sci U S A, 2007. **104**(49): p. 19333.
423. H. Kasai, H. Hatakeyama, M. Ohno, and N. Takahashi, *Exocytosis in Islet β -Cells*, in *Islets of Langerhans*, M.S. Islam, Editor. 2015, Springer Netherlands: Dordrecht. p. 475.
424. S.M. Bindom, C.P. Hans, H. Xia, A.H. Boulares, and E. Lazartigues, *Angiotensin I-converting enzyme type 2 (ACE2) gene therapy improves glycemic control in diabetic mice*. Diabetes, 2010. **59**(10): p. 2540.
425. L. Yuan, C.L. Lu, Y. Wang, Y. Li, and X.Y. Li, *Ang (1-7) protects islet endothelial cells from palmitate-induced apoptosis by AKT, eNOS, p38 MAPK, and JNK pathways*. J Diabetes Res, 2014. **2014**: p. 391476.

-
426. H.S. Spijker, H. Song, J.H. Ellenbroek, M.M. Roefs, M.A. Engelse, E. Bos, A.J. Koster, T.J. Rabelink, B.C. Hansen, A. Clark, F. Carlotti, and E.J. de Koning, *Loss of beta-Cell Identity Occurs in Type 2 Diabetes and Is Associated With Islet Amyloid Deposits*. Diabetes, 2015. **64**(8): p. 2928.
427. A.M. Papinska, N.M. Mordwinkin, C.J. Meeks, S.S. Jadhav, and K.E. Rodgers, *Angiotensin-(1-7) administration benefits cardiac, renal and progenitor cell function in db/db mice*. Br J Pharmacol, 2015.
428. S. Cheepala, J.S. Hulot, J.A. Morgan, Y. Sassi, W. Zhang, A.P. Naren, and J.D. Schuetz, *Cyclic nucleotide compartmentalization: contributions of phosphodiesterases and ATP-binding cassette transporters*. Annu Rev Pharmacol Toxicol, 2013. **53**: p. 231.
429. D. Cheng, J. Ren, and E.K. Jackson, *Multidrug resistance protein 4 mediates cAMP efflux from rat preglomerular vascular smooth muscle cells*. Clin Exp Pharmacol Physiol, 2010. **37**(2): p. 205.
430. Y. Hara, Y. Sassi, C. Guibert, N. Gambaryan, P. Dorfmueller, S. Eddahibi, A.M. Lompre, M. Humbert, and J.S. Hulot, *Inhibition of MRP4 prevents and reverses pulmonary hypertension in mice*. J Clin Invest, 2011. **121**(7): p. 2888.
431. Y. Sassi, A. Abi-Gerges, J. Fauconnier, N. Mougenot, S. Reiken, K. Haghighi, E.G. Kranias, A.R. Marks, A. Lacampagne, S. Engelhardt, S.N. Hatem, A.M. Lompre, and J.S. Hulot, *Regulation of cAMP homeostasis by the efflux protein MRP4 in cardiac myocytes*. Faseb j, 2012. **26**(3): p. 1009.
432. R. Godinho, T. Duarte, and E. Pacini, *New perspectives in signaling mediated by receptors coupled to stimulatory G protein: the emerging significance of cAMP*

- efflux and extracellular cAMP-adenosine pathway*. *Frontiers in Pharmacology*, 2015. **6**(58).
433. A.M. De Souza, A.G. Lopes, C.P. Pizzino, R.N. Fossari, N.C.O. Miguel, F.P. Cardozo, R. Abi-Abib, M.S. Fernandes, D.P.A. Santos, and C. Caruso-Neves, *Angiotensin II and angiotensin-(1–7) inhibit the inner cortex Na⁺-ATPase activity through AT2 receptor*. *Regulatory Peptides*, 2004. **120**(1): p. 167.
434. S. Lara Lda, F. Cavalcante, F. Axelband, A.M. De Souza, A.G. Lopes, and C. Caruso-Neves, *Involvement of the Gi/o/cGMP/PKG pathway in the AT2-mediated inhibition of outer cortex proximal tubule Na⁺-ATPase by Ang-(1-7)*. *Biochem J*, 2006. **395**(1): p. 183.
435. J.W.M.H.D. Baynes, *Medical Biochemistry* 2ed. 2005, Elsevier Mosby.
436. Vicore-Pharma. *RESEARCH of C21*. 2018; Available from: <http://vicorepharma.com/research/>.
437. H. Ebaid, J. Al-Tamimi, A. Metwalli, A. Allam, K. Zoheir, J. Ajarem, A. Rady, I. M. Alhazza, and K. Ibrahim, *Effect of STZ-Induced Diabetes on Spleen of Rats: Improvement by Camel Whey Proteins*. Vol. vol. 47(4). 2015. pp. 1109.
438. M.H. Yousif, B. Makki, A.Z. El-Hashim, S. Akhtar, and I.F. Benter, *Chronic treatment with Ang-(1-7) reverses abnormal reactivity in the corpus cavernosum and normalizes diabetes-induced changes in the protein levels of ACE, ACE2, ROCK1, ROCK2 and omega-hydroxylase in a rat model of type 1 diabetes*. *J Diabetes Res*, 2014. **2014**: p. 142154.
439. K. Zhang, X. Meng, D. Li, J. Yang, J. Kong, P. Hao, T. Guo, M. Zhang, Y. Zhang, and C. Zhang, *Angiotensin(1–7) attenuates the progression of streptozotocin-induced*

- diabetic renal injury better than angiotensin receptor blockade.* Kidney International, 2015. **87**(2): p. 359.
440. H.Y. Qureshi, R. Ahmad, and M. Zafarullah, *High-efficiency transfection of nucleic acids by the modified calcium phosphate precipitation method in chondrocytes.* Anal Biochem, 2008. **382**(2): p. 138.
441. F.L. Graham and A.J. van der Eb, *A new technique for the assay of infectivity of human adenovirus 5 DNA.* Virology, 1973. **52**(2): p. 456.
442. S.I. Sukharev, V.A. Klenchin, S.M. Serov, L.V. Chernomordik, and A. Chizmadzhev Yu, *Electroporation and electrophoretic DNA transfer into cells. The effect of DNA interaction with electropores.* Biophys J, 1992. **63**(5): p. 1320.
443. A.J.F. Griffiths, J.H. Miller, D.T. Suzuki, R.C. Lewontin, and W.M. Gelbart, *An Introduction to Genetic Analysis.* 7th ed. 2000, New York: W. H. Freeman.
444. J.H. Felgner, R. Kumar, C.N. Sridhar, C.J. Wheeler, Y.J. Tsai, R. Border, P. Ramsey, M. Martin, and P.L. Felgner, *Enhanced gene delivery and mechanism studies with a novel series of cationic lipid formulations.* J Biol Chem, 1994. **269**(4): p. 2550.
445. F.R. Bryant, *Construction of a recombinase-deficient mutant recA protein that retains single-stranded DNA-dependent ATPase activity.* J Biol Chem, 1988. **263**(18): p. 8716.
446. A. Froger and J.E. Hall, *Transformation of Plasmid DNA into E. coli Using the Heat Shock Method.* J Vis Exp, 2007(6).
447. H.C. Birnboim, *A rapid alkaline extraction method for the isolation of plasmid DNA.* Methods Enzymol, 1983. **100**: p. 243.

-
448. K. Mullis, F. Faloona, S. Scharf, R. Saiki, G. Horn, and H. Erlich, *Specific enzymatic amplification of DNA in vitro: the polymerase chain reaction*. Cold Spring Harb Symp Quant Biol, 1986. **51 Pt 1**: p. 263.
449. B.A. Sherf, S.L. Navarro, R.R. Hannah, and K.V. Wood, *Dual-luciferase reporter assay: an advanced co-reporter technology integrating firefly and Renilla luciferase assays*, in *Promega Notes Magazine* 1996. p. 2.
450. P.K. Smith, R.I. Krohn, G.T. Hermanson, A.K. Mallia, F.H. Gartner, M.D. Provenzano, E.K. Fujimoto, N.M. Goeke, B.J. Olson, and D.C. Klenk, *Measurement of protein using bicinchoninic acid*. Anal Biochem, 1985. **150**(1): p. 76.
451. U.K. Laemmli, *Cleavage of structural proteins during the assembly of the head of bacteriophage T4*. Nature, 1970. **227**(5259): p. 680.
452. H. Towbin, T. Staehelin, and J. Gordon, *Electrophoretic transfer of proteins from polyacrylamide gels to nitrocellulose sheets: procedure and some applications*. Proc Natl Acad Sci U S A, 1979. **76**(9): p. 4350.
453. S. Aydin, *A short history, principles, and types of ELISA, and our laboratory experience with peptide/protein analyses using ELISA*. Peptides, 2015. **72**: p. 4.
454. M.L. Graham, J.L. Janecek, J.A. Kittredge, B.J. Hering, and H.J. Schuurman, *The Streptozotocin-Induced Diabetic Nude Mouse Model: Differences between Animals from Different Sources*. Comp Med, 2011. **61**(4): p. 356.
455. D. Dufrane, M. van Steenberghe, Y. Guiot, R. Goebbels, A. Saliez, and P. Gianello, *Streptozotocin-Induced Diabetes in Large Animals (Pigs/Primates): Role of GLUT2 Transporter and β -cell Plasticity*. Vol. 81. 2006. 36.

456. S.G. Paik, N. Fleischer, and S.I. Shin, *Insulin-dependent diabetes mellitus induced by subdiabetogenic doses of streptozotocin: obligatory role of cell-mediated autoimmune processes*. Proc Natl Acad Sci U S A, 1980. **77**(10): p. 6129.